SEP -4

REPORT DOCUMENTATION PAGE

AFRL-SR-BL-TR-01-

0583

1. AGENCY USE ONLY (Leave blank)

2. REPORT DATE
August 28, 2001

3. REPORT TYPE AND DATES COVERED
Final Technical Report: 01/01/98 to 09/30/98

4. TITLE AND SUBTITLE
"SHOCK PROPAGATION AND SUPERSONIC DRAG IN LOW TEMPERATURE PLASMAS" Support for AFOSR-SPONSORED WORKSHOP: "Understanding and Control of Ionized High-Speed Flows." Held at Princeton University, Princeton, NJ, Feb. 26-27, 1998

5. FUNDING NUMBERS
AFOSR Grant #F49620-97-1-0497
P00002

6. AUTHOR(S)
Professor Richard B. Miles

7. PERFORMING ORGANIZATION NAME(S) AND ADDRESS(ES)
Princeton University
Dept. Mechanical & Aerospace Engrg.
Olden St.
Princeton, NJ 08544

8. PERFORMING ORGANIZATION REPORT NUMBER

9. SPONSORING / MONITORING AGENCY NAME(S) AND ADDRESS(ES)
AFOSR/NA
801 North Randolph St.
Room 732
Arlington, VA 22203-1977

10. SPONSORING / MONITORING AGENCY REPORT NUMBER

11. SUPPLEMENTARY NOTES

12a. DISTRIBUTION / AVAILABILITY STATEMENT
Approved for public release; distribution is unlimited.

12b. DISTRIBUTION CODE

13. ABSTRACT ***(Maximum 200 Words)***

This grant supported an Air Force-sponsored workshop, "Understanding and Control of Ionized High-Speed Flows," which was conducted at Princeton University, February 26-27, 1998. In recent years, there has been a great deal of interest in the formation mechanisms and properties of air plasmas. This interest is, in part, motivated by experiments conducted in Russia and in the United States which indicate shock propagation in weakly ionized air plasmas is at a higher velocity than would be predicted by presently understood models. If this is, indeed, the case, such plasmas could be used for supersonic/hypersonic drag reduction. In addition, atmospheric plasmas could influence flow control devices, electromagnetic attenuation, and hypersonic propulsion systems. As a consequence, the formation of such plasmas in atmospheric pressure environments, and the study of the properties of these plasmas, are of significant national interest.

2001126 100

14. SUBJECT TERMS
Air plasmas, Weakly ionized air plasmas, AFOSR workshop

15. NUMBER OF PAGES
2 plus 1 Appendix

16. PRICE CODE

17. SECURITY CLASSIFICATION OF REPORT	18. SECURITY CLASSIFICATION OF THIS PAGE	19. SECURITY CLASSIFICATION OF ABSTRACT	20. LIMITATION OF ABSTRACT
Unclassified	Unclassified	Unclassified	UL

NSN 7540-01-280-5500

Standard Form 298 (Rev. 2-89)
Prescribed by ANSI Std. Z39-18
298-102

FINAL TECHNICAL REPORT (Dated 8/28/01)

AFOSR GRANT #F4920-97-1-0497, P00002
(150-6756)

"SHOCK PROPAGATION AND SUPERSONIC DRAG IN LOW TEMPERATURE PLASMAS"

SUPPORT FOR:

AFOSR-SPONSORED WORKSHOP ENTITLED:
"Understanding and Control of Ionized High-Speed Flows"
Princeton University
Princeton, NJ 08544
February 26-27, 1998

ABSTRACT

This grant supported the costs of an Air Force-sponsored workshop, "Understanding and Control of Ionized High-Speed Flows," which was conducted at Princeton University, February 26-27, 1998. In recent years, there has been a great deal of interest in the formation mechanisms and properties of air plasmas. This interest is, in part, motivated by experiments conducted in Russia and in the United States which indicate shock propagation in weakly ionized air plasmas is at a higher velocity than would be predicted by presently understood models. If this is, indeed, the case, such plasmas could be used for supersonic/hypersonic drag reduction. In addition, atmospheric plasmas could influence flow control devices, electromagnetic attenuation, and hypersonic propulsion systems. As a consequence, the formation of such plasmas in atmospheric pressure environments, and the study of the properties of these plasmas, are of significant national interest.

DISCUSSION

The purpose of the workshop was to highlight the basic science issues involved with controlling high-speed flows using weakly-ionized plasmas. The specific objectives of the two-day meeting were to review recent experimental/theoretical research in this area, and to exchange ideas/ understanding on the basic flow physics of the problem, and to discuss future research directions. Princeton University was a natural location for this workshop since work is underway here to examine both drag characteristics and electron discharge physics associated with weakly ionized plasmas.

Sixty individuals, each of whom is considered a leading authority on this issue, attended the two-day workshop (a full listing of the participants is located in Appendix A). The first day of the workshop consisted of four sessions on an agenda of twelve speakers and covered the following topics:

Session I: "Introduction to the Problem" (presentations by B. Ganguly of AFRL and A. Auslender of NASA LaRc).

Session II: "Aerodynamics of Ionized Flow" (presentations by R. Miles of Princeton University, J. Shang of AFRL, N. Malmuth and V. Soloviev of Rockwell Science, and V. Subramanian of The Ohio State University).

Session III: "Theory and Computation of Ionized Flows" (presentations by G. Karniadakis of Brown University, K. Powell of the University of Michigan, and S. Nazarenko of the University of Arizona).

Session IV: "Plasma Generation and Maintenance" (Presentations by S. Kuo of Polytechnic University, J. Kline of Research Support Instruments, and W. Rich of The Ohio State University).

The second day of the workshop, the participants were divided into four separate working groups for further discussion, followed by debriefings and laboratory tours at Princeton.

Appendix A is a complete record of the two-day workshop and includes the final agenda for the meeting, the complete list of participants and their contact information, as well as copies of each of the presentations for all of the four topic areas listed above.

Appendix A

Princeton University

School of Engineering and Applied Science
Department of Mechanical and Aerospace Engineering
P.O. Box CN5263
Princeton, New Jersey 08544-5263

FINAL AGENDA

AFOSR-SPONSORED WORKSHOP:

"UNDERSTANDING AND CONTROL OF IONIZED HIGH-SPEED FLOWS"

February 26-27, 1998

MEETING LOCATION: **Convocation Room (C217) Engineering Quadrangle**
Olden Street, Princeton, NJ 08544

THURSDAY, FEBRUARY 26, 1998:

7:30 AM	*SIGN-IN/COFFEE*	
8:00 AM	OPENING REMARKS:	G.L. Brown--Chairman, MAE Dept., Princeton R. Miles--Princeton S. Walker--AFOSR
8:30 AM	SESSION I:	*INTRODUCTION TO THE PROBLEM* B. Ganguly--AFRL, A. Auslender--NASA LaRC
9:30 AM	DISCUSSION	
10:00 AM	*BREAK*	
10:30 AM	SESSION II:	*AERODYNAMICS OF IONIZED FLOW* R. Miles--Princeton, J. Shang--AFRL, N. Malmuth/V. Soloviev--Rockwell Science V. Subramanian--OSU
11:30 AM	DISCUSSION	
12:00 PM	LUNCH	
1:30 PM	SESSION III:	*THEORY AND COMPUTATION OF IONIZED FLOWS* G. Karniadakis--Brown U., K. Powell--UM, S. Nazarenko--UA
2:30 PM	DISCUSSION	
3:00 PM	*BREAK*	
3:30 PM	SESSION IV:	*PLASMA GENERATION AND MAINTENANCE* S. Kuo--Polytechnic Univ., J. Kline--RSI, W. Rich--OSU
4:30 PM	DISCUSSION	
5:00 PM	FIRST DAY WRAP-UP	
6:00 PM	*RECEPTION, Prospect House*	

FRIDAY, FEBRUARY 27, 1998:

7:30 AM	*SIGN-IN/COFFEE*
8:00 AM	OPENING REMARKS
8:15 AM	WORKING GROUPS
10:30 AM	*BREAK*
11:00 AM	GROUP DEBRIEFINGS
12:00 PM	LUNCH/LABORATORY TOUR

ENGINEERING QUADRANGLE

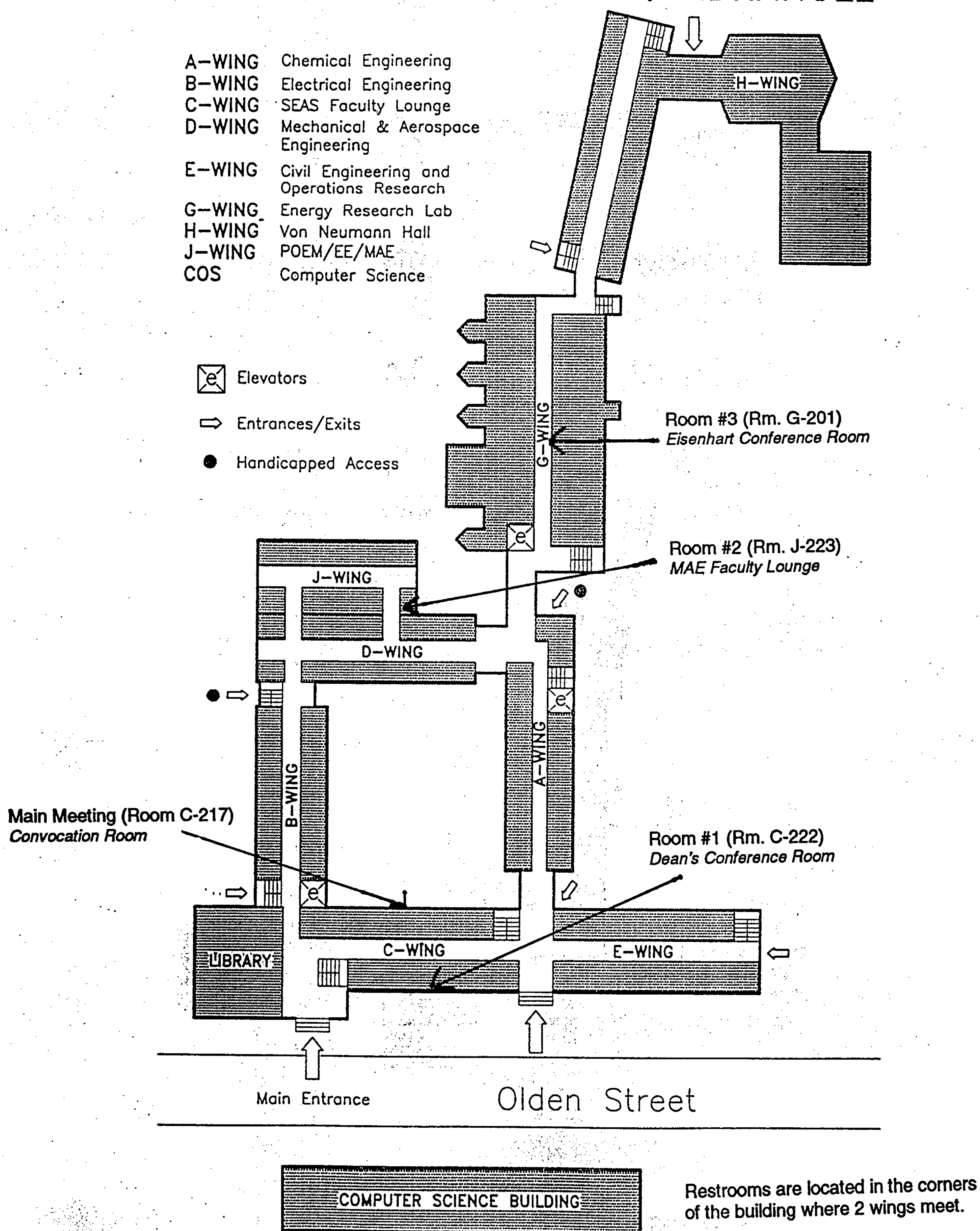

Restrooms are located in the corners of the building where 2 wings meet.

CAMPUS MAP

Nassau Inn

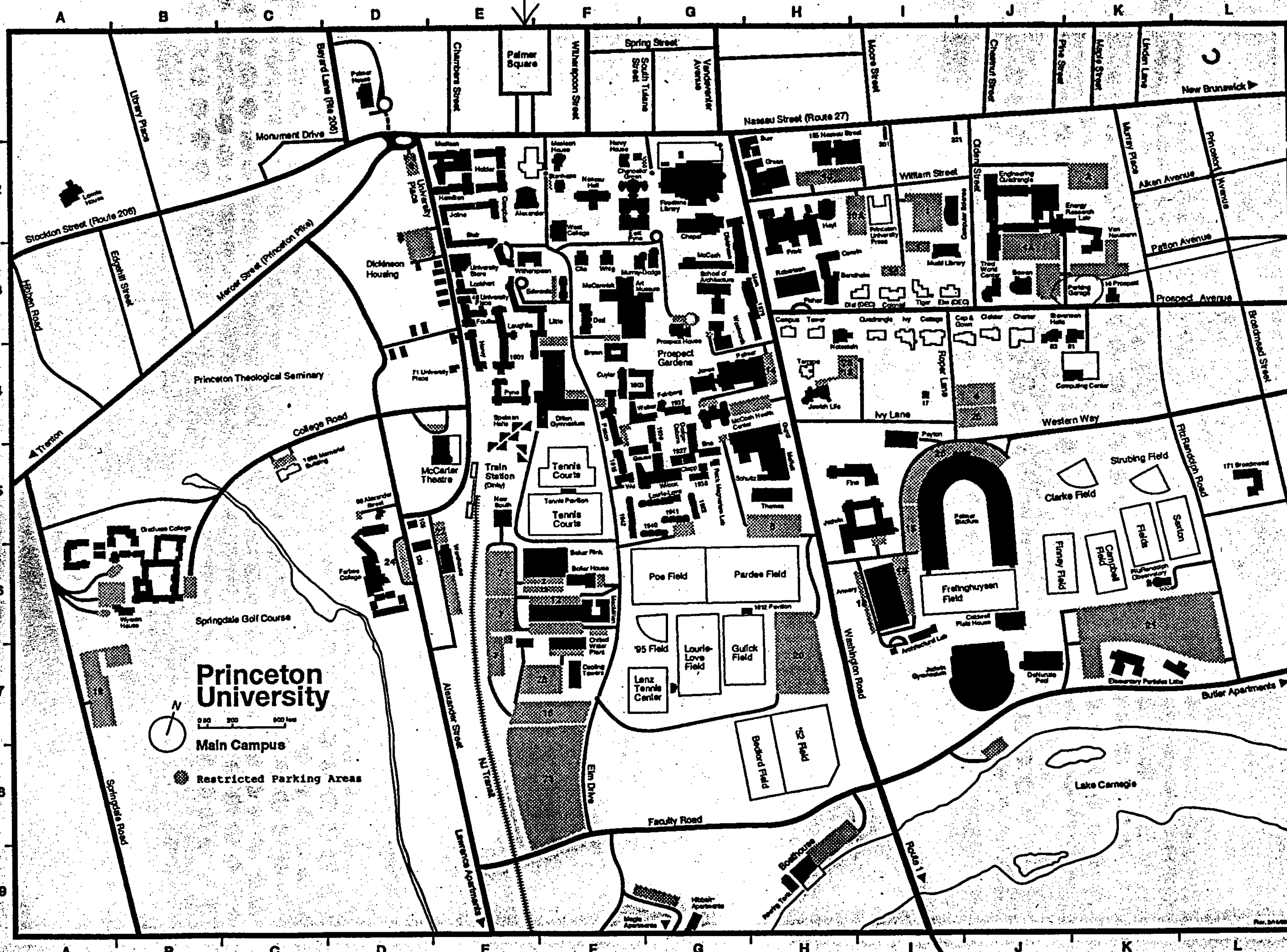

(Parking Garage: Please Use Floors 4 & 5)

South (Trenton/Phila.) ROUTE 1 North (Newark/New York)

PARTICIPANT LIST

AFOSR-SPONSORED WORKSHOP: "UNDERSTANDING & CONTROL OF IONIZED HIGH-SPEED FLOWS"

PRINCETON UNIVERSITY
FEBRUARY 26-27, 1998

NAME	ADDRESS	PHONE/FAX NUMBERS	E-MAIL
ADAMOVICH, Igor	The Ohio State University Dept. Mechanical Engineering 2019 Robinson Laboratory 206 West 18th Avenue Columbus, OH 43216	614-292-0561 (P) 614-292-3163 (F)	Adamo@mps.ohio-state.edu
AUSLENDER, Aaron	NASA-Langley Research Center MS 168 Hampton, VA 23681	757-864-6545 (P)	A.H.Auslender@LaRC.NASA.GOV
BAILEY, William	AFIT/ENP, Dept. of Physics 2950 P Street Wright-Patterson AFB, OH 45433	937-255-3636 x4501 (P) 937-255-2921 (F)	wbailey@afit.af.mil
BAIN, Lee	AFRL/PR Bldg. 18 1950 Fifth St., Suite 10 WPAFB, OH 45433-7251	937-255-1237 (P) 937-656-4659 (F)	Bainwl@wl.wpafb.af.mil
BARKER, Robert	AFOSR/NE 110 Duncan Ave., Suite B115 Bolling AFB, DC 20332	202-767-5011 (P) 202-767-4986 (F)	Robert.barker@afosr.af.mil
BERMAN, Michael	AFOSR/NL 110 Duncan Avenue, Suite B115 Bolling AFB, DC 20332	202-767-4963 (P) 202-404-7475 (F)	Michael.berman@afosr.af.mil
BEUTNER, Thomas J.	WL/FIMO 2145 5th Street Aero-Diagnostics Research Section Wright-Patterson AFB, OH 45433-7005	219-872-5694 (P)	
BRANDENBURG, John	Research Support Instruments 4325-B Forbes Blvd. Lanham, MD 20706	301-306-0010 (P) 301-306-0295 (F)	Rsidc@mindspring.com

NAME	ADDRESS	PHONE/FAX NUMBERS	E-MAIL
BROWN, Garry L.	Princeton University MAE Dept., Rm D-216 E-Quad Olden Street Princeton, NJ 08544	609-258-6083 (P) 609-258-6109 (F)	Glb@princeton.edu
BUSHNELL, Dennis M.	NASA Langley Research Center MS-197 Hampton, VA 23665-5225	757-864-8987 (P) 757-864-8980 (F)	d.m.busnell@larc.nasa.gov
CAMBIER, Jean-Luc	MSE Technology Applications, Inc. PO Box 4078 220 North Alaska Street Butte, MT 59702	406-494-7304 (P) 406-494-7230 (F)	
CAPPELLI, Mark	Stanford Univresity Mechanical Engineering Dept. Stanford, CA 94305-3032	650-725-2020 (P) 650-723-1748 (F)	cap@leland.stanford.edu
CARTER, Campbell D.	Innovative Scientific Solutions, Inc. 2786 Indian Ripple Road Dayton, OH 45440-0001	937-255-8704 (P) 937-656-4652 (F)	Cartered@possum.appl.wpafb.af.mil
CHASE, Raymond L.	ANSER, Inc. Crystal Gateway 1215 Jefferson Davis Highway Arlington, VA 22202-3251	703-416-3290 (P) 703-416-3329 (F)	Chaser@answer.org
CHOUEIRI, Edgar	Princeton University MAE Dept., Rm D-432 E-Quad Olden Street Princeton, NJ 08544	609-258-5220 (P) 609-258-6109 (F)	Choueiri@princeton.edu
DRYER, Frederick L.	Princeton University MAE Dept., Rm D-316 E-Quad Olden Street Princeton, NJ 08544	609-258-5206 (P) 609-258-1939 (F)	Fldryer@phoenix.princeton.edu
EFTHIMION, Philip	Princeton Plasma Physics Laboratory Princeton University B244 C-Site PPPL Princeton, NJ 08544	609-243-3212 (P) 609-243-2874 (F)	Pefthimion@pppl.gov
GAITONDE, Datta	AFRL/VAAC Rm A-120, Bldg 450 2645 Fifth St., Suite 7 WPAFB, OH 45433-7913	937-255-7127 (P) 937-656-4210 (F)	Datta@fim.wpafb.af.mil

NAME	ADDRESS	PHONE/FAX NUMBERS	E-MAIL
GANGULY, Bish	AFRL/PR 2645 Fifth St., Suite 13 Wright-Patterson AFB, OH 45433-7919	937-255-2923 (P) 937-476-4095 (F)	Gangulbn@possum.appl.wpafb.af.mil
GARSCADDEN, Alan	AFRL/PR Building 18 1950 Fifth St., Suite 10 Wright-Patterson AFB, OH 45433-7251	937-255-2246 (P) 937-255-6641 (F)	Garscaa@wl.wpafb.af.mil
JACKSON, Thomas A.	AFRL/PR Building 18 1950 Fifth St., Suite 10 Wright Patterson AFB, OH 45433-7251	937-255-1234 (P) 937-656-4659 (F)	Jacksonta@wl.wpafb.af.mil
JAHN, Robert	Princeton University MAE Dept., Rm. D-334 E-Quad Olden Street Princeton, NJ 08544	609-258-4550 (P) 609-258-6109 (F)	Rgjahn@princeton.edu
KARNIADAKIS, George	Brown University Center for Fluid Mechanics Division of applied Mathematics Providence, RI 02912	401-863-1217 (P)	Gk@cfm.brown.edu
KEEFER, Dennis	Univ. Tennessee Space Institute Gas Diagnostics Research Division Tullahoma, TN 37388-8897	931-393-7475 (P) 931-454-2271	Dkeefer@utsi.edu
KIMMEL, Roger	AFRL/VAAA Bldg. 450 2645 Fifth St., Suite 7 WPAFB, OH 45433-7913	937-255-2193 (P) 937-656-7868 (F)	Kimmelrl@fim.wpafb.af.mil
KLINE, John	Research Support Instruments 4325-B Fores Blvd. Lanham, MD 20706	301-306-0295 (P)	
KORETZKY, Edward	Polytechnic University		
KUO, Spencer	Polytechnic University Route 110 Farmingdale, NY 11735	516-755-4301 (P) 516-755-4404 (F)	Spkuo@poly.edu

NAME	ADDRESS	PHONE/FAX NUMBERS	E-MAIL
KUSHNER, Mark J.	University of Illinois Dept. of Electrical & Computer Engrg. 1406 W. Green St. Urbana, IL 61801	217-244-7096 (P) 217-244-7097 (F)	Mjk@uiuc.edu
LAM, Sau-Hai	Princeton University MAE Dept., Rm. D-302C E-Quad Olden Street Princeton, NJ 08544	609-258-5133 (P) 609-258-6109 (F)	Lam@princeton.edu
LAW, C.K.	Princeton University MAE Dept., Rm D-323 E-Quad Olden Street Princeton, NJ 08544	609-258-5271 (P) 609-258-6233 (F)	Cklaw@princeton.edu
LAWLESS, John	Redwood Scientific, Inc. 1005 Terra Nova Blvd. Pacifica, CA 94044	650-738-8083 (P) 650-738-8086 (F)	70262.363@comuserve.com
LEONE, Stephen	University of Colorado Campus Box 440 Boulder, CO 80309-0440	303-492-5128 (P) 303-492-5504	Srl@jila.colorado.edu
MACHERET, Sergey	Princeton University, MAE Dept. Room D-414 E-Quad Olden St. Princeton, NJ 08544	609-258-5130 (P) 609-258-1139 (F)	Macheret@princeton.edu
MALMUTH, Norman	Rockwell Science Center 1049 Camino Dos Rios Thousand Oaks, CA 91360	805-373-4154 (P) 805-373-4775 (F)	Ndm@norman.risc.rockwell.com
McMICHAEL, James	DARPA/TTO 3701 N. Fairfax Drive Arlington, VA 22203-1714	703-696-2377 (P)	Jmcmichael@darpa.mil
MICCI, Michael M.	Pennsylvania State University Dept. of Aerospace Engineering 233 Hammond Building University Park, PA 16802	814-863-0043 (P) 814-865-7092 (F)	Micci@henry2.aero.psu.edu
MILES, Richard	Princeton University MAE Dept., Rm D414 EQ Olden Street Princeton, NJ 08544	609-258-5131 (P) 609-258-1139 (F)	Miles@hepcat.princeton.edu

NAME	ADDRESS	PHONE/FAX NUMBERS	E-MAIL
MORRIS, Robert	AFRL/VSBP 29 Randolf Road Hanscom AFB, MA 01731	617-377-8758 (P) 617-377-1148 (F)	Morris@plh.af.mil
MURTHY, S.N.B.	Purdue University Thermal Sciences & Propulsion Center School of Mechanical Engineering 1003 Chaffee Hall West Lafayette, IN 47907-1003	765-494-1501 (P) 765-494-0530 (F)	
NACHMAN, Arje	AFOSR/NM 110 Duncan Avenue Bolling AFB, DC 20332	202-767-4939 (P) 202-404-7496 (F)	Arje.nachman.@afosr.af.mil
NAZARENKO, Sergey	University of Arizona Dept. of Mathematics 617 N. Santa Rita Ave. Tucson, AZ 85721		
NELSON, Gordon	MSE Technology Applications, Inc. PO Box 4078 220 North Alaska Street Butte, MT 59702	406-494-7403 (P) 406-494-7230 (F)	Gnelson@buttenet.com
PETERKIN, Robert E.	AFRL/DEHE 3550 Aberdeen Ave., SE Kirtland AFB, NM 87117-5776	505-846-0259 (P)	Bob@ppws07.plk.af.mil
POGGIE, Jonathan	US Air Force Research Laboratory AFRI/VAAA 2645 Fifth St., Suite 7 WPAFB, OH 45433-7913	937-255-5464 (P) 937-656-7868 (F)	Poggiej@fm.wpafb.af.mil
POWELL, Kenneth	University of Michigan Dept. of Aerospace Engineering Ann Arbor, MI 48109-1248	313-764-3331 (P) 734-763-0578 (F)	Powell@engin.umich.edu
RABITZ, Herschel	Princeton University Dept. of Chemistry 129 Frick Lab Princeton, NJ 08544	609-258-3917 (P) 609-258-6746 (F)	Hrabitz@chemvax.princeton.edu
RICH, William	The Ohio State University Robinson Laboratory 206 W. 18th Avenue Columbus, OH 43210-0001	614-292-6309 (P) 614-292-3163 (F)	Rich.2@osu.edu

NAME	ADDRESS	PHONE/FAX NUMBERS	E-MAIL
SCHRECK, Scott	AFOSR/NM 110 Duncan Avenue, Suite B115 Bolling AFB, DC 20332	202-767-7902 (P) 202-404-7496 (F)	Scott.schreck@afosr.af.mil
SHANG, Joseph	AFRL/VA Building 450 2645 Fifth St., Suite 7 Wright-Patterson AFB, OH 45433-7913	937-255-6156 (P)	
SHEROHMAN, John	Lawrence Livermore National Laboratory PO Box 808, L-377 Livermore, CA 94551	510-422-1059 (P) 510-422-4563 (F)	Sherohman1.llnl.gov
SHUMLAK, Uri	University of Washington Aeronautics & Astronautics Dept. Box 352250 Seattle, WA 98195-2250	206-616-1986 (P) 206-543-4719 (F)	Shumlak@aa.washington.edu
SMITS, Alexander	Princeton University MAE Dept., Rm. D-302D E-Quad Olden St. Princeton, NJ 08544	609-258-5117 (P) 609-258-6109 (F)	Asmits@princeton.edu
SOLOVIEV, Victor	Rockwell Science Center 1049 Camino Dos Rios Thousand Oaks, CA 91360		Vics@post.mipt.rssi.ru
SUBRAMANIAM, Vish V.	The Ohio State University Dept. of Mechanical Engineering 2087 Robinson Lab 206 West 18th Avenue Columbus, OH 43210	614-292-6096 (P) 614-292-3163 (F)	Subramaniam.1@osu.edu
TISHKOFF, Julian	AFOSR/NA 110 Duncan Avenue, Suite B115 Bolling AFB, DC 20332	202-767-0465 (P) 202-767-4988 (F)	Julian.tishkoff@afosr.af.mil
TURCHI, Peter	AFRL/DE Kirtland AFB, NM		Turchi.1@osu.edu
VAN WIE, David	Johns Hopkins 11100 Johnbs Hopkins Road Bldg. 10A, Room 115 Laurel, MD 20723-6099	301-953-5194 (P) 410-792-5850 (F)	David.vanwie@jhuapl.edu

NAME	ADDRESS	PHONE/FAX NUMBERS	E-MAIL
WALKER, Steven H.	AFOSR/NA 110 Duncan Ave., Suite B115 Bolling AFB, DC 20332	202-767-4960 (P) 202-767-4988 (F)	Steven.walker@afosr.af.mil
YETTER, Richard	Princeton University MAE Dept., D-312 E-Quad Olden Street Princeton, NJ 08544	609-258-2947 (P) 609-258-1939 (F)	Rich@dante.princeton.edu

Understanding and Control of Ionized High-Speed Flows

AFOSR-Sponsored Workshop

Princeton University

26-27 Feb 98

NEW WORLD VISTAS (NWV)

- 41 Technologies Identified By AFMC And The Air Force Scientific Advisory Board
- 32 NWV Technologies To Receive Basic Research Support
- $14.8M Budget For FY 1997

HYPERSONICS

Objectives

- Investigate Advanced Propellants And Cooling Concepts To Enable Hydrocarbon-Fueled Mach 8+ Aeropropulsion And Combined Cycle Propulsion

- Examine Electromagnetic Manipulation Of Ionized Flowfields To Improve Hypersonic Vehicle Performance

NEW WORLD VISTAS
POWER PROJECTION AND MOBILITY

TOPIC 08 - HYPERSONICS

RESEARCH ISSUE: IMPACT OF WEAKLY IONIZED FLOWS ON VEHICLE/PROPULSION SYSTEM PERFORMANCE

RUSSIAN AYAKS FLIGHT VEHICLE CONCEPT

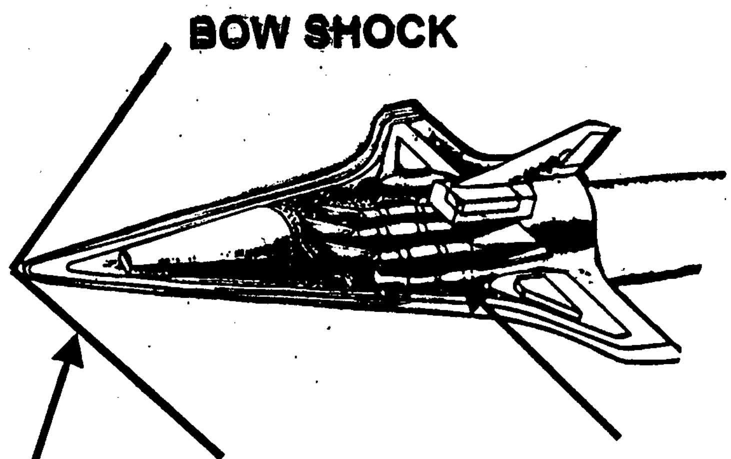

MEASUREMENTS INDICATE THAT UNSTEADY ANALYSIS IS REQUIRED TO DESCRIBE ENERGY TRANSFER BETWEEN SHOCKS AND NONEQUILIBRIUM MEDIA (GANGULY, AFRL/PR)

EXPERIMENTAL RESULTS SHOW THAT REACTION WITH IONIZED AIR CAUSES HYDROCARBON FUEL COMPONENTS TO DECOMPOSE AND FORM REACTIVE FREE RADICALS (MORRIS, AFRL/VS)

Background

- Many experiments have shown large changes in shock strength, speed, and stand-off distance in weakly-ionized flows
- Complete analysis of proposed mechanisms for the observed shock dynamics is lacking
- US interest/research is increasing - USAFA June 97 workshop

Purpose of Workshop

- Highlight basic science issues involved with controlling high-speed flows using weakly-ionized plasma
  - Review recent basic research in the area
  - Technical exchange on flow physics
  - Discuss future directions

FINAL AGENDA

AFOSR-SPONSORED WORKSHOP:

"UNDERSTANDING AND CONTROL OF IONIZED HIGH-SPEED FLOWS"

February 26-27, 1998

MEETING LOCATION: **Convocation Room (C217) Engineering Quadrangle**
Olden Street, Princeton, NJ 08544

THURSDAY, FEBRUARY 26, 1998:

7:30 AM	*SIGN-IN/COFFEE*	
8:00 AM	OPENING REMARKS:	G.L. Brown--Chairman, MAE Dept., Princeton R. Miles--Princeton S. Walker--AFOSR
8:30 AM	SESSION I:	*INTRODUCTION TO THE PROBLEM* B. Ganguly--AFRL, A. Auslender--NASA LaRC
9:30 AM	DISCUSSION	
10:00 AM	*BREAK*	
10:30 AM	SESSION II:	*AERODYNAMICS OF IONIZED FLOW* R. Miles--Princeton, J. Shang--AFRL, N. Malmuth/V. Soloviev--Rockwell Science V. Subramanian--OSU
11:30 AM	DISCUSSION	
12:00 PM	LUNCH	
1:30 PM	SESSION III:	*THEORY AND COMPUTATION OF IONIZED FLOWS* G. Karniadakis--Brown U., K. Powell--UM, S. Nazarenko--UA
2:30 PM	DISCUSSION	
3:00 PM	*BREAK*	
3:30 PM	SESSION IV:	*PLASMA GENERATION AND MAINTENANCE* S. Kuo--Polytechnic Univ., J. Brandenburg--RSI, W. Rich--OSU
4:30 PM	DISCUSSION	
5:00 PM	FIRST DAY WRAP-UP	
6:00 PM	*RECEPTION, Prospect House*	

FRIDAY, FEBRUARY 27, 1998:

7:30 AM	*SIGN-IN/COFFEE*
8:00 AM	OPENING REMARKS
8:15 AM	WORKING GROUPS
10:30 AM	*BREAK*
11:00 AM	GROUP DEBRIEFINGS
12:00 PM	LUNCH/LABORATORY TOUR

Rules of Engagement

- Let's keep this science-oriented but relevant; we'll let someone else actually build AJAX
- Let's really attempt to better understand this stuff before we leave
- Let's critique the work, but not criticize the people
- Please don't say, "It's just a thermal effect"; prove it.
- Don't be afraid to ask questions; we have people from many diverse technical backgrounds here
- Government people never say stupid things (by default)
- Please treat the second day as your <u>collective</u> chance to shape the future AF basic research investment in this area
- Let's have <u>fun</u> - 2 days without email, voice mail, dept. chairs, supervisors, etc.

AFOSR
Workshop

Princeton Univ

Feb 26, 1998

Dr. Bish Ganguly

Nonequilibrium Air Plasma

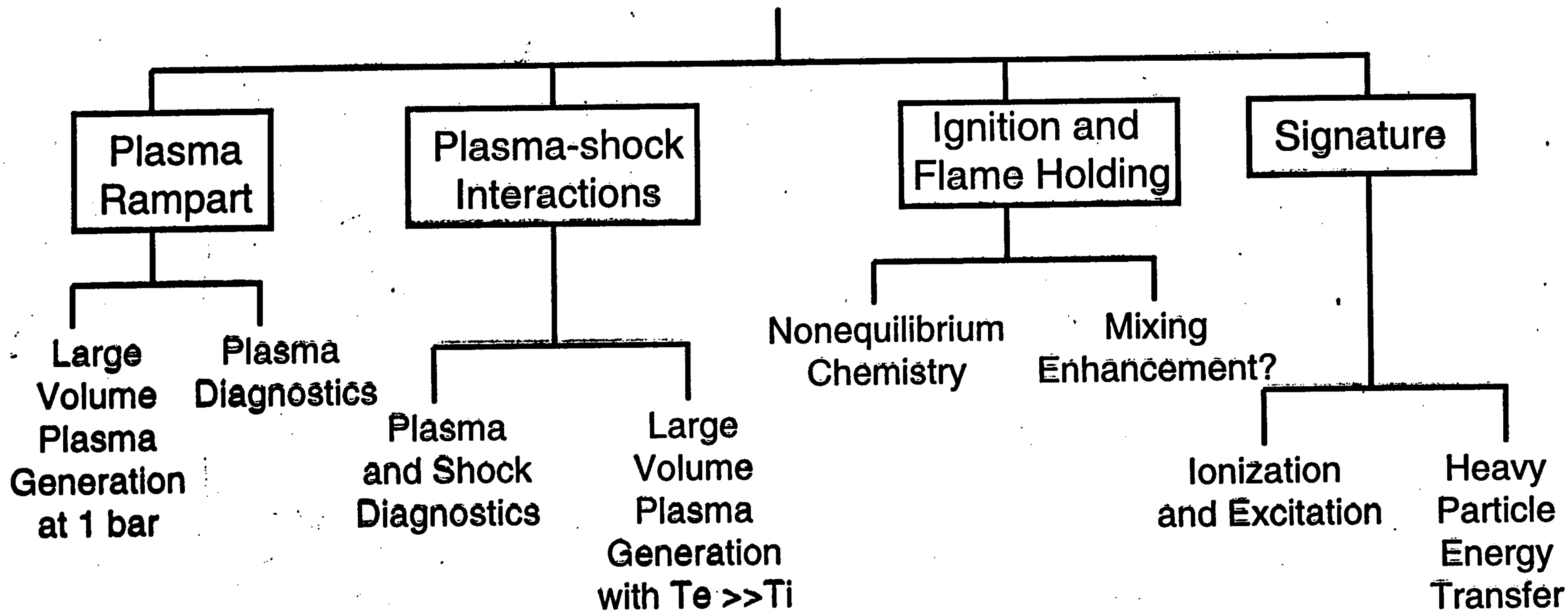

POTENTIAL PAYOFFS OF NONEQUILIBRIUM PLASMAS TO HYPERSONICS

- Thermal problem minimized - shock wave dissipation by nonequilibrium plasmas
- Combustion efficiency improvement - mixing enhancement by plasma interactions
- Drag reductions through boundary layer control
- Improve ignition and flame holding for subsonic to hypersonic combustor by nonequilibrium plasma chemistry

EXPERIMENTAL OBSERVATIONS OF PLASMA-SHOCK INTERACTIONS

- Shock wave dispersion, damping and velocity increase (super thermal) are observed in glow discharges of both atomic and molecular gases
    a. fractional ionization - 10^{-7} to 10^{-3}
    b. gas temperature - 300 to 1400 K

- Similar features are not observed in thermal plasmas

- Weak magnetic field impacts sound velocity

- Sound velocity change depends on T_e

- UV illumination of the plasma is <u>claimed</u> to increase speed of sound in plasma

CURRENT STATUS OF THE RESEARCH RESULTS

- SEVERAL GROUPS HAVE REPORTED INCREASED DISPERSION AND DAMPING OF SHOCK WAVES IN WEAKLY IONIZED PLASMAS, ALSO HIGHER SHOCK PROPAGATION VELOCITIES
- SOME OF THE RESEARCHERS ASCRIBED THE EFFECTS TO THE NONEQUILIBRIUM PLASMAS, OTHERS TO THE TEMPERATURE GRADIENT FORMED IN PLASMAS
- ACCURATE THEORETICAL MODEL EXISTS FOR SMALL AMPLITUDE AUDIO FREQUENCY ACOUSTIC WAVE PROPAGATION IN PLASMAS
- ACCURATE MODEL DOES NOT EXIST FOR SHOCK WAVE PROPAGATION IN NONEQUILIBRIUM PLASMAS

Shock Wave Propagation in a Weakly Ionized Low-pressure Discharge

Plasma Parameters

$p = 30$ torr
$J = 3$ mA/cm^2
$T_g = 800$ K

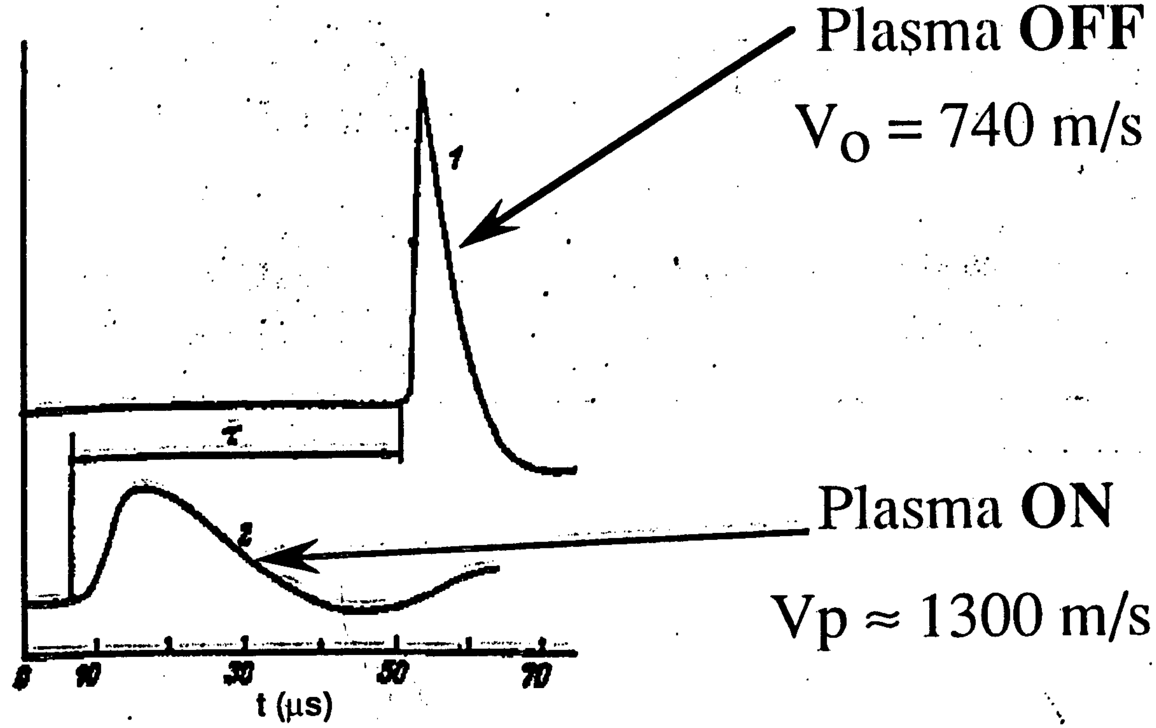

A. I. Klimov et al., Sov. Tech. Phys. Lett. **8**, 192 (1982)

Shock Standoff Comparison to Predictions

(0.75 in. diam, 30 torr)

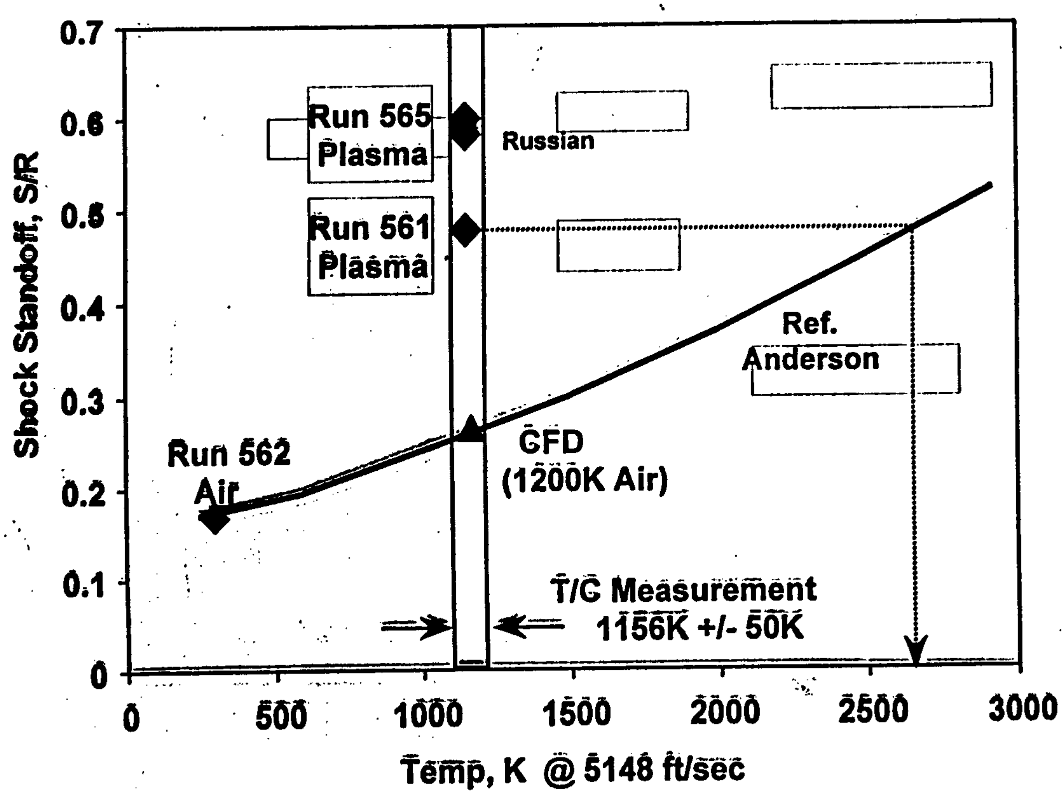

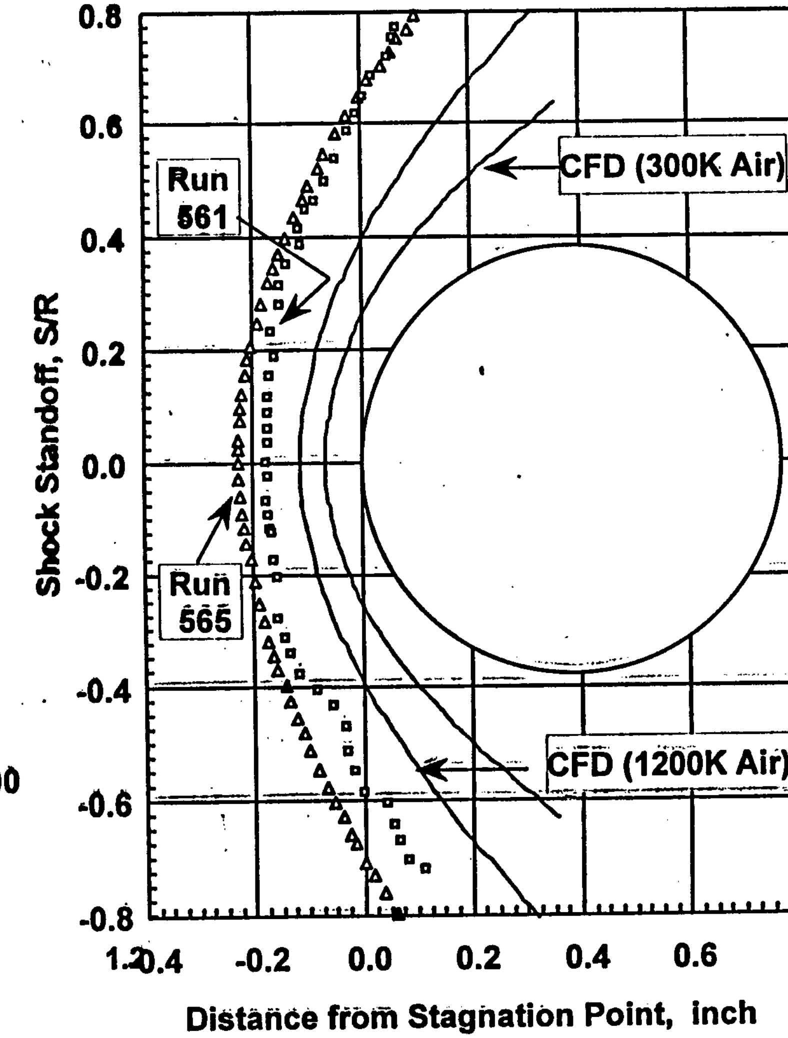

RESEARCH TOPICS OF INTEREST

- MACH NO. DEPENDENT SHOCK WAVE ATTENUATION AND DISPERSION VS. GAS PRESSURE AND CURRENT DENSITY

- SIMULTANEOUS MULTIPOINT MEASUREMENTS
  - GAS HEATING EFFECTS
  - LINEAR/NONLINEAR ENERGY COUPLING
  - ENERGY TRANSFER MECHANISM

- ENERGY EXCHANGE MECHANISMS
  - CHARGE EXCHANGE EFFECTS
  - ELECTRON ENERGY ENHANCEMENT BY AMBIPOLAR ELECTRIC FIELD
  - KINETIC TO ELECTROSTATIC ENERGY TRANSFER

Initial Replication of Russian Results at AEDC

(0.75-in diam sphere, 30 torr)

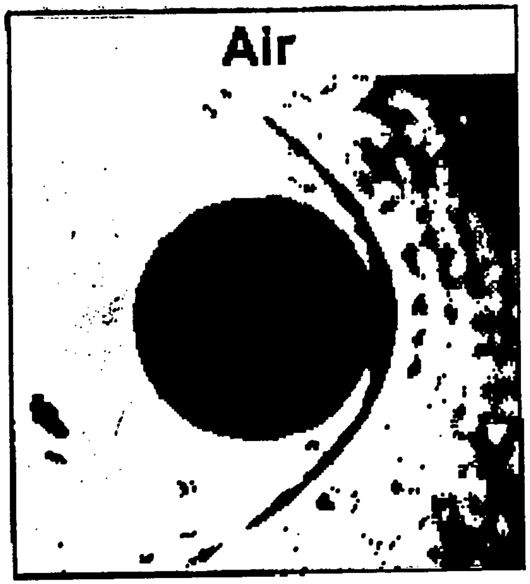

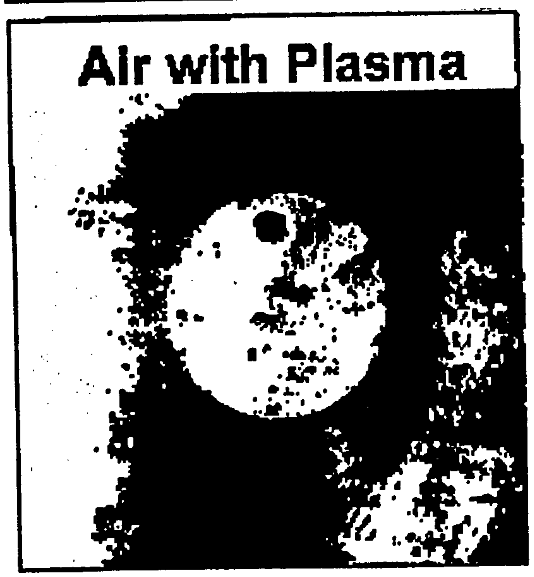

Holography Images

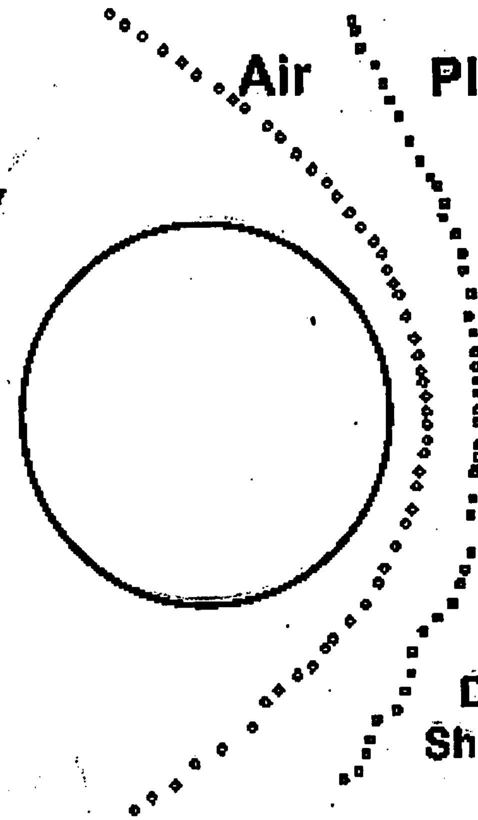

Digitized Shock positions

Weakly Ionized Gas Research

Russian Ballistic Tests (G. Mishin & A. Kilmov, 1978)

- Effect of pre-ionization on the flow around a sphere at Mach 6 in air

(a) Without Pre-ionization

M = 6

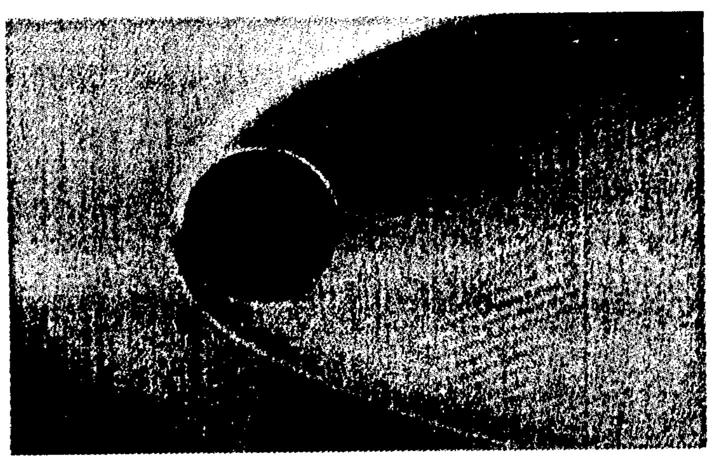

(b) With Pre-ionization

M = 6

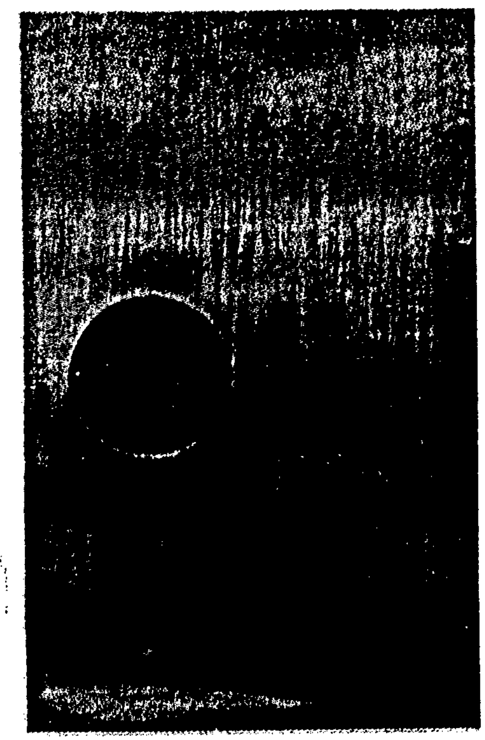

Schematic of Experiment

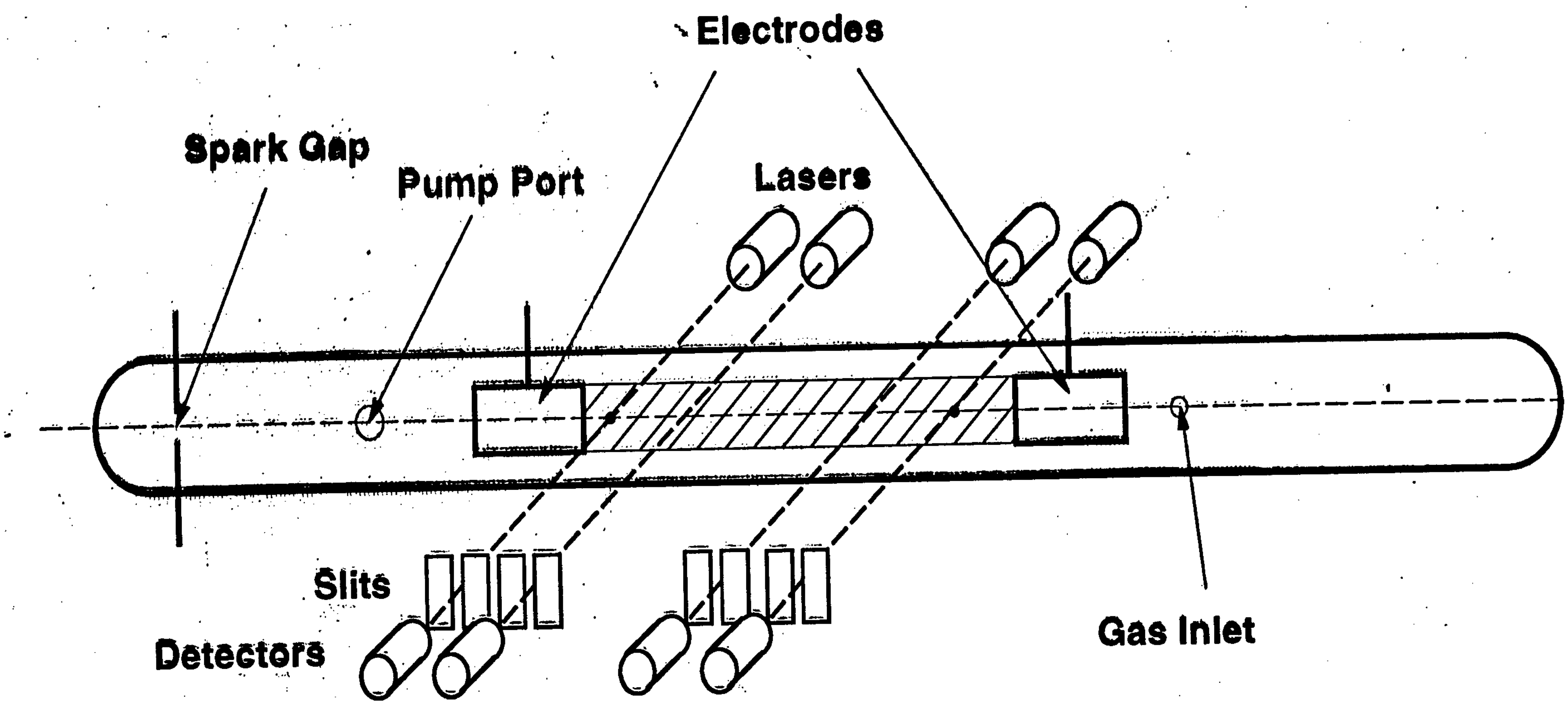

Local Velocity in Discharge as Function of Discharge Current

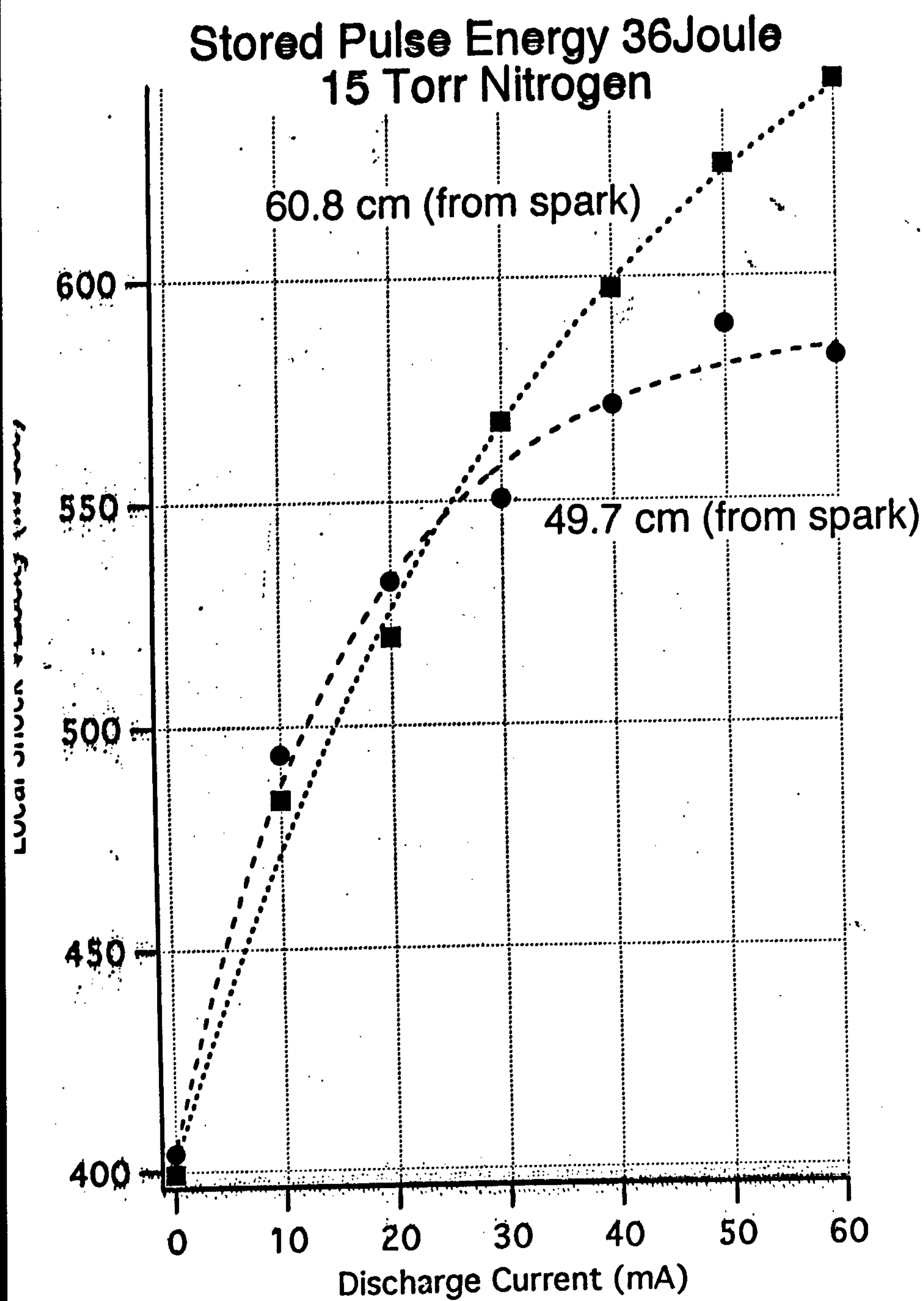

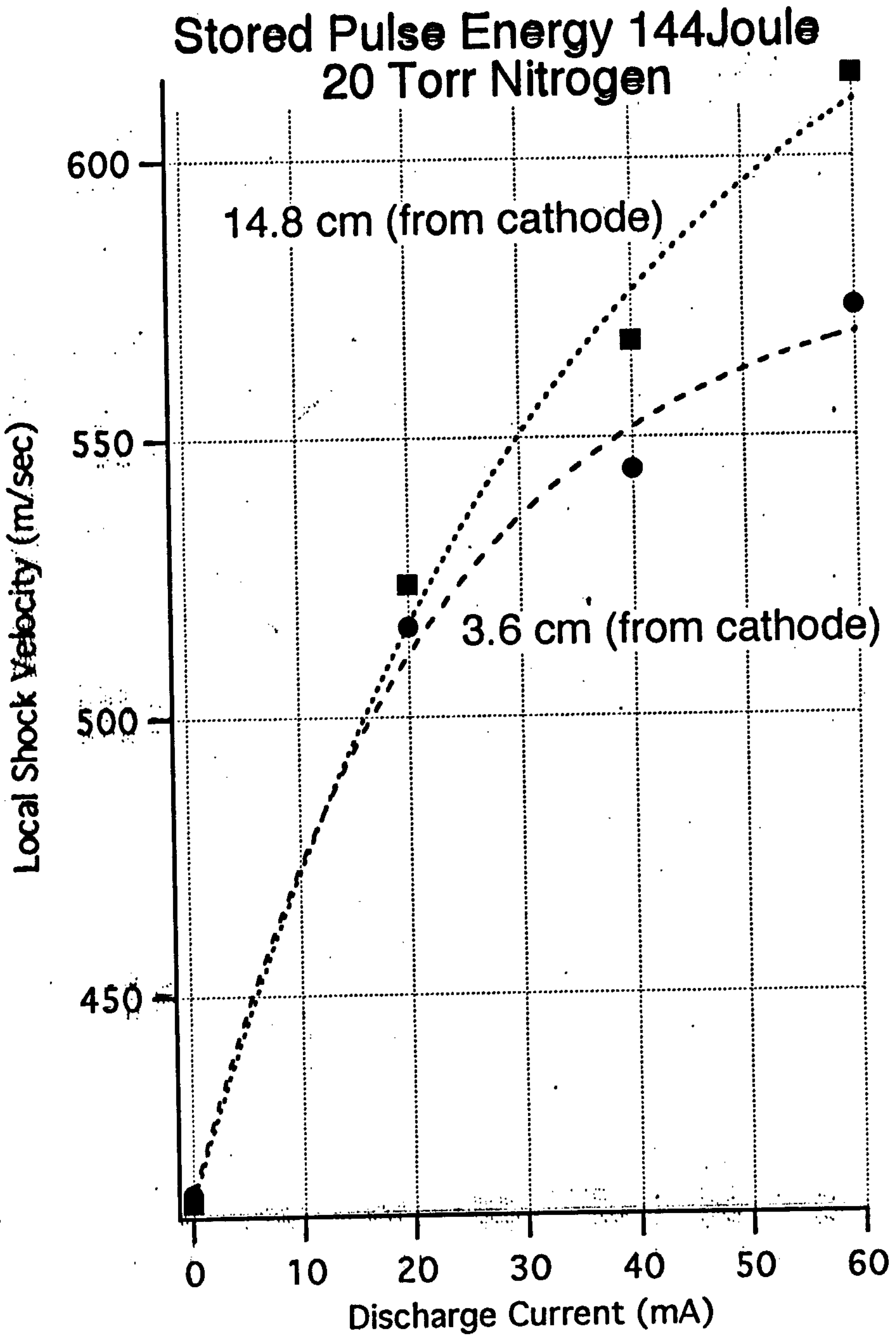

SHOCK WAVE INTERACTIONS WITH WEAKLY IONIZED GASES

- Confirmed shock wave relaxation in nonequilibrium plasmas
- Occurs even at 10^{-7} fractional ionization
- Measurements demonstrated highly non-linear interactions of acoustic shock wave with non-equilibrium weakly ionized plasmas
- Measurements need to be performed to quantify interaction mechanisms and energy balance
- Data will be required to permit energy efficiency analysis of plasma based drag reduction and shock wave amplitude control

OUR PLANNED RESEARCH FOR FY98-99

- Simultaneous multi-point local shock wave velocity measurements.
- Spectroscopic measurement of gas temperatures.
- Shock wave structure recovery in decaying plasma and neutral gas.
- 2-D Schlieren imaging of shock profiles.
- Spectroscopic measurement of shock wave density profile.
- Shock dispersion measurements in pulsed and radio frequency discharges.
- Shock propagation in double layer plasmas.
- Shock induced electric field modulation measurements.

SUMMARY

- Data show the dissipation of supersonic shock waves is nonlinearly dependent on amplitude in weakly ionized nonequilibrium plasmas

- Spatially resolved measurements indicate that shock propagation velocity change and dispersion cannot be explained by gas heating <u>only</u>

- Shock wave dispersion and damping are dependent on the gas number density and fractional ionization

- The energy coupling mechanisms are not understood at present

- Plasma energy density and single particle collision frequency are inadequate to explain the observed phenomena

- Long range cooperative interactions may be important

A Comparison of the Shock Thickness With a 0.8 mm Diameter Wire , 30 Torr Argon , Pulser Voltage 9kV

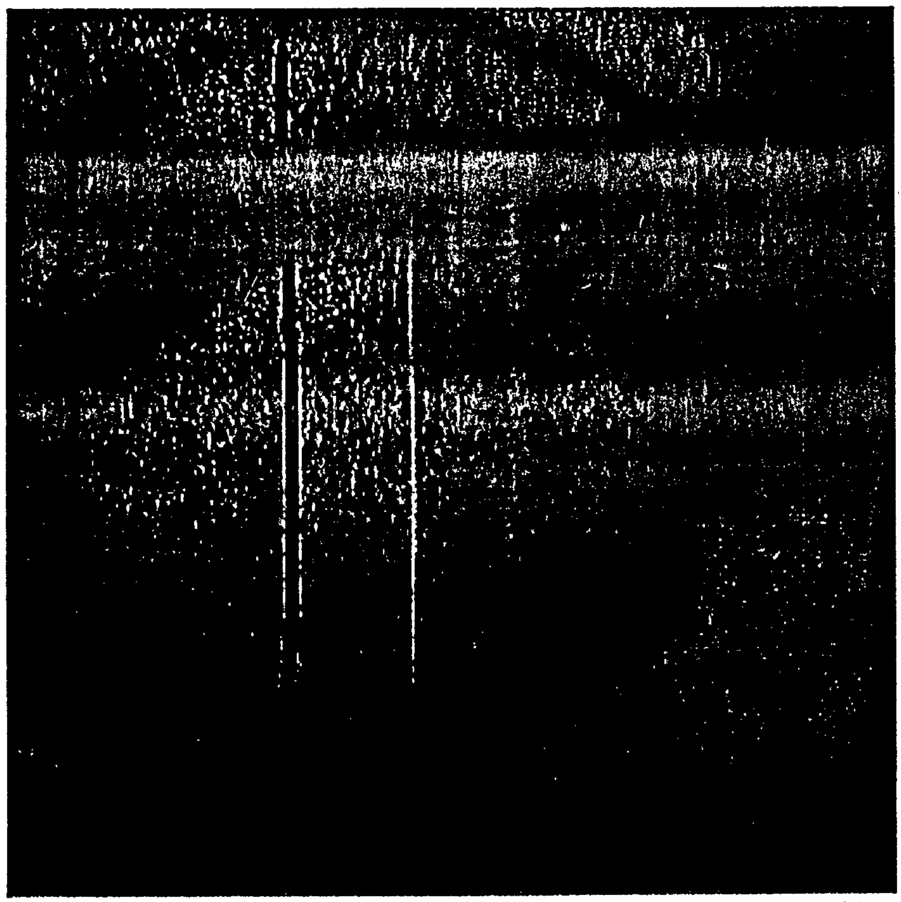

Discharge Tube Dimensions and Location of Laser Beams

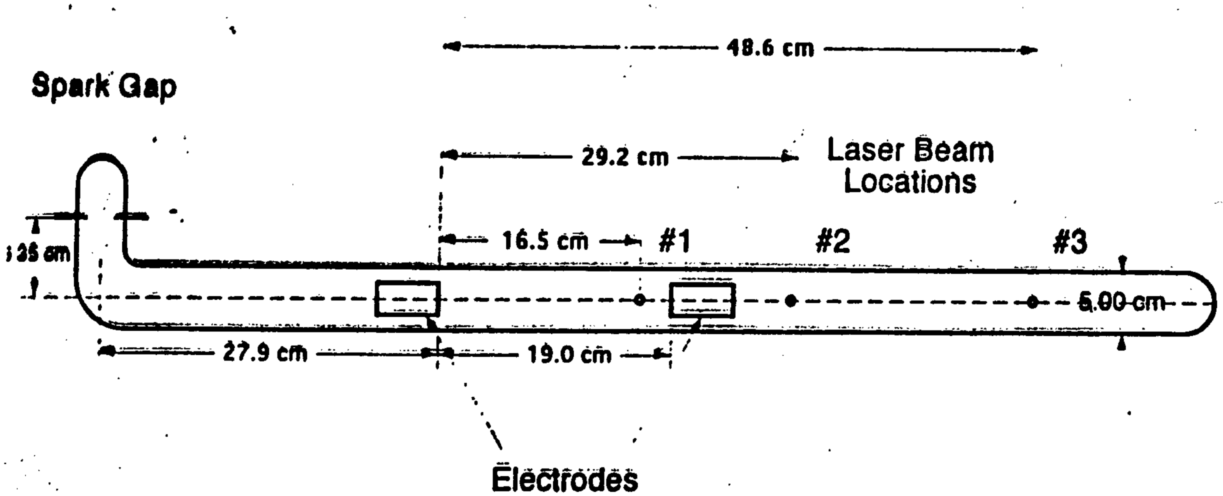

Argon 30 Torr, 10kV 2μF, 42.2cm

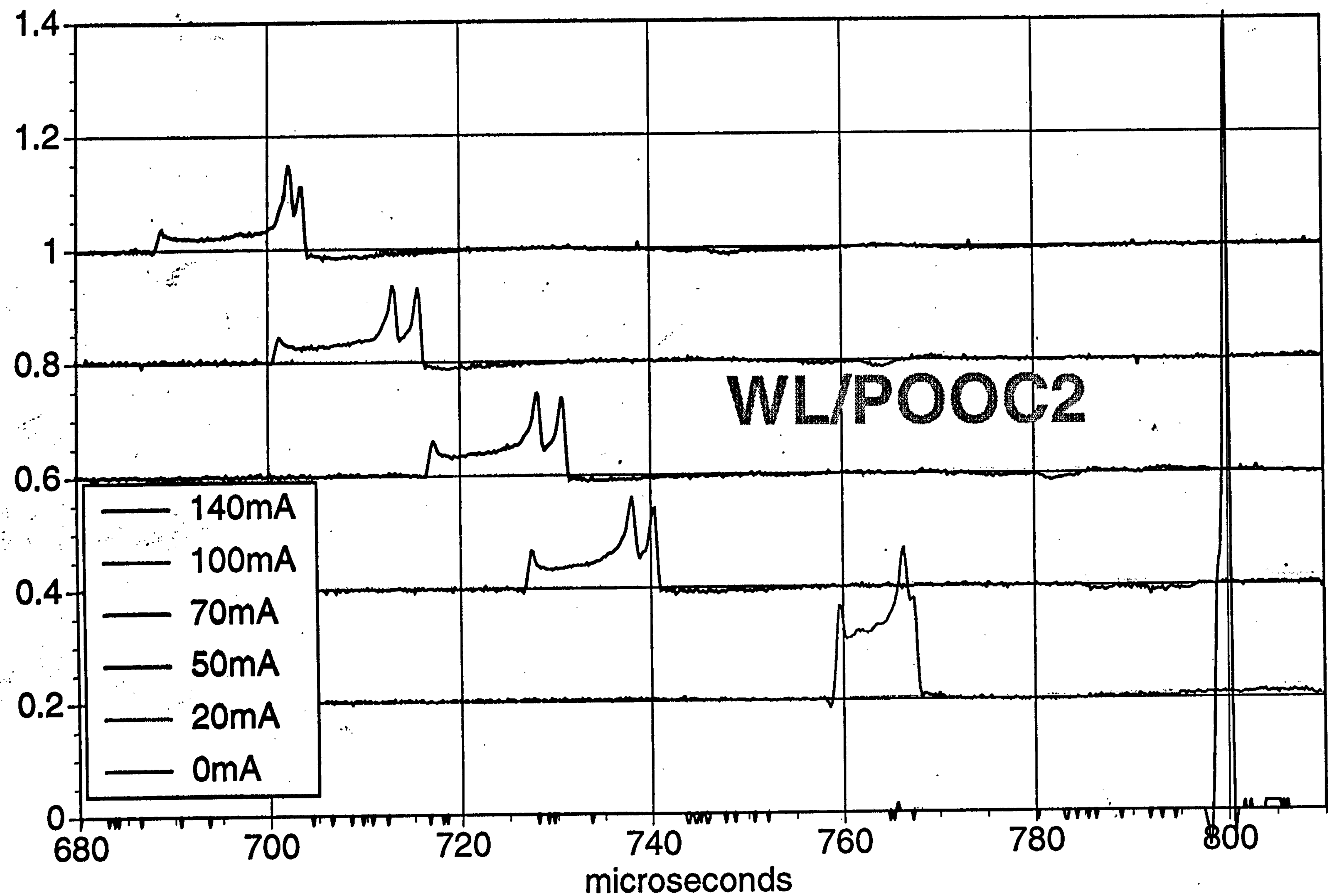

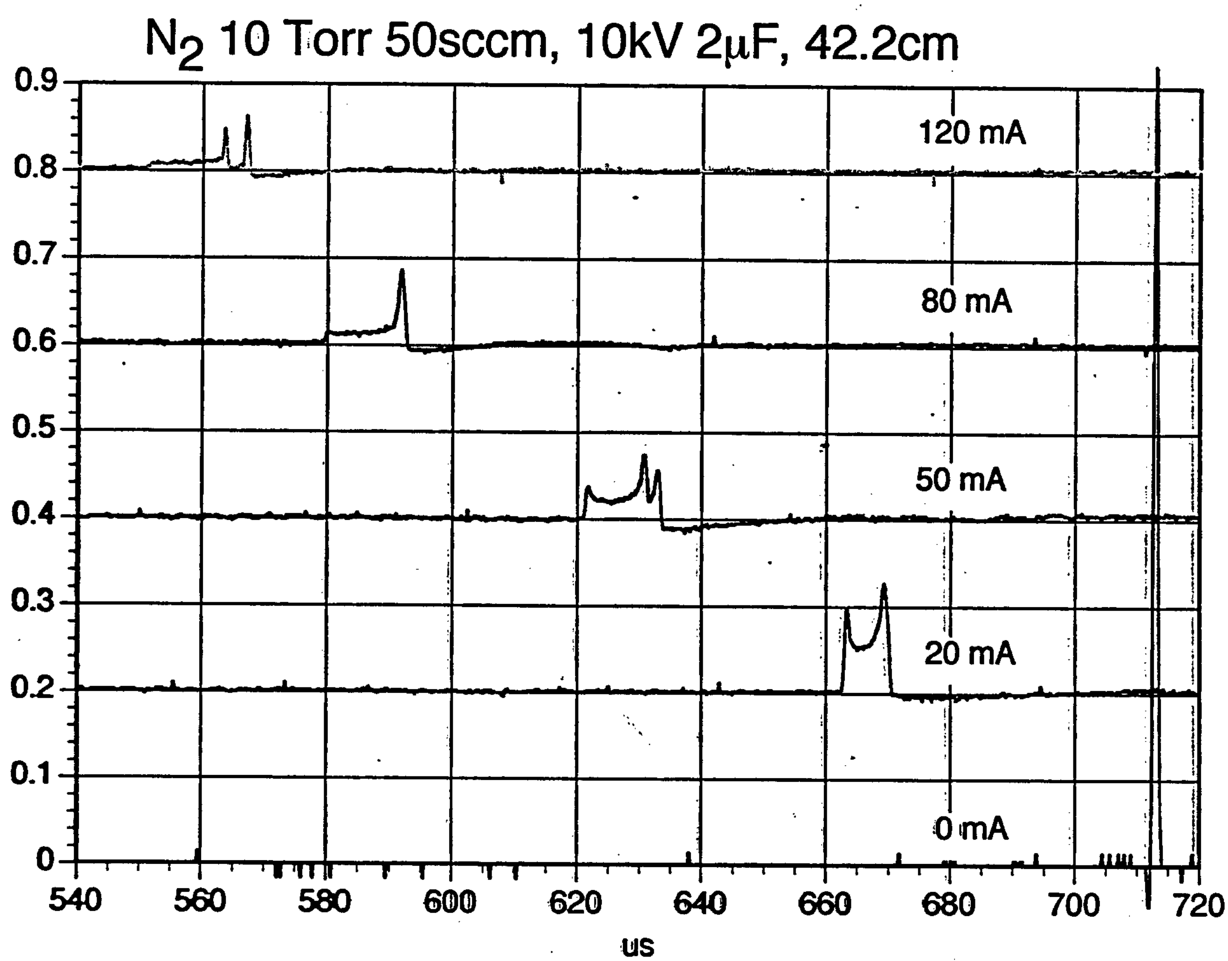

N2 10 Torr 50sccm, 10kV 2μF, 42.2cm
120 mA
80 mA
50 mA
20 mA
0 mA
0.9
0.8
0.7
0.6
0.5
0.4
0.3
0.2
0.1
0
540
560
580
600
620
640
660
680
700
720
us

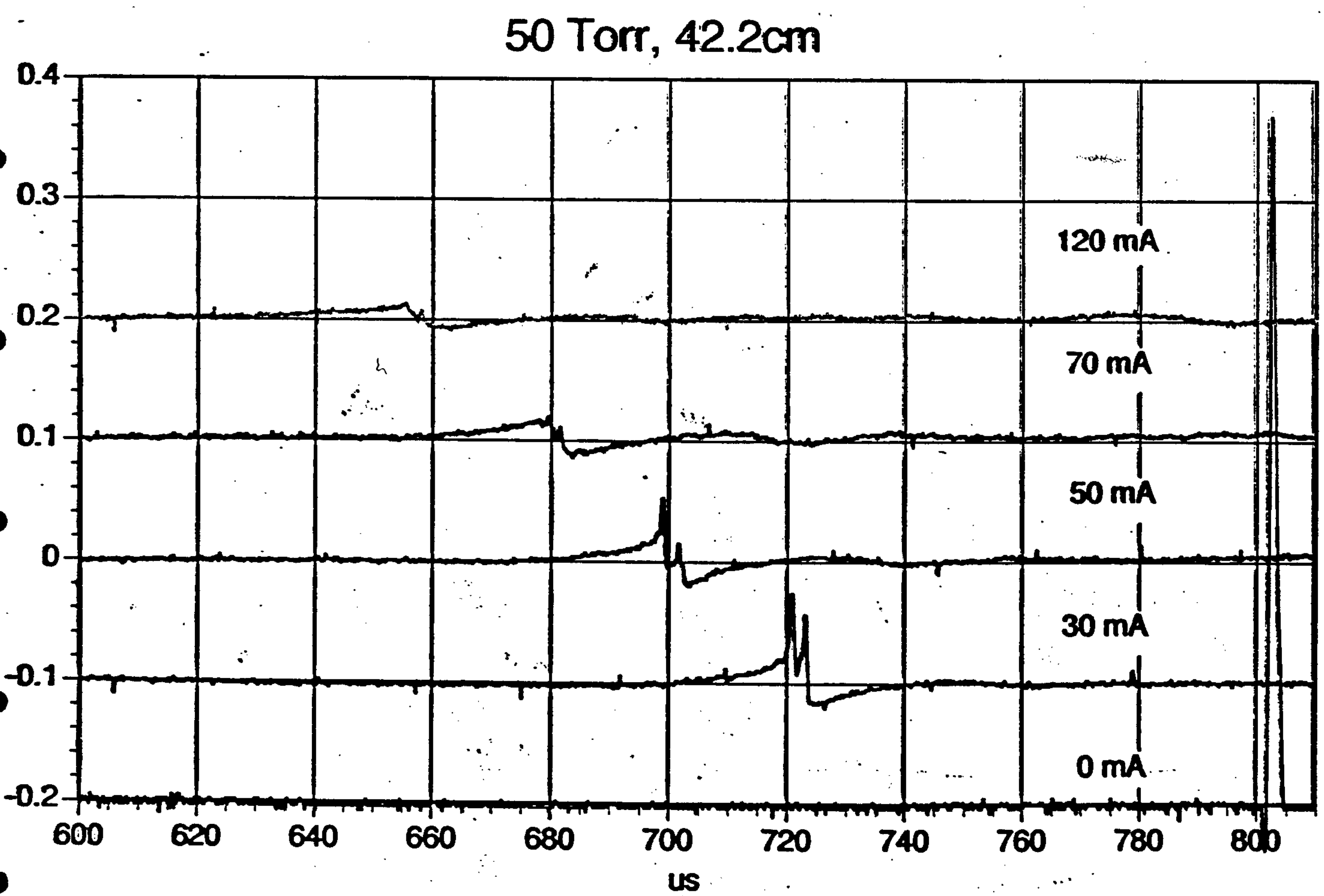

50 Torr, 42.2cm
120 mA
70 mA
50 mA
30 mA
0 mA
0.4
0.3
0.2
0.1
0
-0.1
-0.2
600
620
640
660
680
700
720
740
760
780
800
us

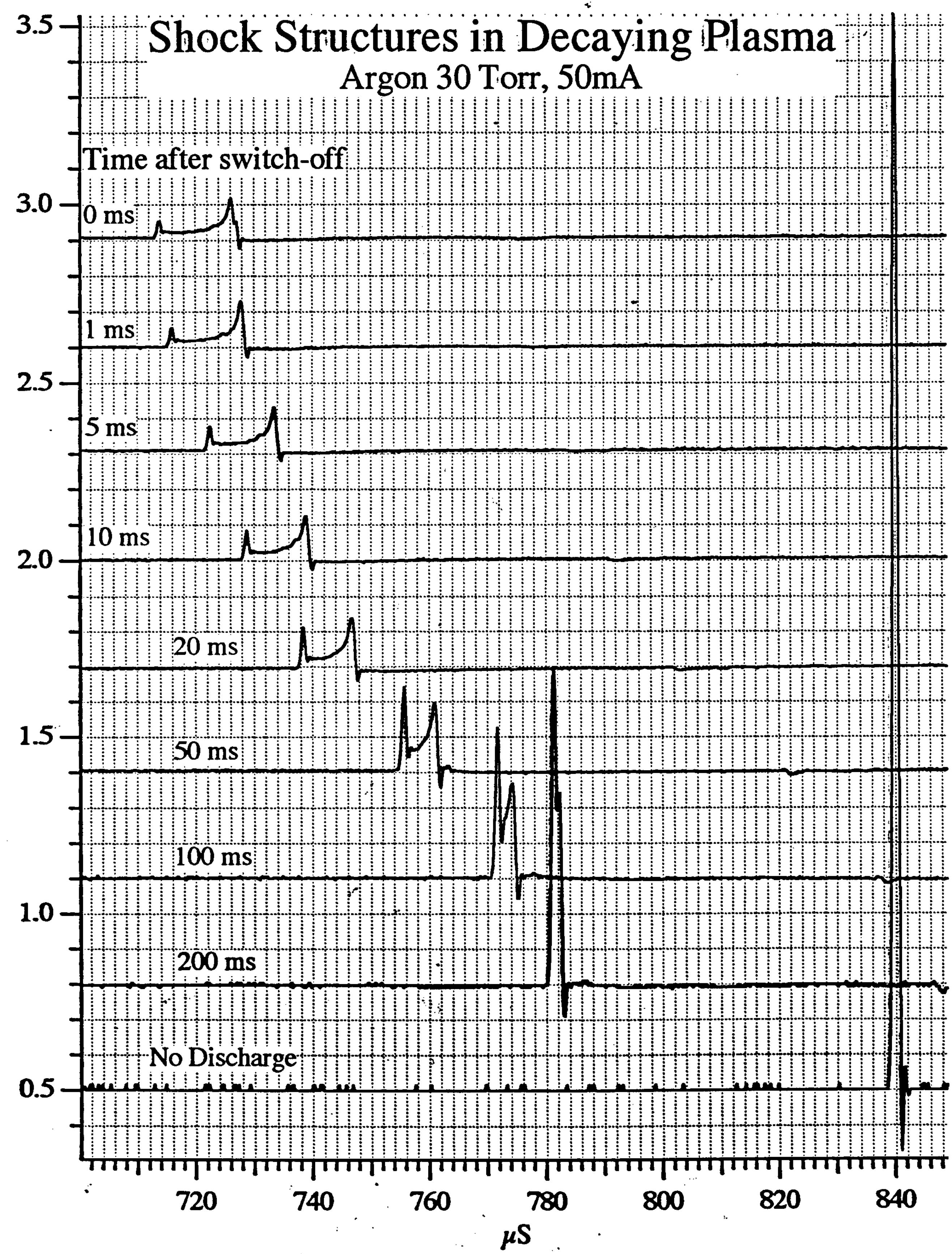

Shock Structures in Decaying Plasma
Argon 30 Torr, 50mA
Time after switch-off
0 ms
1 ms
5 ms
10 ms
20 ms
50 ms
100 ms
200 ms
No Discharge
3.5
3.0
2.5
2.0
1.5
1.0
0.5
V
720
740
760
780
800
820
840
μS

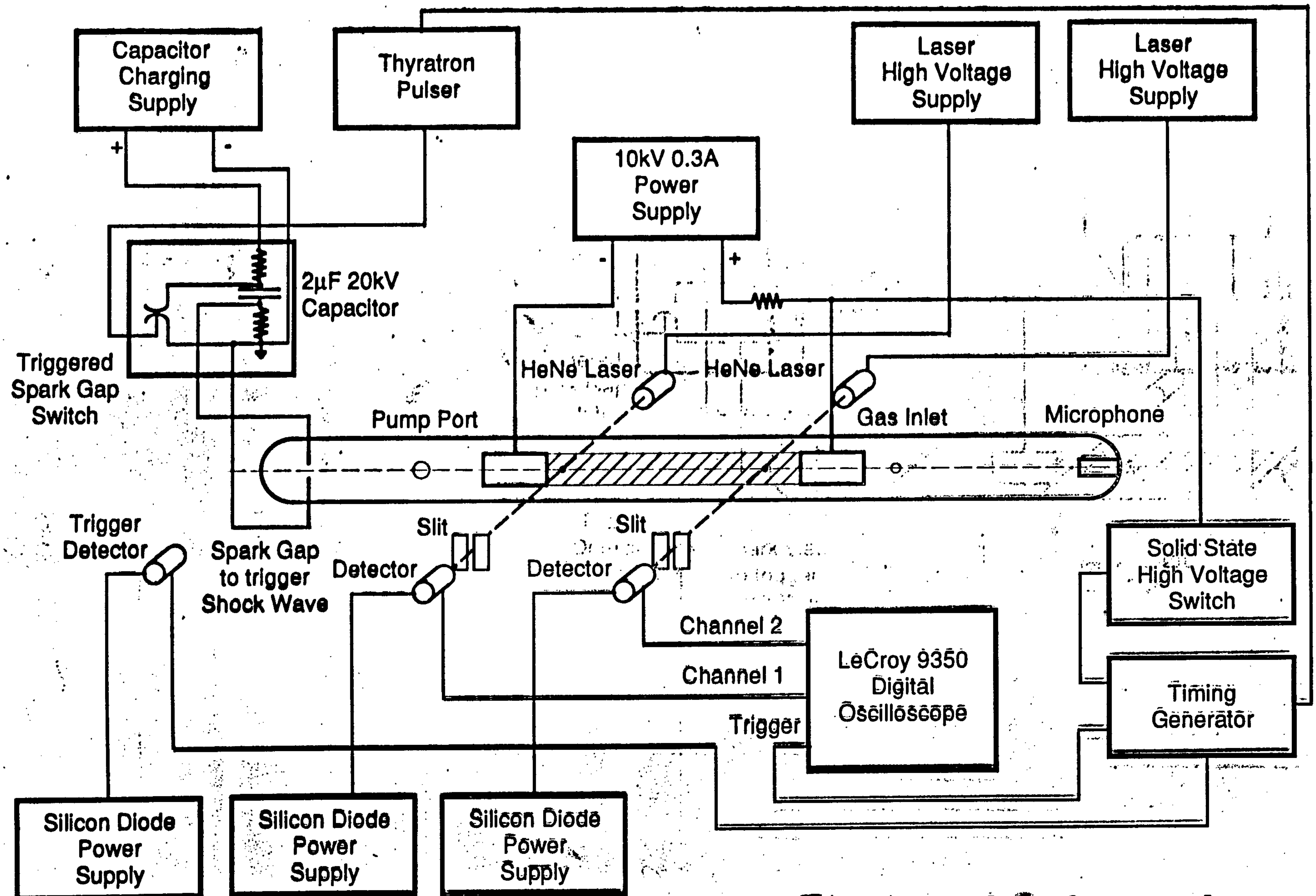

Electrical Schematic for typical measurement

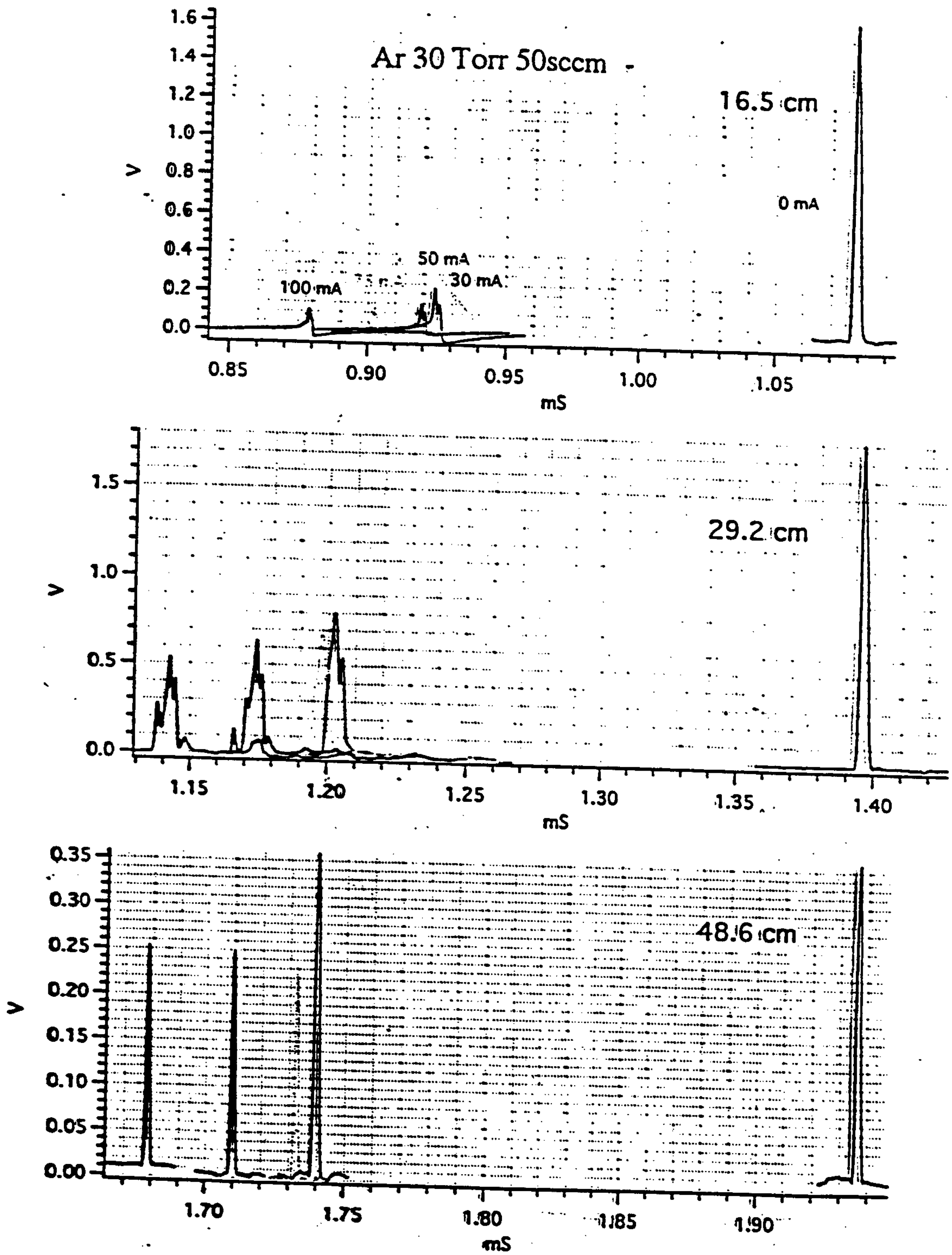
Ar 30 Torr 50sccm
16.5 cm
0 mA
50 mA
100 mA
30 mA
V
mS
29.2 cm
48.6 cm

Average Velocity of Front and Back Boundaries of Shockwave at Center and Off-Axis as Function of Discharge Current

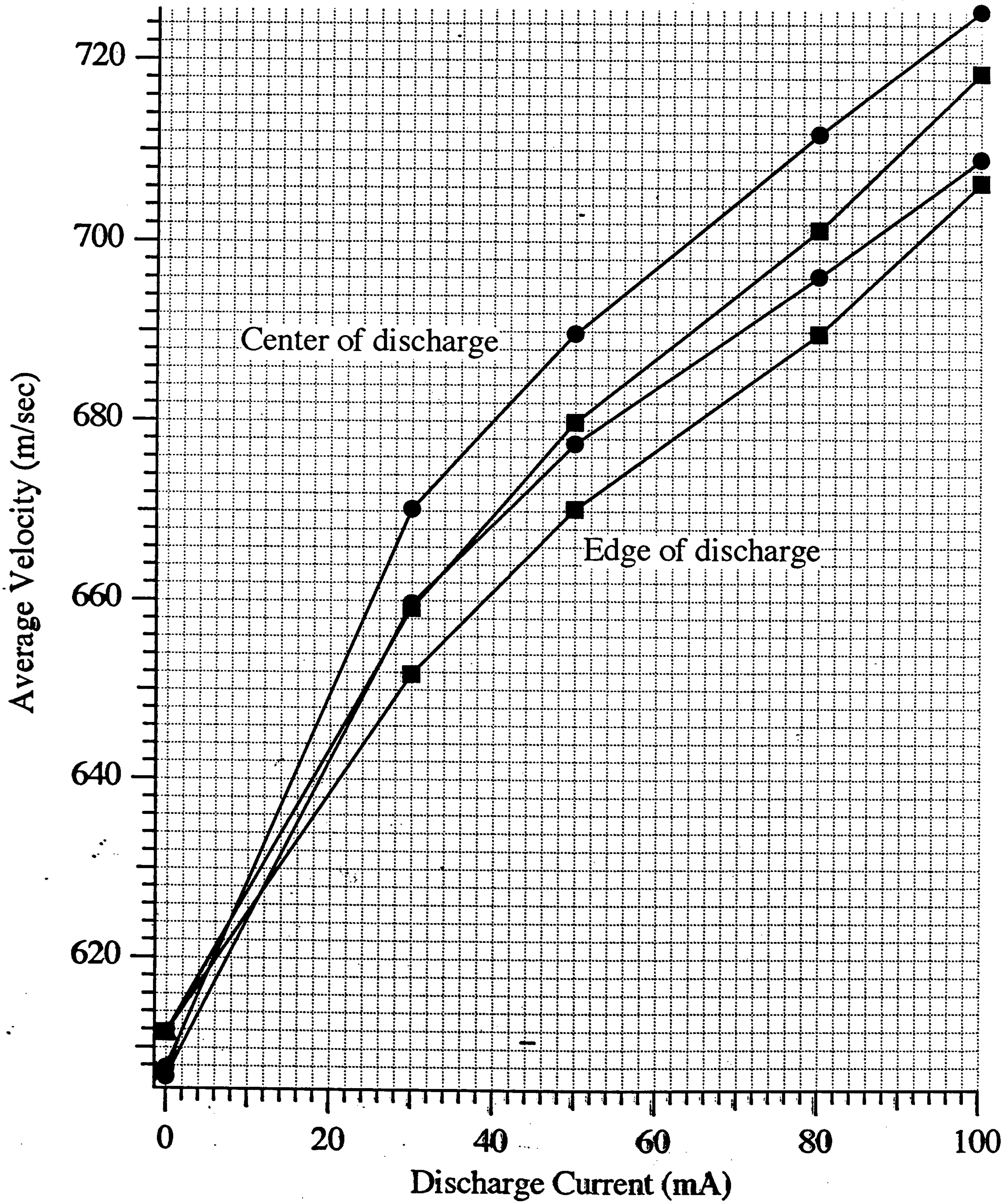

Deflection Signals Downstream of Discharge

Pulse Energy 81 Joule

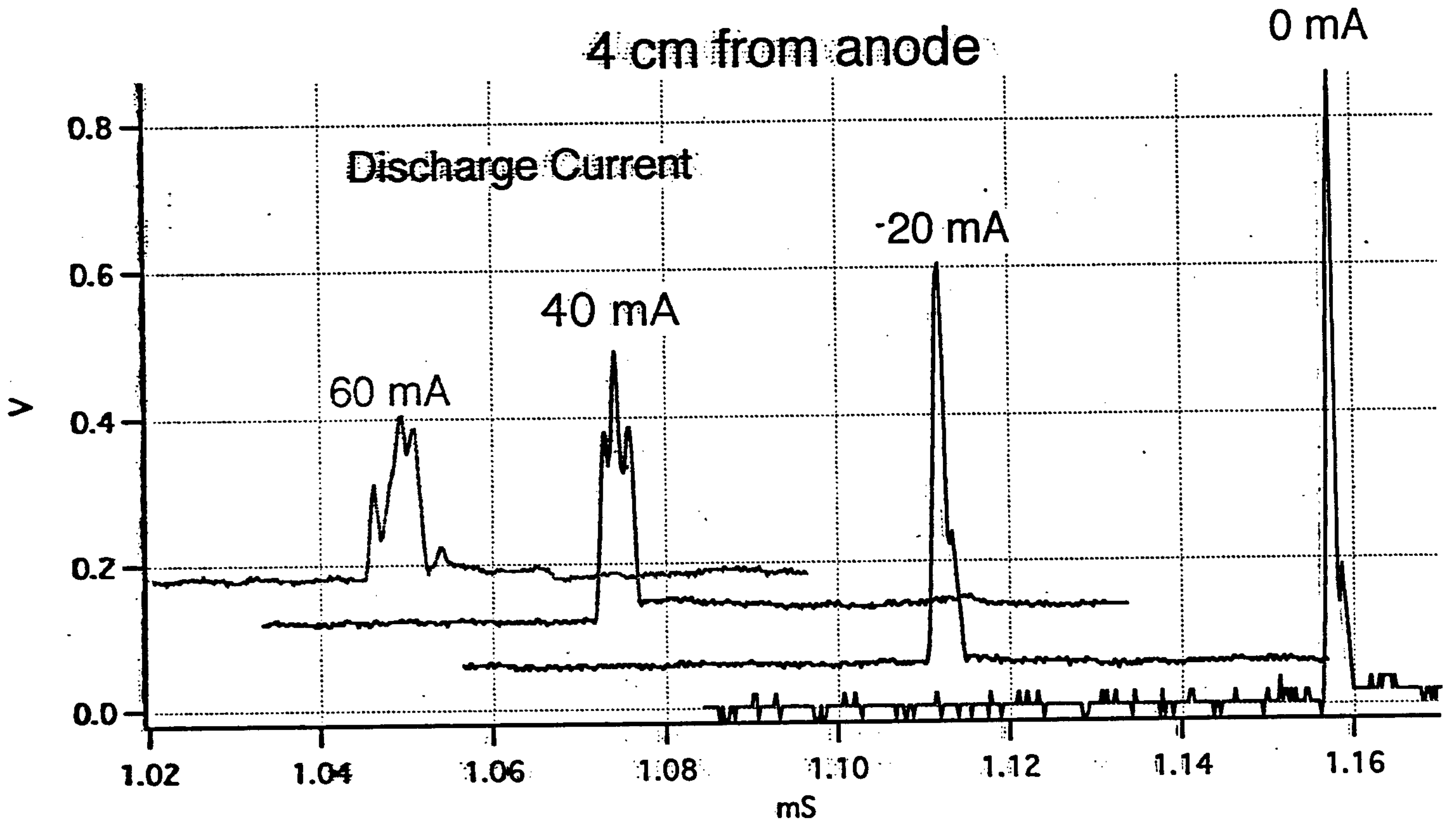

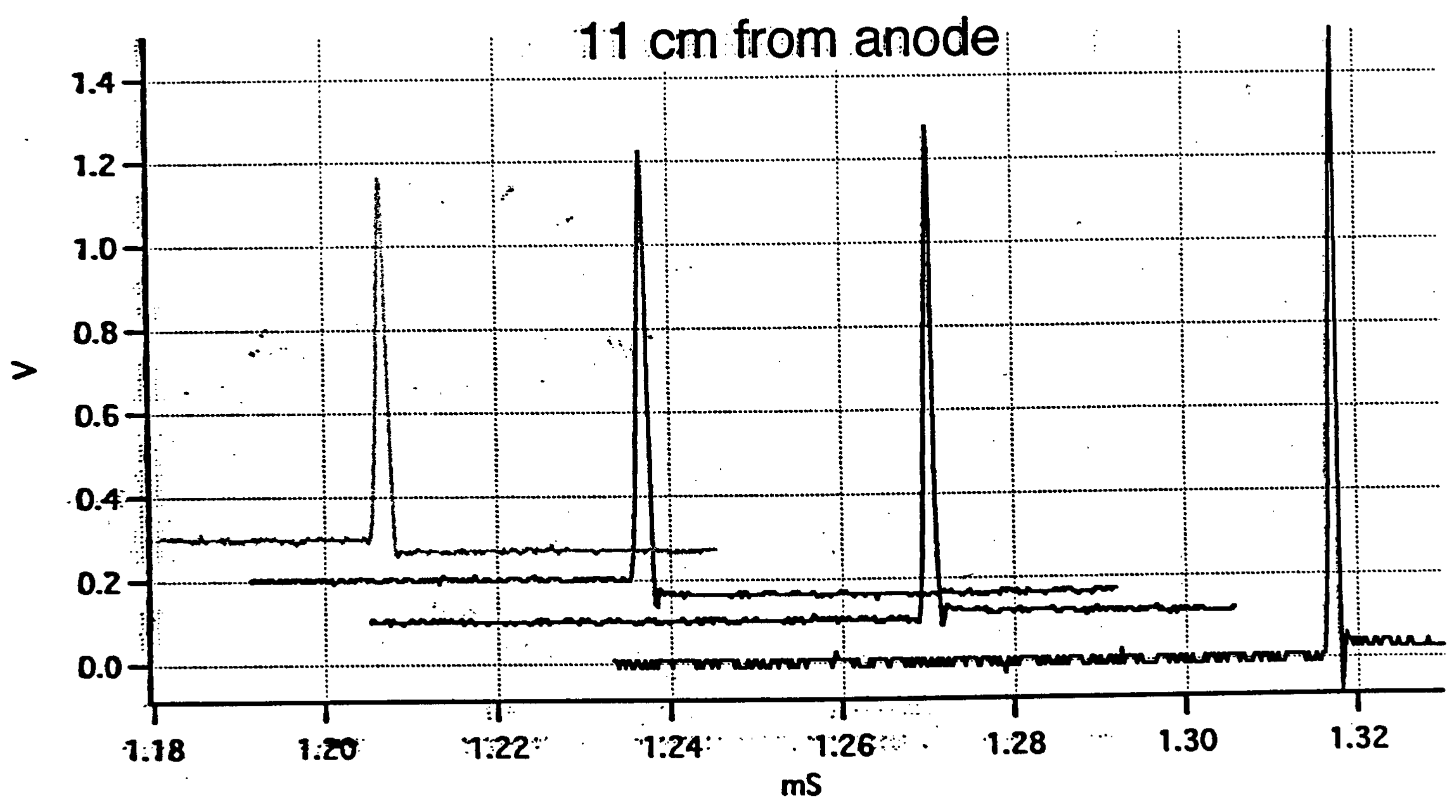

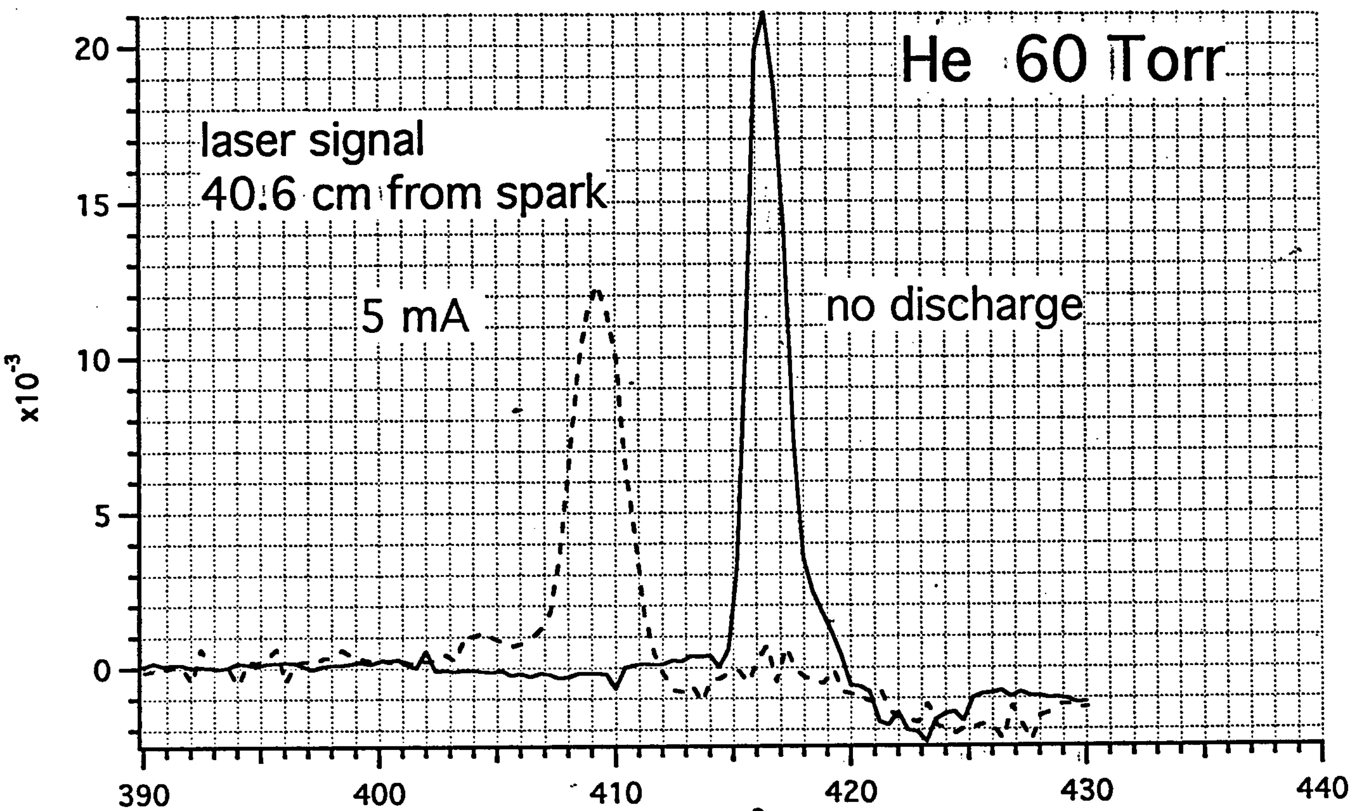
He 60 Torr
laser signal
40.6 cm from spark
5 mA
no discharge
x10^-3
0
5
10
15
20
390
400
410
420
430
440

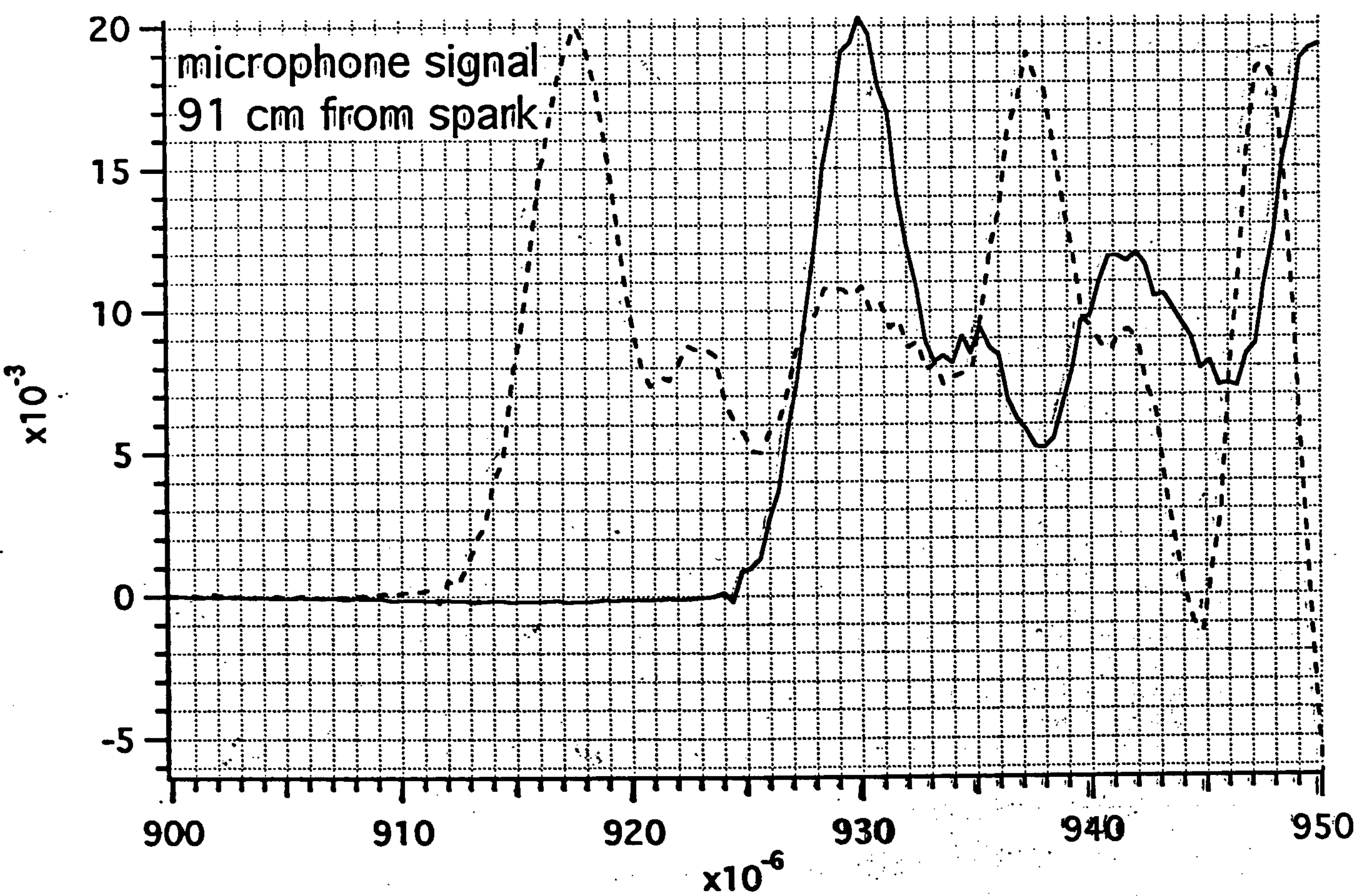
microphone signal
91 cm from spark
x10^-3
-5
0
5
10
15
20
900
910
920
930
940
950
x10^-6

UNDERSTANDING AND CONTROL OF IONIZED
HIGH-SPEED FLOWS

AFOSR WORKSHOP
PRINCETON UNIVERSITY
FEBRUARY 26–27, 1998

Plasma Drag Reduction — An Overview of the Issues

Aaron Auslender
NASA Langley Research Center

OUTLINE

- Problem Statement and Related Issues
- Present Research Focus — NASA/LaRC and ICASE
- Analysis of Air Force Experiments — ODU
- Ballistic Range Mechanisms — ODU
- Onboard-Microwave Experiments — NASA/LaRC
- Shock Tube Experiments — FA&M

Flow around a sphere moving supersonically in a gas-discharge plasma

G. I. Mishin, Yu. L. Serov, and I. P. Yavor

(Submitted April 11, 1991)
Pis'ma Zh. Tekh. Fiz. 17, 65–71 (June 12, 1991)

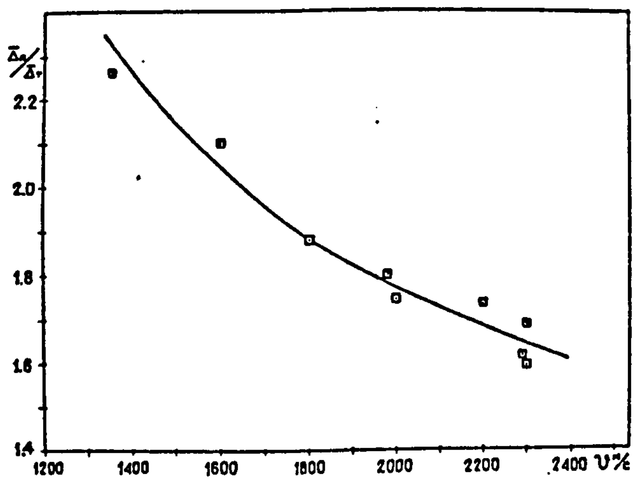

FIG. 2. Ratio of experimentally determined relative standoff distance of the bow shock from a sphere moving through a glow-discharge plasma to the corresponding calculated value of the relative standoff distance in air at the same temperature as the plasma ($\bar{\Delta}_p$ is the relative standoff distance of the bow shock in the plasma, $\bar{\Delta}_T$ is the relative standoff distance in air at $T = 1350$ K, and v is the velocity of the sphere).

414 Sov. Tech. Phys. Lett. 17(6), June 1991

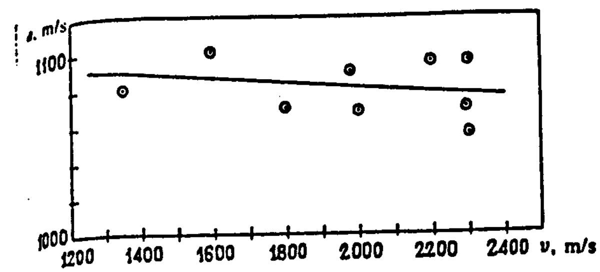

FIG. 3. "Effective" (governing the flow pattern) sound velocity in a plasma in the range of velocities of a spherical model 1350–1300 m/s (a is the effective sound velocity, and v is the velocity of the sphere).

The main series of experiments was carried out in a steadily burning discharge at a gas pressure of 40–50 torr and a discharge current density of 25–50 mA/cm^2. The electron density was $\approx 10^{-11}$–10^{-12} cm^{-3}, the ionization coefficient was $\alpha = 10^{-5}$–10^{-6}, and the electron temperature was $T_e \approx$ 1–4 eV. The gaskinetic temperature T_a of the plasma was determined by several techniques: by measuring the density of the gas from interferograms, by means of Chromel—Alumel thermocouple, by radiation pyrometry, and from the electron vibration—rotation spectra of the molecules.[2] The measurements showed that the temperature distribution along the diameter is bell-shaped, with $T_a \leq 1400$ K on the axis of the discharge.

• no shock case(s)

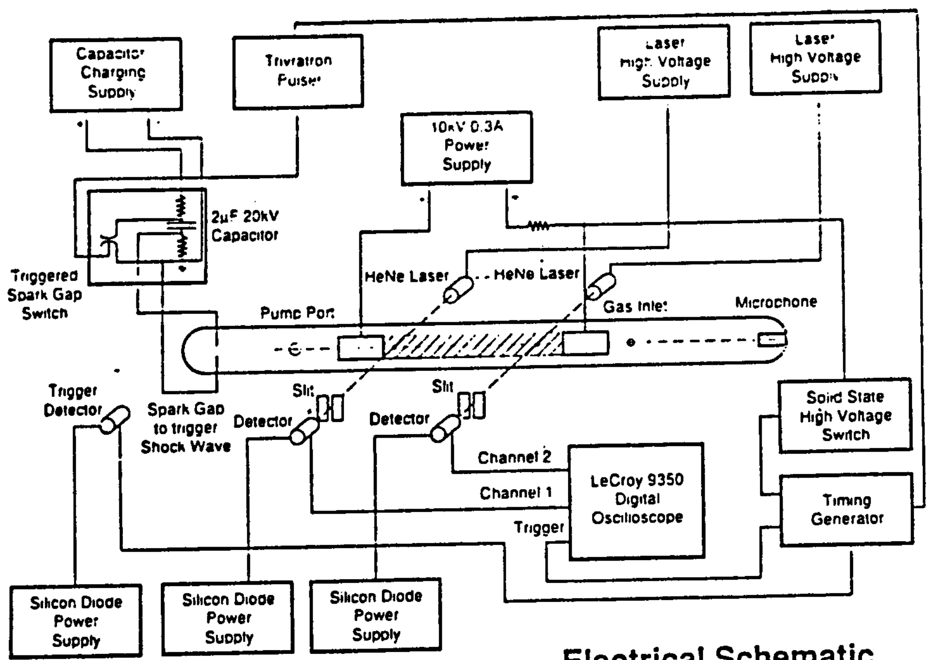

Electrical Schematic
for typical measurement

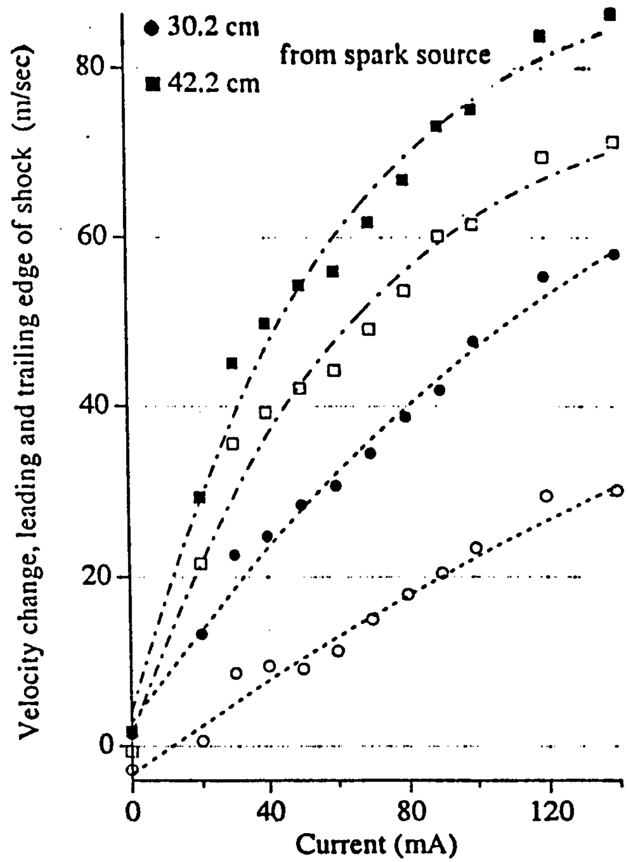

ACOUSTIC SHOCK WAVE PROPAGATION IN NONEQUILIBRIUM NITROGEN AND ARGON PLASMAS

B. N. GANGULY AND P. BLETZINGER
WRIGHT LABORATORY, WRIGHT-PATTERSON AFB

Physics of the Undercritical Microwave Discharge and Its Influence on the Supersonic Aerodynamics and Shock Waves

K. Khodataev (MRTI)

Absorption Ability of the Microwave Streamer Discharge

Each filament element (streamer) being heated by microwave radiation explodes and generates the shock wave. The phase trajectory M(r) of the shock wave gives the energy absorbed by filament length unit E_1

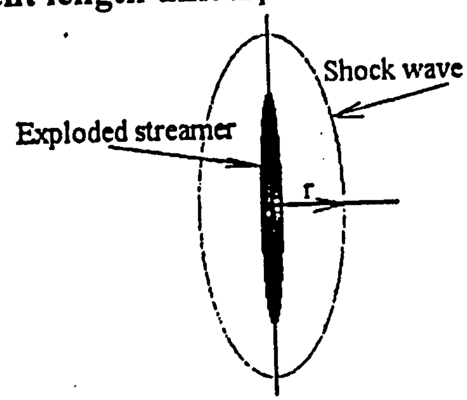

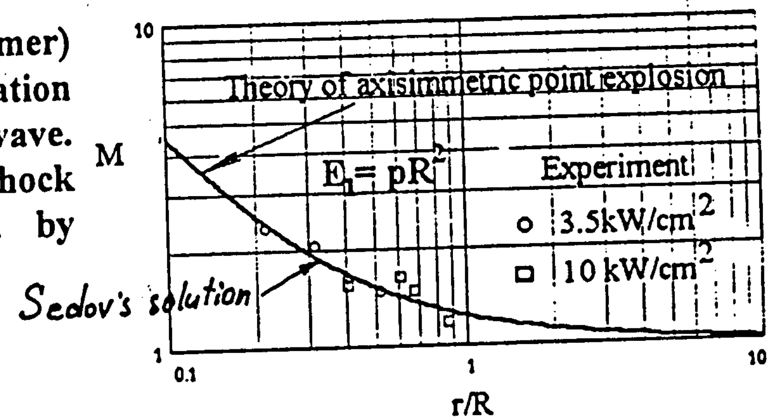

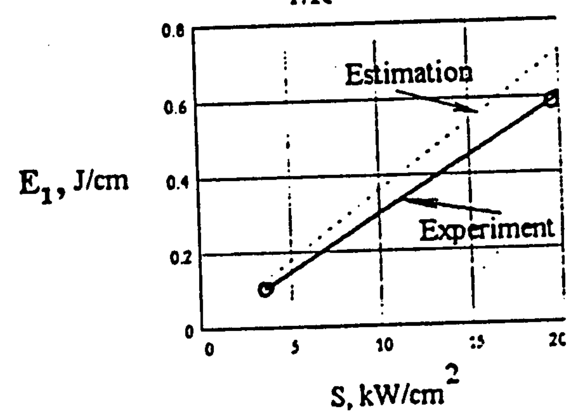

The net of the microwave discharge filaments absorbs whole radiation flux.

The Experimental Data about a Shock Wave Attenuation in a Microwave Discharge

The scheme of the experiment

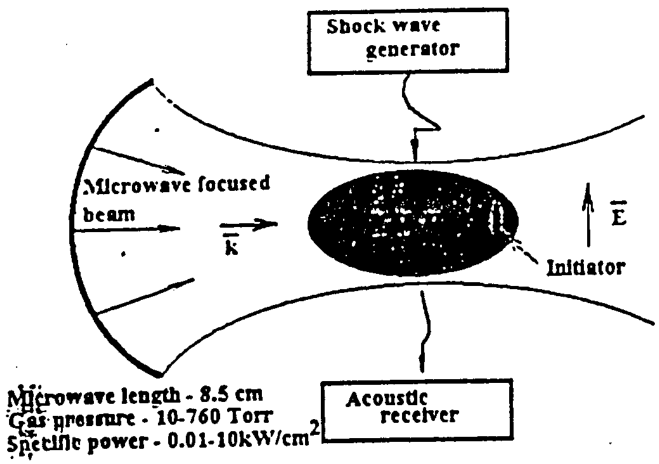

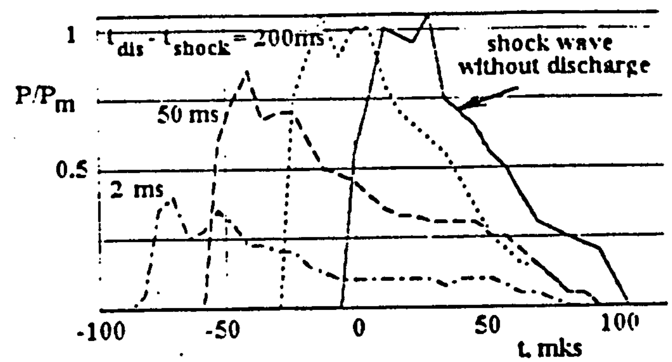

p = 30 Torr

The typical oscillograms

The measurements show that discharge region:

- *attenuates the pulse shock waves,*
- *increases the pulse shock wave time duration,*
- *the memory time of discharge region equals more than 0.1 s.*

The Acoustic Interferometry Study of the *Microwave Discharge Region*

The sound velocity dependence on wave number $C_s(k)$ in the decaying microwave discharge plasma.

The delay time after discharge: 20 ms -solid, 50 ms -dot, 200 ms-dash line.

The dependence show that:

the discharge region

- *is heated in average,*
- *has microscale hot inhomogeneties,*
- *has a memory time up to 0.2s.*

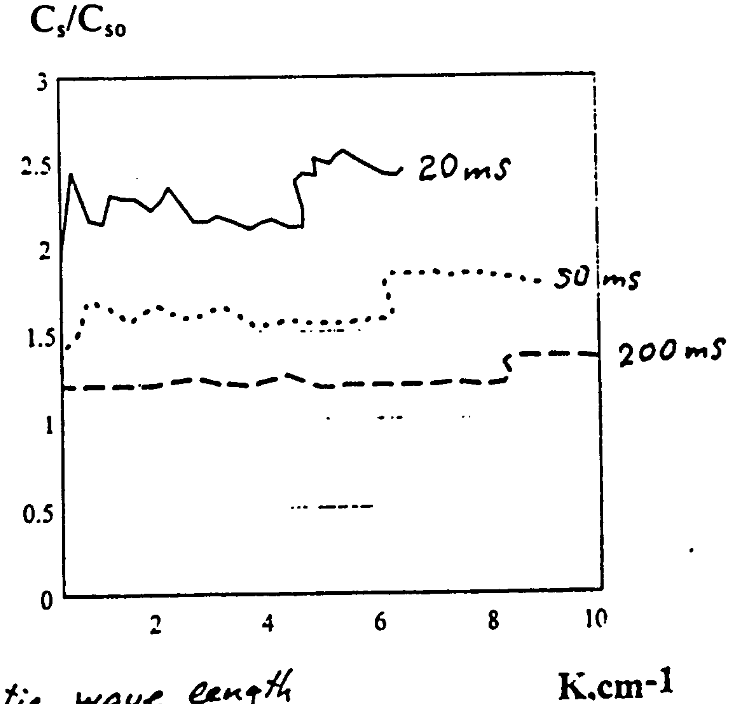

$K = \frac{2\pi}{\lambda}$ - acoustic wave length

$$\begin{aligned} \frac{\partial \mathbf{v}_n}{\partial t} &= -c_n^2 \nabla \rho_v / \rho_{0v} - \omega_{ni}(\mathbf{v}_n - \mathbf{v}_i) \\ \frac{\partial \rho_v}{\partial t} &= -\rho_{0v} \nabla \cdot \mathbf{v}_n \\ \frac{\partial \mathbf{v}_i}{\partial t} &= -c_i^2 \nabla \rho_u / \rho_{0u} - \omega_{in}(\mathbf{v}_i - \mathbf{v}_n) \\ \frac{\partial \rho_u}{\partial t} &= -\rho_{0u} \nabla \cdot \mathbf{v}_i \end{aligned} \tag{1}$$

$$\begin{aligned} \mathbf{v}_n &= \nabla \phi_n \\ \mathbf{v}_i &= \nabla \phi_i \end{aligned} \tag{2}$$

$$\begin{aligned} \frac{\partial^2 \phi_n}{\partial t^2} - c_n^2 \nabla^2 \phi_n + \omega_{ni}\left(\frac{\partial \phi_n}{\partial t} - \frac{\partial \phi_i}{\partial t}\right) = 0 \\ \frac{\partial^2 \phi_i}{\partial t^2} - c_i^2 \nabla^2 \phi_i + \omega_{in}\left(\frac{\partial \phi_i}{\partial t} - \frac{\partial \phi_n}{\partial t}\right) = 0 \end{aligned} \tag{3}$$

$$\begin{vmatrix} -\omega^2 + c_n^2 k^2 - i\omega\omega_{ni} & i\omega\omega_{ni} \\ i\omega\omega_{in} & -\omega^2 + c_i^2 k^2 - i\omega\omega_{in} \end{vmatrix} = 0 \tag{4}$$

- **Analysis assumed:**

(1) Uncoupled Speed-of-Sound Ratio "Fast-Wave" to the "Slow-Wave" equals ten

(2) Ionization Fraction is constant

- **Conclusion:**

(1)"Slow-Wave" only propagates in the long-wave-length limit

(2) Large Ionization Fractions are required ("Slow-Wave")

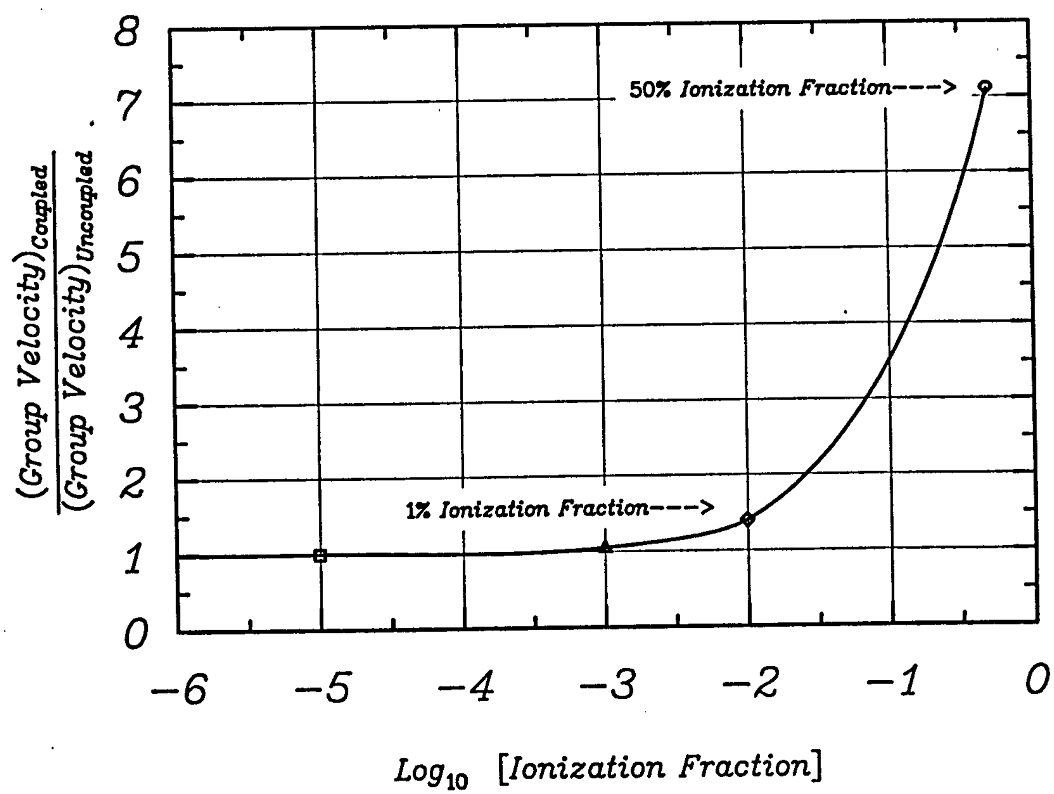

PRESENT RESEARCH EFFORTS

- Kinetics
  - Excited State —> reactions —> "hot" electron production
  - Metastable States —> "long-lived" neutrals

- Far-From Equilibrium Effects —> neutral particle stationary solutions of the Boltzmann kinetic equation having sources/sinks (fluxes)
  —> influences speed-of-sound
  —> yields mass/momentum/energy fluxes in the shock region (OSU)

- Far-From Equilibrium Effects (OSU, NASA/LaRC and ICASE)
  - DSMC Modelling (NASA/LaRC and ICASE) employing a central forcing function of the class: $Force = \alpha_0 \; e^{-(X - X_{SHOCK})^2/\alpha_1}$ to assess the magnitude of the required mechanism(s)
  - Development of related mechanism(s) and analysis of the relevant "fluid" equation set (OSU)

Shock-Wave Structure in a Rigid Sphere Gas[1]

G. A. BIRD[2]
Department of Mechanics of Fluids, University of Manchester, Manchester, England

Translational Equilibrium in a Rigid Sphere Gas

G. A. Bird
Department of Aeronautical Engineering, University of Sydney, Sydney, Australia
(Received 10 May 1963)

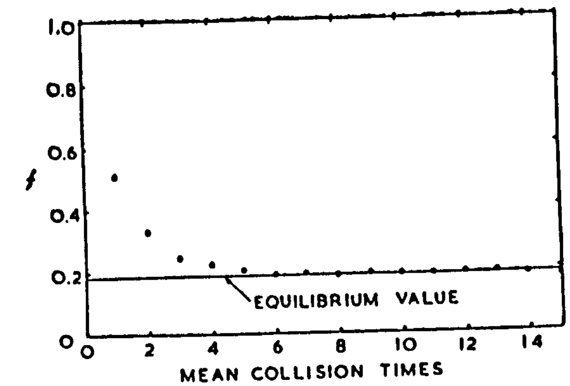

FIG. 2. Fraction of molecules in range 0.9 to 1.1 v_s.

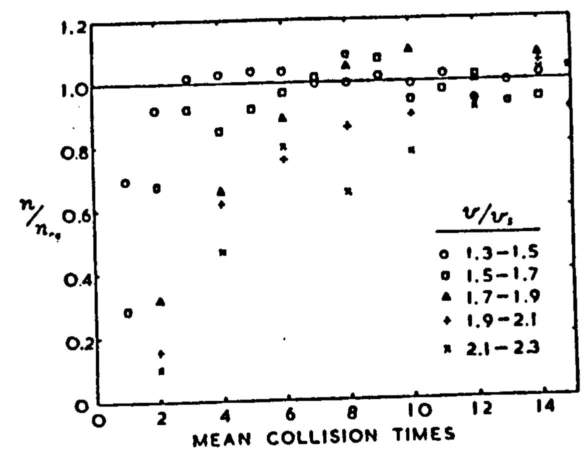

FIG. 3. Approach to equilibrium in higher speed ranges.

Exact power-law solutions of the particle kinetic equations

A. V. Kats, V. M. Kontorovich, S. S. Moiseev, and V. E. Novikov

Khar'kov Research Institute for Metrology, Institute for Radiophysics and Electronics, Ukrainian Academy of Sciences, and Physico-technical Institute, Ukrainian Academy of Sciences
(Submitted November 21, 1975)
Zh. Eksp. Teor. Fiz. 71, 177–192 (July 1976)

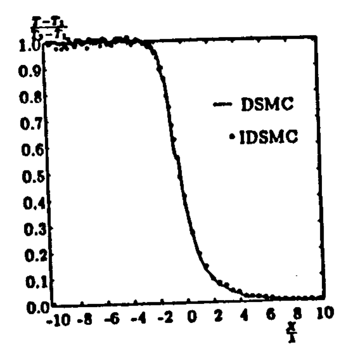

6.11 shock-wave

ODU Research Activity

- Analysis of planar-wave experiments
  - shock front propagation
- Analysis of ballistic range experiments
  - standoff distance
- Determination of underlying physical mechanisms
  - distribution of internal energy
  - collisional dynamics during relaxation
  - influence of double electric layer on charged and excited particles
  - nonequilibrium effects
- Shock dispersion experiments and plasma generation
  (future work)

“Anomalous” Effects in Atomic & Molecular Gases at $T_e >> T_n$

- Not observed at $T_e = T_n$.
- Not dependent on direction of applied electric field.
- Reduced/nonexistant at transverse magnetic field of below/above ~500 G.
- Increase with ultraviolet irradiation.
- Rise-time from plasma inception ~100 μs.
- Afterglow decay time depends on gas species.
  Can be >100 ms.

Generic Experiments

- A. Shock wave propagation through a DC glow discharge
  1. parallel-plate
     transverse propagation
  2. cylindrical
     coaxial propagation
- B. Supersonic flow in weakly ionized gas around a spherical model (ballistic range experiments)

A.1.

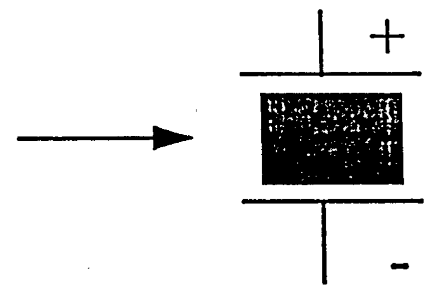

A. 2.

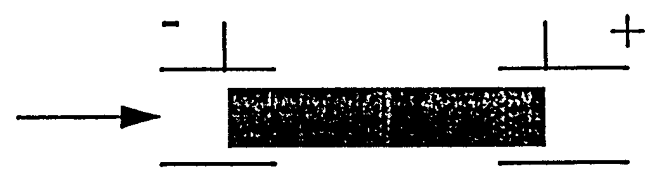

B.

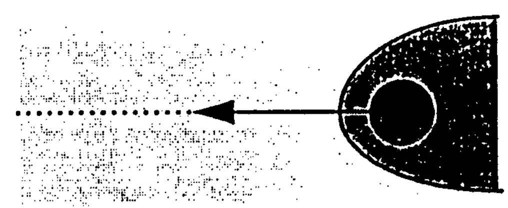

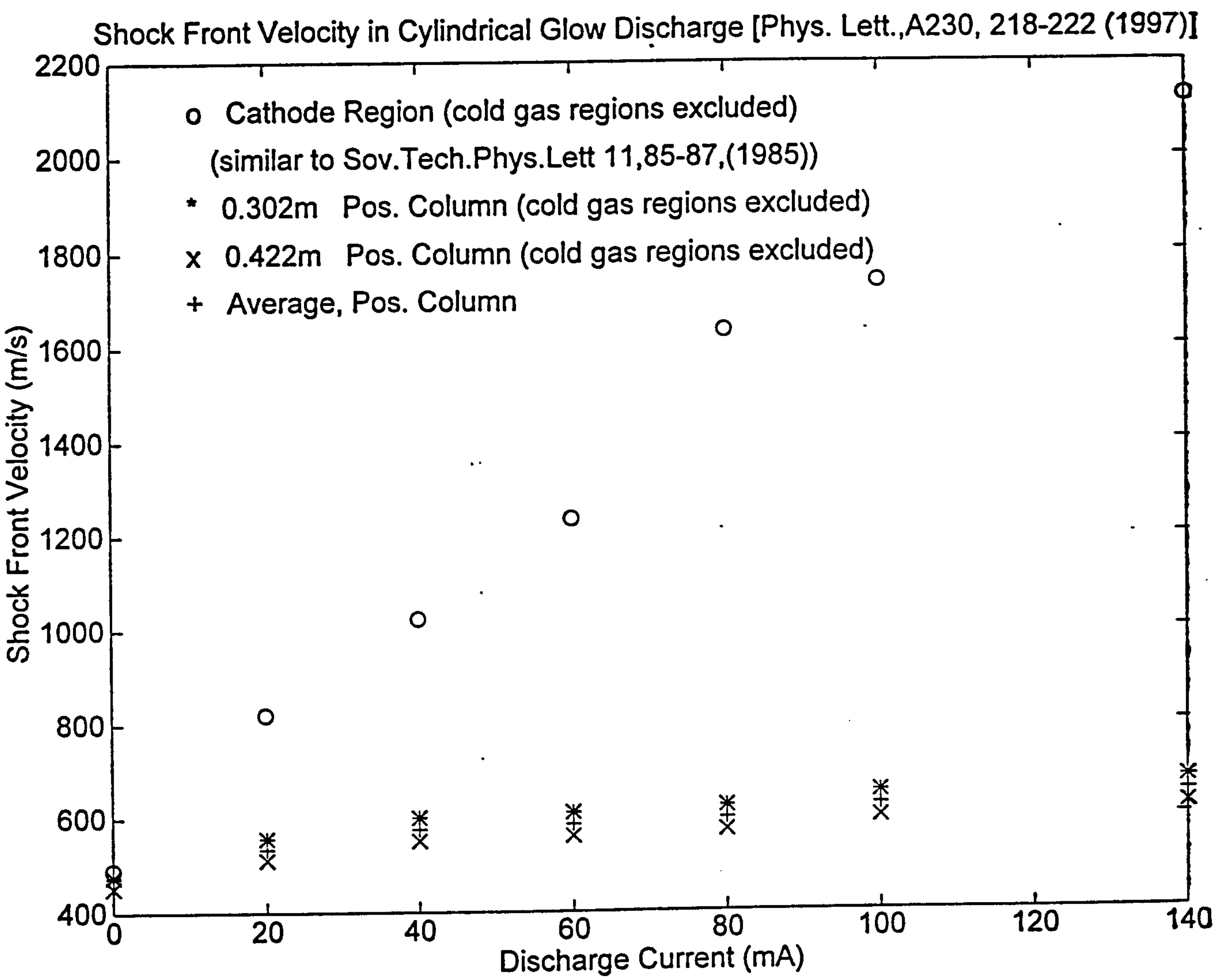

Shock Front Velocity in Cylindrical Glow Discharge [Phys. Lett.,A230, 218-222 (1997)]
o Cathode Region (cold gas regions excluded)
(similar to Sov.Tech.Phys.Lett 11,85-87,(1985))
* 0.302m Pos. Column (cold gas regions excluded)
x 0.422m Pos. Column (cold gas regions excluded)
+ Average, Pos. Column
Shock Front Velocity (m/s)
2200
2000
1800
1600
1400
1200
1000
800
600
400
0
20
40
60
80
100
120
140
Discharge Current (mA)

Metastable States

• Oxygen	$a^1\Delta_g$	(0.97 - 5) eV
• Nitrogen	$A^3\Sigma_u^+$	(6.17 - 8.83) eV
• Argon	$1s_{3,5}$	11.55 eV & 11.72 eV
	2p	(12.91 - 13.48) eV

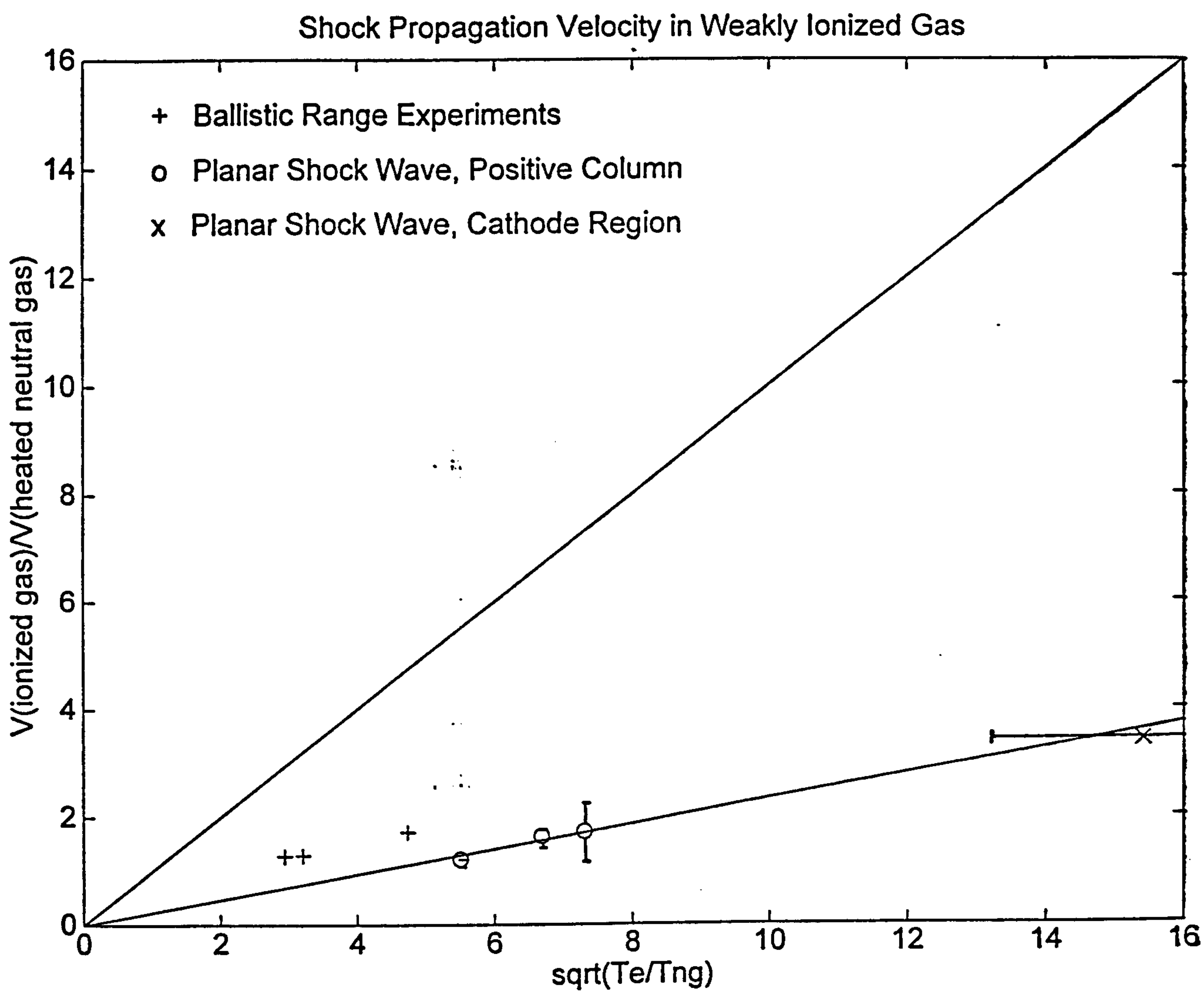

Shock Propagation Velocity in Weakly Ionized Gas
+ Ballistic Range Experiments
o Planar Shock Wave, Positive Column
x Planar Shock Wave, Cathode Region
V(ionized gas)/V(heated neutral gas)
sqrt(Te/Tng)
0
2
4
6
8
10
12
14
16

Relevant Collision Processes

- Electron impact ionization

  Dominant ionization mechanism at high pressures.

  $Ar^* + e^- \Rightarrow Ar^+ + e^-_{(0\ \mathrm{to}\ 4\ \mathrm{eV})}$

- Energy pooling reactions

  Dominant ionization mechanism at medium pressures.

  $Ar^* + Ar^* \Rightarrow Ar + Ar^+ + e^-_{(5\ \mathrm{to}\ 15\ \mathrm{eV})}$

  $\Rightarrow Ar^* + Ar^+ + e^-_{(0\ \mathrm{to}\ 4\ \mathrm{eV})}$

  (Density breakdown, "oven effect" of Rydberg states).

- Charge Transfer

  $Ar^+_{(fast)} + Ar \Rightarrow Ar_{(fast)} + Ar^+$

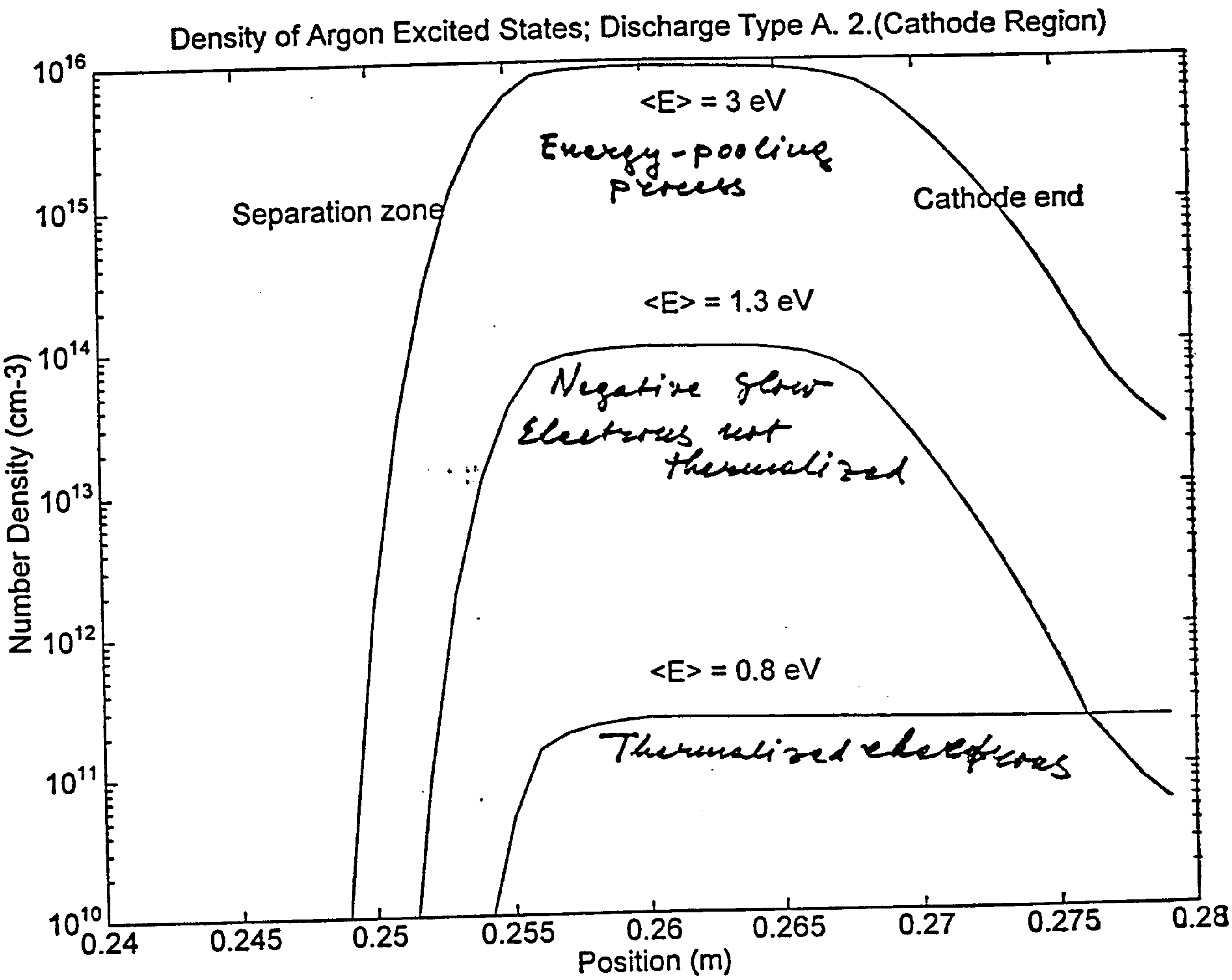

Density of Argon Excited States; Discharge Type A. 2.(Cathode Region)
<E> = 3 eV
Energy-pooling process
Separation zone
Cathode end
<E> = 1.3 eV
Negative glow
Electrons not thermalized
<E> = 0.8 eV
Thermalized electrons
Number Density (cm-3)
Position (m)
10^{16}
10^{15}
10^{14}
10^{13}
10^{12}
10^{11}
10^{10}
0.24
0.245
0.25
0.255
0.26
0.265
0.27
0.275
0.28

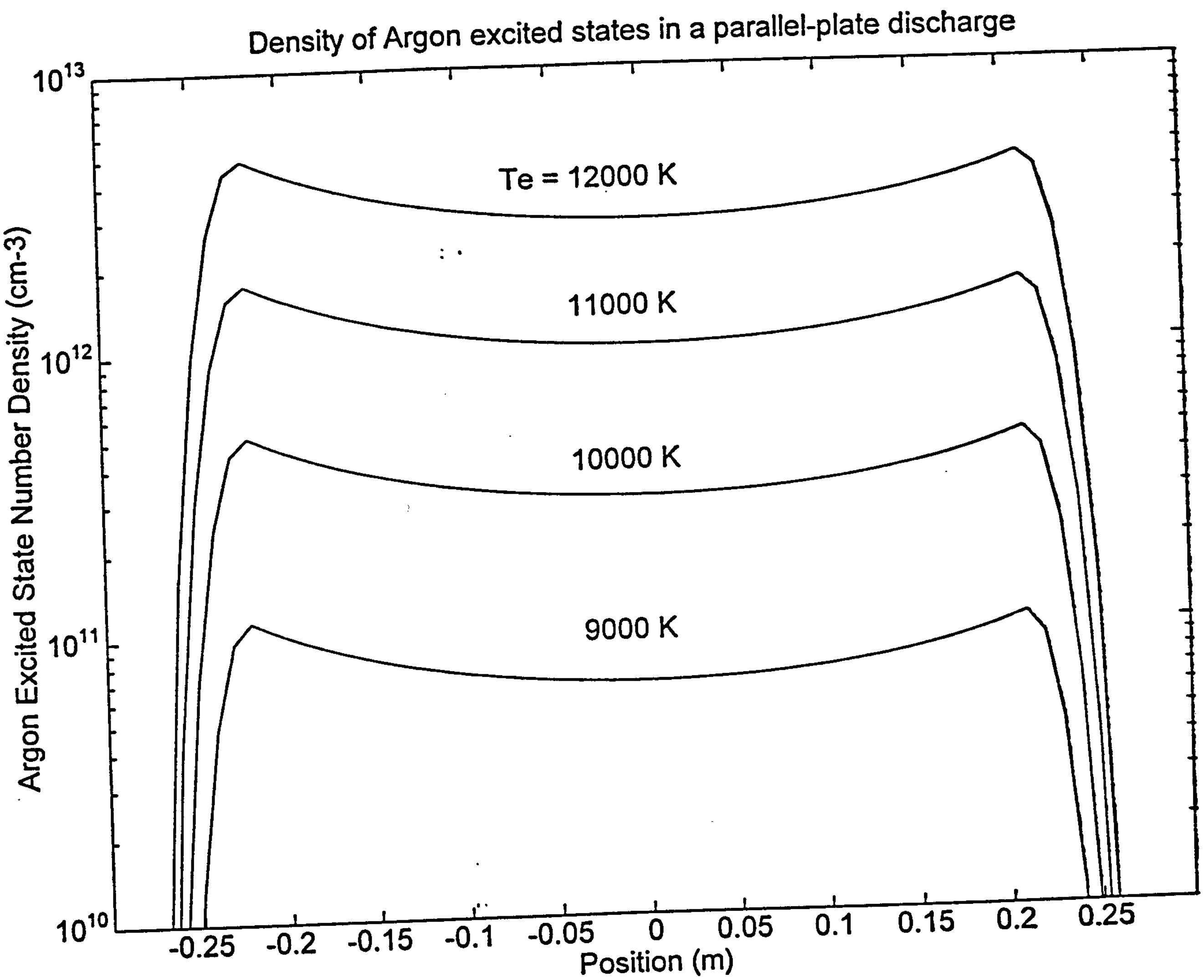

Density of Argon excited states in a parallel-plate discharge
Argon Excited State Number Density (cm-3)
10^{13}
10^{12}
10^{11}
10^{10}
Te = 12000 K
11000 K
10000 K
9000 K
-0.25 -0.2 -0.15 -0.1 -0.05 0 0.05 0.1 0.15 0.2 0.25
Position (m)

EM Field at DEL

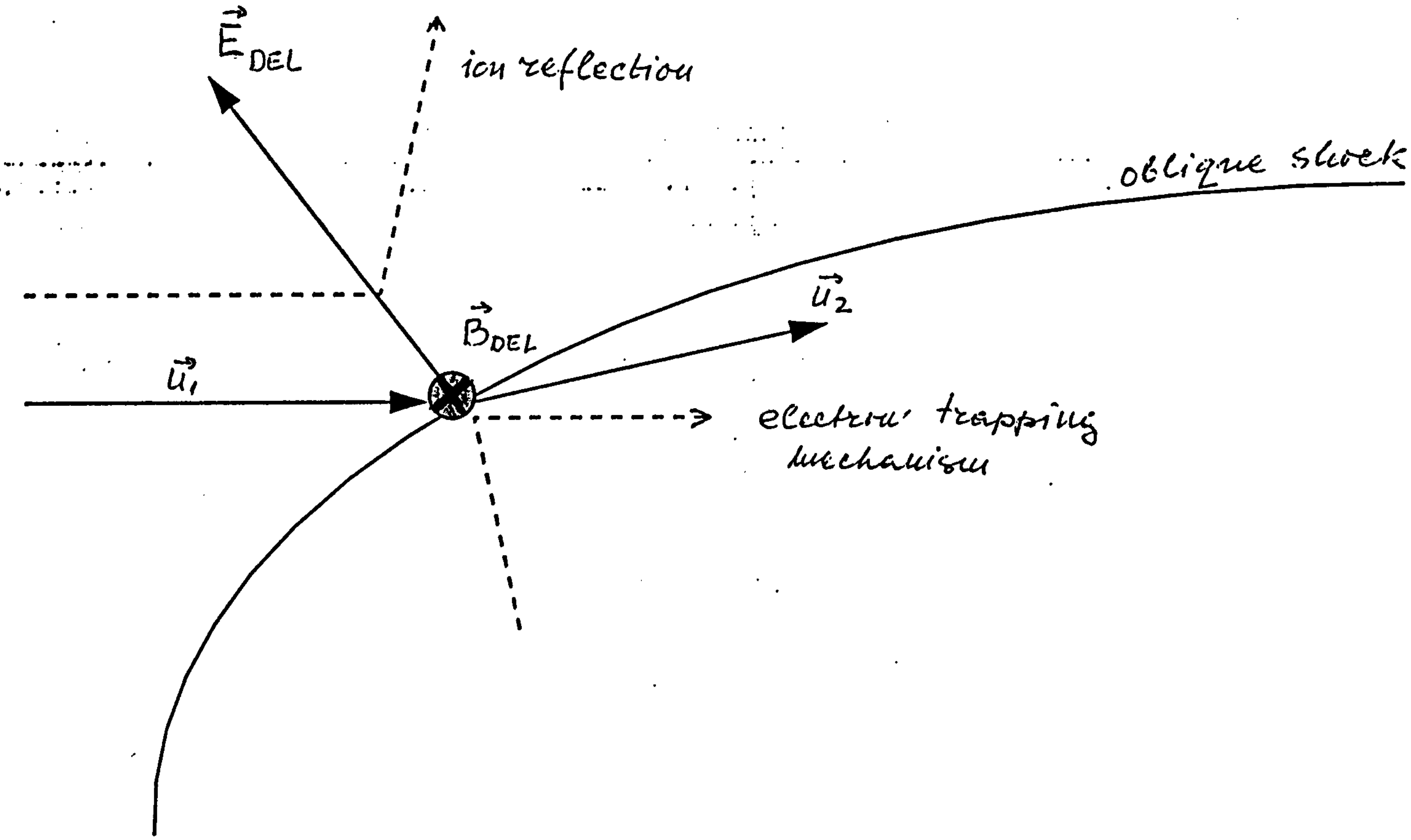

Electric Potential Distribution on the Centerline

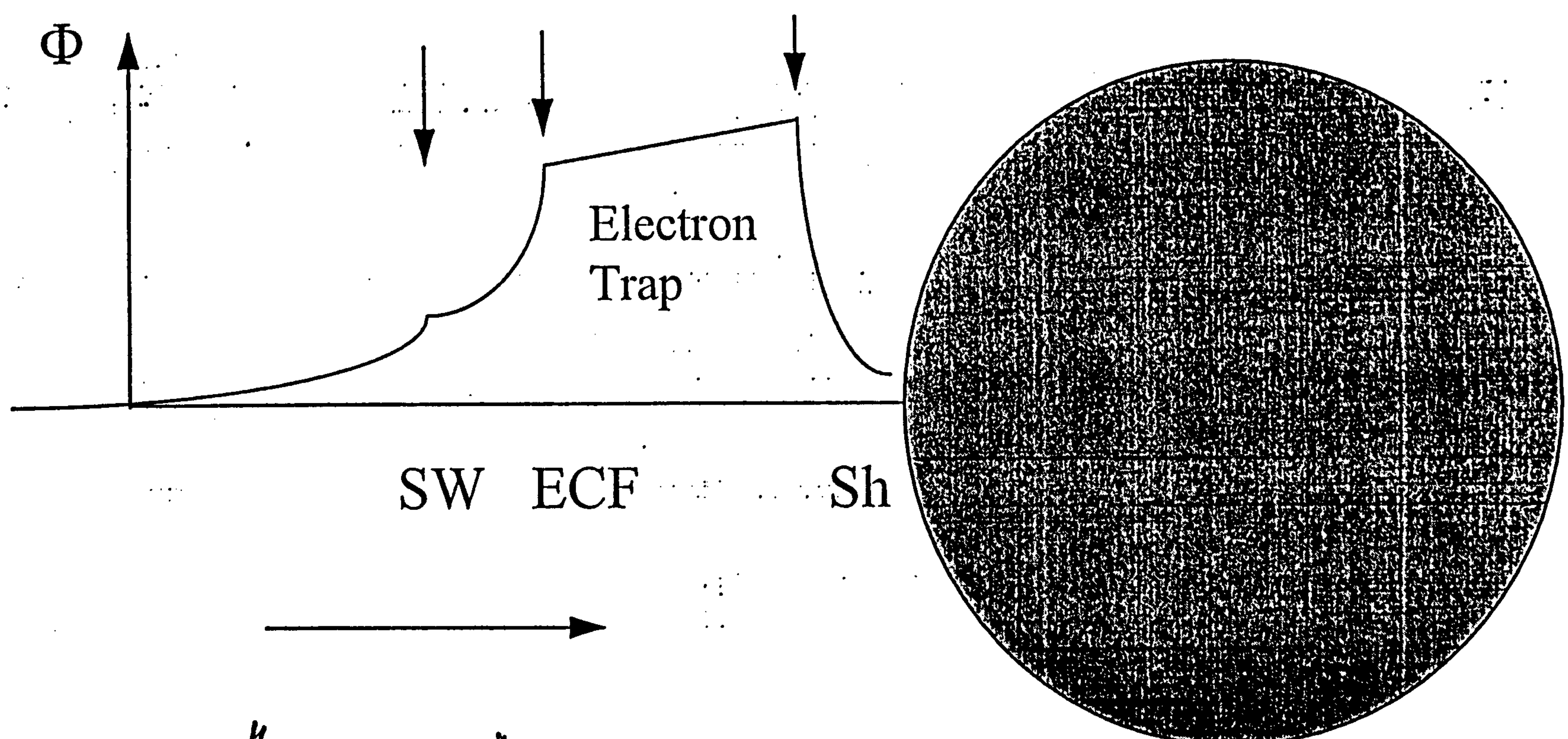

"Storage" mechanism

(most energy stored in "electron trap" region)

Shock Structure

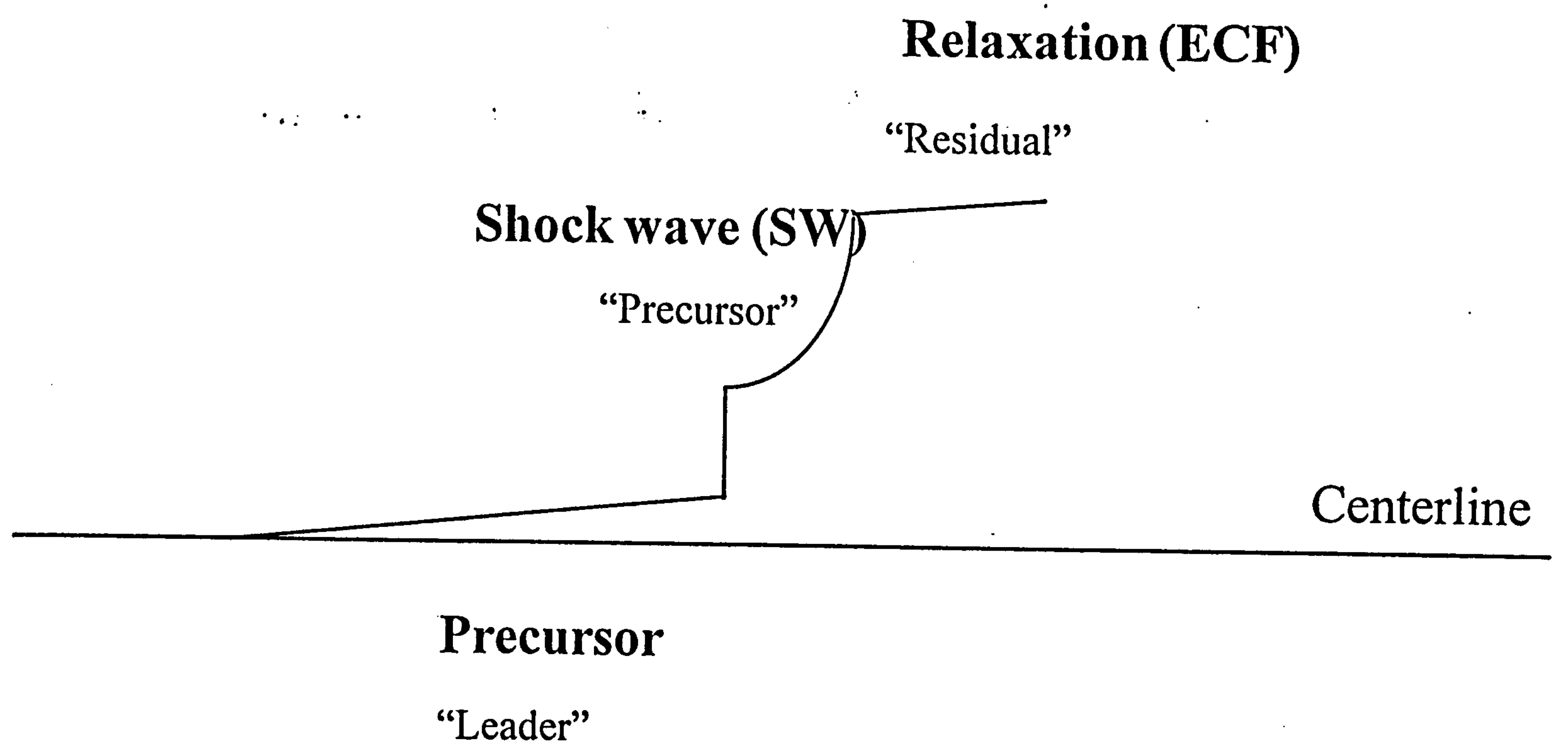

Effects which Follow Initial Perturbation

- Ion dynamics
  - Shock wave generates a Double Electric Layer (DEL).
  - DEL generates an ion acoustic wave.
  - Local increase of ion density traveling with the wave.
  - Slow ions reflected from DEL.
- Electron dynamics
  - Moving DEL induces transversal **B** field.
  - **B** field confines slow electrons.
  - Fast electrons escape DEL.
  - Most electrons trapped in relaxation zone
  - Electrons heated by inverse bremstrahlung.

Precursor

- Fast Ions reflected and accelerated on DEL
  - able to excite and ionize atoms and molecules
- Fraction of hot electrons heated by:
  - *inverse bremstrahlung* (observed difference in population of resonant and metastable states)
  - *energy pooling reactions*
- Mechanisms:
  - A. Ion-acoustic wave
  - B. Ionization wave generated by heavy particles (fast ions and neutrals)?
  - C. Onset of turbulence by angular momentum transfer in energy pooling reactions?

ON-BOARD GENERATION OF A "PRECURSOR" MICROWAVE PLASMA AT MACH 6: EXPERIMENT DESIGN

R. J. EXTON

NASA AERONAUTICS AND SPACE ADMINISTRATION

LANGLEY RESEARCH CENTER

MACH 6 PLASMA/DRAG REDUCTION TEAM

MEMBER	PRIMARY RESPONSIBILITY
R. J. EXTON	EXPERIMENT DEFINITION
R. J. BALLA	VISUALIZATION/LASERS
G. J. BRAUCKMANN	MODELS/FACILITY
M. DIFULVIO	FACILITY
W. E. LIPFORD	OPTICAL SUPPORT
J. FUGITT*	MICROWAVE (EXPERIMENT)
M. C. BAILEY	MICROWAVE (THEORY)
W. C. KELLIHER	NUCLEAR SOURCES
I. A. CARLBERG	NUCLEAR SOURCES
G. C. HERRING	ELECTRON DENSITY
B. SHIRINZADEH	NEUTRAL DENSITY
P. D. BABB	SAFETY
A. H. AUSLENDER	CPD
D. B. RHODES	SCHLIEREN
S. JONES	SCHLIEREN

*DOE JEFFERSON LAB

OBJECTIVES:

1. Experimentally demonstrate a concept for on-board generation of a microwave plasma;

2. Develop plasma diagnostic techniques for low density (cold) plasmas;

3. Clarify the physics underlying the phenomenon in conjunction with a parallel CFD effort.

APPROACH

- Design model/microwave horn for Mach 6 facility conditions
- Measure the forces on the model (plasma on/off)
- Characterize the plasma flow field (shock standoff and shape, electron density and temperature, neutral density profile)
- Investigate both cw and pulsed microwave power amplifiers as plasma generators

"Precursor" Microwave Plasma at Mach 6

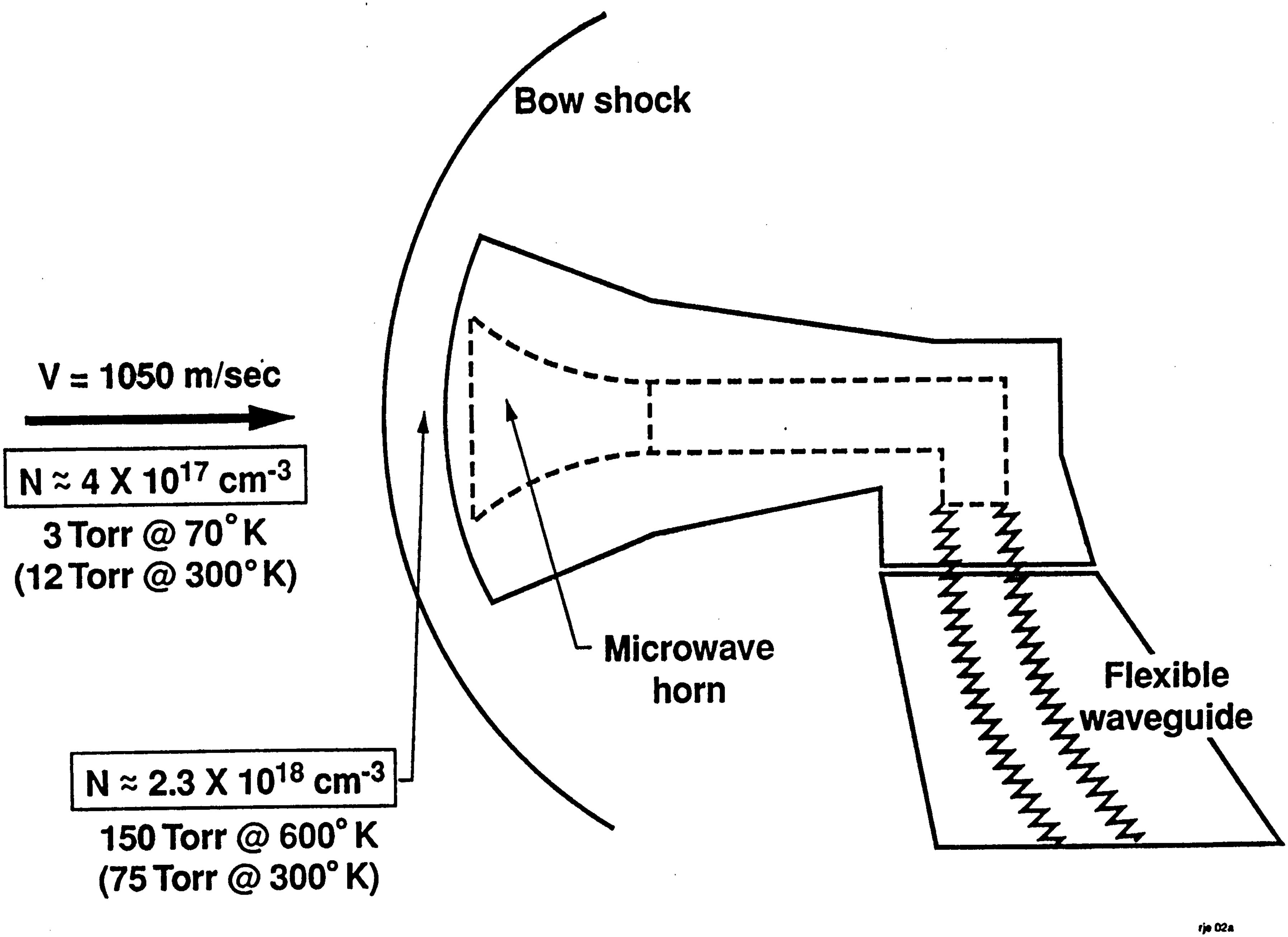

"Precursor" Microwave Plasma at Mach 6

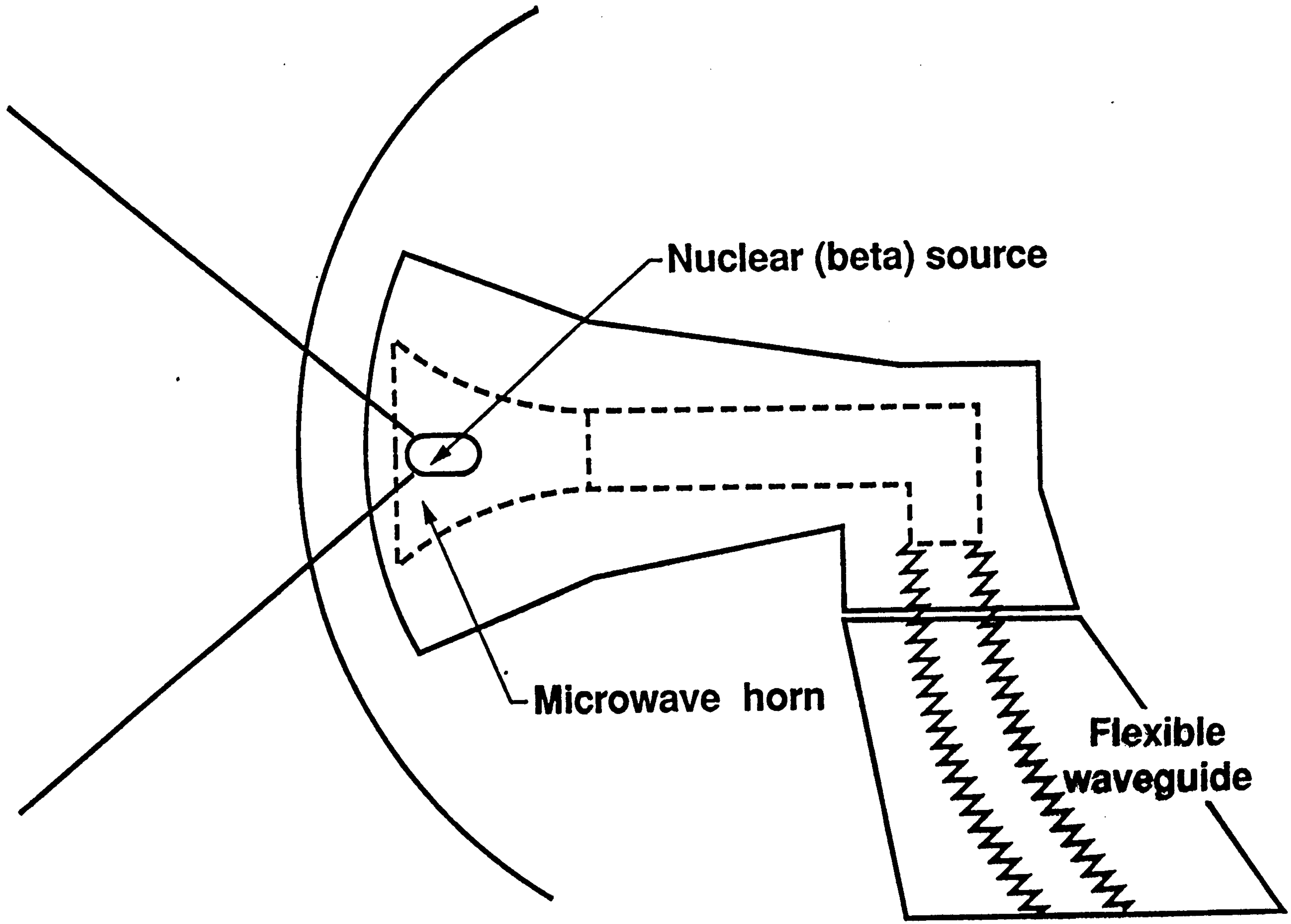

rje 02e

"Precursor" Microwave Plasma at Mach 6

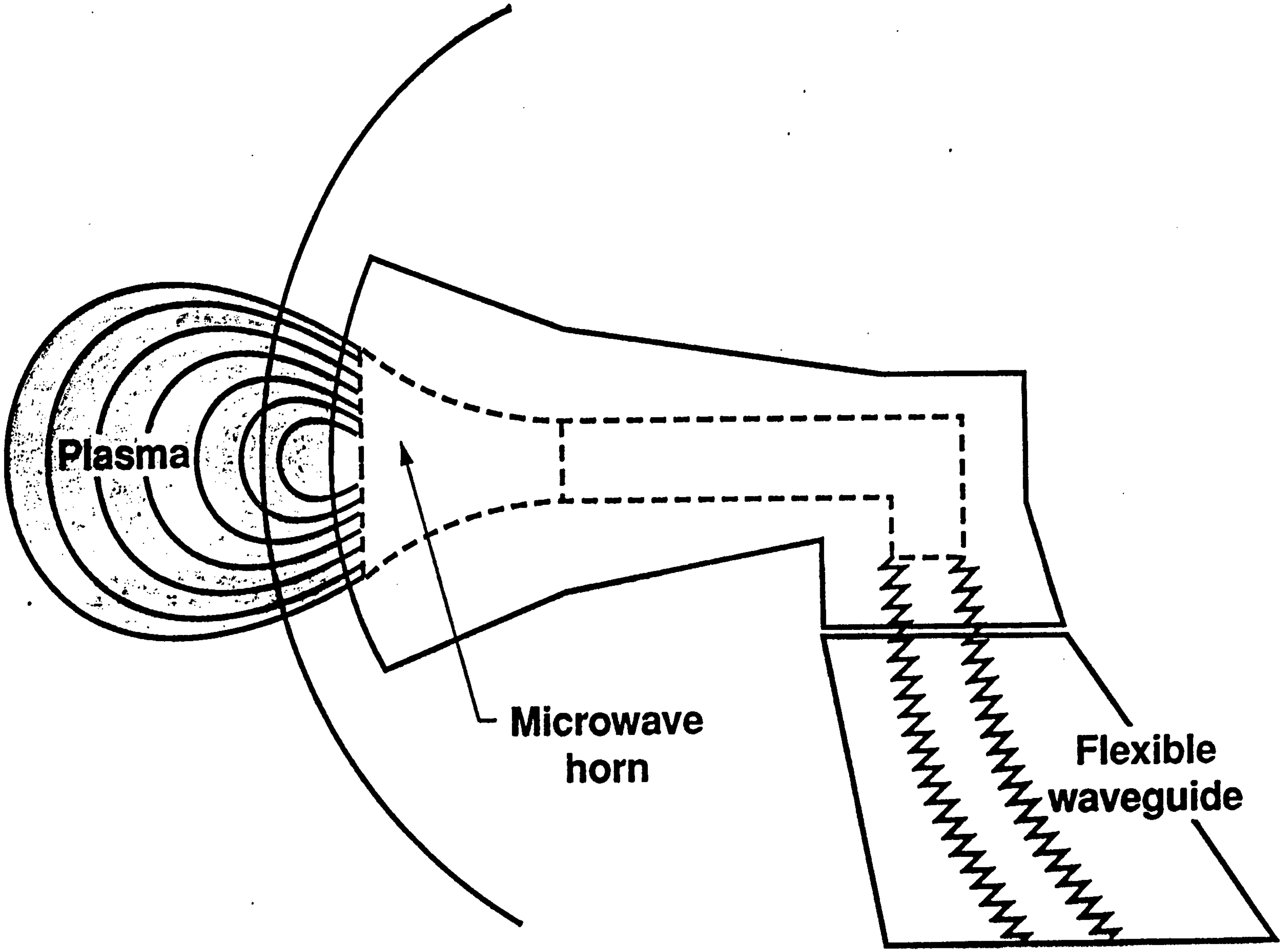

rje 02d

Microwave Breakdown in Air, O, and N

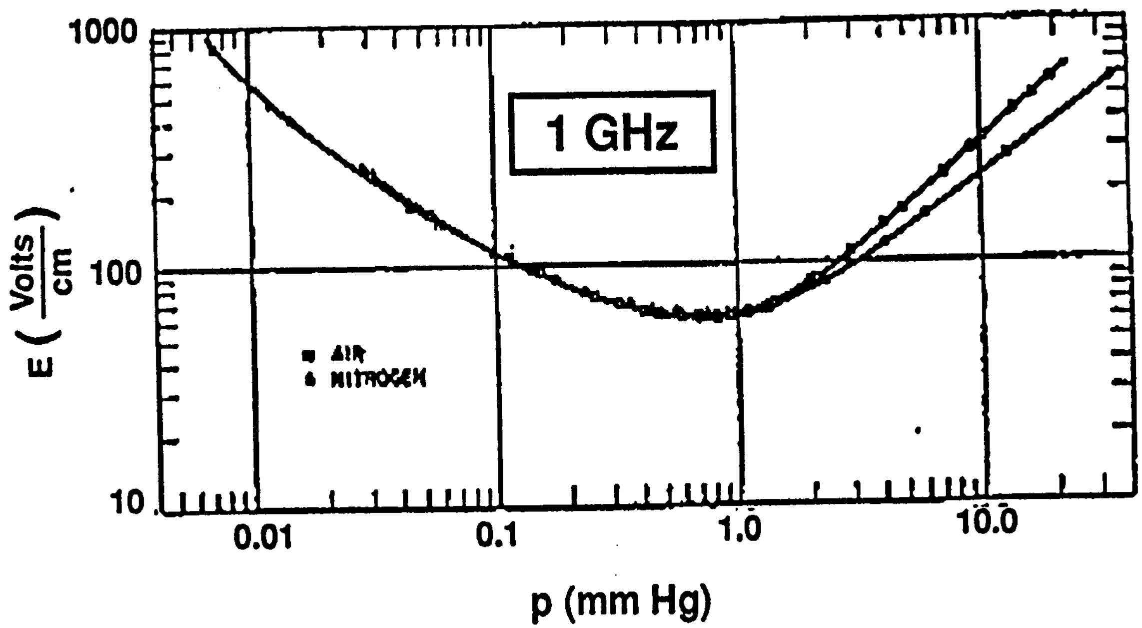

Cw breakdown fields for air and nitrogen at a frequency of 994 Mc/sec.
(Characteristic diffusion length A = 2.65 cm)
A. D. MacDonald et. al. Phys. Rev. 130, 1841 (1963)

Microwave Breakdown in Air, O, and N

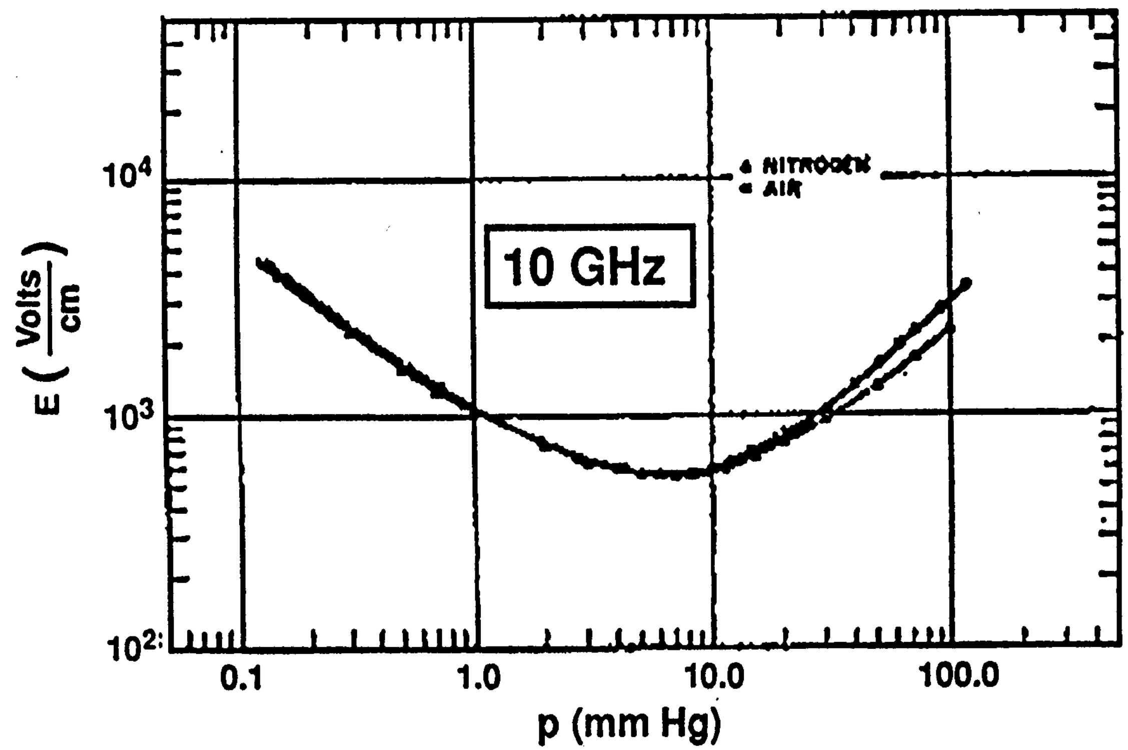

Cw breakdown fields for air and nitrogen at a frequency of 9.4 kMc/sec.
(Characteristic diffusion length A = 0.22 cm)
A. D. MacDonald et. al. Phys. Rev. 130, 1841 (1963)

PLASMA DRAG REDUCTION MODEL

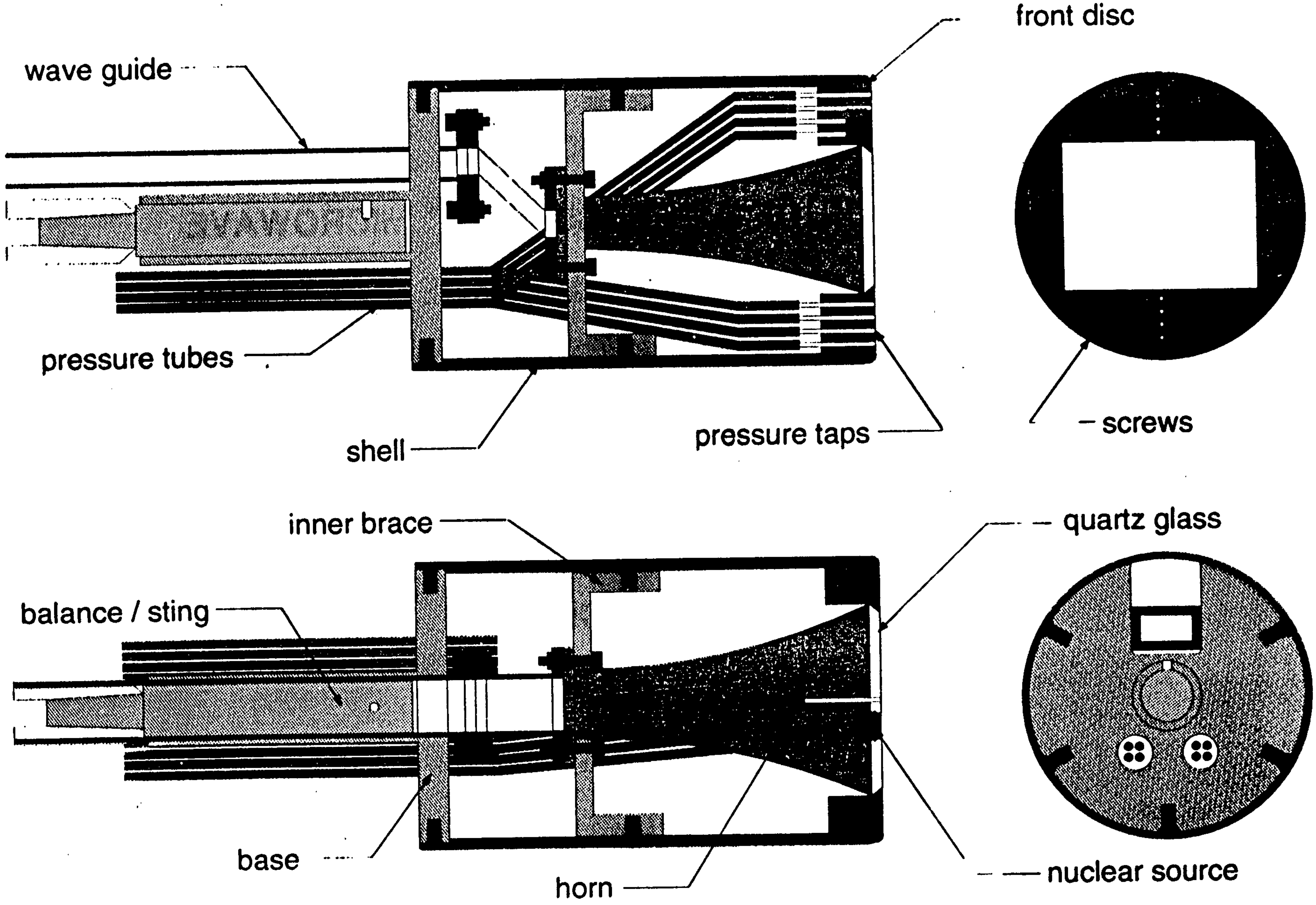

DIAGNOSTICS

INITIAL ENTRY

- o PULSED, DIGITAL SCHLIEREN
- o GATED, CCD CAMERA
- o OPTICAL MULTICHANNEL ANALYZER (200-900 NM)

FUTURE ENTRIES

- o EXCIMER LASER (NEUTRAL PROFILE)
- o LASER/MICROWAVE INTERFEROMETRY

  (ELECTRON DENSITY)

DIAGNOSTICS

INITIAL ENTRY

- o PULSED, DIGITAL SCHLIEREN
- o GATED, CCD CAMERA
- o OPTICAL MULTICHANNEL ANALYZER (200-900 NM)

FUTURE ENTRIES

- o EXCIMER LASER (NEUTRAL PROFILE)
- o LASER/MICROWAVE INTERFEROMETRY

  (ELECTRON DENSITY)

SCHEDULE/MICROWAVE POWER

SCHEDULE-MACH 6

INITIAL ENTRY ~AUG 97

2ND ENTRY--FY98

POWER AMPLIFIERS (AVAILABILITY)

CW

- 200 W, 8-18 GHz (AVAILABLE)
- 500 W, 8-18 GHz (POSSIBLE LOANER)
- 2 kw @ 14 GHz (COMMERCIAL)
- 10 kw @ 18 GHz (?????)

PULSED

- 26 kw PEAK, X-BAND (8.2-12.4 GHZ) 5% DUTY 1.3 kw AVG. (POSSIBLE LOANER)
- 100 kw PEAK, X-BAND (8.2-12.4 GHz) (POSSIBLE LOANER)
- 100 kw PEAK, KU-BAND (12.4-18.0 GHz) 3 MICROSEC PULSE 100 Hz (POSSIBLE LOANER)

CONCERNS

- o SUFFICIENT FIELD STRENGTH FOR BREAKDOWN (~700 V/CM @ 10-15 TORR)
- o PLASMA EXTENT SUFFICIENT TO ATTAIN "PRECURSOR" STATUS
- o ELECTRON DENSITY AND TEMPERATURE ADEQUATE TO BRING ABOUT SHOCK MODIFICATION

SOLUTION

MORE POWER

Program Overview

Shock Wave Dynamics in Weakly Ionized Plasmas

at

Laboratory for Modern Fluid Physics, Florida A&M University (FAMU), Tallahassee, FL

Prof. J. A. Johnson III, Distinguished Prof. of Science and Engineering
Dr. Richard Appartaim, Research Associate in Physics
Mr. Kester Thompson, Graduate Student, Mechanical Engineering

Overall FAMU Purpose

To determine the roles which turbulence and/or nonequilibrium effects in weakly ionized gases play in shock wave transport dynamics through:

(a) comprehensive optical diagnostics of the interactions of shock waves with turbulence and/or nonequilibrium plasmas in the low supersonic and hypersonic regimes;

(b) rigorous analyses of the associated physics, including quantumechanical as well as classical phenomena;

(c) explorations of potential modalities for the implementation of plasma drag reduction of operational aircraft.

Recent FAMU Achievements

-> Evidence of shock wave strength reduction from a turbulence manipulated nonequilibrium flow in a pressure ruptured shock tube;

-> Preliminary evidence of shock wave acceleration in our new Supersonic Shocked Plasma Facility where a Mach 2 shock wave moves from a plasma free region into one with a weak plasma;

-> Preliminary evidence from our Hypersonic Arc Driven Shock Tube of highly localized energy transfer from small scale turbulent nonequilibrium fluctuations into large scale flow of the sort which can weaken the strength of a resident shock wave.

-> Preliminary experimentally testable explanations of the influence of turbulence and/or nonequilibrium effects on standard macroscopic transport quantities

Specific Immediate FAMU Plans

-> Modifications of our current Supersonic Shocked Plasma Facility to afford a wider variety of manipulations in the shock wave-plasma interaction, including the introduction of seed molecules and microwave probes;

-> System-specific modelling of the plasma and atomic processes so as to determine the underlying physics along with a full range of test modalities, including those relevant to ballistic ranges, flight, and other configurations different from our own;

-> The implementation of a new Turbulent Stark Velocimetry as a program of developement of relevant portable diagnostics suitable for possible near term introduction on operational airframe platforms.

AERODYNAMIC APPLICATIONS OF WEAKLY IONIZED PLASMAS

R. Miles, S. Macheret, S.H. Lam, P. Efthimion, L Martinelli
Princeton University

- Drag Reduction
- Plasma Ramparts
- Flow Control
    - By Localized Energy Addition
    - By J x B forces
- Control and Intiation of Chemical Processes
- Power Extraction
    - MHD in an engine inlet (AJAX)
    - MHD in ionized flow
- Hypersonic Wind Tunnel Drivers
    - By Energy Addition through microwaves
    - By MHD acceleration
- Suppression of shock strength and sonic boom

SUSTAINING A PLASMA IN HIGH SPEED FLOW

- Important for Drag reduction, Plasma Ramparts, Flow Control, Shock Suppression, MHD, and Combustion Initiation and Control

- Discharge may be blown out

- Thermal (equilibrium) plasma will need to be reinitiated - a thermal plasma cannot propagate at supersonic speed

- Nonequilibrium plasma will require high electric field and high power

- A filamentary plasma may serve the purpose and will require less power (a small portion of the volume is ionized)

- Filaments may be guided by laser or electron beams

- A high power microwave may be the preferred source.

SUSTAINING MICROWAVE DRIVEN PLASMAS IN ATMOSPHERIC PRESSURE AIR

- Thermal Regime
    - Requires $T_{min} > 4000K$
    - Needs relatively low microwave power (kilowatts/cm^2) the power offsets the thermal losses
    - Long lifetime (cooling time)

- Nonequilibrium Regime
    - Requires high power microwaves to overcome the electron recombination and attachment rates
    - Diffuse plasma (low pressure)
        - Low temperature neutral species
    - Filamentary discharge (high pressure)
        - High temperature localized streamers

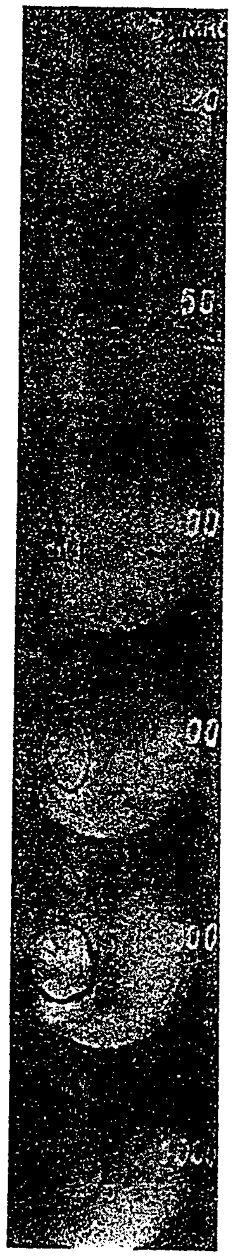
20
50

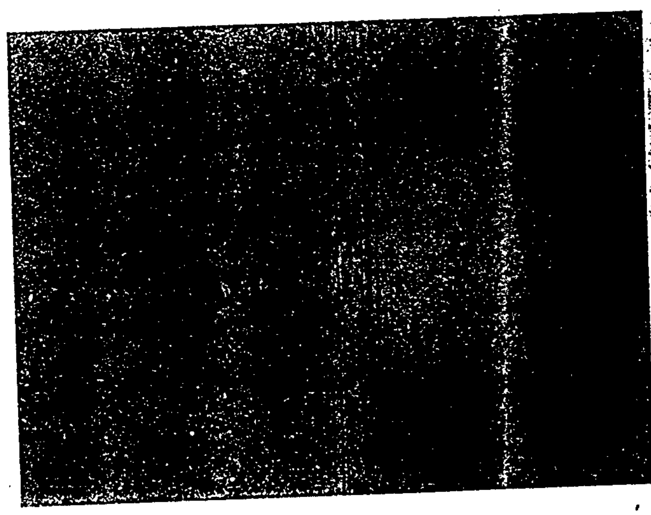

FILAMENTATION OF ATMOSPHERIC MICROWAVE DRIVEN PLASMA

Grachev, Esakov, Mishin and Khodataev

Moscow RadioTechnical Institute

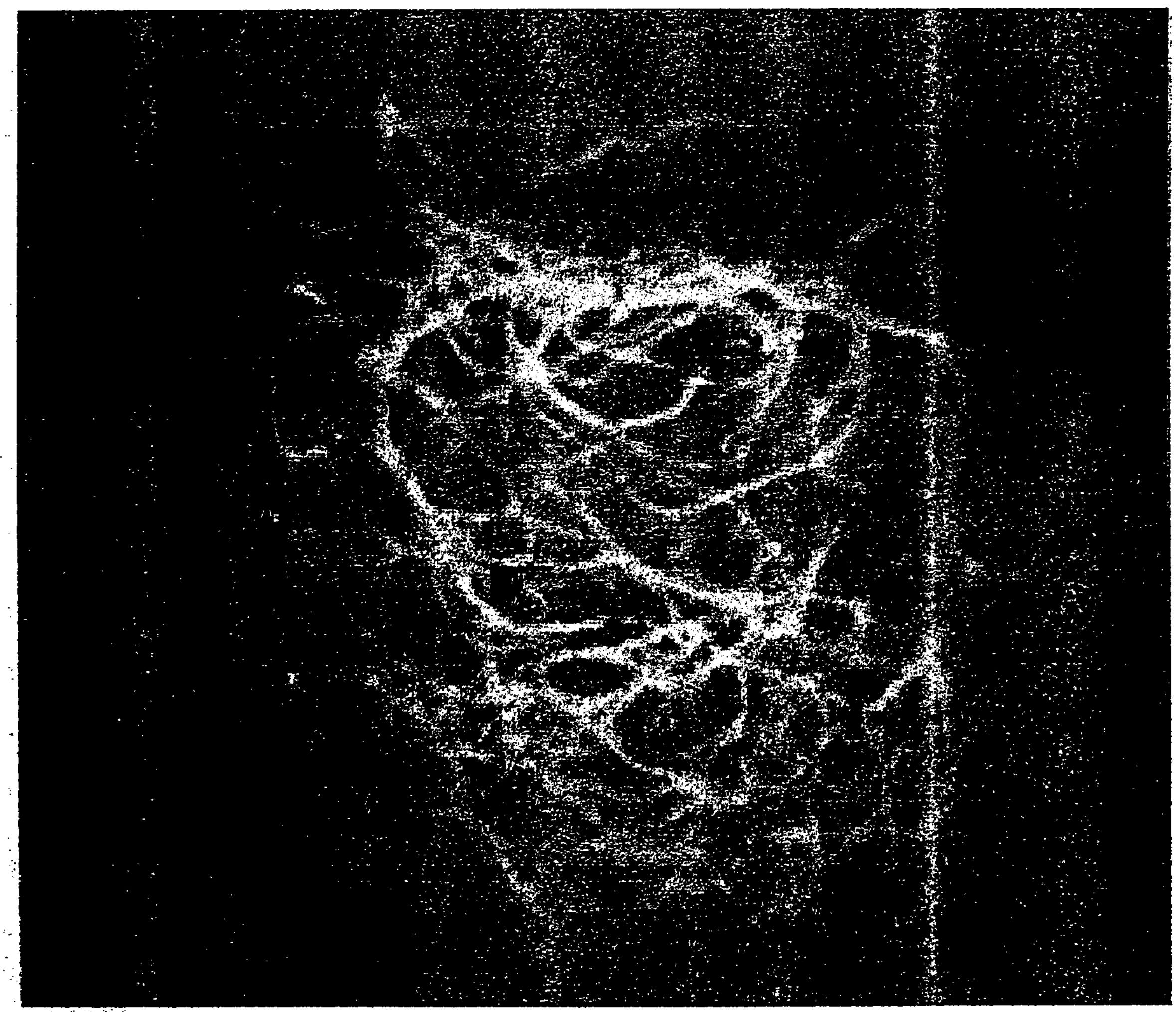

LASER GUIDED ARC FORMATION

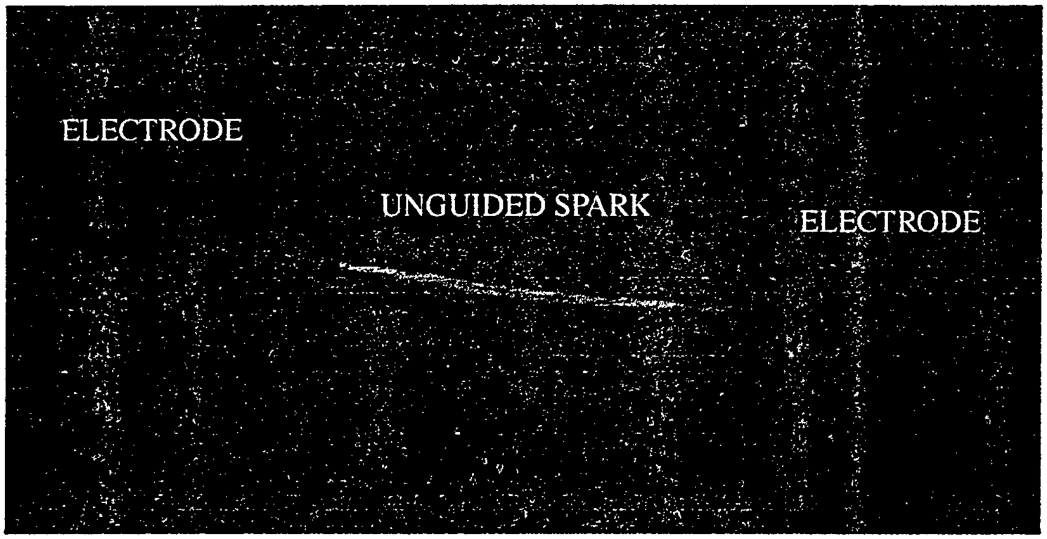

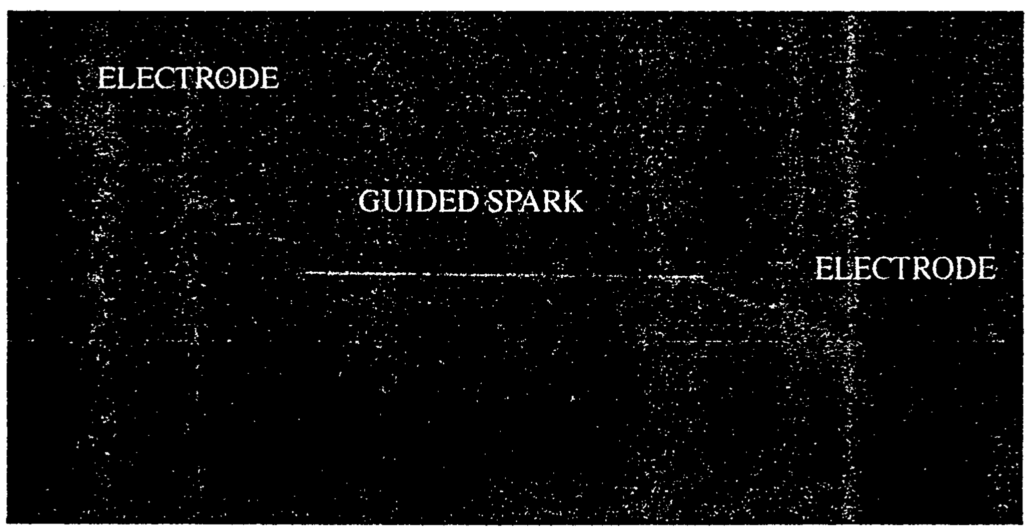

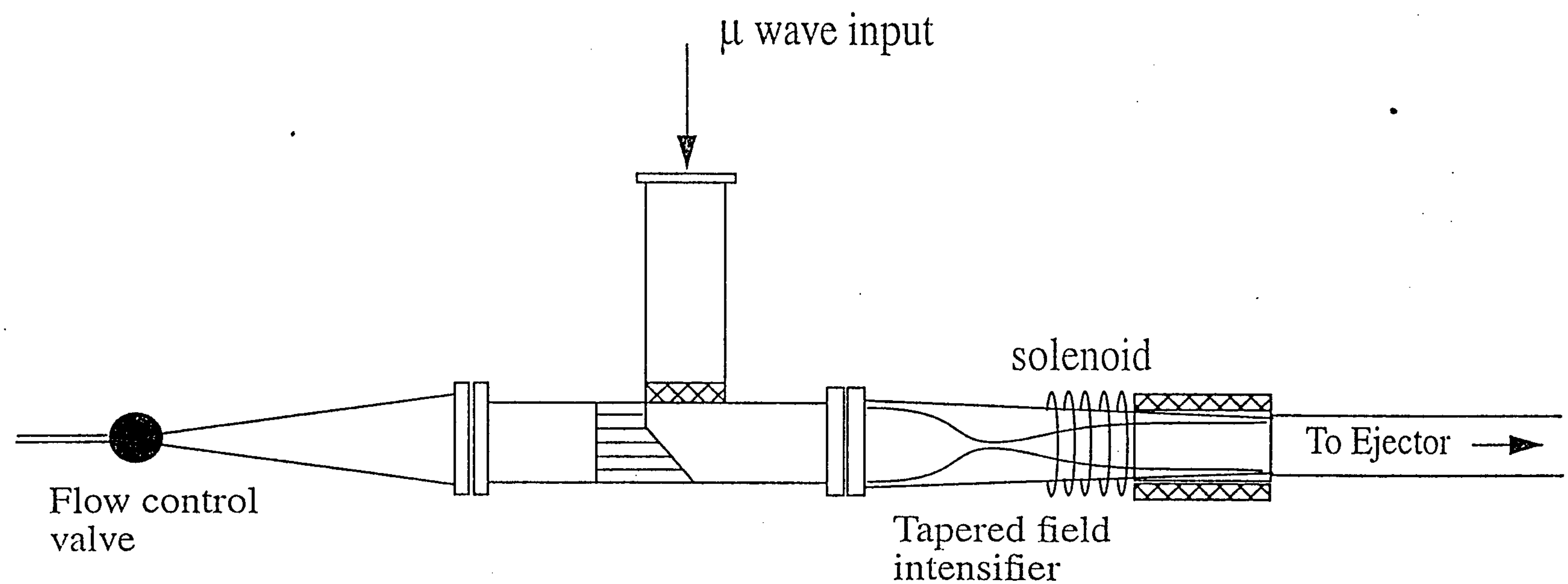
μ wave input
solenoid
To Ejector
Flow control
valve
Tapered field
intensifier

DRAG REDUCTION
Experimental Observations

- Shocks Accelerate Upon Entry Into Plasmas From Neutral Gas

- Dramatic Changes In Structure:
  - Shock Front Broadens
  - Amplitude Decreases
  - Shock Typically Splits Into Two or Three

- Effect Persists for Quite a Long Time (up to 1 - 10 msec)

- Observations Were Made In Various Discharges (Longitudinal And Transverse),In Various Gases (Air, Argon, Hydrogen, Helium, Etc.) Using Various Diagnostics.

- Ballistic Range Experiments Seem to Imply a Change in the Effective Speed of Sound, and Show Decrease in Supersonic Drag.

Thermal diaphragm
Density Contours

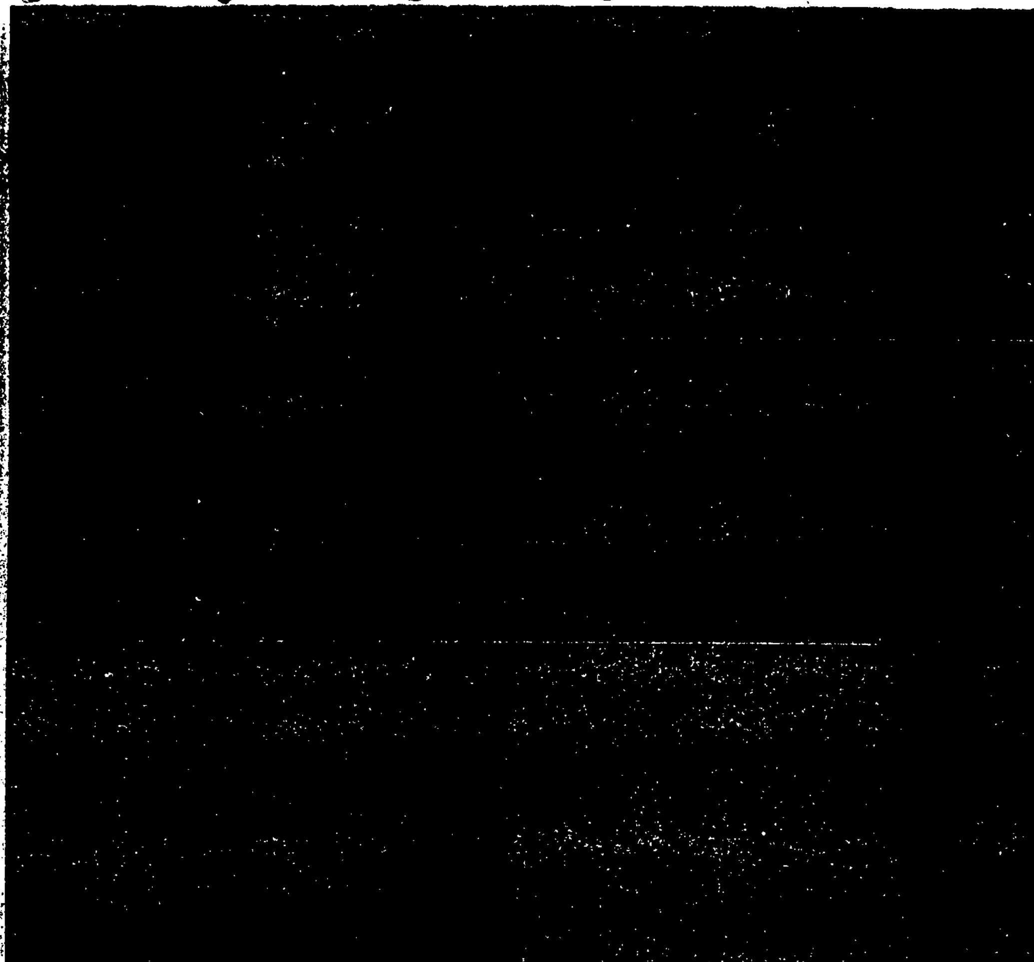

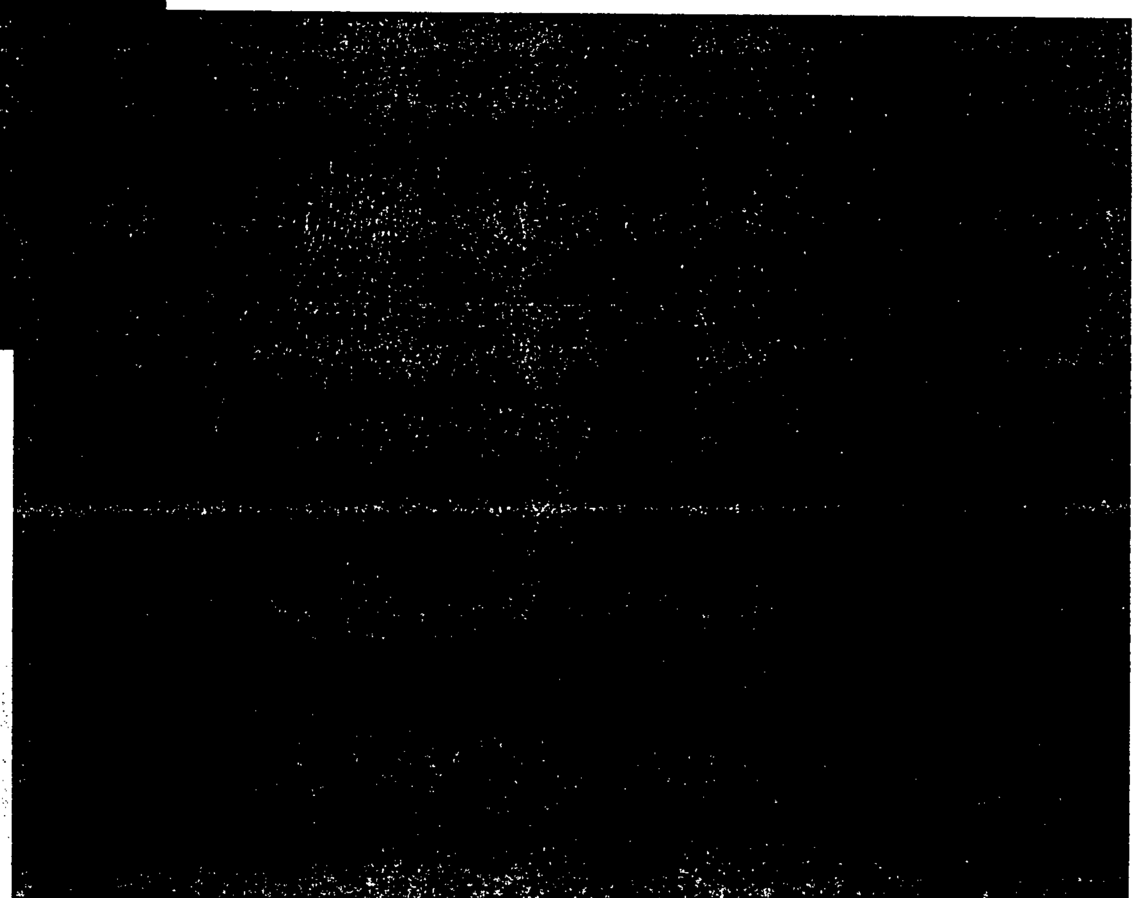

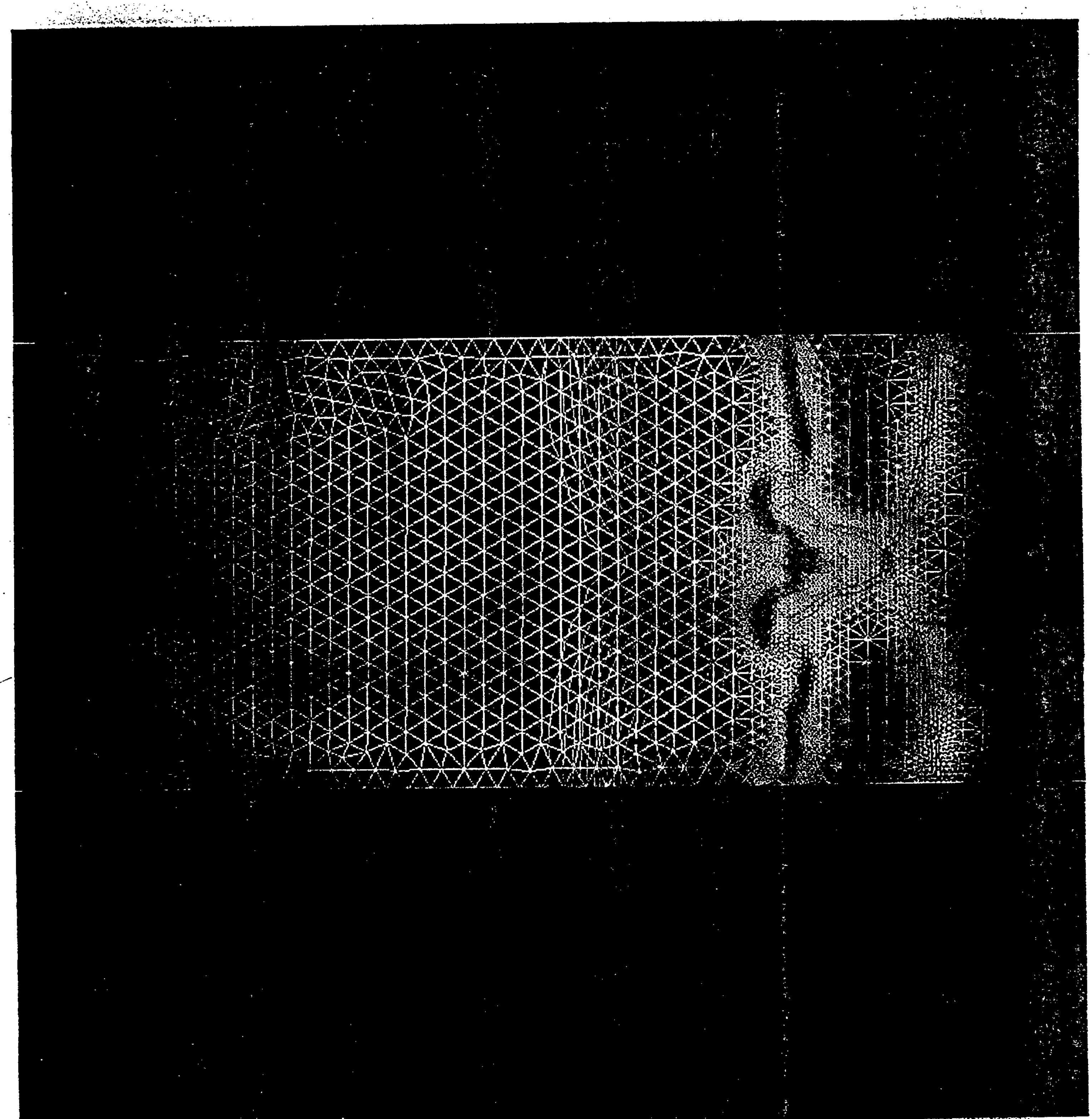

DENSITY PROFILE ACROSS THE SHOCK IN "THERMAL DIAPHRAGM" CASE (CURVED BOUNDARY BETWEEN HOT AND COLD REGIONS) CUT ALONG THE CENTER LINE.

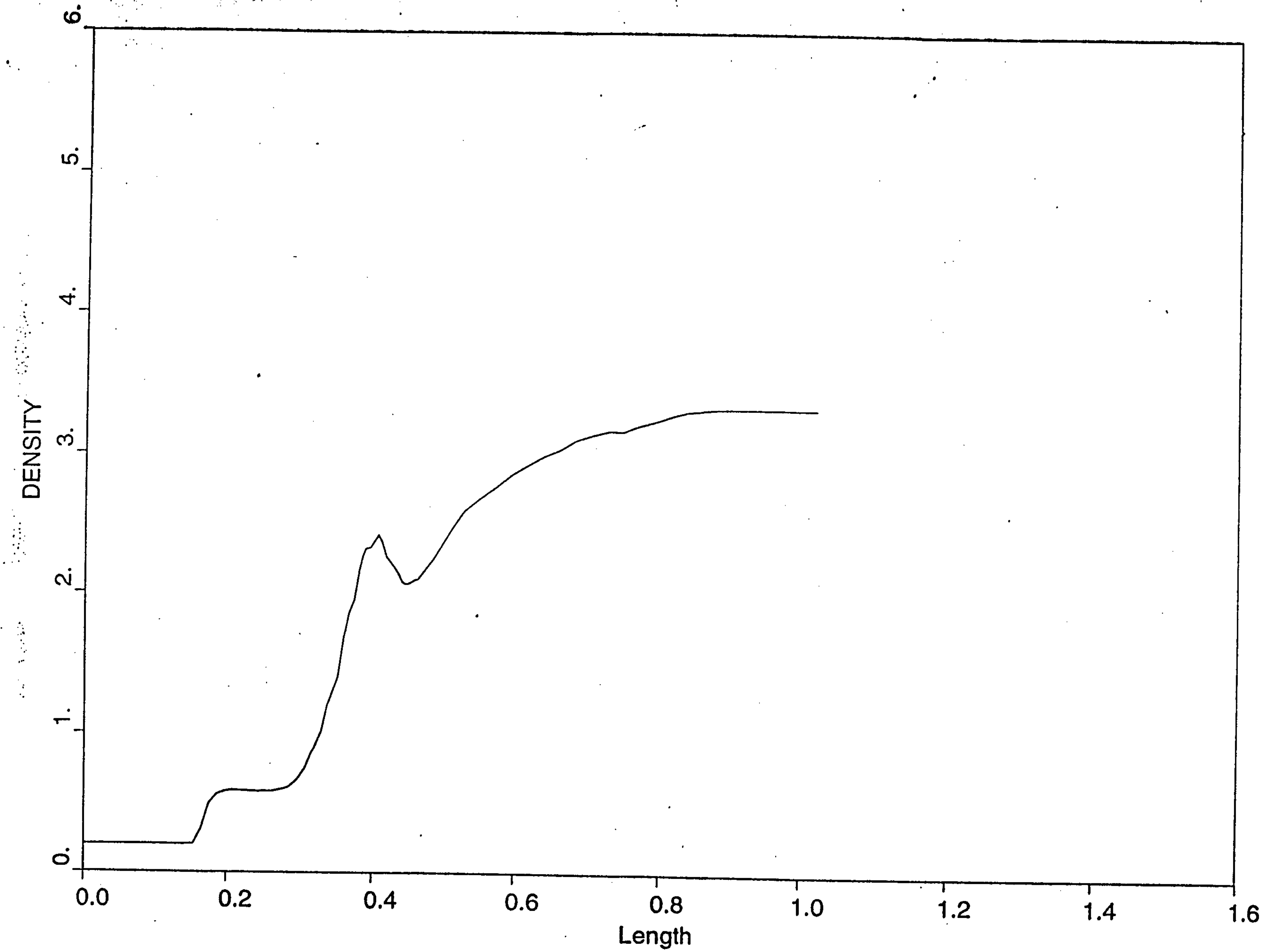

Planar Cut @ (0.83, -0.24, 0.25)(0.83, 0.74, 0.25)(1.82, -0.24, 0.25)

DENSITY PROFILE ACROSS THE SHOCK IN "THERMAL DIAPHRAGM" CASE
(CURVED BOUNDARY BETWEEN HOT AND COLD REGIONS)
SIDE CUT

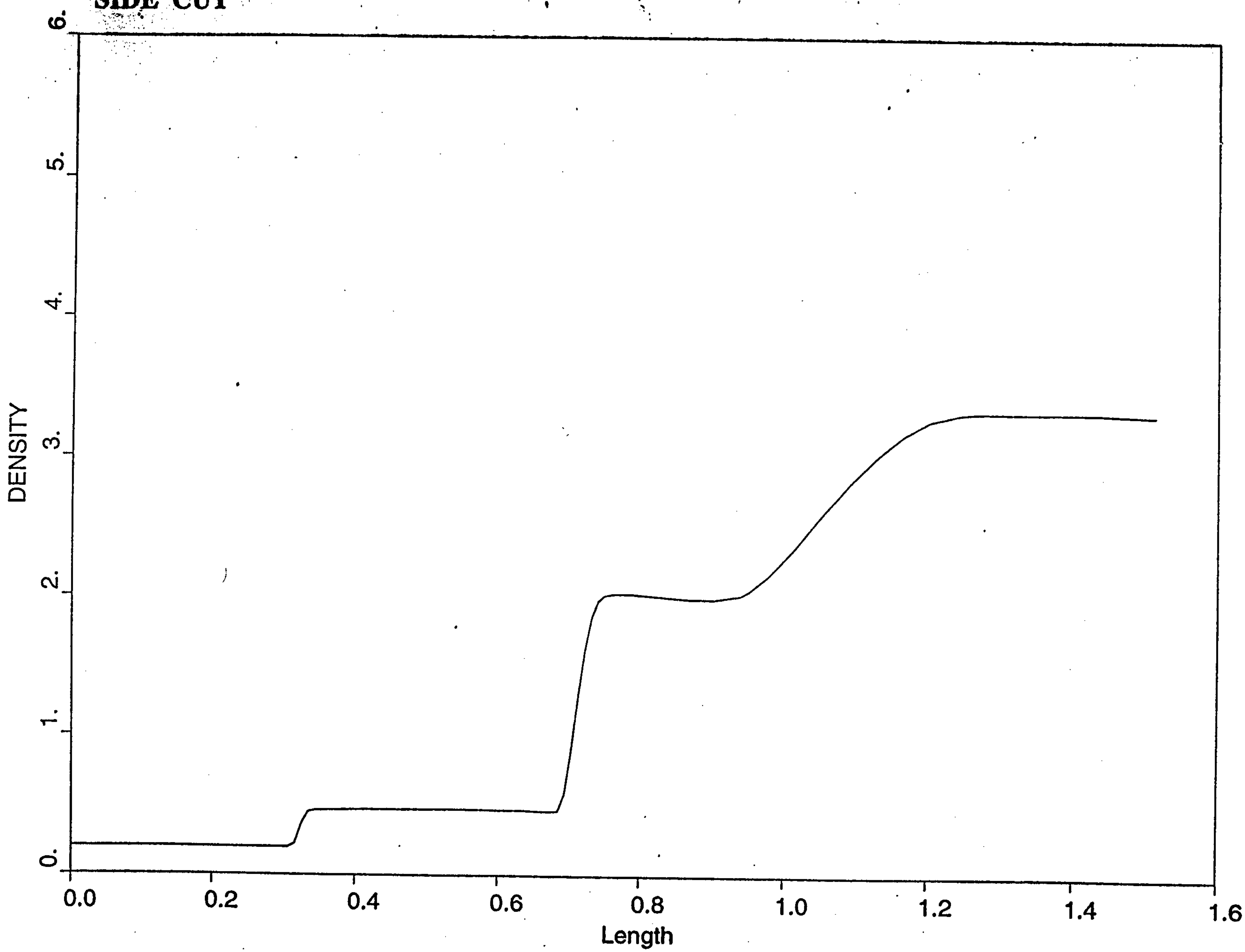

Planar Cut @ (1.01, -0.28, 0.25)(1.01, 1.26, 0.25)(2.55, -0.28, 0.25)

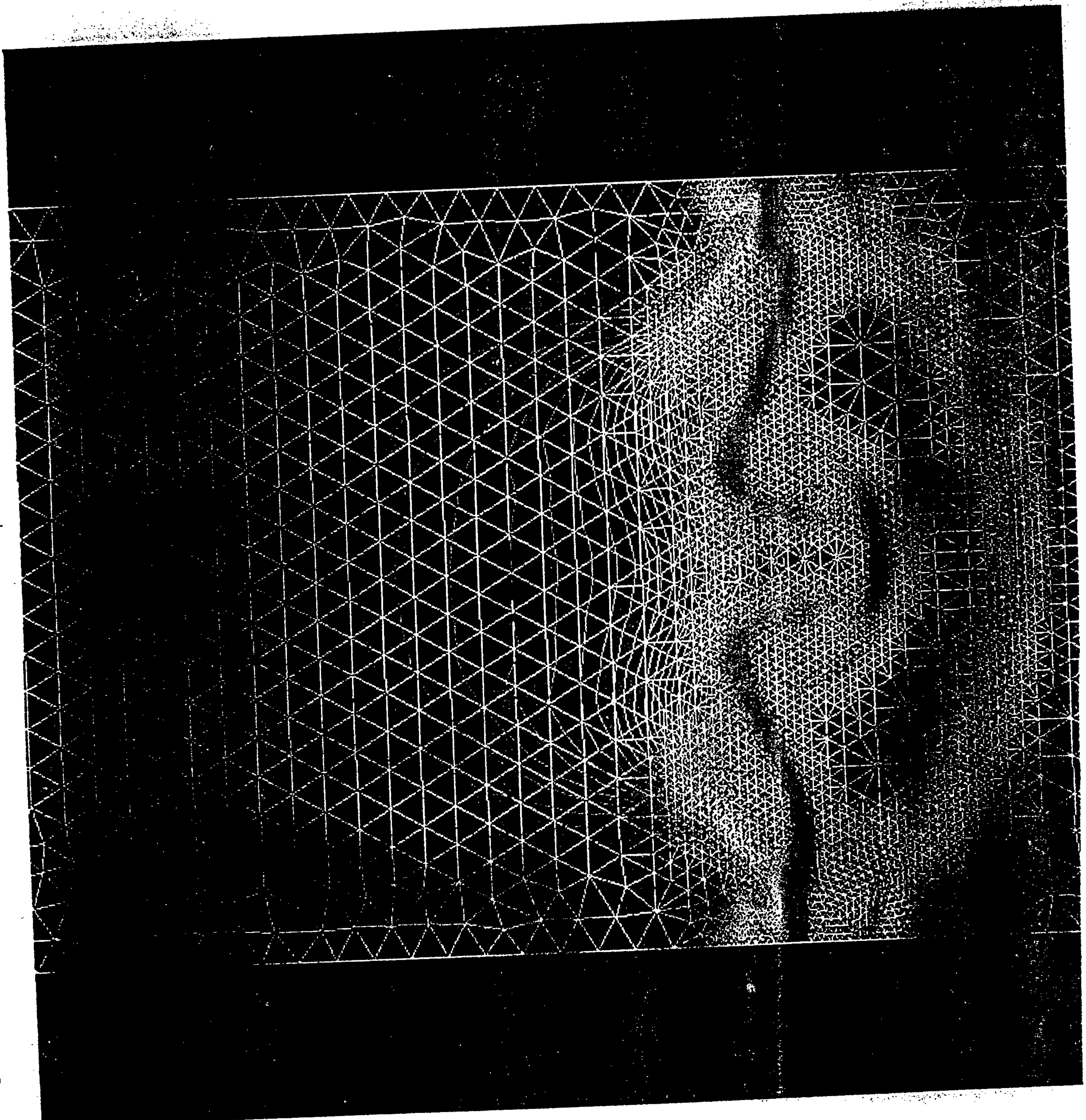

EXPERIMENTAL CONCERNS

- Temperature

  - In all the experiments, the temperature of the neutral gas has not been directly measured.

- Temperature Profile

  - A transverse temperature profile or a curved thermal boundary will lead to complex shock structure. This may occur as the shock passes through the hot cathode or anode fall regions of the discharge. (Well away from the centerline of the experiment)
  - Models indicate the apparent shock splitting and the density rise echo experimental observations

- Nonuniform Temperature Field

  - Shock splitting has been seen in turbulent mixtures of gases. If the plasma has hot and cold regions, a similar shock break-up may occur.

-

M = 1.03 SHOCK PROPAGATION THROUGH
HE + R 12 TURBULENT MIXTURE
Hesselink and Sturtevant

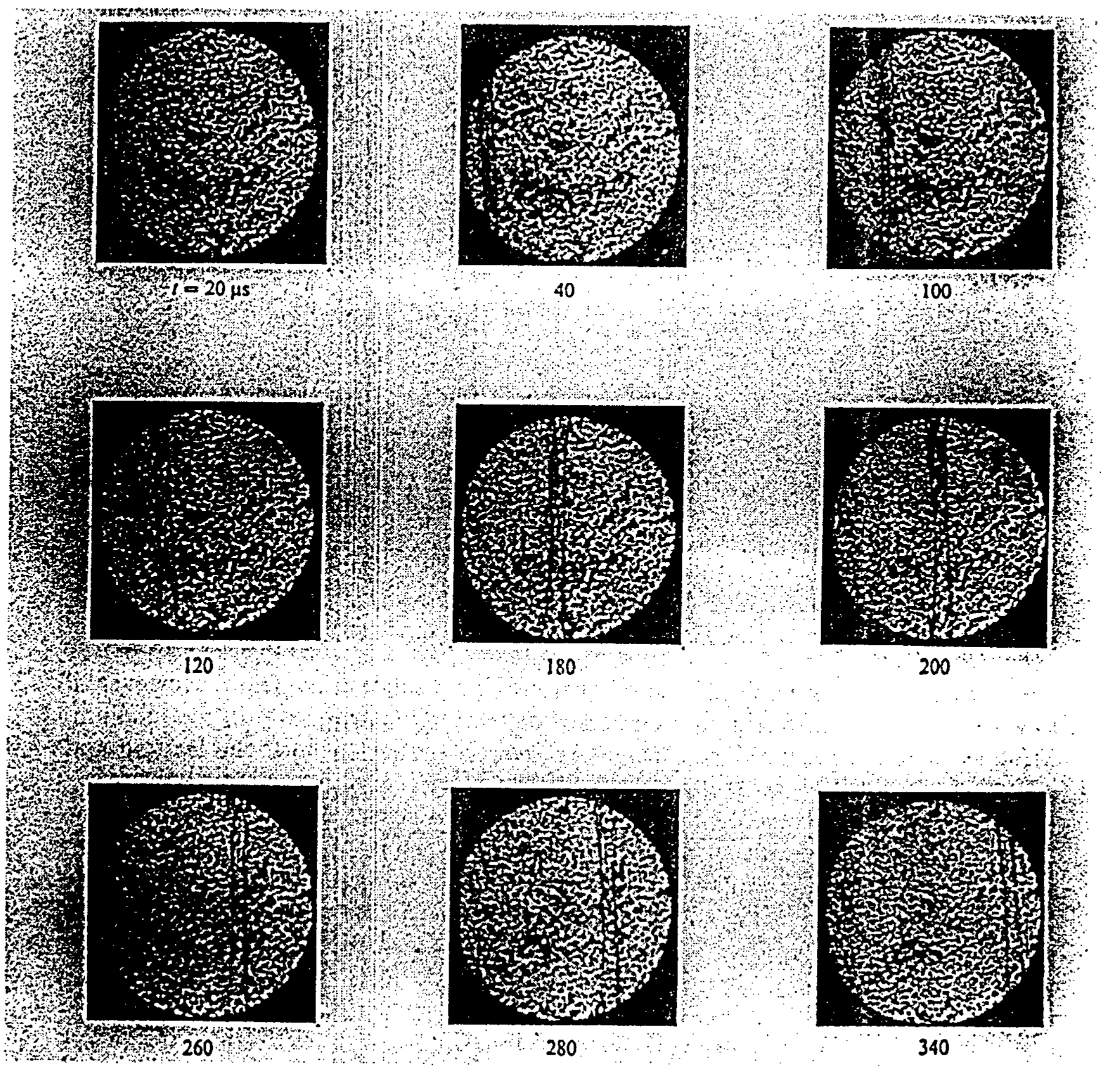

CONCLUSIONS ON DRAG REDUCTION

- All the experimental phenomena we examined are consistent with thermal gradient effects

- Ballistic range data needs to be studied in more detail

- Accurate temperature and density measurements need to be made

- There may be some effects of thermal gradients, unsteady phenomena, vorticity, and random or flickering heat addition.

PRINCETON PROGRAM

- Development of new diagnostics for temperature and density imaging

- New World Vistas
  - Sustaining microwave driven plasmas in a Mach 3 flow
  - Plasma effects on the bow shock in a Mach 3 flow.
  - Study of basic mechanisms of acoustic wave interactions and shock dynamics in stationary plasmas

- Plasma Ramparts
  - Experimental studies of the control of plasma filamentation
  - Kinetic model development for pulsed ionized air plasmas
  - Modeling nonequilibrium molecular processes
  - High power microwave driven discharge dynamics
  - Stabilizing and extending microwave driven plasmas with magnetic fields

- Mariah II (Radiatively Driven Wind Tunnel augmented by MHD)
  - Sustaining conductivity in atmospheric pressure air with electron beams
  - Acceleration and deceleration of supersonic flows in MHD channels
  - Energy coupling into high pressure air
  - MHD acceleration with filamentary discharges

PLASMA TEMPERATURE MEASUREMENT BY FILTERED RAYLEIGH SCATTERING

- Rayleigh Scattering
  - Total Scattering is Proportional to Density
  - Linewidth is proportional to $\sqrt{T}$
  - Signal is weak
  - Background scattering is at nearly the same frequency

- Filtered Rayleigh Scattering
  - Eliminates Background Scattering
  - Permits Measurement of Linewidth

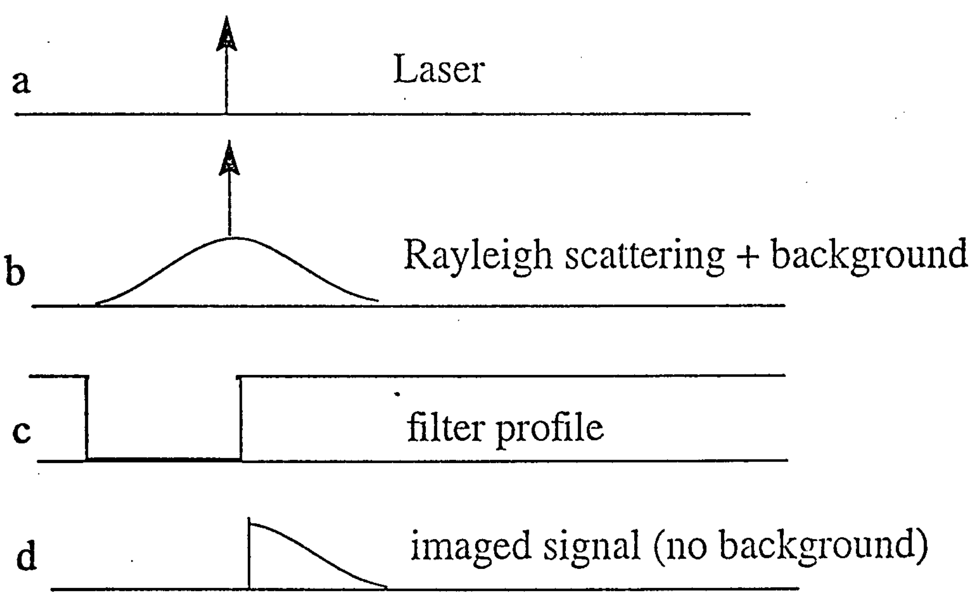

FILTERED RAYLEIGH SCATTERING IMPLEMENTATION

- Source
  - Tunable Ultraviolet, Injection Locked Laser
  - Ti:sapphire with "Ramp and Lock" Technology (Schwartz Electro-Optics)
- Filter
  - Atomic Mercury Vapor
  - 2" Diameter Cell Held at 40°C with a hot water bath (vapor pressure 1 Torr)
- Camera
  - UV Sensitive, Intensified CCD (Princeton Instruments)

SEQUENTIAL RAYLEIGH IMAGES OF MACH 2.5 SHOCKWAVE / BOUNDARY LAYER INTERACTION AT A 14° WEDGE

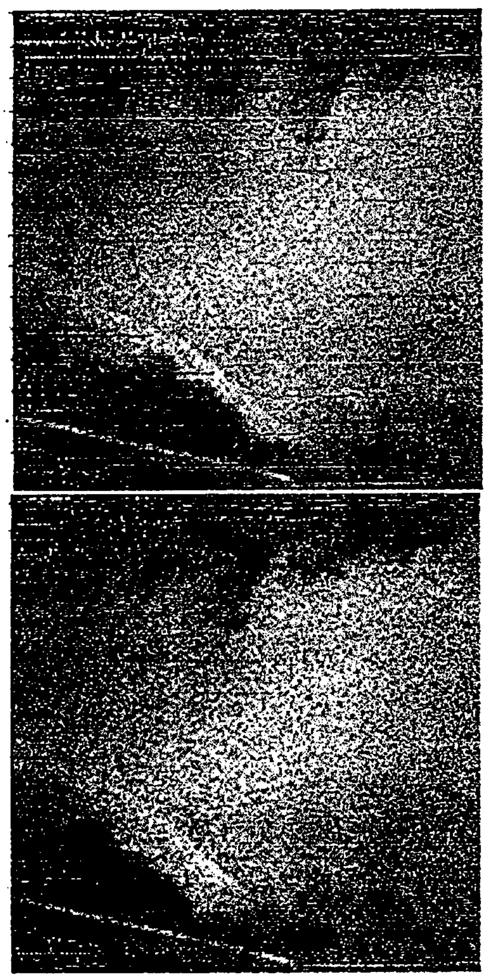

Framing rate is 500,000 images per second

Mariah II

- No wind tunnel can at present be run to accurately simulate flight conditiona at higher than Mach 8
  - 240K, (120,000 ft) requires 2800K, 8 atm in plenum
  - NO contamination
  - Low static T or low static P (enthalpy too low or entropy too high)
  - Short time operation

- Radiatively Driven concept adds energy downstream of the throat in the supersonic section
  - Static temperature stays low
  - Low temperature but high pressure in the plenum
  - Concept is driven by lasers or electron beams
  - Demonstrated with 10KW laser in December at Wright Labs

- MHD section is to be added to further accelerate the flow after the Radiative section
  - Reduces the front end pressure requirement
  - Extends the envelop of the tunnel
  - Requires electron beam sustained conductivity
  - Must operate at close to room temperature and at pressures on the order of .1 atm.

Energy Addition by Lasers

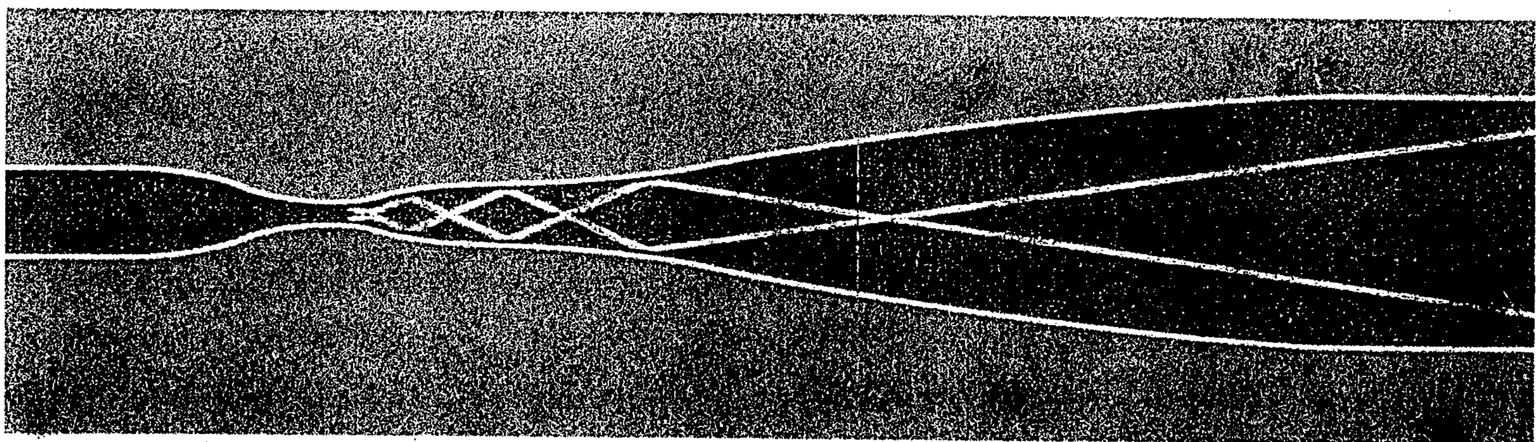

RDHWT Review April 23 - 24, 1997

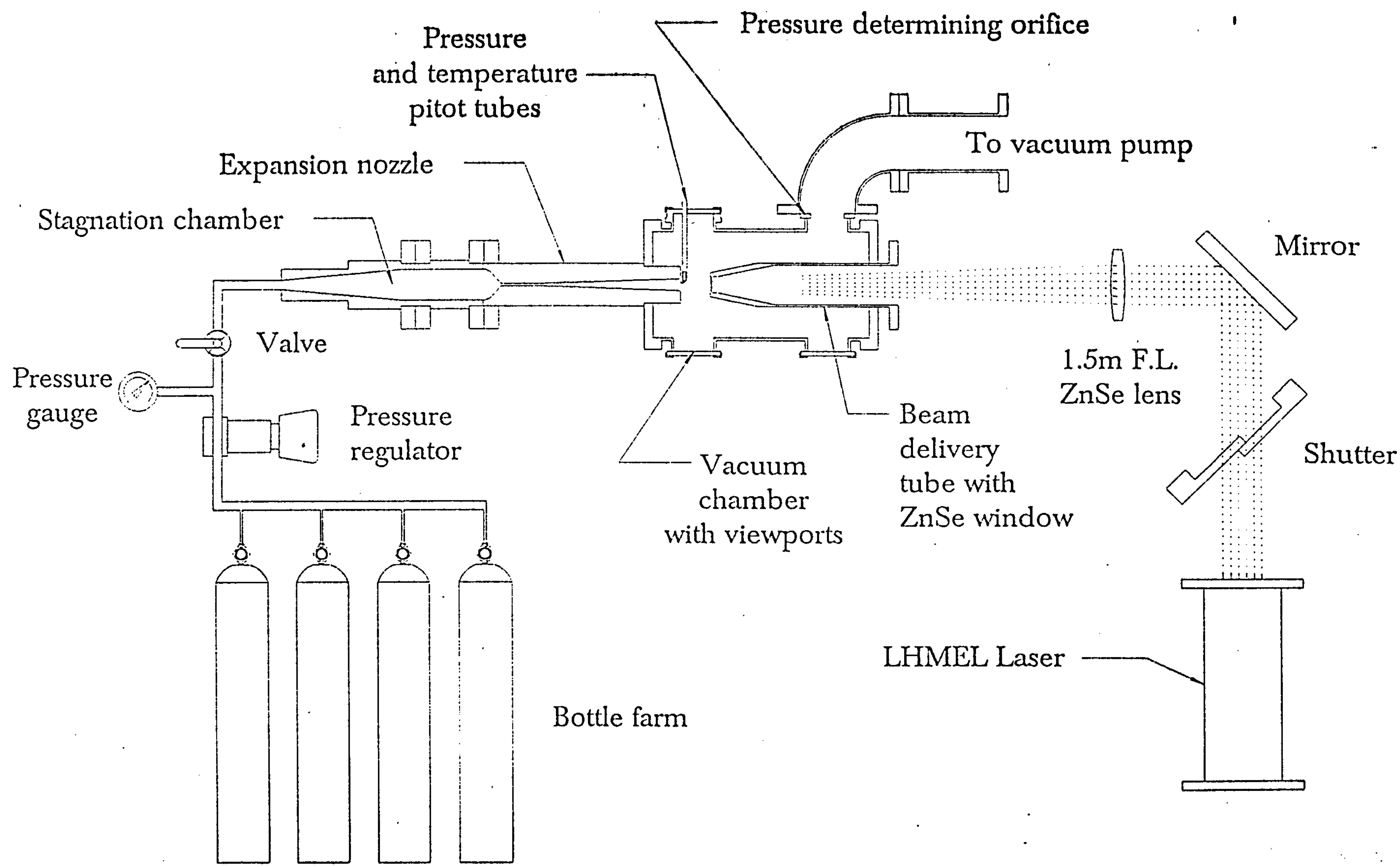

Figure 1. Diagram of 10 kw laser energy addition experiment

CFD - Energy Addition

- At exit $\Delta M \sim 1$

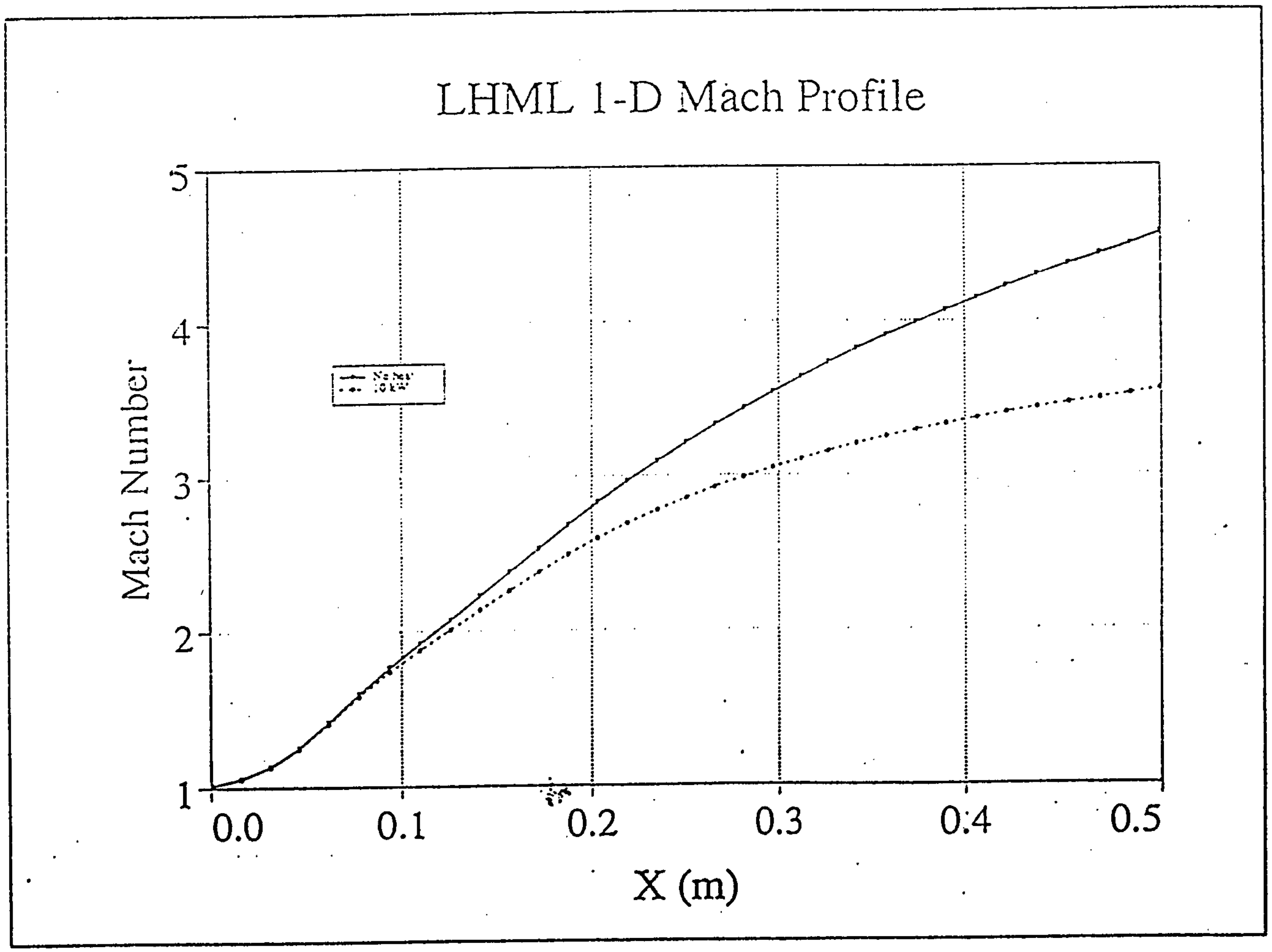

Thermodynamic Comparison of Philosophies

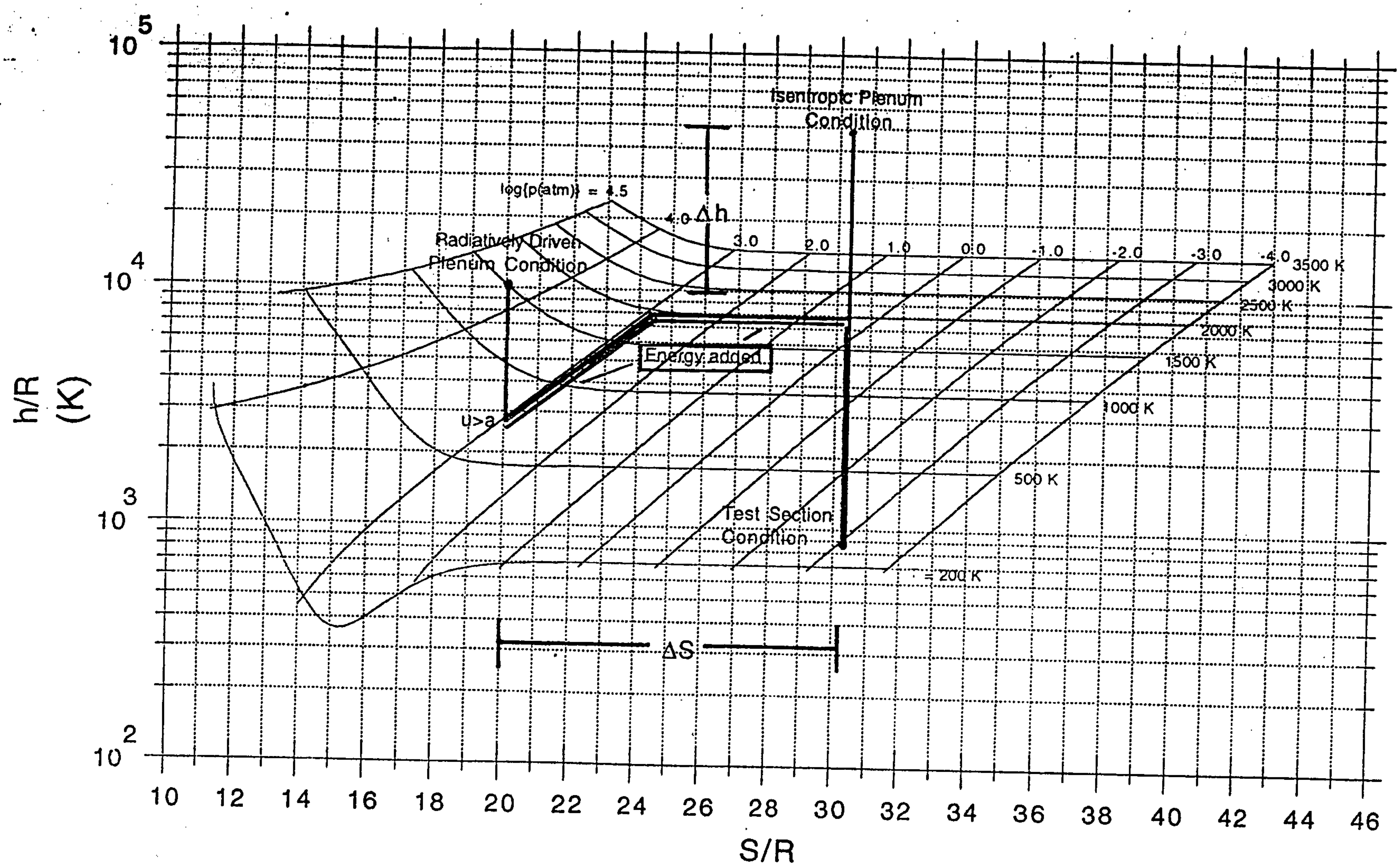

Energy equal to the energy deficit between the two plenum conditions is added along the highlighted path which is determined by the tunnel profile. An effective temperature, $\Delta h/\Delta s$, indicates the mean temperature at which the enthalpy must be coupled. Note that real gas effects are significant in the plenum region so that enthalpy is a function of pressure.

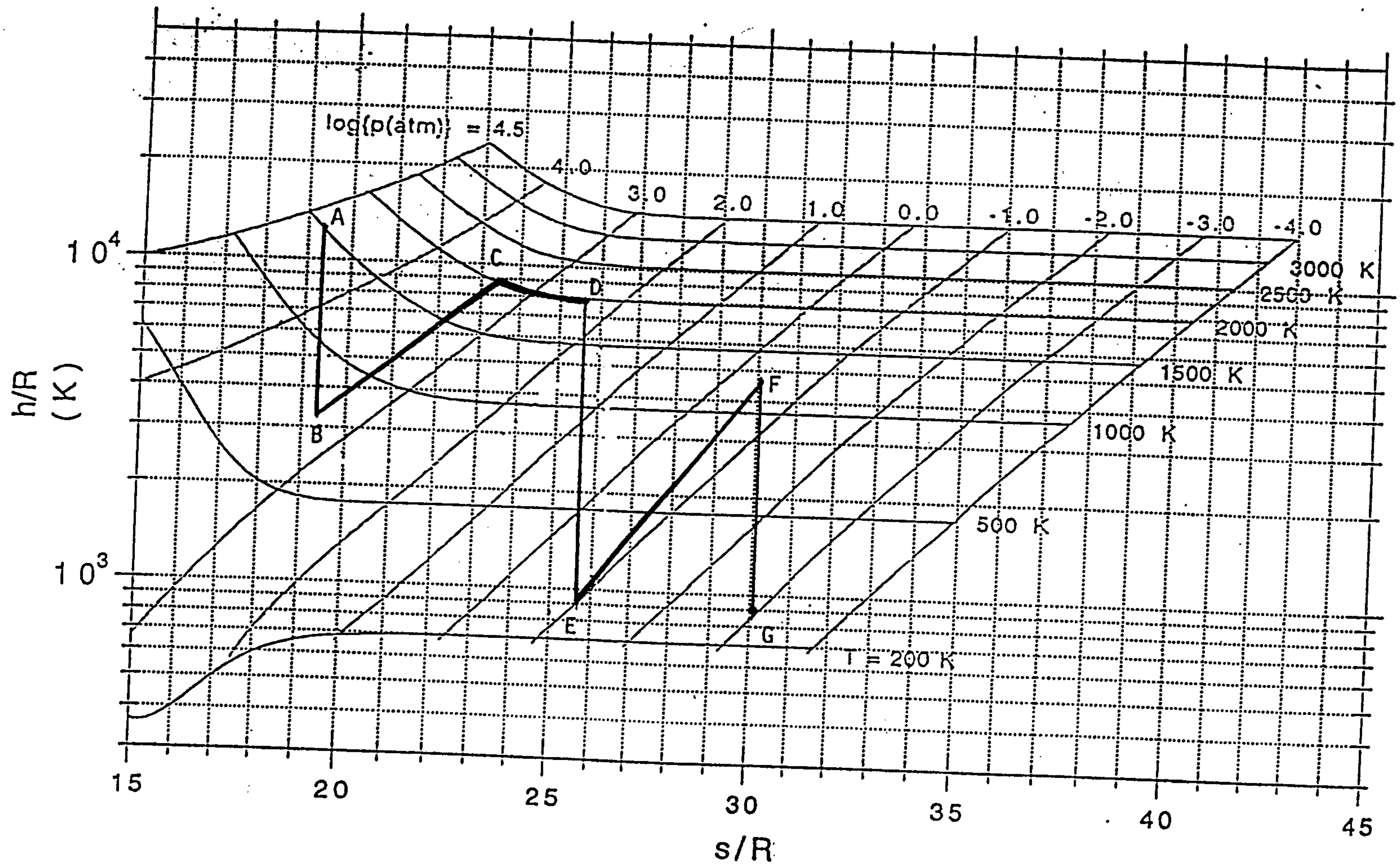

log(p(atm)) = 4.5
4.0
3.0
2.0
1.0
0.0
-1.0
-2.0
-3.0
-4.0
3000 K
2500 K
2000 K
1500 K
1000 K
500 K
T = 200 K
A
B
C
D
E
F
G
h/R
(K)
10^4
10^3
15
20
25
30
35
40
45
s/R

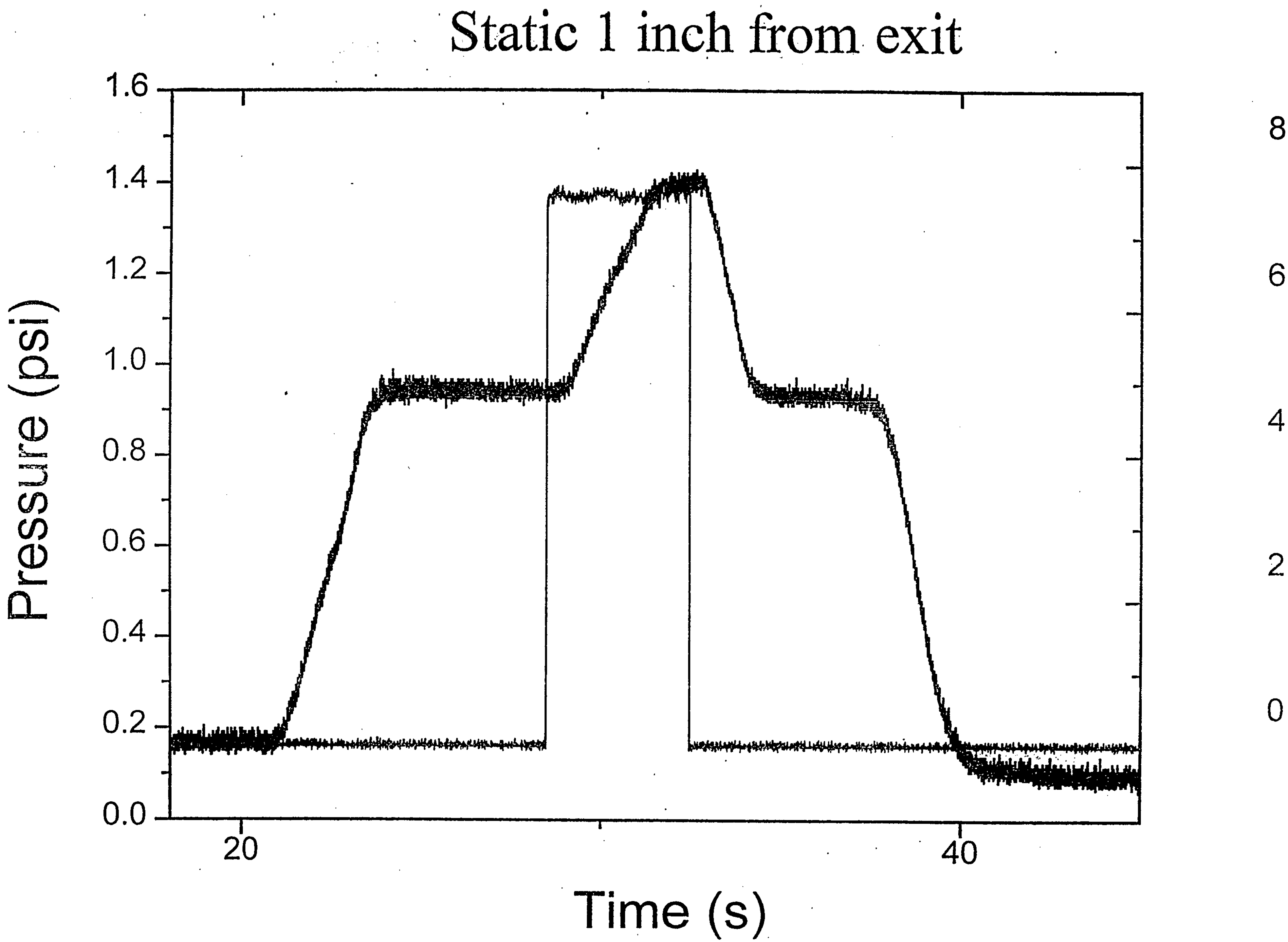

Static 1 inch from exit
Pressure (psi)
1.6
1.4
1.2
1.0
0.8
0.6
0.4
0.2
0.0
8
6
4
2
0
20
40
Time (s)

Flow Around Probe

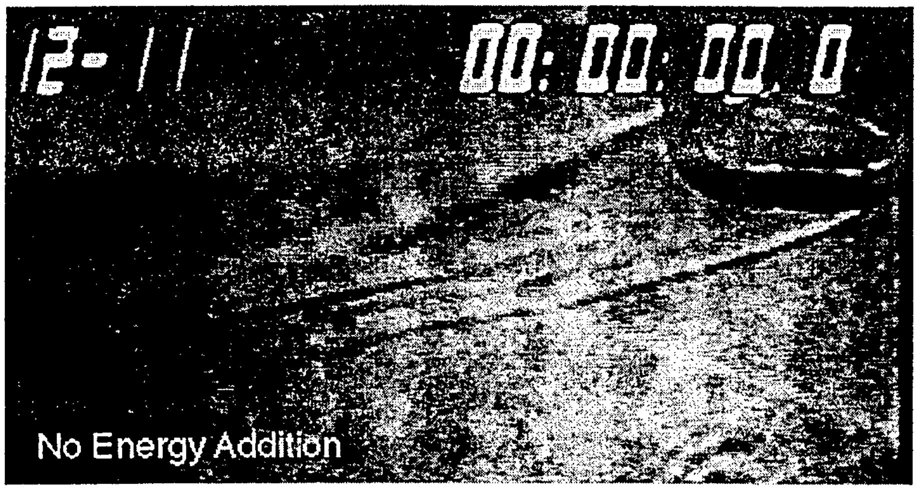

Laser Off
M = 4.3

Laser On
M = 3.9

Results verified by Pitot Measurements

Energy Addition by Electron Beams

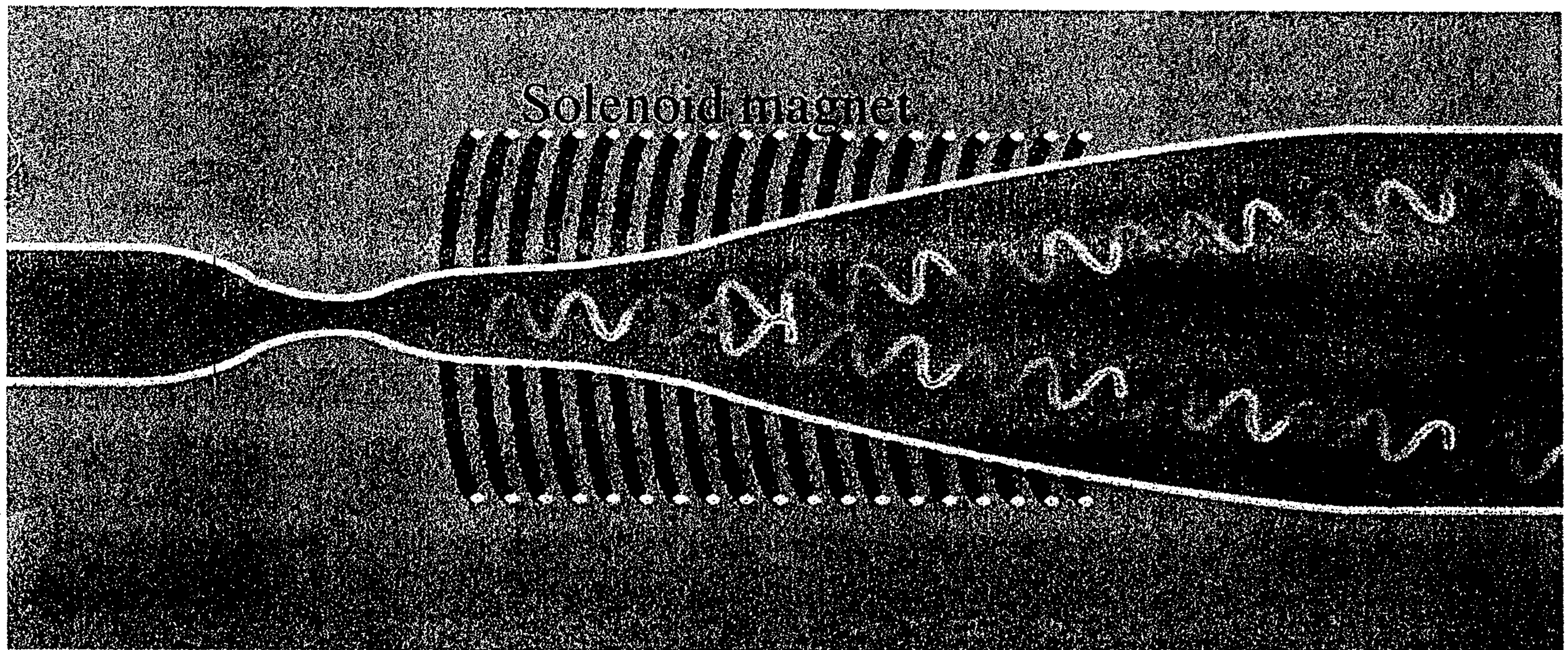

Hybrid Hypersonic Wind Tunnel with E-beam Heating and MHD Acceleration
Mach 14, 3.0-m Exit Diameter

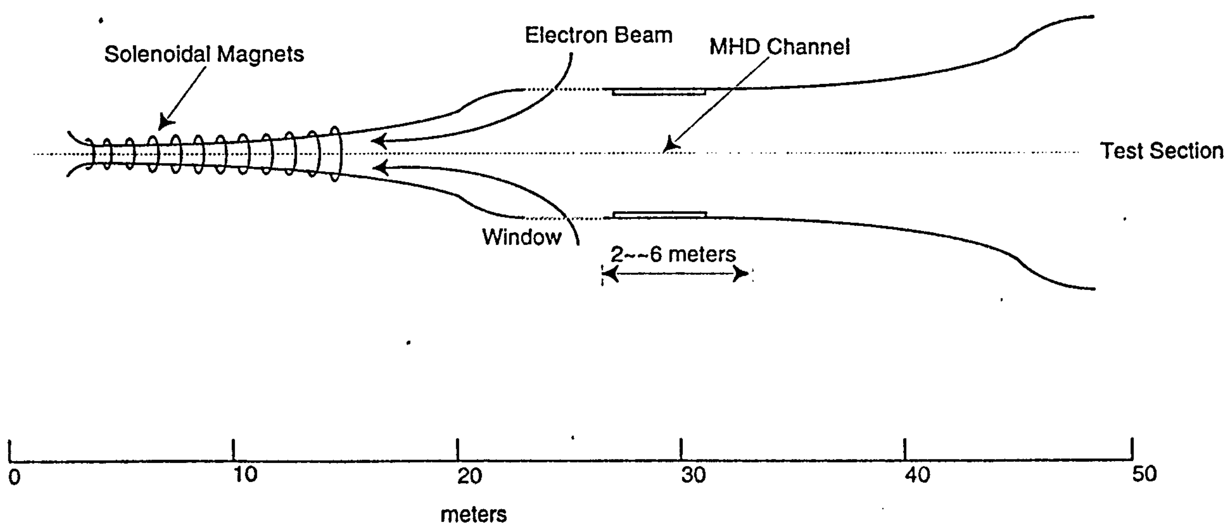

Thermodynamic limit of RDHWT:

$$\Delta h = T_a \Delta s$$

T_a can't be extremely high (erosion, chemistry); minimum s is defined by incompressibility; maximum s is defined by test section requirements.

THERMODYNAMIC ADVANTAGE OF MHD

Total enthalpy augmentation:

$$\Delta h_t = \frac{K}{K-1} T \Delta s$$

where $K \equiv E/(uB) =$ (Energy added)/(Push work)

The best thermodynamically:
when $K \to 1$, Δh_t can be large even for small $T \cdot \Delta s$
(non-entropy-generating energy addition).

However, when $K \to 1$, $j = \sigma \cdot (E - uB) \to 0$,
and to add

$$\Delta h_t = \sigma K(K-1) u B^2 L/\rho \,,$$

very large conductivity, σ, and/or length, L, would be required

AJAX

Proposed by Russians in 1990

(Vladimir Freistadt -

State Hypersonic Systems Scientific Research Enterprise

St. Petersburg)

- MHD converter in the inlet connected to MHD accelerator in the nozzle to by-pass free stream kinetic energy and reduce the entropy rise in the inlet.

  - Reduces the flow to subsonic in the combustor
  - MHD conditions almost the same as Mariah II
  - Requires some method to sustain conductivity

- Reduction in vehicle drag by cold plasma injection at the nose

- Increase of combustion volume and efficiency within the engine by plasma injection or injection of materials ahead of the fuel injectors

- Reforming of kerosene and water into hydrogen and CO for fuel.

Computational Hypersonics Initiative in Air Force Research Laboratory

J. S. Shang
Air Vehicle Directorate
Air Force Research Laboratory
Wright-Patterson Air Force Base, Ohio 45433

Objective

- Rekindle a multidisciplinary computational modeling and simulation research to support the USAF New World Vista Vision.
- Develop an enabling critical simulation technology for aerospace vehicle in hypersonic flight regime.
- Research the potential of electromagnetics/shock interaction as a new flowfield control mechanism.

Scientific "Findings" in Plasma/Shock Interaction

- Appearance of a shock precursor and increase standoff distance of bow shock wave in weakly ionized gas.
- Shock propagation velocity increases and shock front disperses in plasma medium.
- Intermingled reflected compression and rarefaction waves propagation in inhomogeneous plasma media.
- Aerodynamic drag and heat transfer to solid surface are modified by weakly ionized gas.
- Magnetic field suppresses laminar-turbulent transition bypass.

Macroscopic Conservation Equations

$$
\begin{aligned}
\frac{\partial \rho \alpha_i}{\partial t} &+ \nabla . \left(\rho \alpha_i \bar{u} + \rho \alpha_i \bar{u}_i \right) = \dot{r}_i \\
\frac{\partial \rho}{\partial t} &+ \nabla . \left(\rho \bar{u} \right) = 0 \\
\frac{\partial \rho \bar{u}}{\partial t} &+ \nabla . \left(\rho \bar{u} \bar{u} - \bar{\bar{\tau}} \right) = \rho \sum \bar{f}_i \\
\frac{\partial \rho e}{\partial t} &+ \nabla . \left(\rho e \bar{u} + \bar{u} . \bar{\bar{\tau}} - k \nabla T + \rho \sum \alpha_i h_i \bar{u}_i + \dot{q}_r \right) + \sum_i \dot{r}_i \Delta h_i^o \\
&= \rho \sum \alpha_i \bar{f}_i . \left(\bar{u} + \bar{u}_i \right)
\end{aligned}
$$

In numerical simulations of hypersonic flows, this system of conservative equations is usually written in strong conservation form.

$$\frac{\partial U}{\partial t} + \frac{\partial F}{\partial x} + \frac{\partial G}{\partial y} + \frac{\partial H}{\partial Z} = 0$$

Arrhenius equation

In order to apply the law of mass action, the rate of reactions is assumed to be independent of whether or not the system is in equilibrium. This commonly accepted assumption is consistent with the local equilibrium approach. The rate constant is given as $K_{c,j} = K_{f,j}/K_{b,j} = \Pi(X_i)^{\nu''_{i,j}}/\Pi(X_i)^{\nu'_{i,j}}$ Only when the gas mixture is in chemical equilibrium, the forward andreverse reactions are in dynamic balance, and the net rate of change in compostion vanishes.

$$\left(\frac{dX_i}{dt}\right)_j = \left(\nu''_{i,j} - \nu'_{i,j}\right) K_{f,j} \left[\Pi\,(X_i)^{\nu'_{i,j}} - \frac{1}{K_{c,j}}\Pi\,(X_i)^{\nu''_{i,j}}\right]$$

The so-called rate constant has been experimentally recognized as

$$K_{c,j} = C\,\exp\left(-\frac{\epsilon_a}{KT}\right)$$

This is the well-known Arrhenius equation, and the constant ϵ_a is often refered to as the Arrhenius activation energy. This equation has been modified to better fit to measurements as

$$K_{c,r} = CT^{\eta}\exp\left(-\frac{\epsilon_a}{KT}\right)$$

Internal Degree of Excitation of Gas Medium

The partition function of a microscopic particle is fundamentally important in relating atomic/molecular structure,which influence the energy level, and thermodynamic behavior.

$$Z = \sum_i g_i \ \exp\left\{-\frac{\epsilon_i}{kT}\right\}$$

Usually, the coupling of internal degrees of freedom of gas medium is neglected, this assumption leads to the factorization property of partition functions.

$$Z = Z_{trs}.Z_{rot}.Z_{vib}.Z_{el}$$

The energy of different internal degree of excitations is additive, the total internal energy is then found by summing the translational, rotational, vibrational, and electronic modes.

$$E_i = E_t + E_r + E_v + E_e$$

Partition Functions of Internal Degree of Freedom

$$
\begin{aligned}
\text{Translational DOF} \quad Z_{trs} &= \left(\frac{2\pi mkT}{h^2}\right)^{\frac{3}{2}} V \\
\text{Rotational DOF} \quad Z_{rot} &= \frac{T}{\sigma\theta_r} \\
\text{Vibrational DOF} \quad Z_{vib} &= \frac{1}{1 - \ \exp\left\{\frac{\theta_v}{T}\right\}} \\
\text{Electronic DOF} \quad Z_{el} &= g_o + \sum_i g_i \ \exp\left(-\frac{\theta_{e,i}}{T}\right)
\end{aligned}
$$

Shortcomings in Computational Hypersonics

- Inadequate description of transport property.
- Unreliable non-equilibrium kinetic models for vibration-vibration and vibration-translation energy transfer.
- Marginal numerical accuracy and low computational efficiency.
- Sparse or non-existent verification data base.

Mobility of Charged Particles

Langevin's Formula

$$D = \frac{3}{8}\sqrt{\frac{\pi}{2}}\frac{1}{nS_D}(\frac{m+M}{mM}kT)^{\frac{1}{2}}$$

$$\frac{u}{E} = \frac{3}{8}\sqrt{\frac{\pi}{2}}\frac{q}{nS_D}(\frac{m+M}{mM}\frac{1}{kT})^{\frac{1}{2}}$$

Mobility of Heavy Ions

$$D = \frac{3}{8}\sqrt{\pi}L(\frac{m+M}{mM}kT)^{\frac{1}{2}}$$

$$\frac{u}{E} = \frac{3}{8}\sqrt{\pi}qL(\frac{m+M}{mM}\frac{1}{kT})^{\frac{1}{2}}$$

$$L = \frac{1}{\sqrt{2}nS_d}$$

Mobility of Free Electrons

$$\frac{u_e}{E} = \frac{2}{3}\sqrt{\frac{2}{\pi}}\frac{eL_e}{(mkT)^{\frac{1}{2}}}$$

$$L_e = 4\sqrt{2}L$$

Understanding and Control of Ionized High-Speed Flows

AFOSR Workshop

Plasma Aerodynamics Studies

N. Malmuth, V. Soloviev, H. Hornung, V. Bytchkov
V. Krivstov, A. Konchakov, A. Tseskis and V. Velikodnyi

February 26, 1998

Rockwell
Science Center

Other Team Members

- W. Beaulieu, Boeing Aircraft and Missile Systems
- P. Bellan, Caltech
- A. Fedorov, Moscow Institute of Physics and Technology
- I. Goldberg, Rockwell Science Center
- A. Klimov, Moscow Technical Club
- K. Lee, Rockwell Science Center
- S. Leonov, Moscow Technical Club
- D. Ota, Rockwell Science Center
- S. Palinswamy, Metacomp
- S. Ramakrishnan, Rockwell Science Center

Rockwell Science Center

Plasma Aerodynamics
Objectives/Approach

- Program Objectives
  - Determine basic physical processes of plasma aerodynamic augmentation
  - Develop analytical and computational models of these processes
  - Provide links with experiments
    - F-15 flight test
      - Ground and on-board flight instrumentation
      - Plasma generator technology
    - Wind tunnel , ballistic range, discharge tube and other ground tests
      - coupling with analytical model development, *e.g.* cross-validations
      - design and intepretation of experiments

Objectives/Approach (cont'd)

- Approach
  - Study importance of key physical mechanisms in flow such as:
    - plasma energy addition to flow such as Joule heating
    - anomalous dispersion
    - ion-acoustic waves
    - non-equilibrium phenomena
    - second viscosity and other transport parameter modification
    - electromagnetic effects such as induced *B* fields and Lorentz forces
  - Use solutions of unit problems such P1-P4 (for which limited experimental databases exist) to isolate these important mechanisms
  - Interface with experiments
    - Design new experiments
    - Compare evolving theoretical models with previous datasets

Supercruise Fighter

Plasma Aerodynamic Enhancements

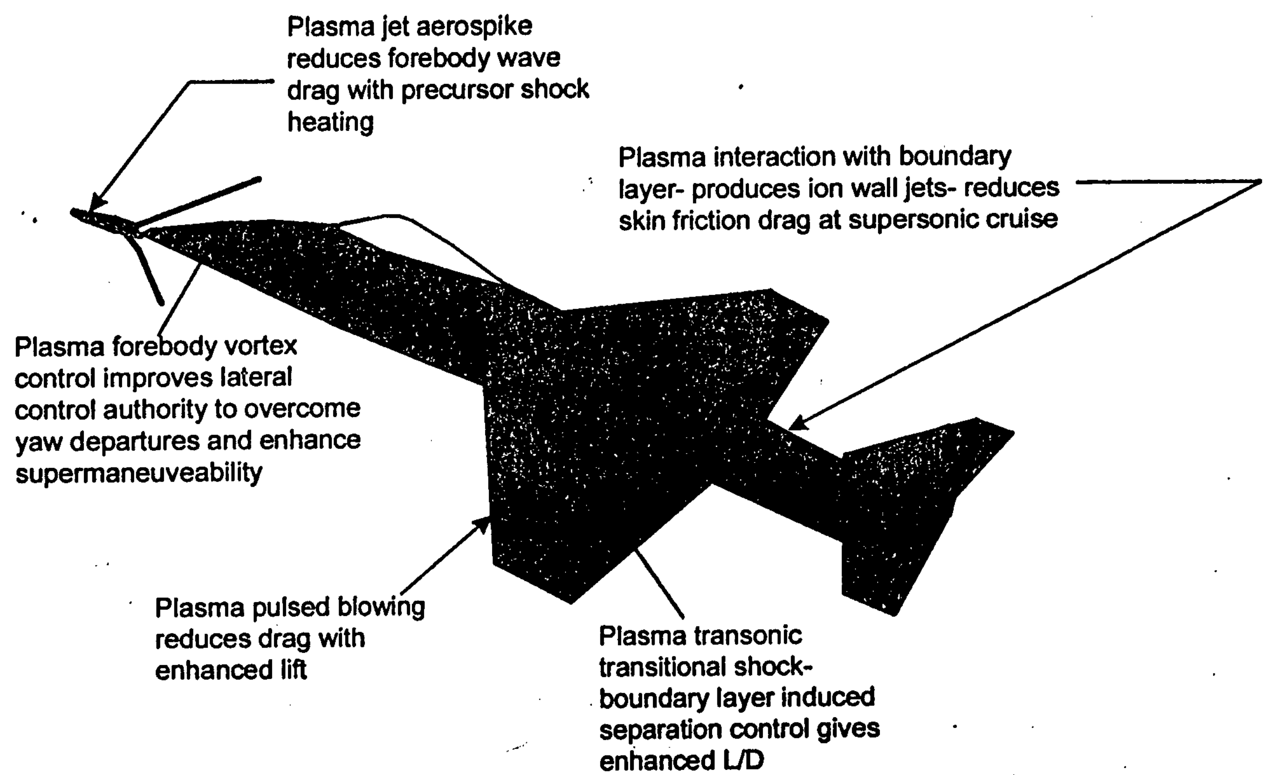

Noseboom Plasma Flow Control

(Problem P4)

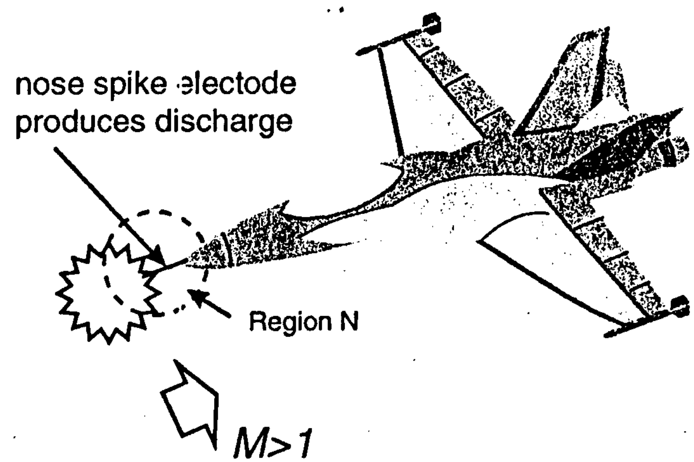

- Basic hypotheses:
  - dissipative processes in plasma lead to
    - Joule heating that reduces pressure drag
    - control of nose separation and nose shocks
- Problem is a useful departure point for treatment of:
  - Problem 3: erosive plasma + RF discharge on F-15
  - 1-D shock structure
  - hypersonic applications
- P4 study useful since experimental dataset available to test models

Problems

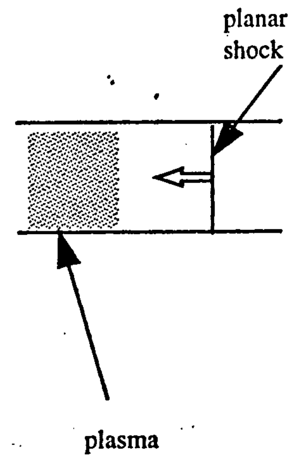

Problem 1

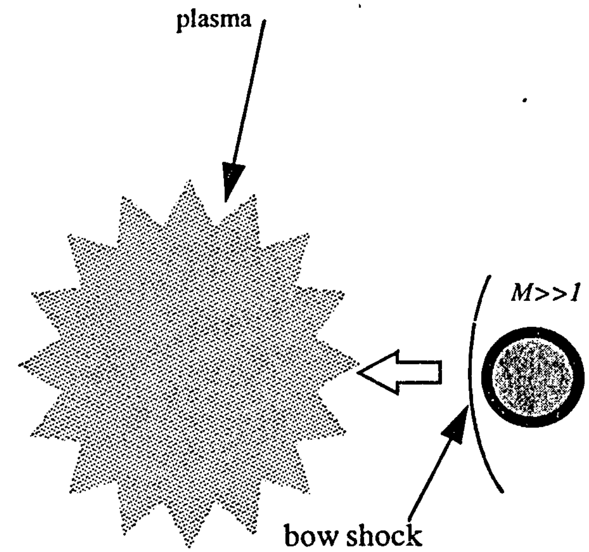

Problem 2

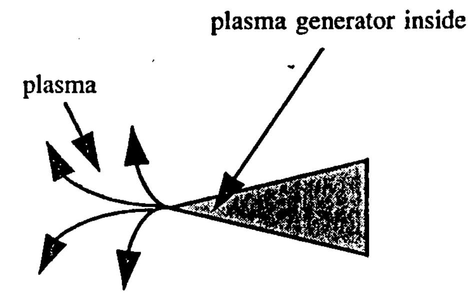

Problem 3 - (F-15)

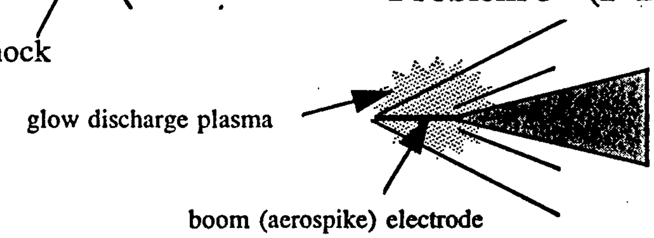

Problem 3a - (F-15)

3

Plasma Shock Structure

- Modify 1-D Navier Stokes equations to model
  - electric field and other plasma terms
  - second viscosity
  - relaxation
  - anomalous dispersion
- Examine scaling of shock thickness with strength from Russian experiments

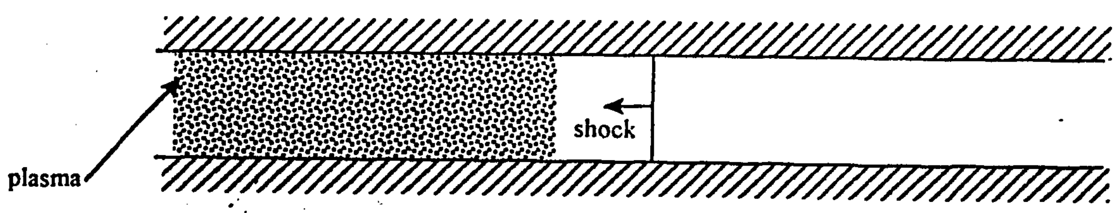

1-D shock propagating into a plasma

Perfect Gas Shock-Layer Problem

Equations of Motion

Continuity

$$\frac{d}{dx}(\rho u) = 0$$

Momentum

$$\rho u \frac{du}{dx} + \frac{dp}{dx} = \frac{d}{dx}\left(\mu'' \frac{du}{dx}\right)$$

Energy

$$\rho u \frac{dh}{dx} - u \frac{dp}{dx} = \frac{d}{dx}\left(\frac{\mu''}{\mathrm{Pr}''} \frac{dh}{dx}\right) + \mu''\left(\frac{du}{dx}\right)^2$$

$\mu'' \approx 2\mu + \lambda$, $\mu \equiv$ shear viscosity, $\lambda \equiv$ "second" viscosity, $\mathrm{Pr}'' \equiv$ Prandtl Number

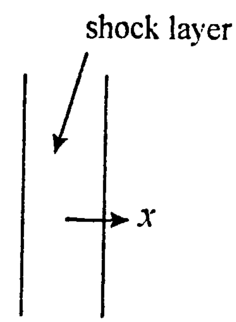

Boundary conditions

$$\frac{du}{dx}, \frac{dh}{dx} \to 0, \text{ as } x \to \pm\infty$$

Solution for Shock Thickness

$$\delta = \frac{32\left(\gamma + (\gamma - 1)\left(\frac{1}{\mathrm{Pr}''} - 1\right)\right)\nu'}{3(\gamma + 1)\left(V_f - V_i\right)}$$

$\delta \equiv$ viscous shock layer thickness

$V_f - V_i \equiv$ shock strength

$\gamma \equiv$ specific heat ratio

Scaling of Shock Attenuation with Thickness in a Plasma

SC.4052CS.022398

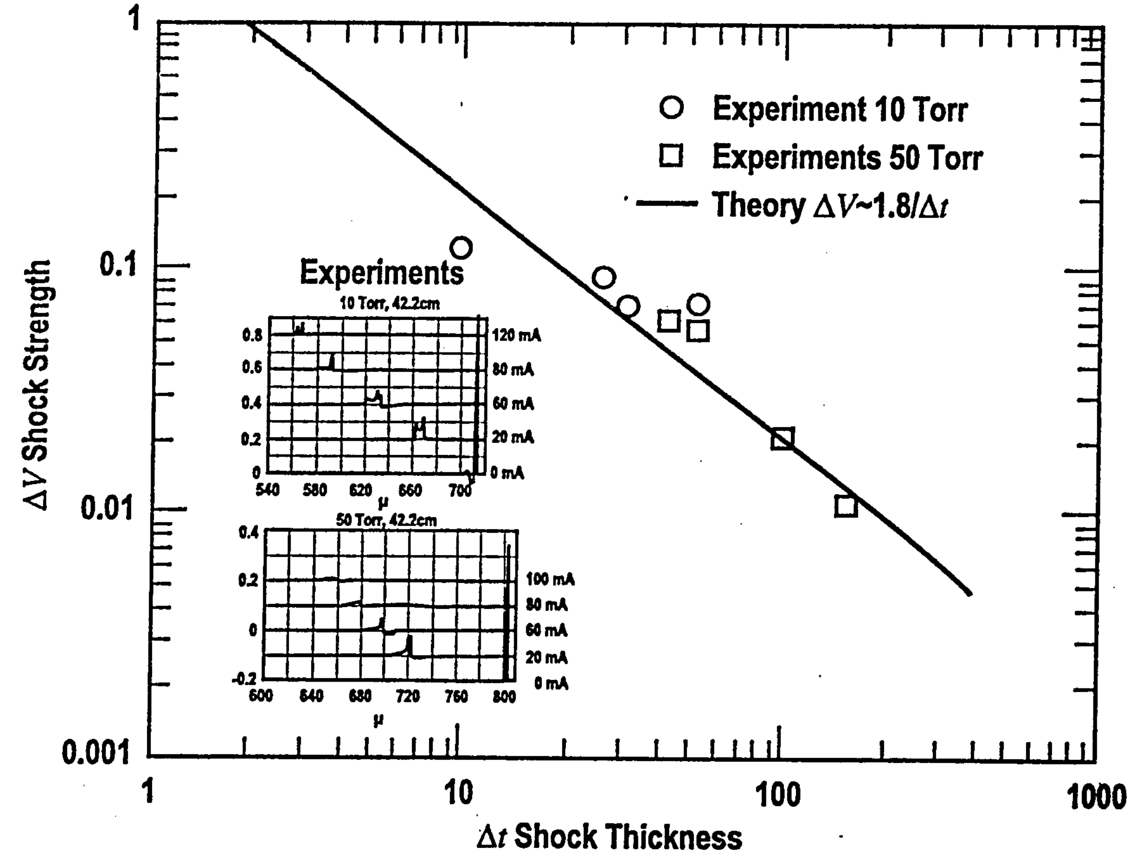

BOEING®

Rockwell Science Center

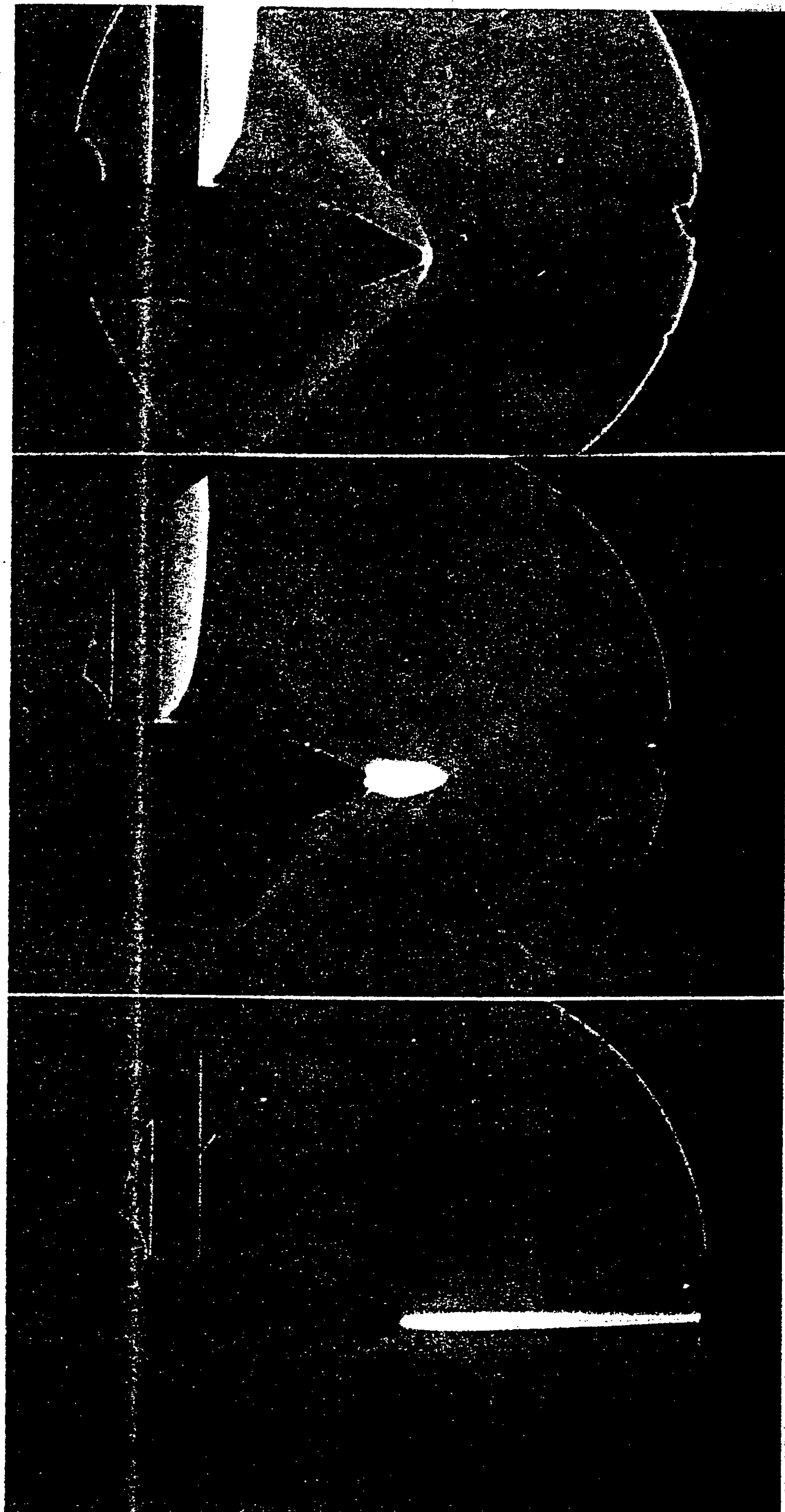

Drag Reduction Mechanisms

- Plasma jet aerospike extension
  - aerospike reduces drag by making a shallow oblique shock out of blunt nose detached almost normal shock
  - creates low pressure separation in front of blunt nose to give a net suction thrust increment
- Transverse shock due to plasma heating leading to rarefaction of separation region
- Interaction of separation and transition over the aerospike

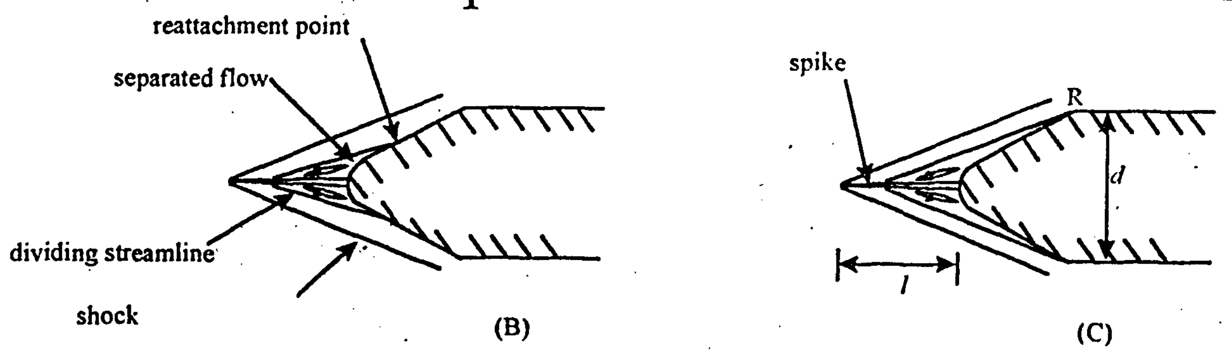

Flow Configurations

8

12

Aerospike Effect on Pressures

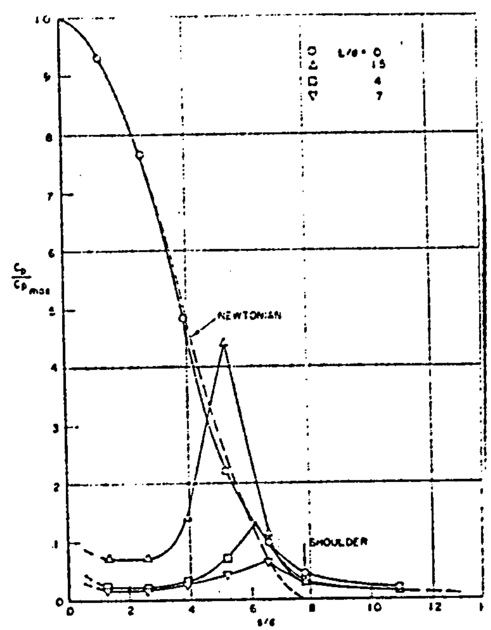

Bogdanoff and Vas JAS 1959

- Spike produces peak in pressures near reattachment point
- Peak attenuates with increasing spike length reducing drag
- Needs to be traded against high heat transfer near peak
- Plasma heating can affect reattachment and therefore pressure peak

Estimate of Drag Reduction

Approximate formula based on Newtonian on blunt nose and cone part

$$C_p = 2\left(\sin^2\varepsilon + \frac{1}{\gamma M_\infty^2}\right)(1-\alpha^2) + \frac{P_{\text{plateau}}\alpha^2}{q} - \frac{2}{\gamma M_\infty^2}\left(1-\left(\frac{r_{base}}{r_d}\right)^2\right)$$

$P_{\text{plateau}} \equiv$ pressure in separation region

$r_d \equiv \frac{d}{2}$

$\alpha \equiv \frac{r_j}{r_d}$

$r_j \equiv$ radius at juction of spherical nose tip with cone portion

$\varepsilon \equiv$ cone semiapex angle

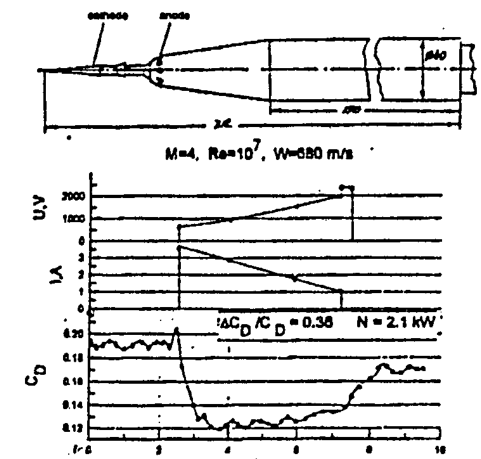

Figure 5 Wind Tunnel Experiments of the Electric Discharge Influence on Drag at TsAG

	Experiment	Estimated	Remarks/assumptions in separation zone
current off	.19	.216	plateau pressure=1/2 normal shock value
current on	.12	.07	vacuum due to plasma

Plasma On

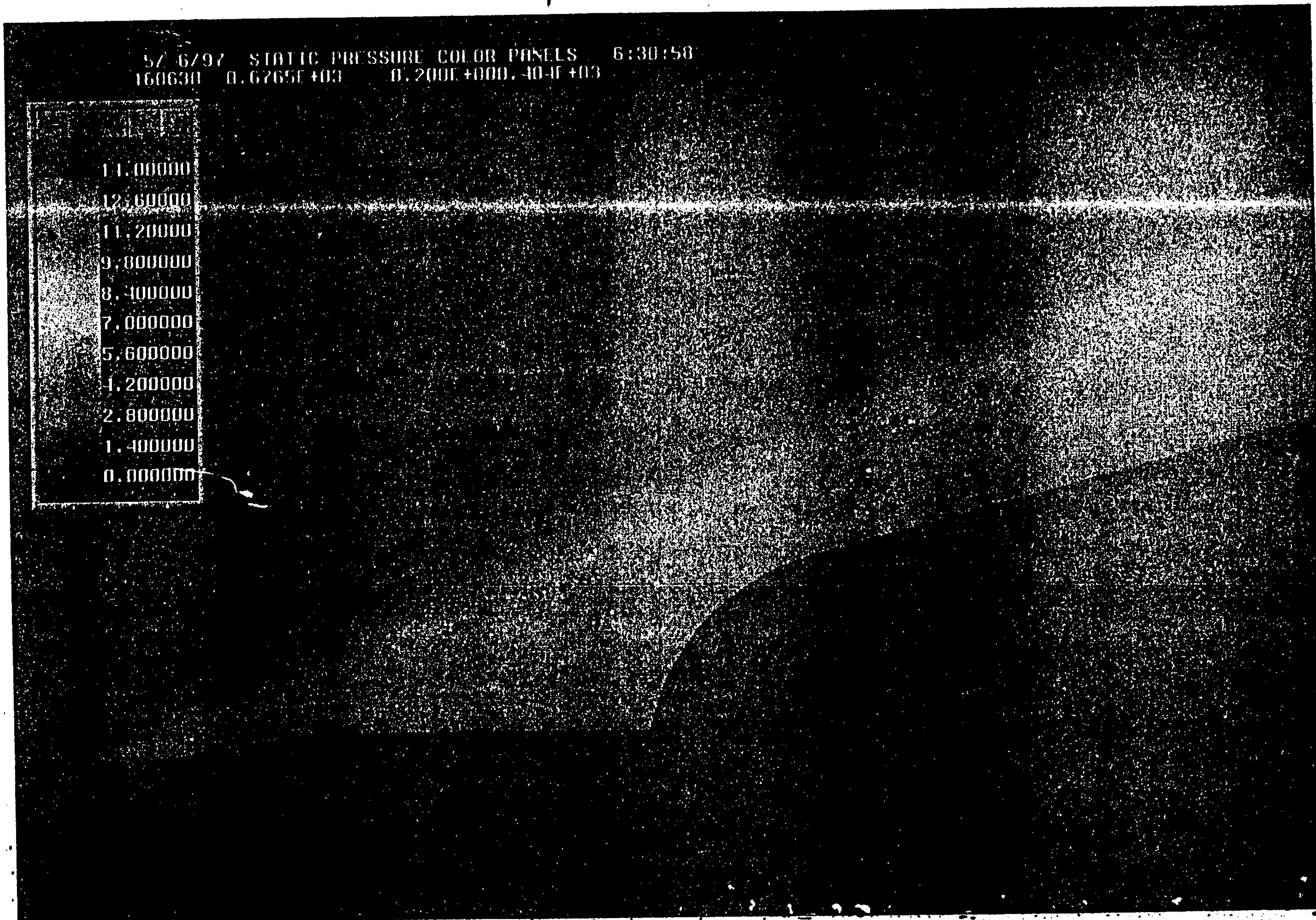

5/ 6/97 STATIC PRESSURE COLOR PANELS 6:30:58
160630 0.6765E+03 0.200E+000.404E+03
11.00000
12.60000
11.20000
9.800000
8.400000
7.000000
5.600000
4.200000
2.800000
1.400000
0.000000

Plasma Off

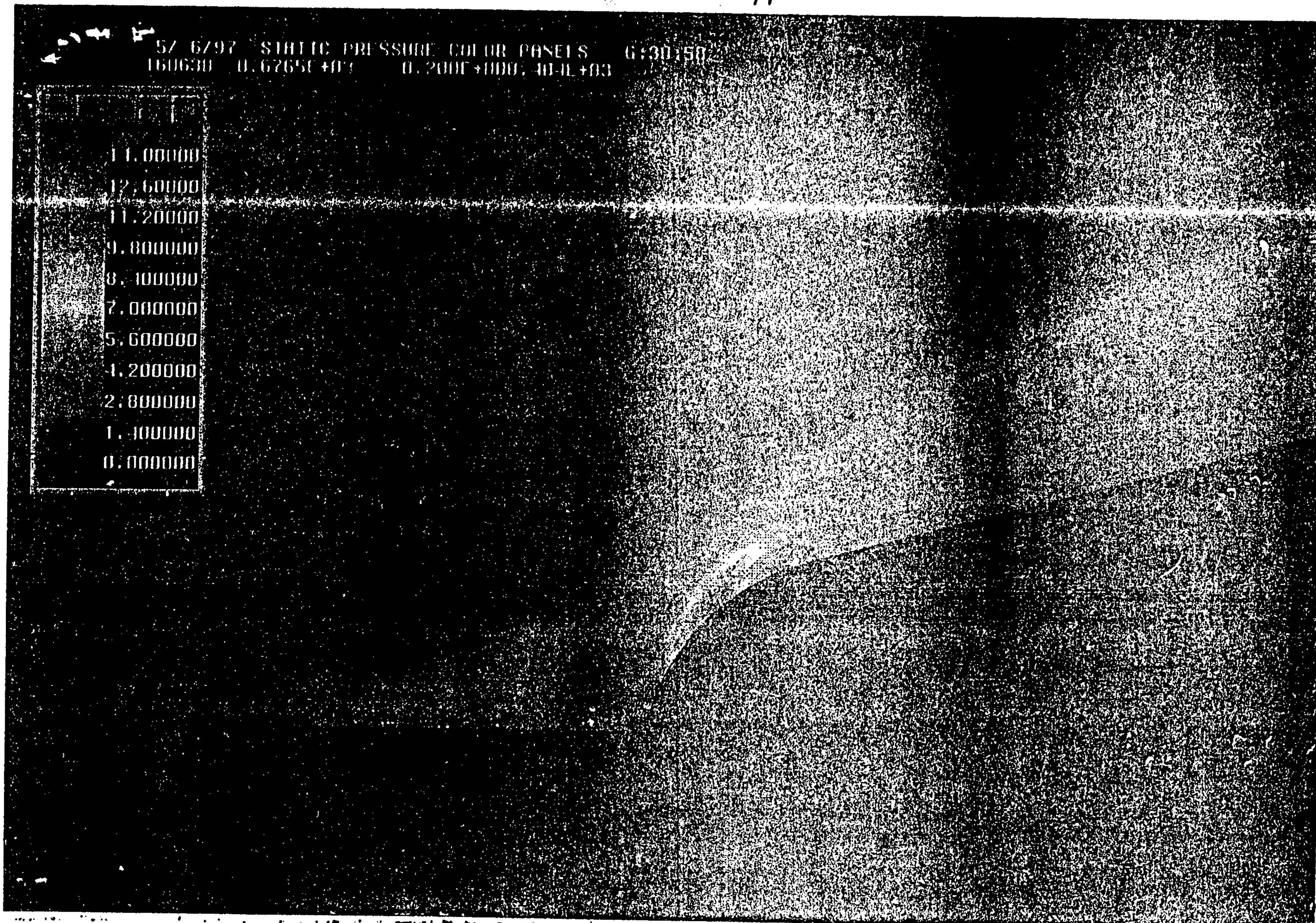

57 6797 STATIC PRESSURE COLOR PANELS 6:30:50
14.00000
12.60000
11.20000
9.800000
8.400000
7.000000
5.600000
4.200000
2.800000
1.400000
0.000000

Pressure and Skin Friction Distributions With Plasma Heating

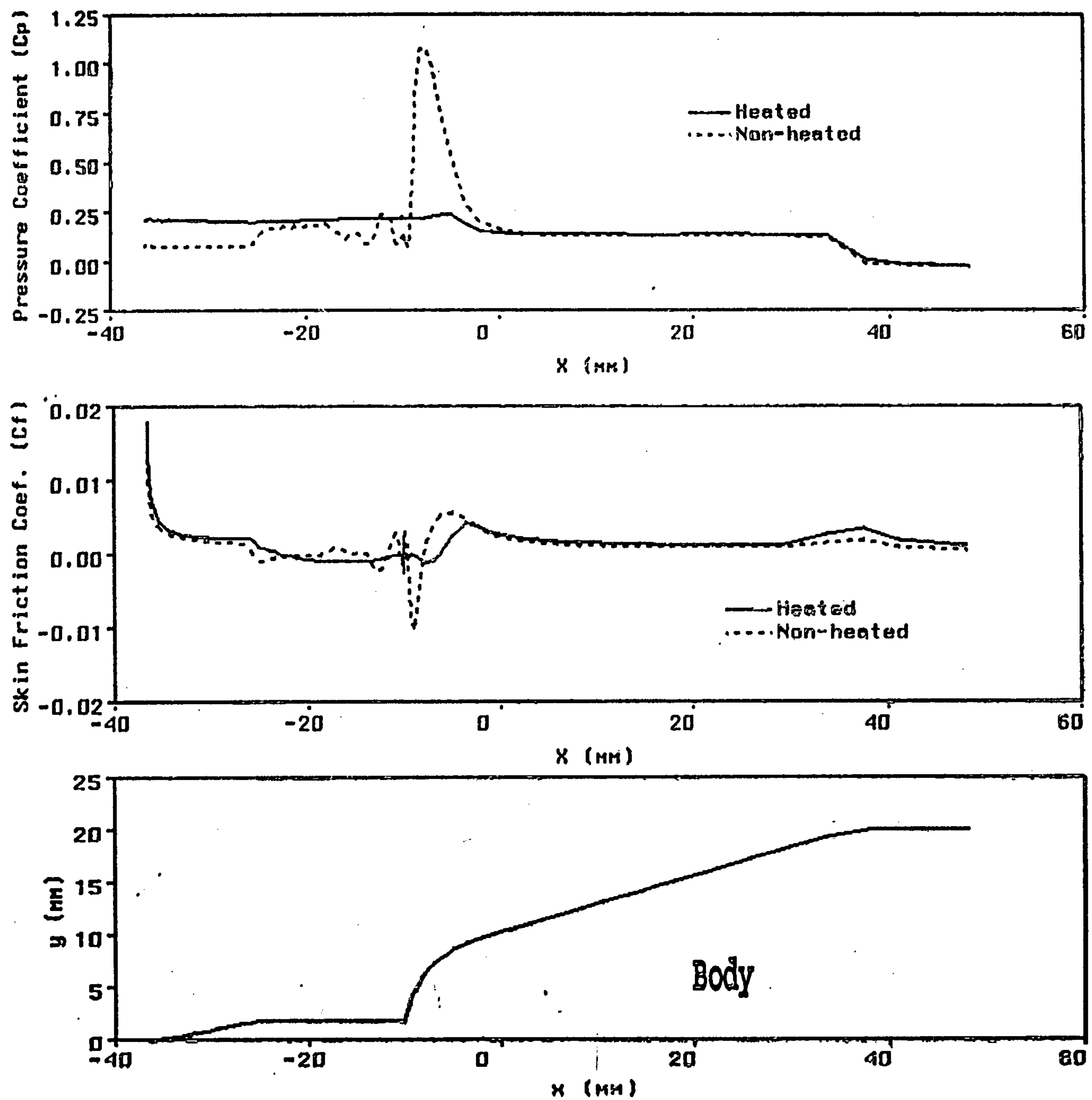

Cumulative Pressure and Skin Friction Drag with Plasma Heating

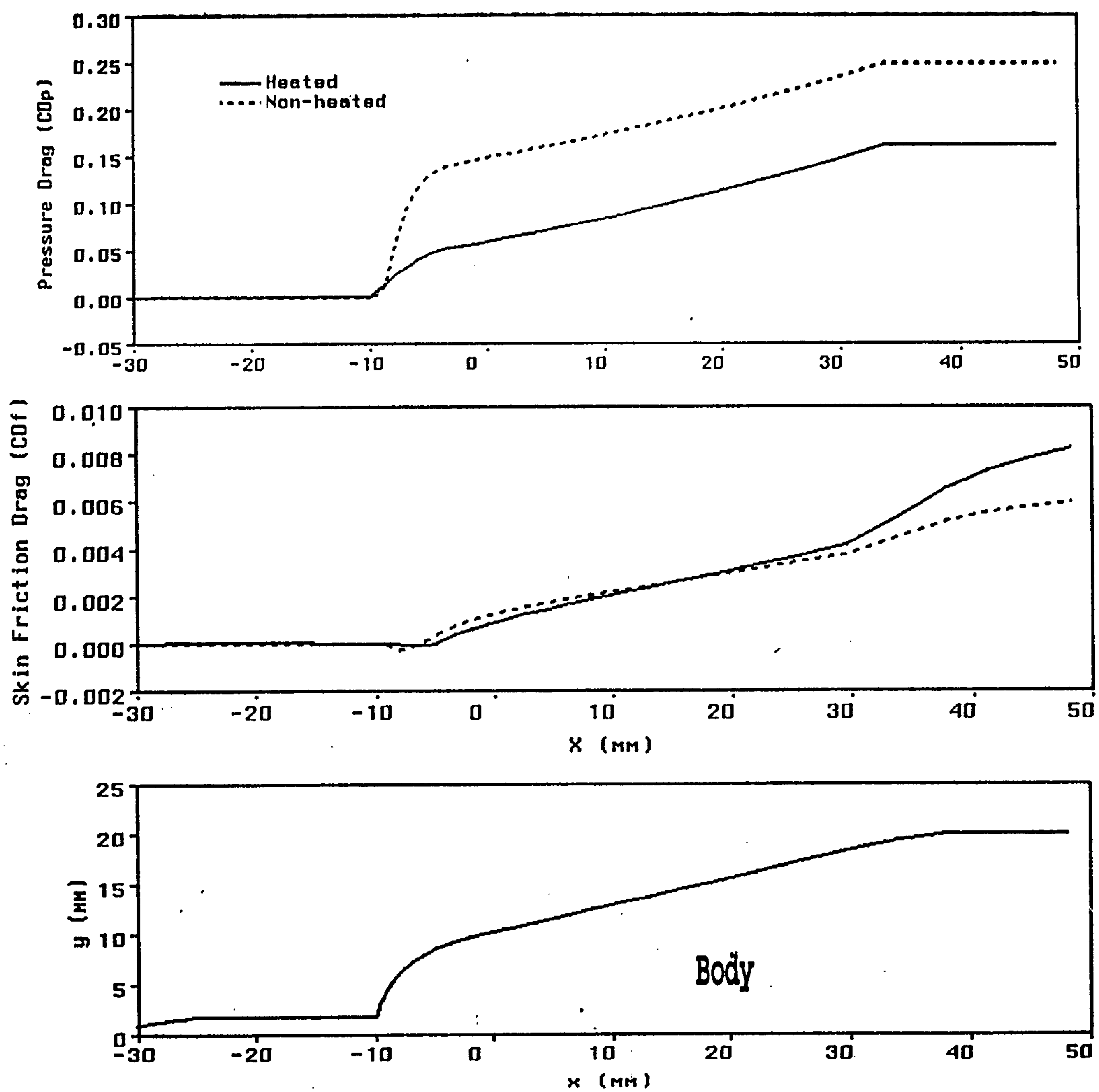

Comparison of Predicted Drags With Russian Experiments

	Rockwell Science Center Computation*	Russian Experiment
C_D (Plasma off)	0.254	0.220
C_D (Plasma on)	0.170	0.180
$\Delta C_D / C_D$	0.33	0.18

*Laminar Navier Stokes model with plasma power uniformly distributed over spike electrode surface

- Discrepancies above within experimental errors
- Heat source model may give dominant physics of spike electrode problem
- Computed relative drag changes agree with experimental order of magnitude

Rockwell
Science Center

Forebody drag of a cone-cylinder with counterflow jet in supersonic flow

- Objectives
  - Study competition of jet momentum drag with surface pressure drag
  - Study basic physical mechanisms
  - Relate to plasma jet effects

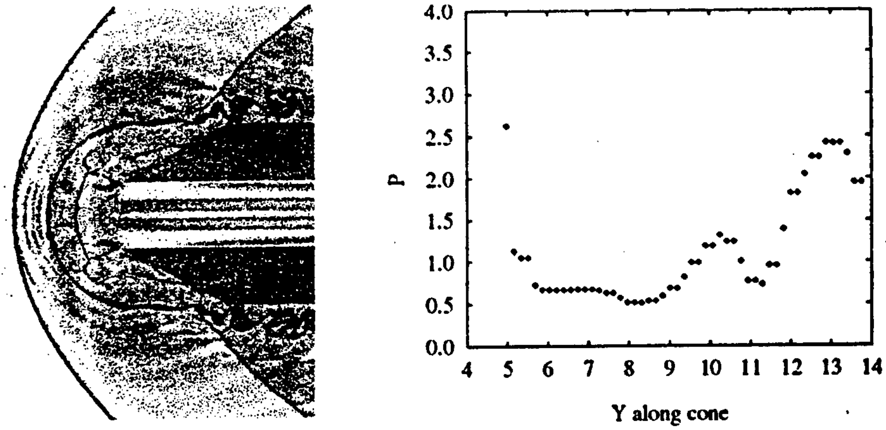

$p_4/p_\infty = 15.0$, $C_{D_c} = 0.395$, $C_{D_t} = 0.462$, $C_D = 0.857$

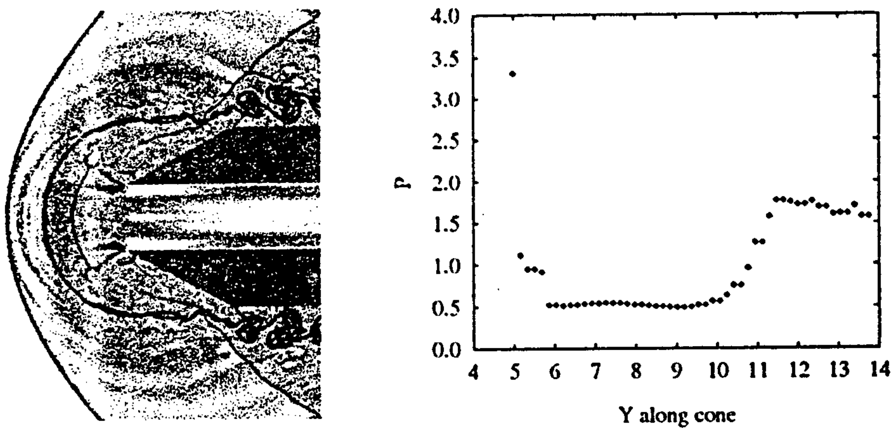

$p_4/p_\infty = 18.0$, $C_{D_c} = 0.342$, $C_{D_t} = 0.553$, $C_D = 0.895$

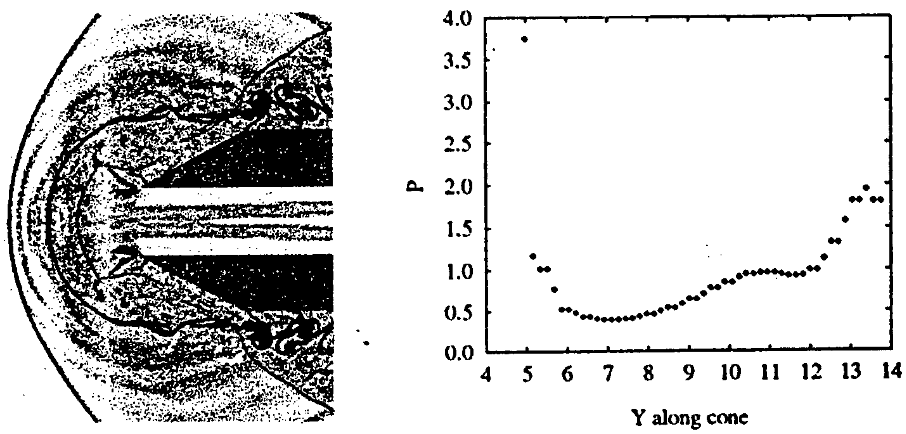

$p_4/p_\infty = 21.0$, $C_{D_c} = 0.312$, $C_{D_t} = 0.646$, $C_D = 0.957$

Counterflow jet, $M_\infty = 2.0$, $T_4/T_\infty = 10$, $\gamma = 1.4$.

Forebody drag of a cone-cylinder with counterflow jet in supersonic flow

- Flow field features
  - Small pressure ratios<12, (subsonic jets)
    - jet insufficiently powerful to counter freestream, contact surface is an effective blunt body
    - leads to saddle point singularity from which contact interface issues
    - jet separation over body causing a low pressure region giving a thrust
  - Large pressure ratios >12, (supersonic jets)
    - Goes through normal shock prior to impingment with freestream
    - Free shear layer stagnates on shoulder, leading to eddies, baroclinic vorticity, multiple secondary shocks and instabilities

Forebody drag of a cone-cylinder with counterflow jet in supersonic flow

- Conclusions
  - Two competing tendencies
    - Jet momentum flux- increases drag
    - Pressure thrust on forebody-decreases drag
  - Drag can be lower thatn the forebody drag of an equivalent sharp cone or cone frustrum
  - Minimum drag occurs when the jet to freestream pressure ratio is approximately 11

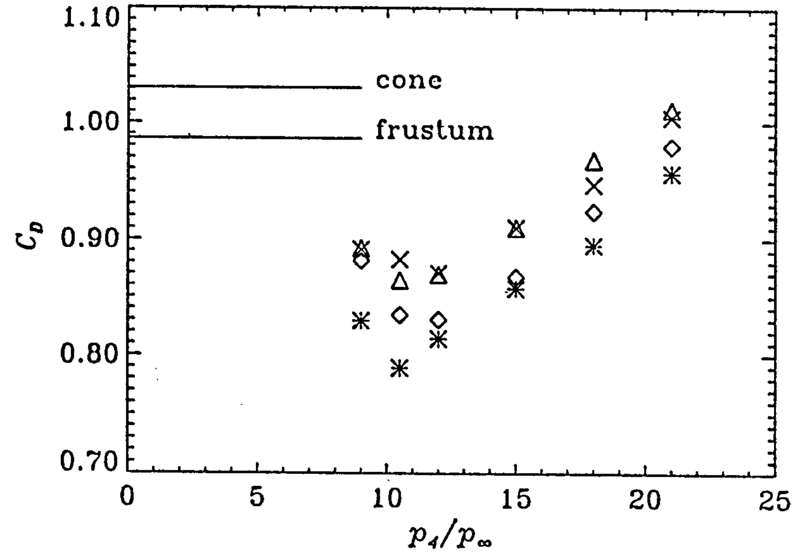

Figure 7: Forebody drag coefficient as a function of p_4/p_∞ for different values of T_4/T_∞ as follows: crosses:1, triangles:3, diamonds:6, asterisks:10. The forebody drag coefficients of the sharp cone and the cone frustum are shown as lines for reference. $M_\infty = 2$, $\gamma = 1.4$

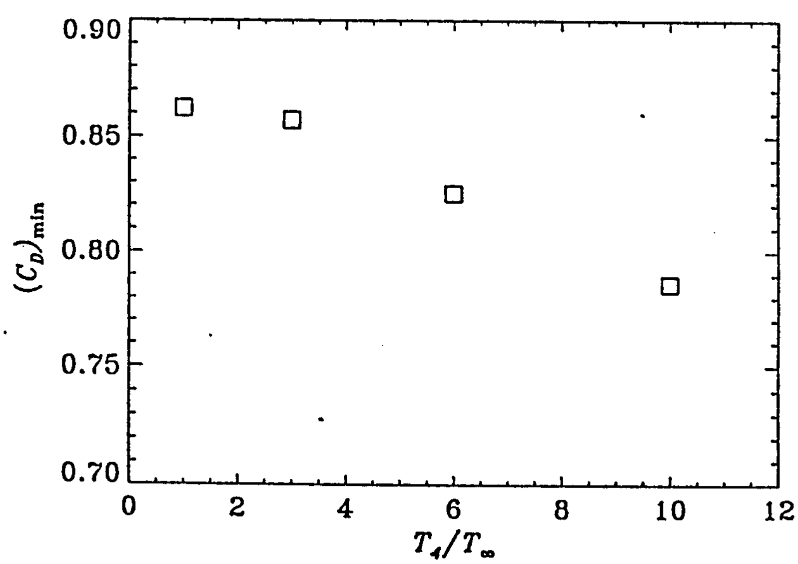

Figure 8: The minimum value of the forebody drag coefficient as a function of T_4/T_∞. $M_\infty = 2$, $\gamma = 1.4$

Propagation of 1-D Shock Waves Through Weakly Ionized Plasmas

V.R.Soloviev, V.M.Krivtsov, A.M.Konchakov
Moscow Institute of Physics and Technology, Russia

N.Malmuth
Rockwell Science Center, CA, USA

Main topics of the model

- Hugoniot relations on a shock wave (SW) in a weakly ionized plasma
- Estimations of the energy stored in different excited states for glow discharge plasma
- The existence of high situated metastable states in Ar and N_2 , which serve as a 'new ground state' for higher states excitation by electron impact
- Highly excited atomic and/or molecular states store sufficient energy to produce SW acceleration and attenuation
- Inclusion of highly excited atom energy release behind the SW front dramatically improves agreement of theory with experiment for 1-D shock penetrating into a plasma and hypersonic sphere entering a plasma

Hugoniot relations on a shock wave (SW) in a weakly ionized plasma

A set of gas mass, momentum and energy conservation equations in SW coordinates

$$\frac{\partial \rho}{\partial t}+\frac{\partial(\rho u)}{\partial \xi}=0,$$

$$\frac{\partial(\rho(u+D))}{\partial t}+\frac{\partial}{\partial \xi}(\rho u(u+D)+p)=\frac{\partial}{\partial \xi}\left[\frac{4}{3}\mu\frac{\partial u}{\partial \xi}\right]+f_\xi,$$

$$\frac{\partial}{\partial t}\left[\rho\left(h+\frac{(u+D)^2}{2}\right)-p\right]+\frac{\partial}{\partial \xi}\left[\rho u\left(h+\frac{(u+D)^2}{2}\right)\right]=\frac{\partial}{\partial \xi}\left[\frac{\lambda}{c_p}\frac{\partial h}{\partial \xi}\right]+$$
$$+\frac{4}{3}\mu\frac{\partial^2}{\partial \xi^2}\left(\frac{(u+D)^2}{2}\right)+f_\xi(u+D)+Q_r$$

$$h=c_pT_a=\frac{\gamma}{\gamma-1}\frac{p}{\rho},$$

ρ, p, h are density, pressure and enthalpy of the gas; v is its velocity;

λ, μ are thermal conductivity and dynamic viscosity coefficients;

c_p, γ are specific heat at a constant pressure and the ratio of specific heats;

D is the SW velocity;

The f_ξ and Q_r terms describe the plasma influence on the gas.

Hugoniot relations

$$\rho_1 u_1=\rho_0 D,$$

$$\rho_1 u_1^2+p_1=\rho_0 D^2(1-\varepsilon_{u1})+p_0,$$

$$h_1+\frac{u_1^2}{2}=h_0(1+\varepsilon_h)+\frac{D^2}{2}(1-2\varepsilon_{u2}),$$

where

$$\varepsilon_{u1}=\frac{1}{\rho_0 D^2}\int_{-\infty}^{\infty} f_\xi d\xi \;,\; \varepsilon_{u2}=-\frac{1}{\rho_0 D^3}\int_{-\infty}^{\infty} f_\xi u d\xi,\quad \varepsilon_h=\frac{1}{\rho_0 D h_0}\int_{-\infty}^{\infty} Q_r d\xi$$

- To produce a plasma effect on SW propagation it is necessary ε_{u1}, ε_{u2}, or ε_h to be of the order of 1.

The typical cold glow discharge plasma parameters in SW - discharge interaction experiments

gas pressure (gas density)	$p \approx 3$ - 30 Torr ($N \approx 10^{17}$ - 10^{18} cm^{-3})
gas temperature	$T \approx 300$ K
current density	$j \approx 1$ - 100 mA/cm^2
electric field strength	$E \approx 100$ V/cm
E/N value	$(2$ -$10) \times 10^{-16}$ V$\times$cm^2
discharge specific power	$W \approx 0.1$ - 10 W/cm^3
electron temperature	$T_e \approx 1$ - 3 eV
electron density	$n_e \approx 10^{10}$ - 10^{12} cm^{-3}
metastable atom (or molecule) density	$N_m \approx 10^{11}$ - 10^{13} cm^{-3}

The energy stored in different excited states

- freestream gas enthalpy $\quad h_0 = Nc_pT \sim 10^{16}$ eV/cm^3
- ionization $\quad n_iE_i \sim 10^{12}$ eV/cm^3, $\quad \varepsilon_h = n_iE_i / Nc_pT \sim 10^{-4}$
- metastable atoms (or molecules) $N_mE_m \sim 10^{14}$ eV/cm^3, $\varepsilon_h = N_mE_m / Nc_pT \sim 10^{-2}$
- specific discharge energy supply
  during the time of unit length SW pass $\quad \varepsilon_h = W \times 1\text{cm}/D\ Nc_pT \sim 10^{-2}$ - 10^{-1}
- the vibrational energy is shown to be unsuitable to explain the SW anomalious propagation effects because of large vibrational-translational relaxation time $\tau_{VT} \sim 10^{-3}$s

The scheme of Ar and N_2 electronic excited states

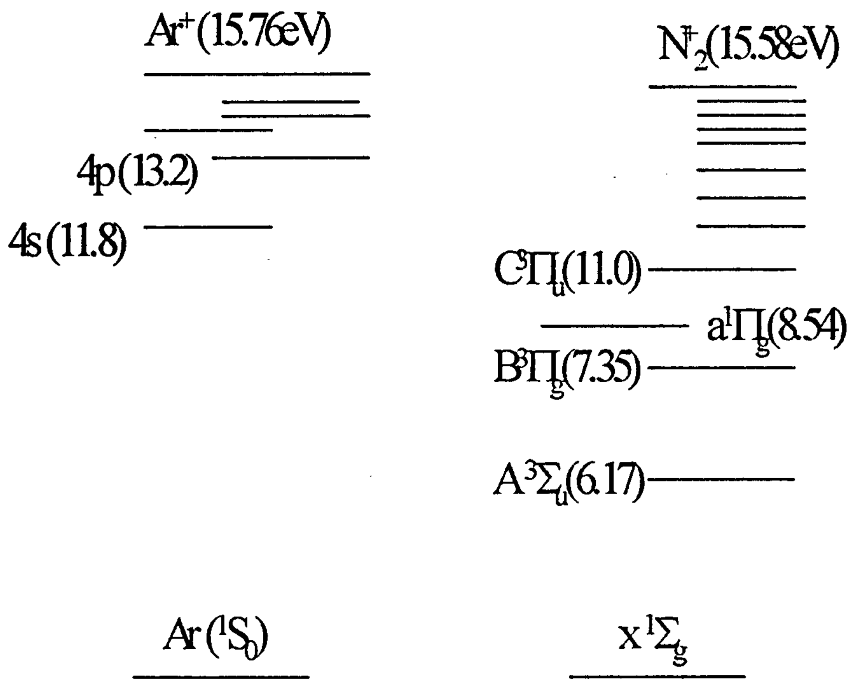

Ar(4s) and $N_2(A^3\Sigma)$ are the metastable states

The Ar metastable state quenching and building up

Process	Rate constant	Quenching time for $p=10$ Torr, $n_e=10^{11}cm^{-3}$ and 1% N_2 diluent in Ar
$Ar(4s) + 2Ar \rightarrow Ar^*_2 + Ar$	$10^{-32}\ cm^6/s$	0.8 ms
$Ar(4s) + e \rightarrow Ar + e + 11.8ev$	$10^{-8}\ cm^3/s$	1ms
$Ar(4s) + N_2 \rightarrow Ar + N_2(C, B, ...)$	$3.6\times10^{-11} cm^3/s$	0.01ms
$Ar(4s) + Ar(4s) \rightarrow Ar^+ + Ar + e$	$10^{-9}\ cm^3/s$	$1ms\times(10^{12}/n(4s)[cm^{-3}])$
$Ar(4p) + Ar \rightarrow Ar(4s) + Ar$	$\sim 10^{-11}$ - $10^{-12} cm^3/s$	0.3 - 3mcs
$Ar(4p) \rightarrow Ar(4s) + h\nu$	$3.2\times10^7\ s^{-1}$	0.03mcs

The $N_2(A^3\Sigma)$ metastable state quenching and building up

$N_2(A^3\Sigma) + Ar \rightarrow N_2(X) + Ar$	$<4\times10^{-14} cm^3/s$	$> 0.1ms$
$N_2(A^3\Sigma) + N_2(X) \rightarrow 2\ N_2(X)$	$<4.5\times10^{-17} cm^3/s$	$>100ms$
$N_2(A^3\Sigma) + O_2 \rightarrow N_2(X) + O_2$	$3.6\times10^{-12} cm^3/s$	4mcs (for air composition)
$N_2(A^3\Sigma) + N_2(X,v) \rightarrow N_2(B^3\Pi) + N_2(X)$	$\sim 10^{-10} cm^3/s$	
$N_2(A^3\Sigma) + N_2(A^3\Sigma) \rightarrow N_2(B,C,...) + N_2(X)$	$10^{-9} cm^3/s$	$1ms\times(10^{12}/n(A)[cm^{-3}])$
$N_2(B^3\Pi) + N_2(X) \rightarrow N_2(A^3\Sigma) + N_2(X)$	$2\times10^{-11} cm^3/s$	0.15mcs
$N_2(B^3\Pi) \rightarrow N_2(A^3\Sigma) + h\nu$	$1.5\times10^5\ s^{-1}$	6.5mcs
$N_2(C^3\Pi) \rightarrow N_2(A,B) + h\nu$	$2.7\times10^7\ s^{-1}$	0.037mcs

The discharge fractional power input into different excited states for Ar, N_2 and Ar-N_2 mixture

E-is electric field strength, **N** - is gas number density

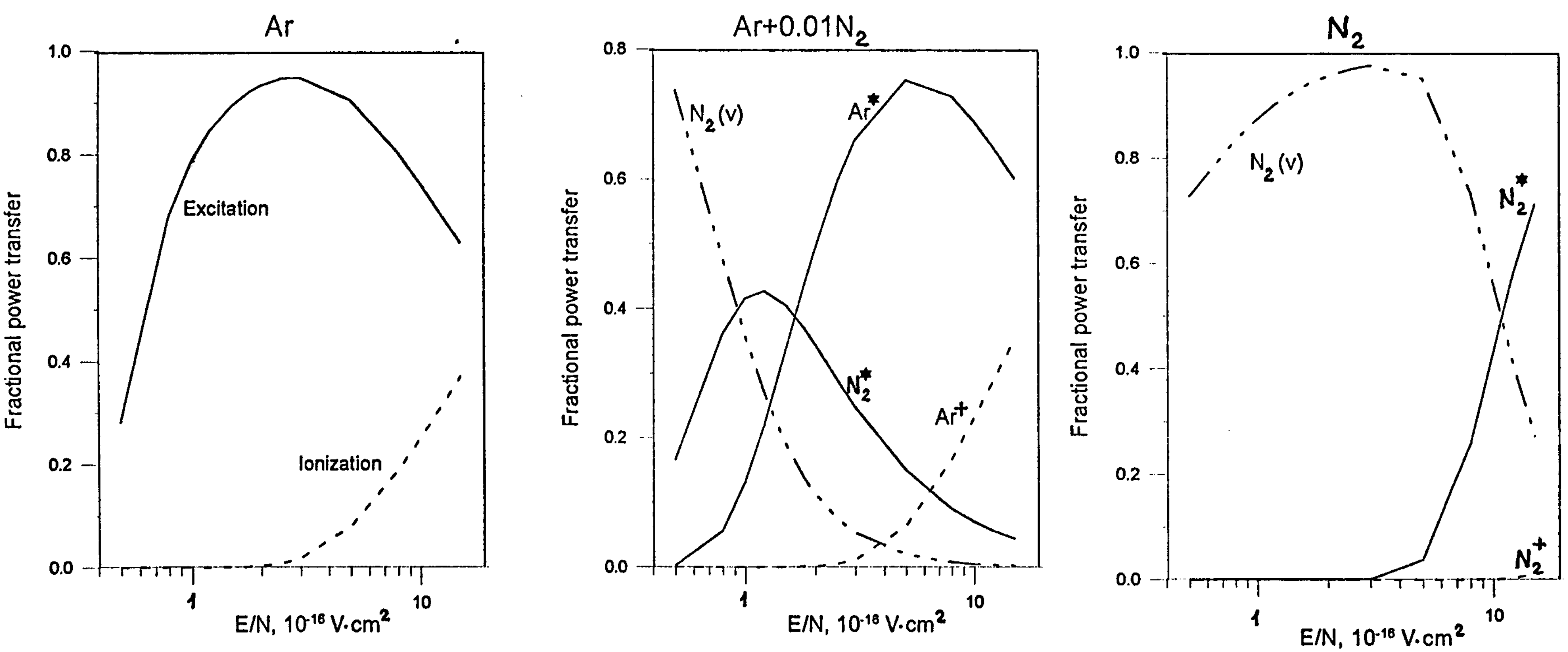

The mean electron energy (electron temperature) and electron drift velocity versus E/N value for Ar, Ar+0.01N_2 and N_2 discharges

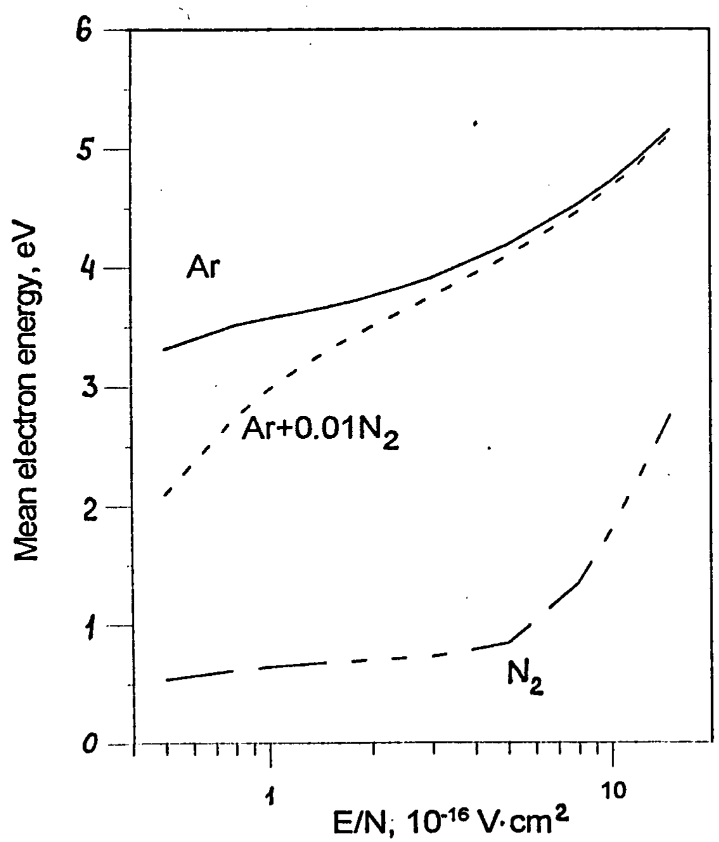

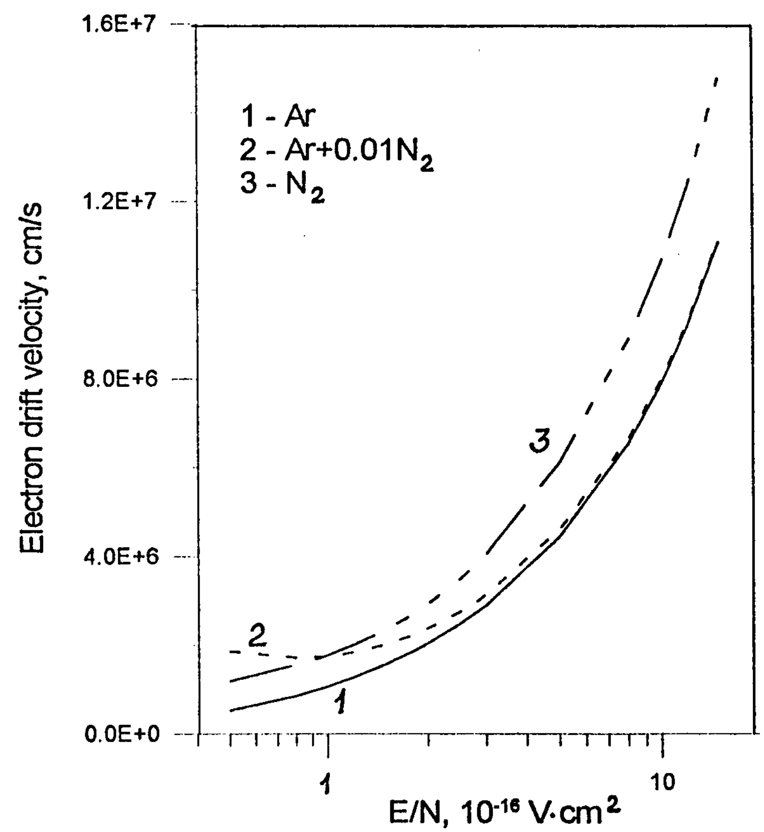

The kinetic model of energy storing in highly excited states

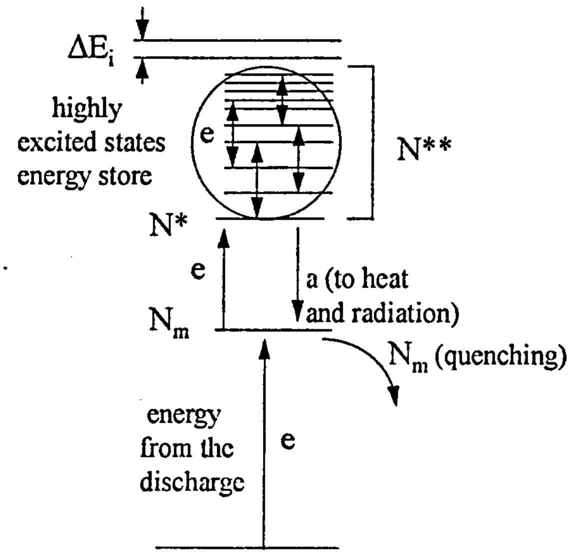

The system of balance equations for excited states

$$\frac{\partial N_m}{\partial t} = \frac{W\eta}{E_m} - N_m\left(k_p N_m + \frac{1}{\tau_q}\right) - k_e n_e N_m + N^*(k_q N + A_R\theta)$$

$$\frac{\partial N^*}{\partial t} = k_e n_e N_m - N^*(k_q N + A_R\theta)$$

$$N^{**} = \sum_{n=n^*}^{n_f} N^* \frac{g_n}{g_{n^*}} \exp\left(-\frac{E_n - E_{n^*}}{T_e}\right), \qquad \text{for } n>n^* \quad k_e n_e >> k_q N \frac{\Delta E_{n,n+1}}{T_e},$$

$$\Delta E_{n,n+1} \approx \frac{2Ry}{n^3}, \quad n^* \approx \sqrt[3]{\frac{2Ry}{T_e}\frac{k_q N}{k_e N_e}} \approx 4-5, \quad E_i - E^* \approx 0.5\text{-}1\text{eV}$$

Ry =13.6eV is the Rydberg constant

W = jE - is the discharge specific power;

η~1 - is the discharge fractional power input into excitation;

E_m, E_n - are the energies of the different states excitation from the ground state;

k_p - is the metastable atom Penning process rate constant;

τ_q - is the metastable state quenching time in other processes;

k_e - is the electron excitation rate constant from metastable to N^* states;

k_q - is the gas quenching rate constant for N^* states;

A_R - is the radiative decay rate for N^* states;

θ - is the probability of radiation trapping;

ΔE_i - is the decrease of ionization potential due to excited atom electron - ion interaction;

For the tube radius R $$\theta = \frac{1}{3\sqrt{\pi \sigma_{abs} N_m R}}$$

For Ar(4p) → Ar(4s) transitions $\theta \approx 3\times10^{-2}\,(10^{12}/N_m)^{0.5}$ followed by

$$A_R\theta << k_q N$$

The steady state values of N_m and N^* :

$$N_m \approx \sqrt{\frac{W\eta}{k_p E_m}} \approx 2.5\times10^{13}\sqrt{W[W/cm^3]},\, cm^{-3}$$

$$N^* \approx N_m \frac{k_e n_e}{k_q N} \approx 3.5\times10^{12}\,\frac{\sqrt{W[W/cm^3]}}{p[Torr]},\, cm^{-3}$$

The equilibrium highly excited hydrogen-like states population

$$n_f \approx \sqrt{\frac{Ry}{\Delta E_i}} \approx \sqrt{\frac{Ry}{e^2 N_i^{\frac{1}{3}}}}$$ - the upper limit of principle quantum number for hydrogen-like states;

$n_f \approx 100$ for $N_i \approx 10^{11}\,cm^{-3}$

$$N^{**} \approx N^* \frac{2n_f^3}{3g^*}\exp\left(-\frac{E_i - E^*}{T_e}\right) \sim 10^4 N^*$$

g^* ~30 is the degeneracy of N^* state

The energy stored in highly excited states

$$\varepsilon^{**} \approx (E^* - E_m)\frac{n_f^3}{g^*}\frac{k_e N_e}{k_q N}\sqrt{\frac{W\eta}{E_m k_p}}\exp(-\frac{E_i - E^*}{T_e})$$

$$\varepsilon^{**} \approx 10^{17}\frac{\sqrt{W[W/cm^3]}}{p[Torr]}, \frac{eV}{cm^3},$$

$$\frac{\varepsilon^{**}}{c_p NT} \approx 1$$

The energy released to heat behind the shock wave

$$\Delta\varepsilon \approx \varepsilon^{**}(1 - \frac{N_0 N_{e1}}{N_1 N_{e0}})$$

0 and 1 indexes correspond to the gas and plasma parameters before and behind the shock

The relaxation length behind the SW front

$$\xi_r \approx D\frac{N_0}{N_1}\frac{1}{k_p N_m} \approx 4\times 10^{-5}\frac{N_0}{N_1\sqrt{W[W/cm^3]}}D[cm/s], \quad cm$$

Inclusion of Plasma Effects Dramatically Improves Agreement of Theory with Experiment for 1-D Shock Penetrating Into a Plasma

Physical System

$1.3<M<3.5$, $M = D_0/a_0$,
a_0=sound velocity

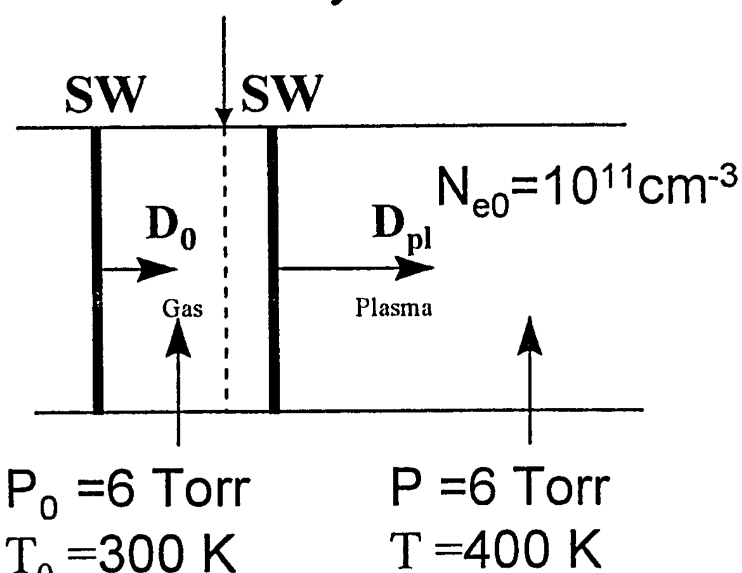

Dependence of shock speed in plasma D_{pl} versus the initial shock speed D_0 in undisturbed gas.

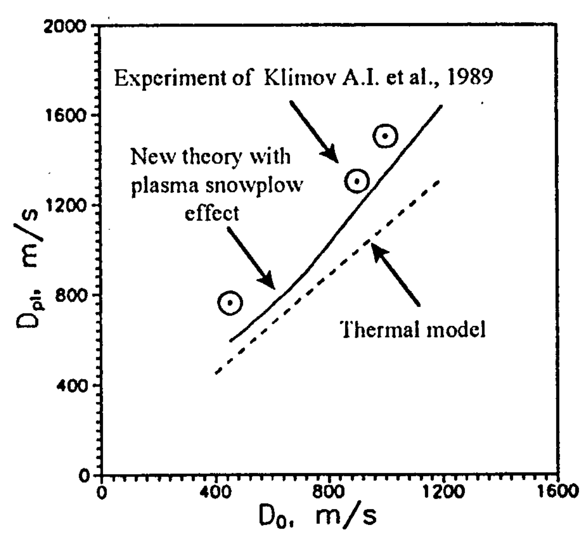

Rockwell Science Center

Inclusion of Plasma Effects Dramatically Improves Agreement of Theory with Experiment for Hypersonic Sphere Entering a Plasma

Physical System

P_0=45 Torr, T_0=1350 K, N_{e0}=10^{11}cm^{-3},

1.7<M<3.2, $M=V_{sph}/a_0$, R_{sph}=20 mm

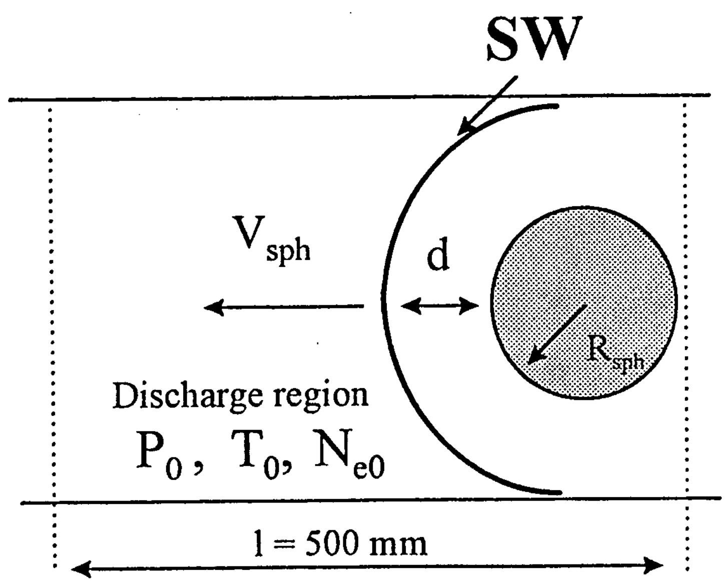

Dependence of relative shock standoff distance d/R_{sph} from the sphere versus the speed of the sphere V_{sph}.

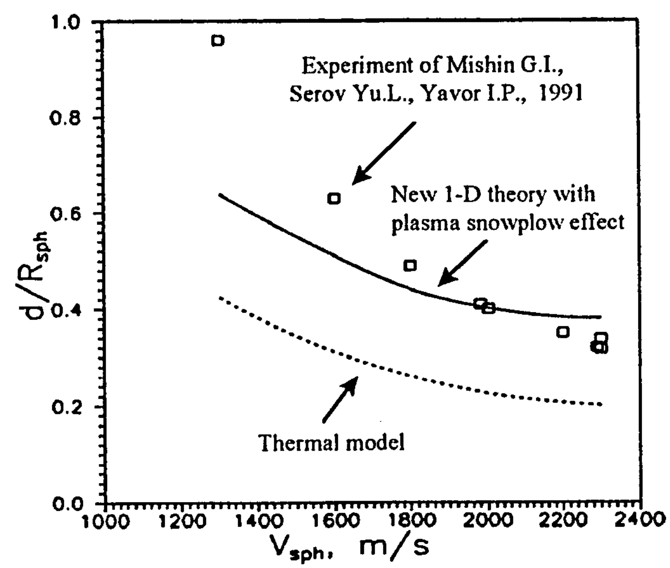

Rockwell Science Center

Conclusions

- The mechanism of shock wave (SW) acceleration and attenuation due to interaction with a weakly ionized plasma really exists

- Preliminary calculations of 1-D SW speed in plasma are in a good agreement with experimental results when the highly excited states energy release behind the SW front is taken into account

- SW acceleration is accompanied by decrease of density and velocity jump with a small increase of static pressure jump through the SW front

- The foregoing results in a decrease of dynamic pressure jump through the SW front

- The creation of a discharge plasma IN FRONT OF the shock wave courses the SW attenuation and drag reduction for supersonic and hypersonic vehicles

- More detailed kinetic analysis is necessary to obtain more precise results

Anomalous Behavior of Shocks in Weakly Ionized Gases - Theory & Modeling

Vish V. Subramaniam
Department of Mechanical Engineering
and Chemical Physics
The Ohio State University
Columbus, Ohio 43210

- Anomalous effects seen in two different types of experiments:

(1) Ballistic range

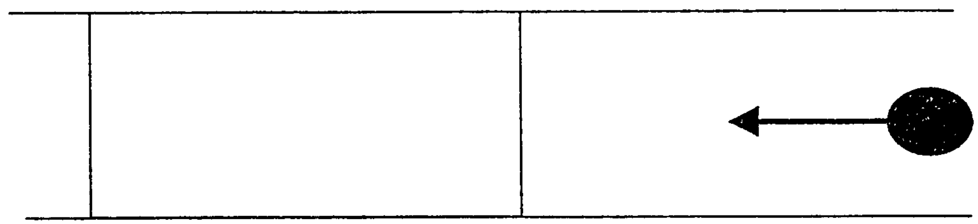

(2) Spark-generated shock launched into a glow discharge (WPAFB)

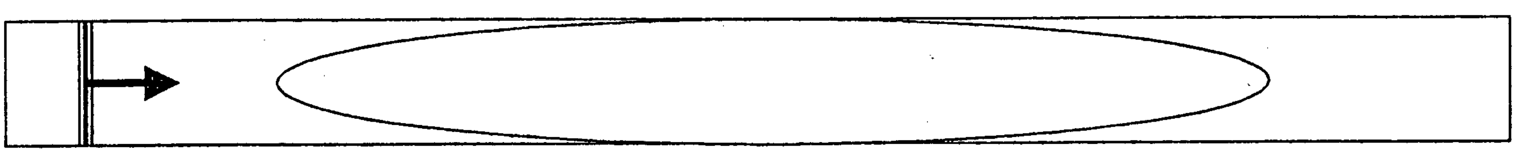

Effects of purely axial thermal gradients

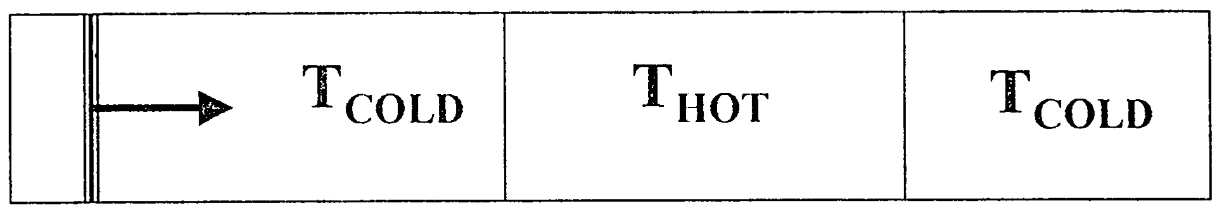

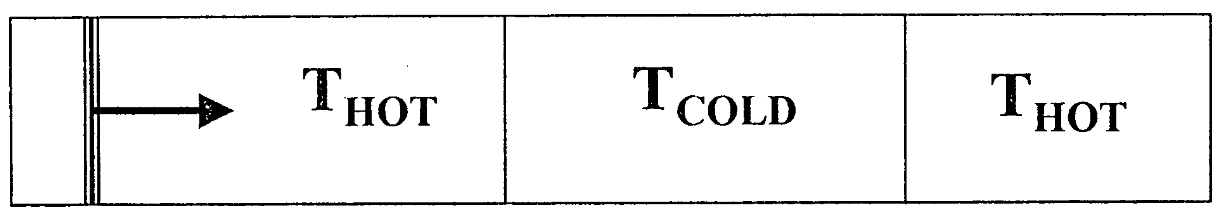

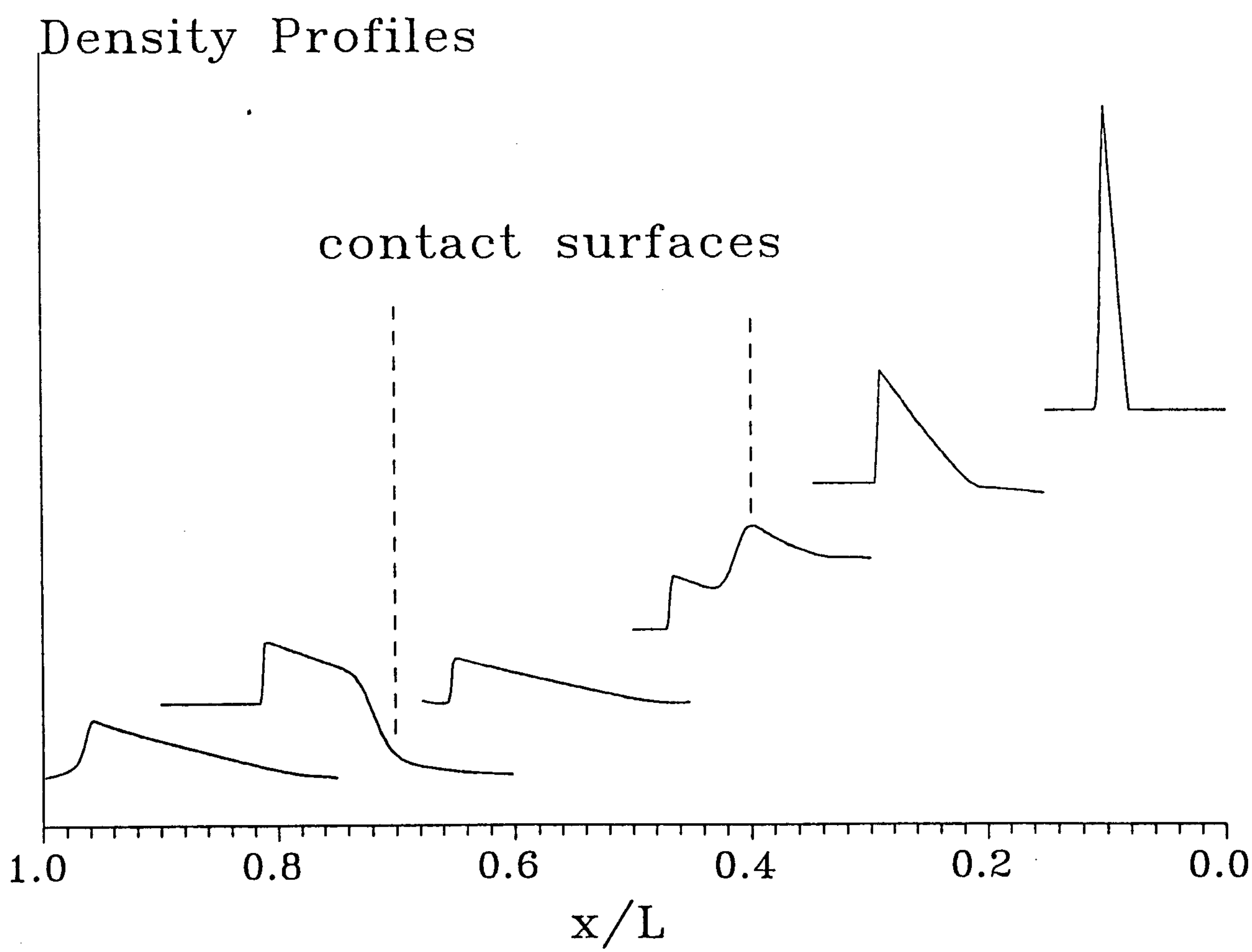

Density Profiles
contact surfaces
1.0
0.8
0.6
0.4
0.2
0.0
x/L

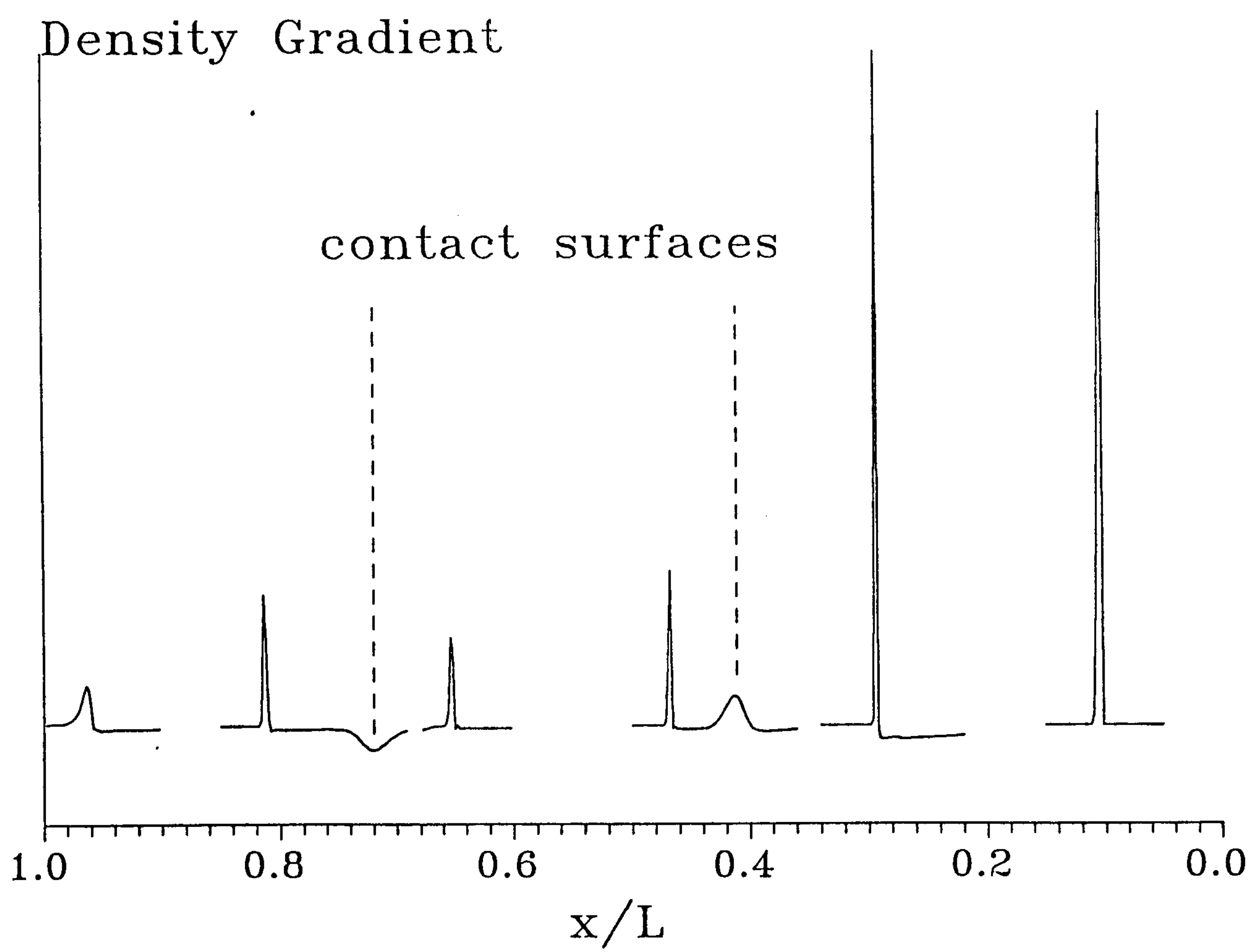

Density Gradient
contact surfaces
1.0
0.8
0.6
0.4
0.2
0.0
x/L

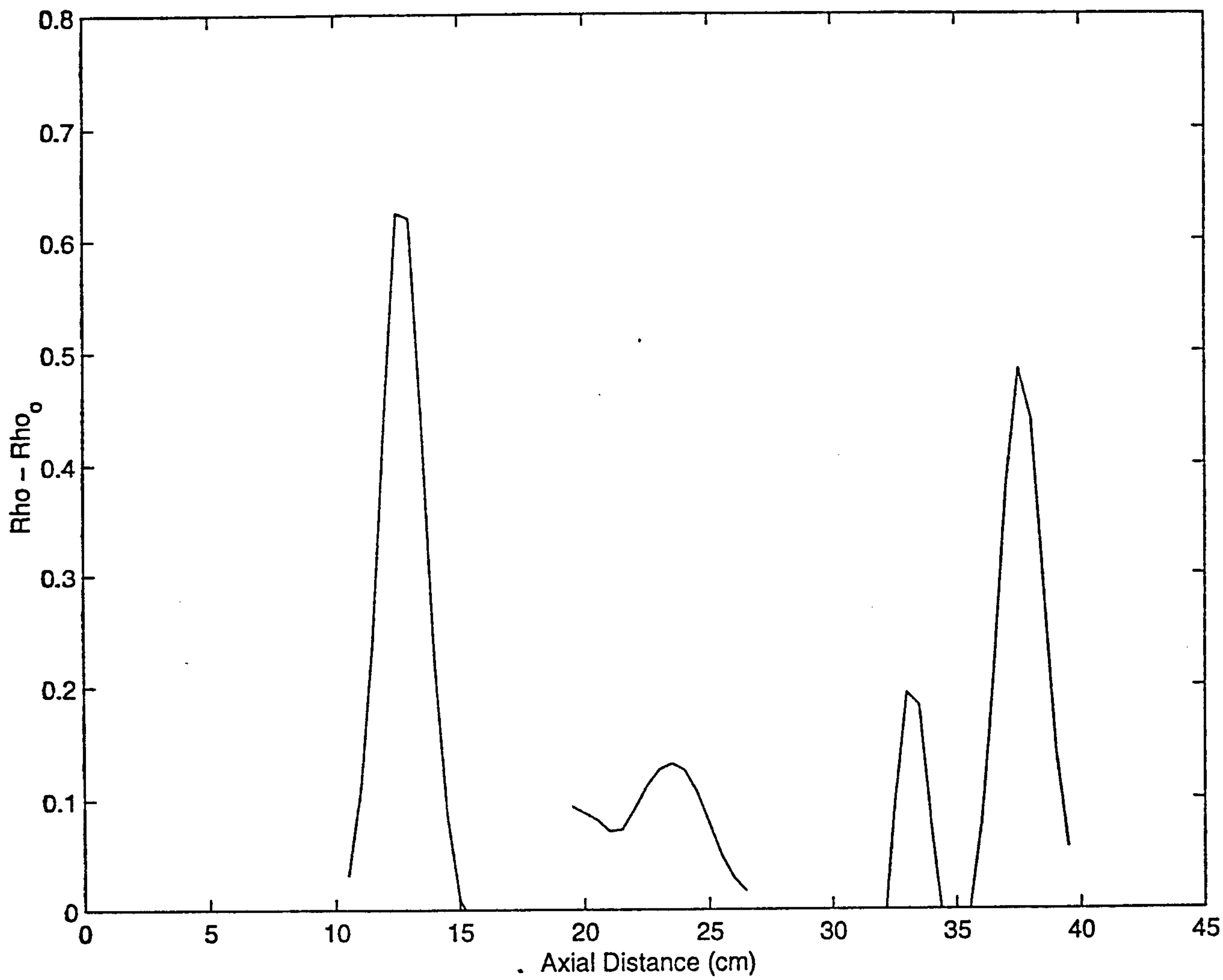

0.8
0.7
0.6
0.5
0.4
0.3
0.2
0.1
0
Rho - Rho$_o$
0
5
10
15
20
25
30
35
40
45
Axial Distance (cm)

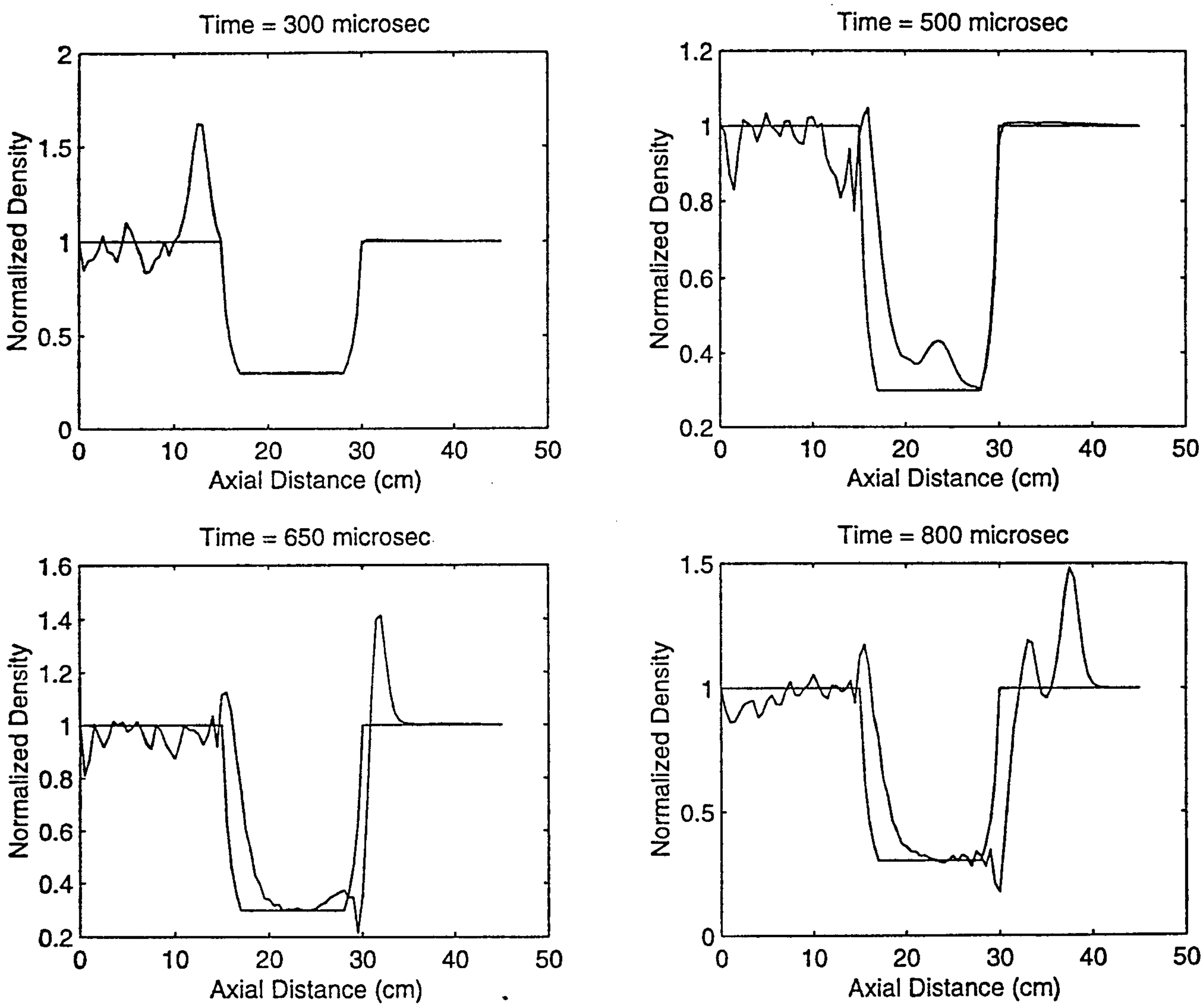

Time = 300 microsec
Normalized Density
Axial Distance (cm)
Time = 500 microsec
Normalized Density
Axial Distance (cm)
Time = 650 microsec
Normalized Density
Axial Distance (cm)
Time = 800 microsec
Normalized Density
Axial Distance (cm)

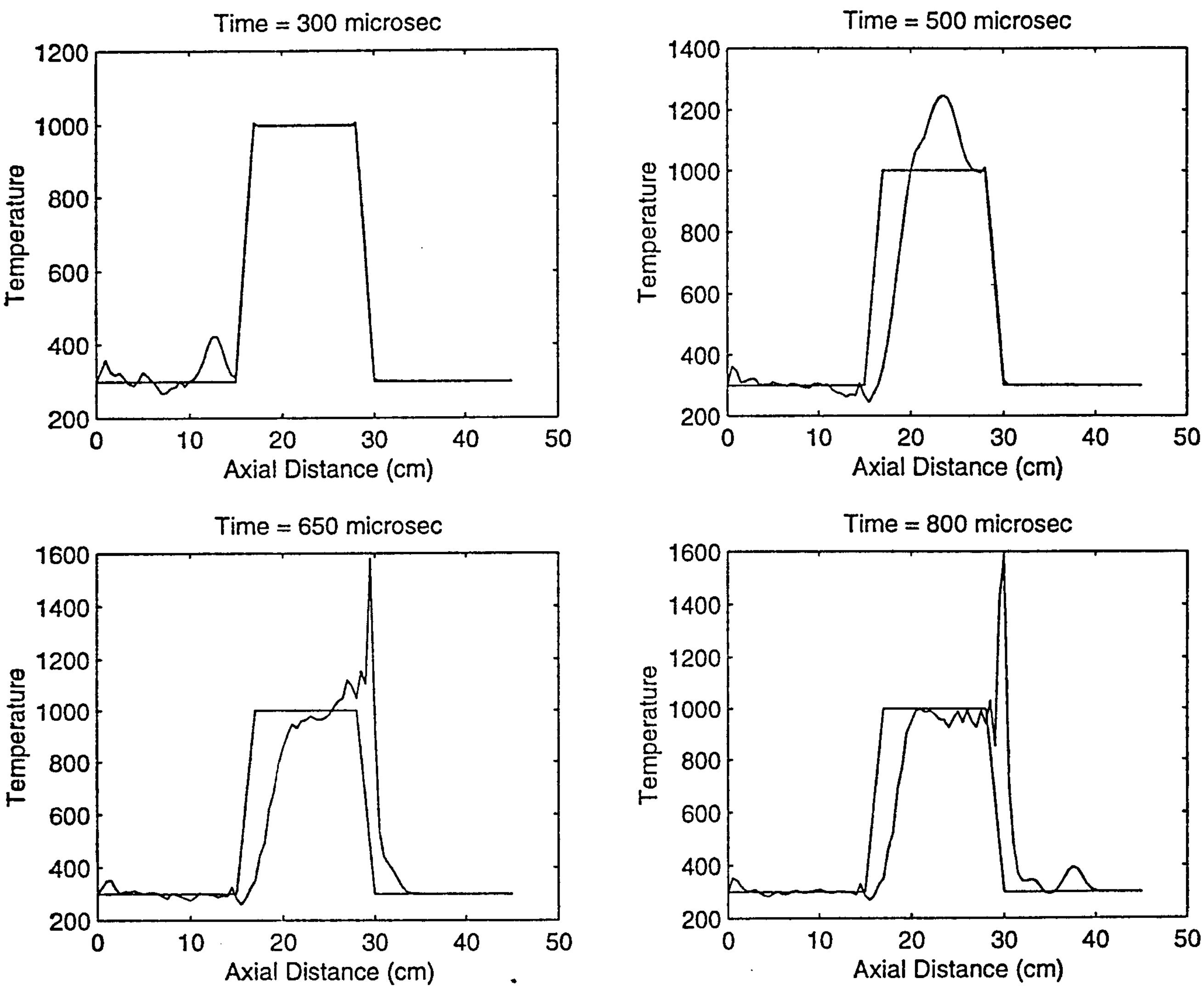
Time = 300 microsec
Time = 500 microsec
Time = 650 microsec
Time = 800 microsec
Temperature
Axial Distance (cm)
200
400
600
800
1000
1200
1400
1600
0
10
20
30
40
50

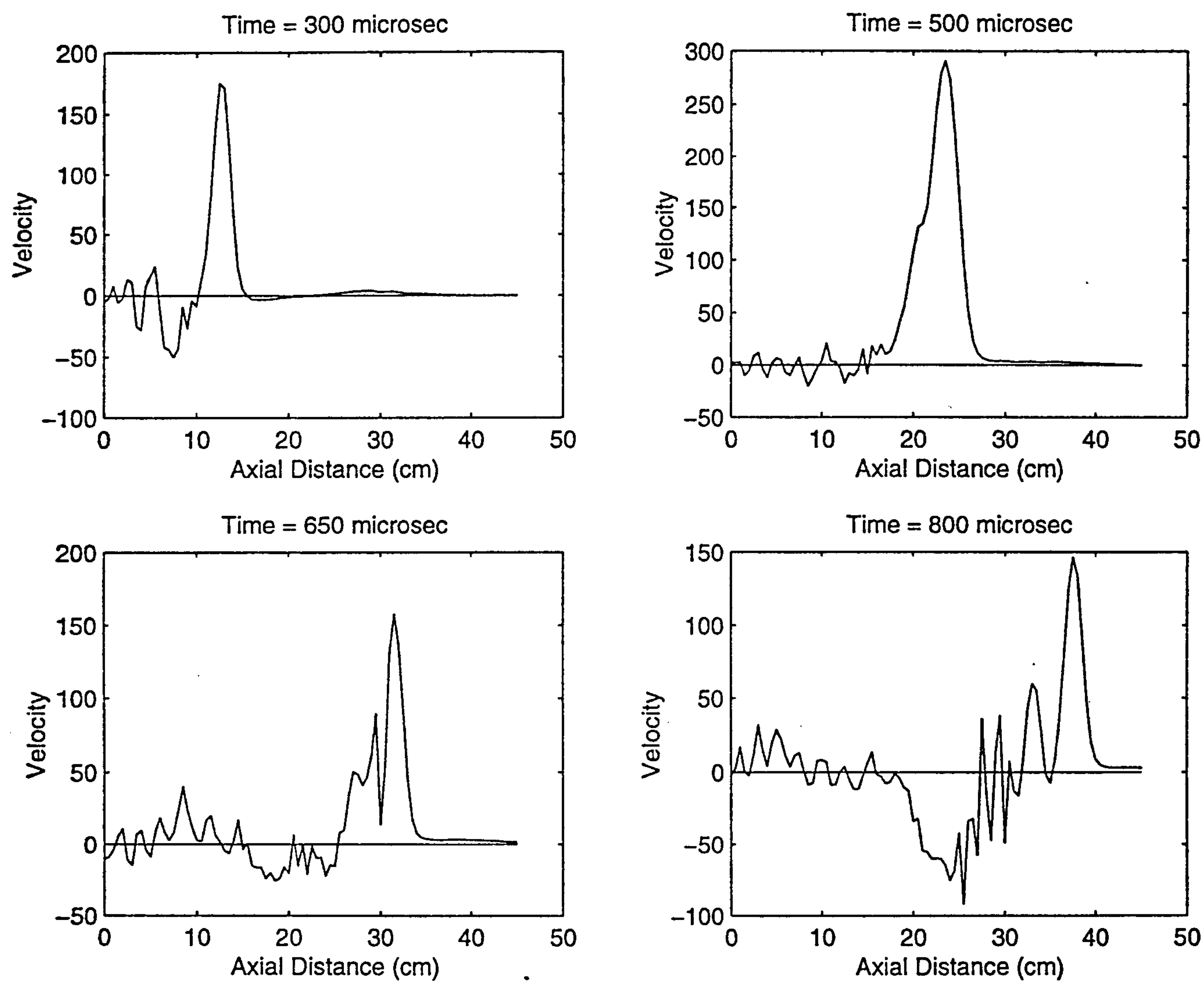

Time = 300 microsec
Time = 500 microsec
Time = 650 microsec
Time = 800 microsec
Velocity
Axial Distance (cm)

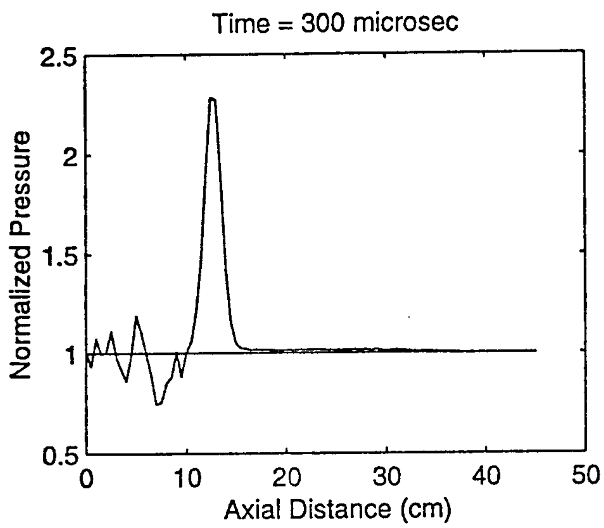
Time = 300 microsec
Normalized Pressure
Axial Distance (cm)
2.5
2
1.5
1
0.5
0
10
20
30
40
50

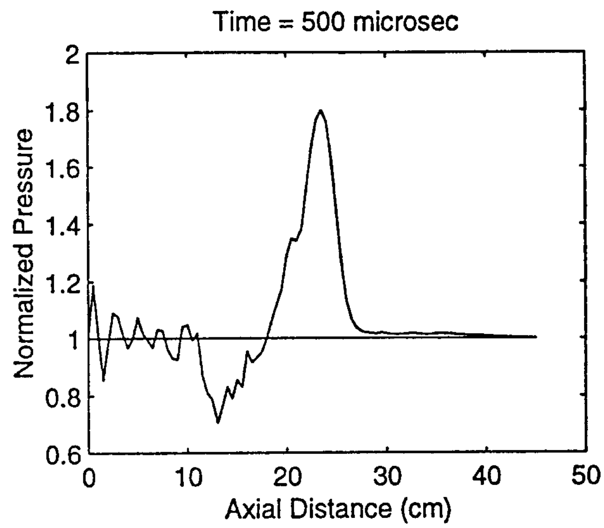
Time = 500 microsec
Normalized Pressure
Axial Distance (cm)
2
1.8
1.6
1.4
1.2
1
0.8
0.6
0
10
20
30
40
50

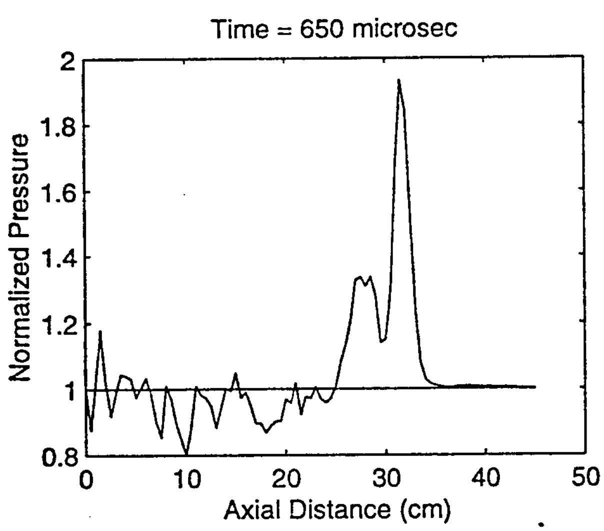
Time = 650 microsec
Normalized Pressure
Axial Distance (cm)
2
1.8
1.6
1.4
1.2
1
0.8
0
10
20
30
40
50

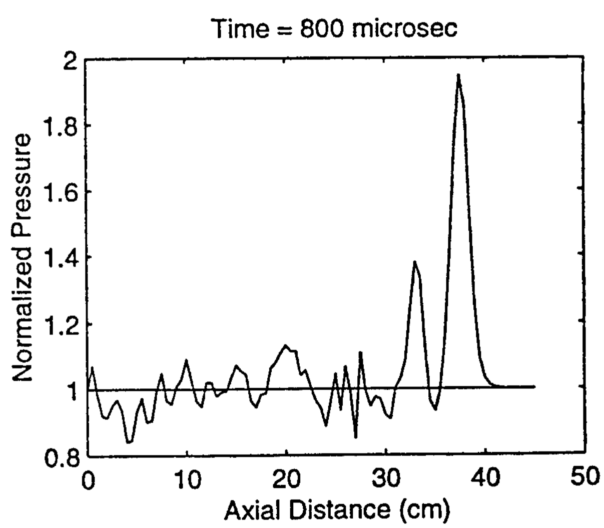
Time = 800 microsec
Normalized Pressure
Axial Distance (cm)
2
1.8
1.6
1.4
1.2
1
0.8
0
10
20
30
40
50

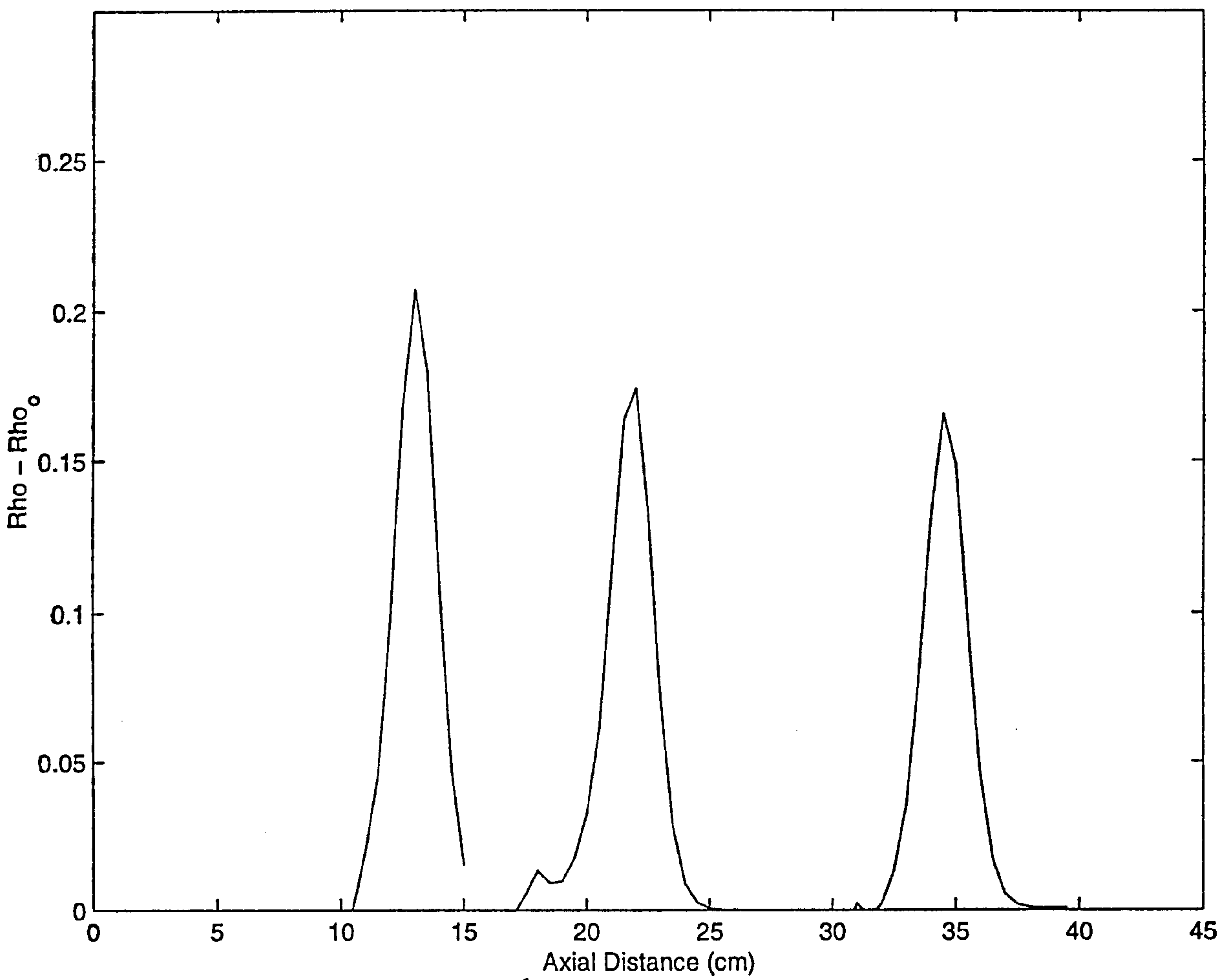
0.25
0.2
0.15
0.1
0.05
0
Rho - Rho$_o$
0
5
10
15
20
25
30
35
40
45
Axial Distance (cm)

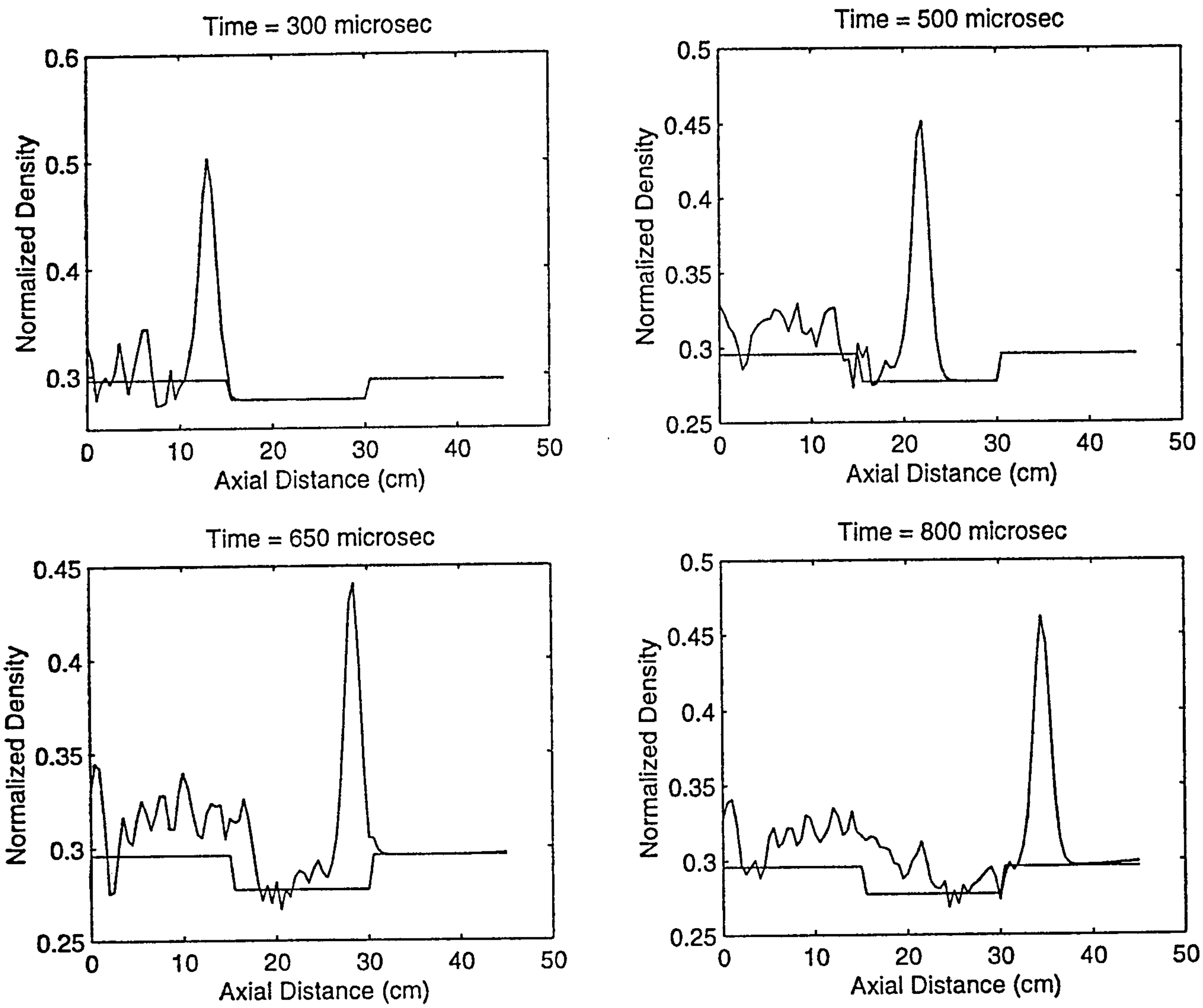
Time = 300 microsec
Time = 500 microsec
Time = 650 microsec
Time = 800 microsec
Normalized Density
Axial Distance (cm)
0.6
0.5
0.45
0.4
0.35
0.3
0.25
0
10
20
30
40
50

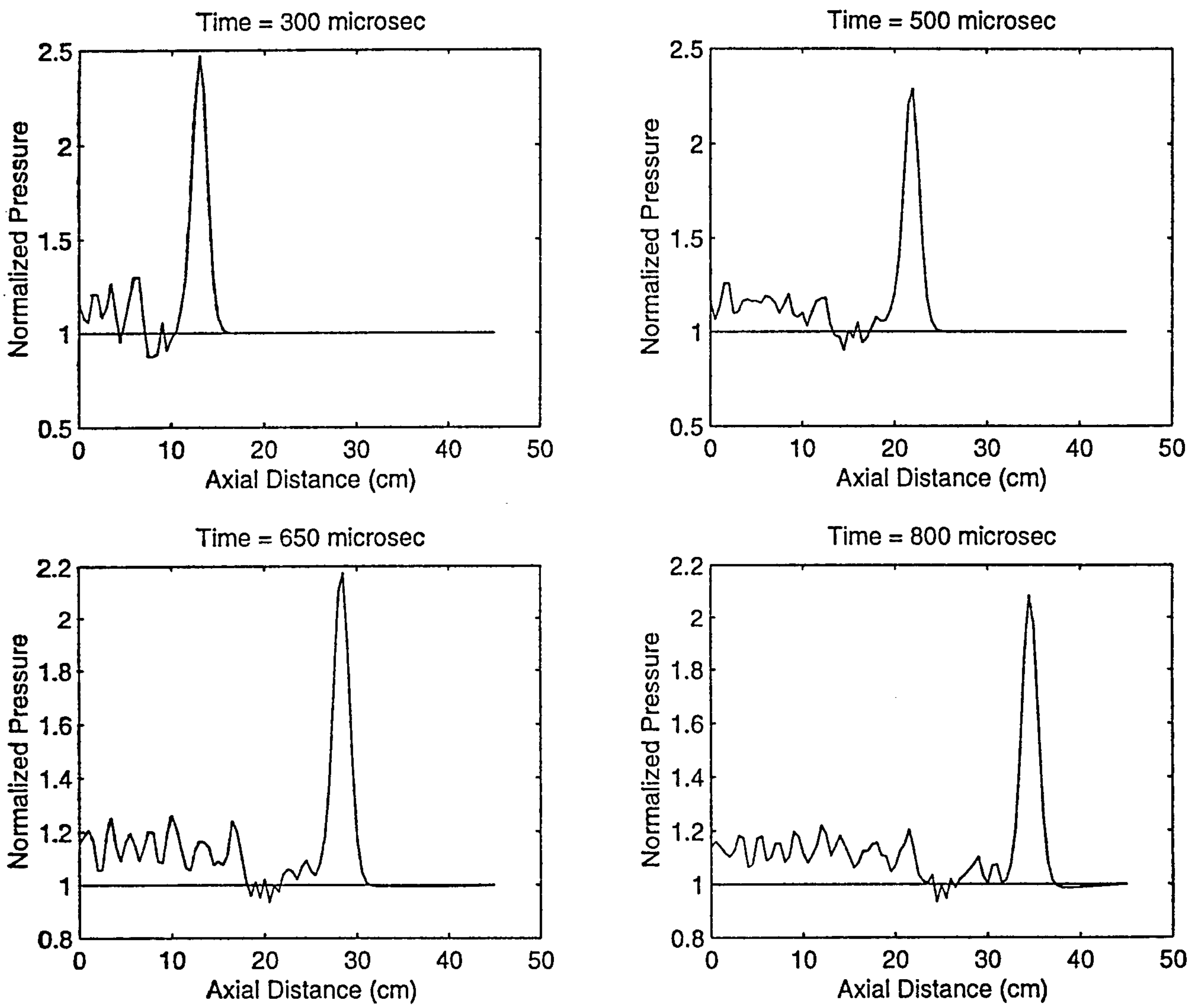

Time = 300 microsec
Time = 500 microsec
Time = 650 microsec
Time = 800 microsec
Normalized Pressure
Axial Distance (cm)
2.5
2
1.5
1
0.5
2.2
2
1.8
1.6
1.4
1.2
1
0.8
0
10
20
30
40
50

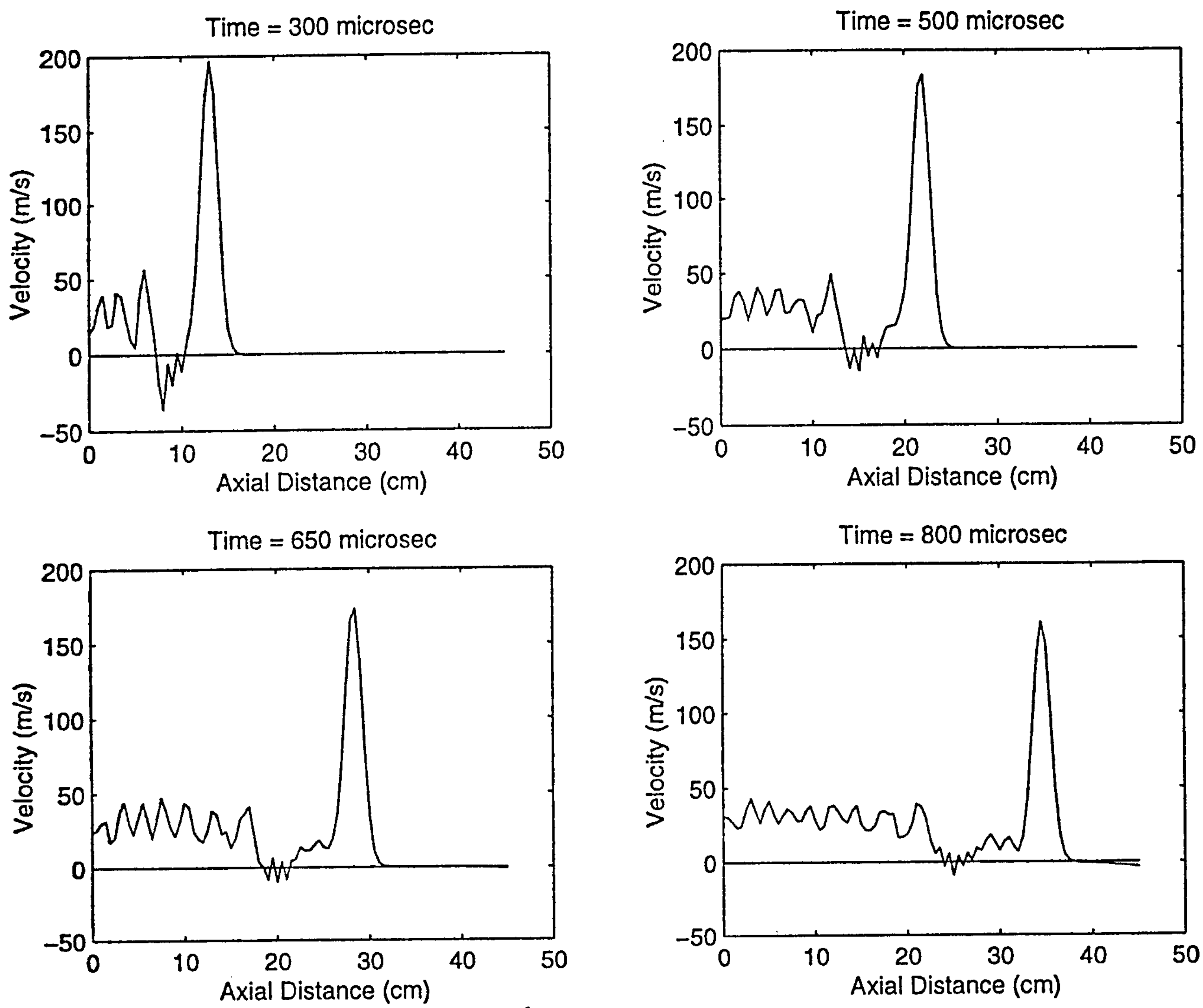
Time = 300 microsec
Time = 500 microsec
Time = 650 microsec
Time = 800 microsec
Velocity (m/s)
Axial Distance (cm)
200
150
100
50
0
−50
0
10
20
30
40
50

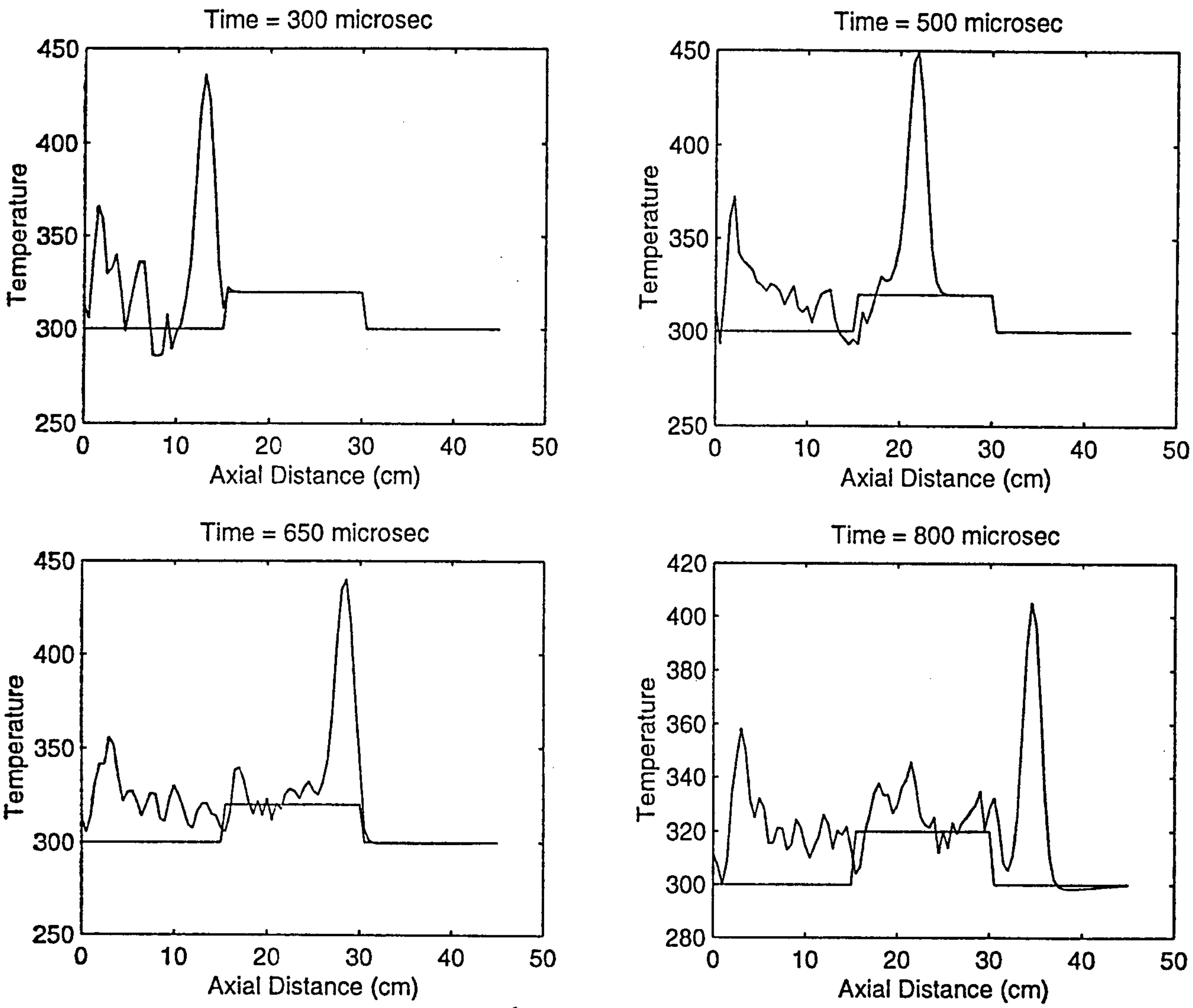
Time = 300 microsec
Time = 500 microsec
Time = 650 microsec
Time = 800 microsec
Temperature
Axial Distance (cm)

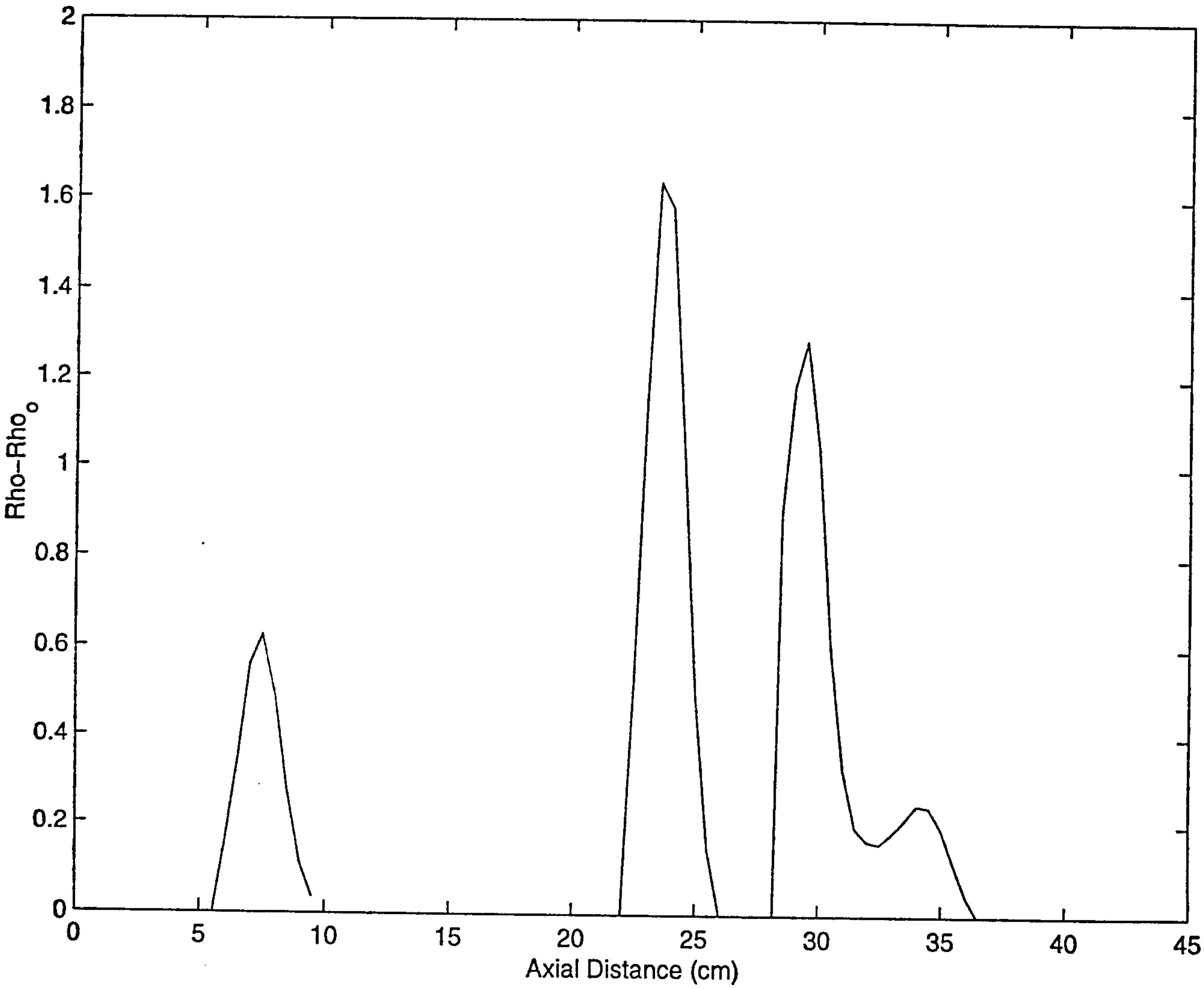

Rho-Rho_o
2
1.8
1.6
1.4
1.2
1
0.8
0.6
0.4
0.2
0
0
5
10
15
20
25
30
35
40
45
Axial Distance (cm)

1500/300/1500

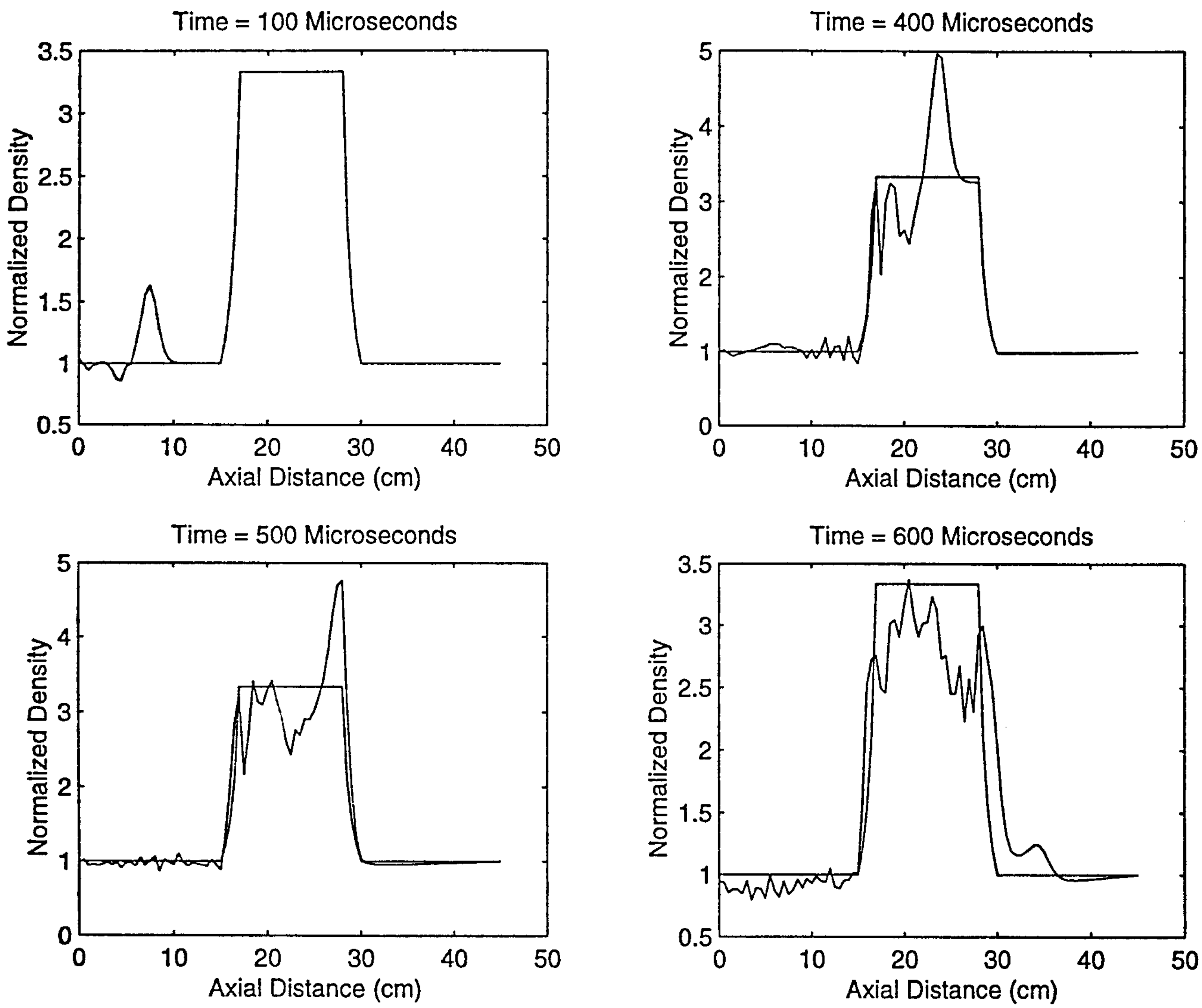

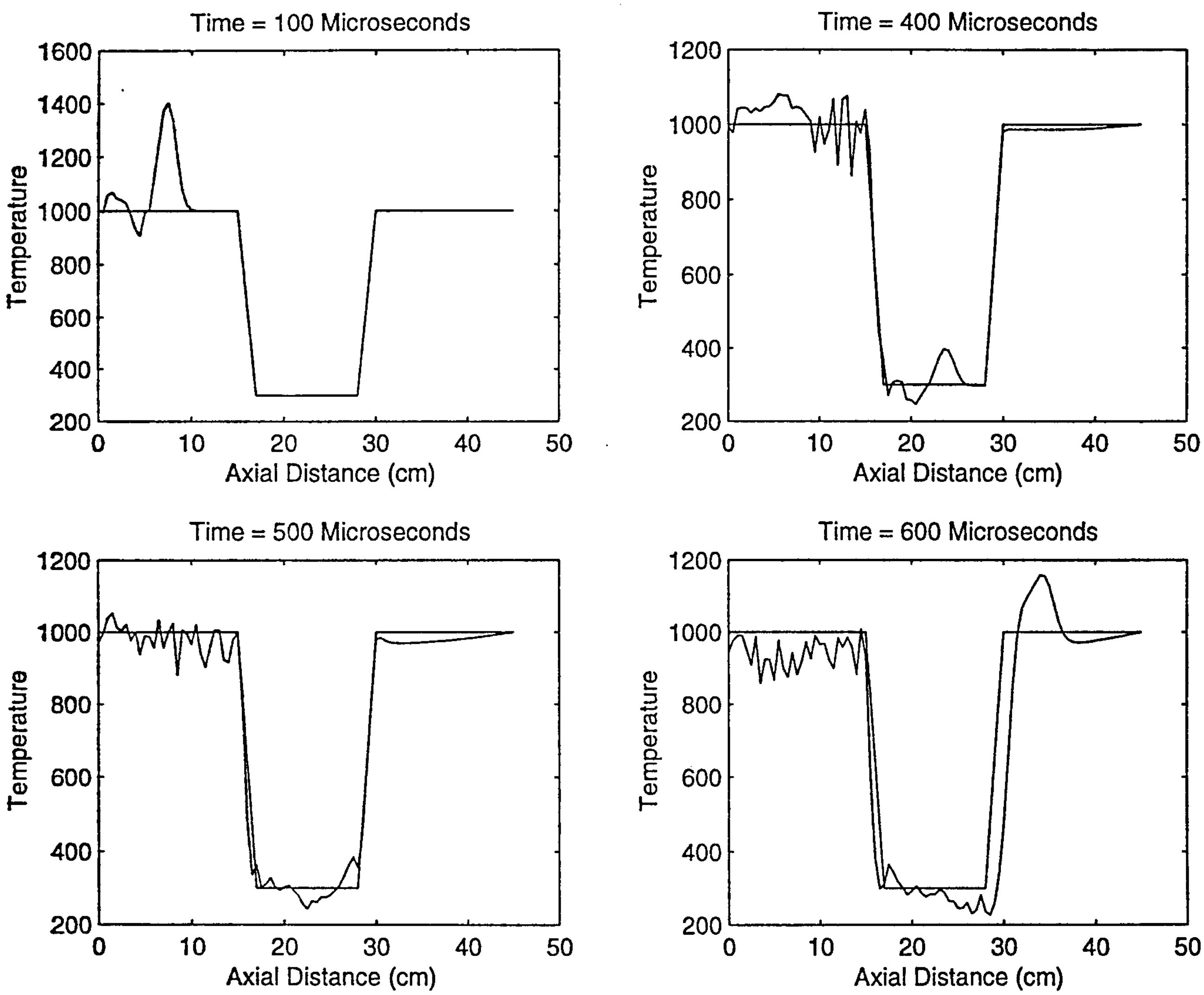
Time = 100 Microseconds
Time = 400 Microseconds
Time = 500 Microseconds
Time = 600 Microseconds
Temperature
Axial Distance (cm)
1600
1400
1200
1000
800
600
400
200
0
10
20
30
40
50

150, 150/1000

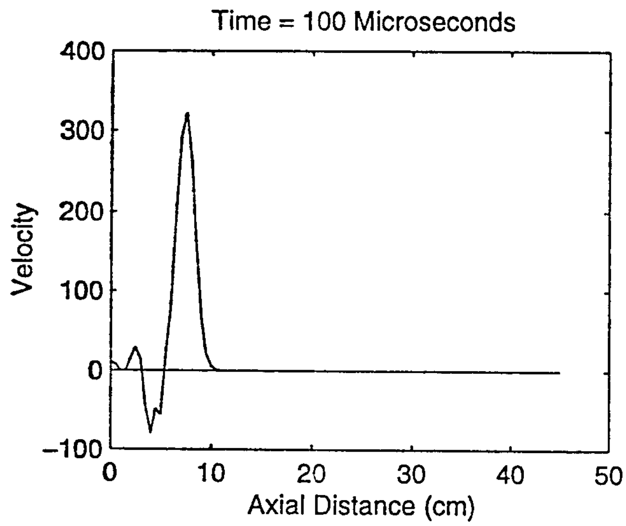

Time = 100 Microseconds
Velocity
Axial Distance (cm)

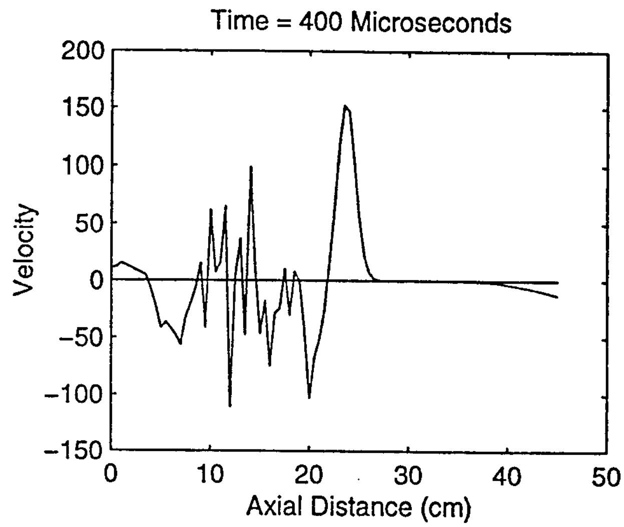

Time = 400 Microseconds
Velocity
Axial Distance (cm)

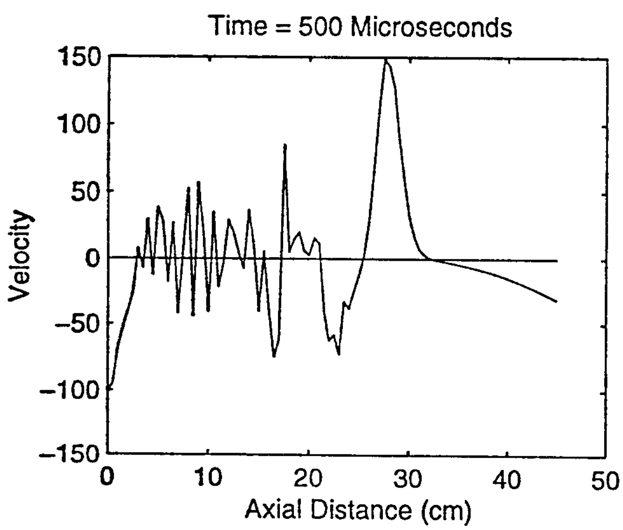

Time = 500 Microseconds
Velocity
Axial Distance (cm)

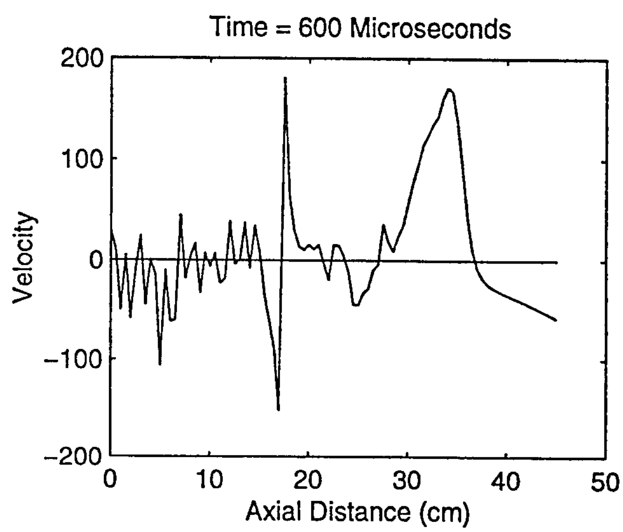

Time = 600 Microseconds
Velocity
Axial Distance (cm)

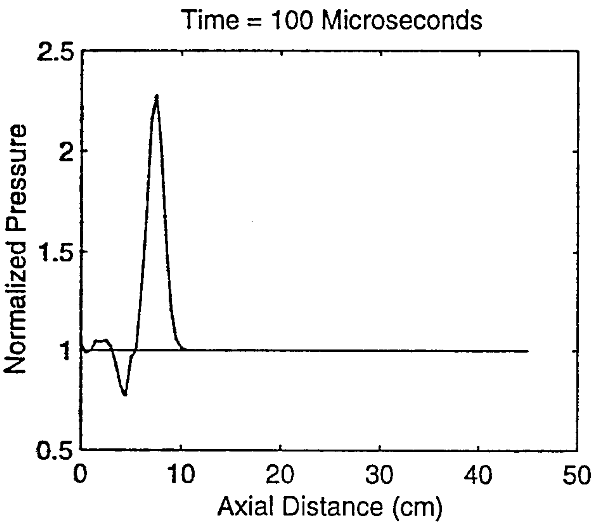
Time = 100 Microseconds
Normalized Pressure
2.5
2
1.5
1
0.5
0
10
20
30
40
50
Axial Distance (cm)

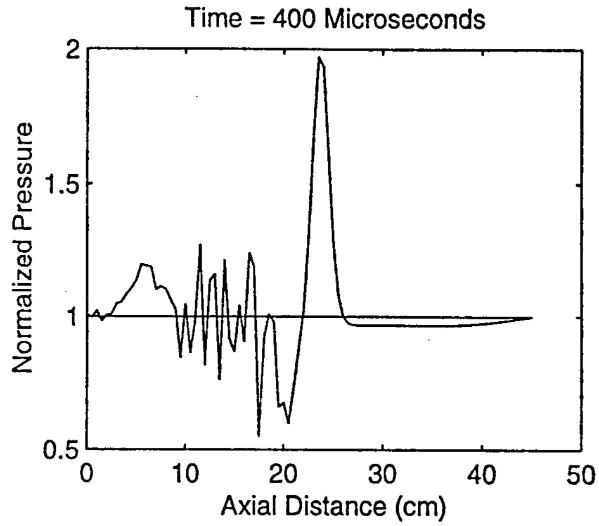
Time = 400 Microseconds
Normalized Pressure
2
1.5
1
0.5
0
10
20
30
40
50
Axial Distance (cm)

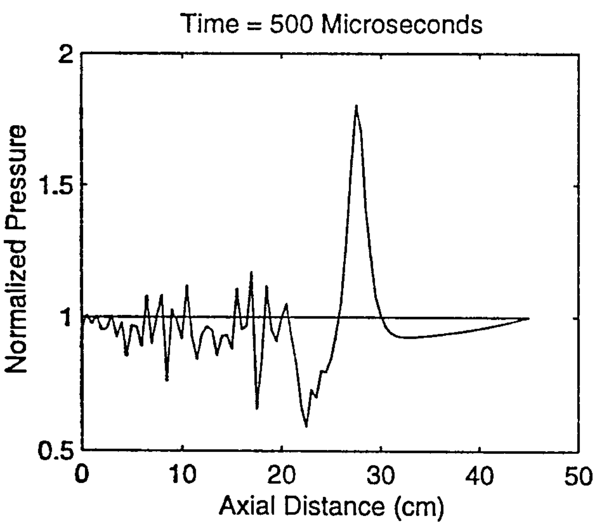
Time = 500 Microseconds
Normalized Pressure
2
1.5
1
0.5
0
10
20
30
40
50
Axial Distance (cm)

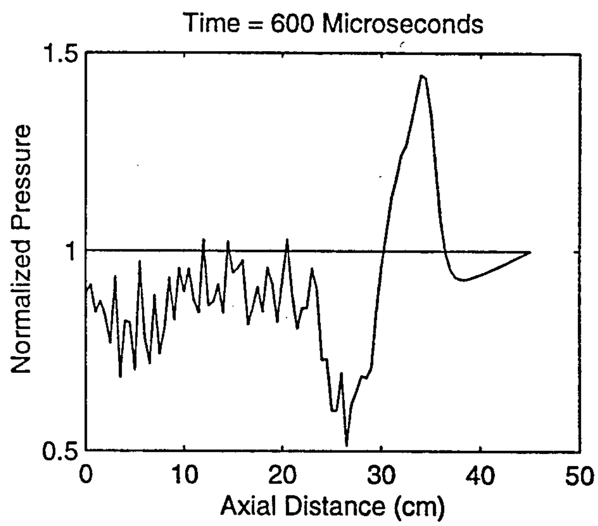
Time = 600 Microseconds
Normalized Pressure
1.5
1
0.5
0
10
20
30
40
50
Axial Distance (cm)

8/98

1) No radial temp grad

2) Triangular axial temp grad

3) No plasma.

CASE III

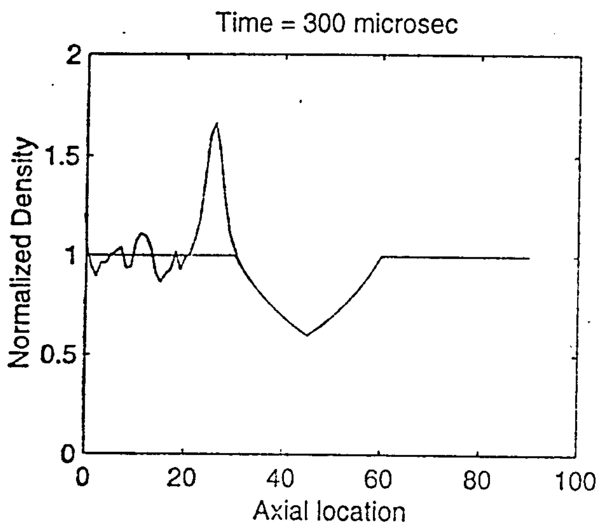

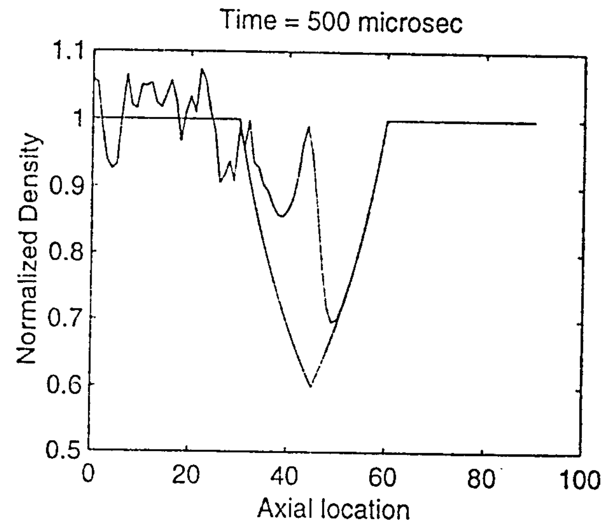

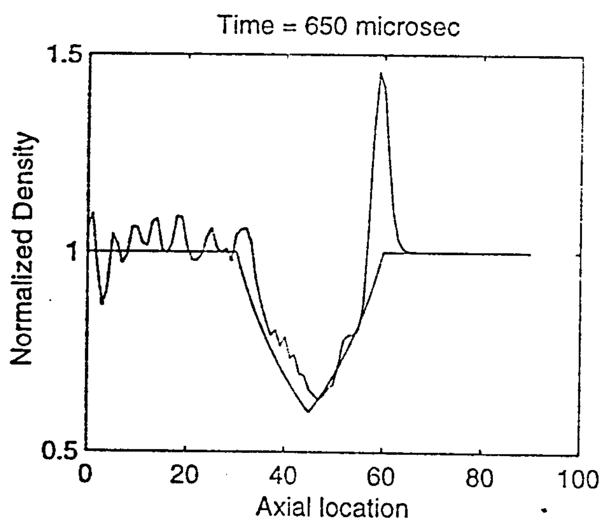

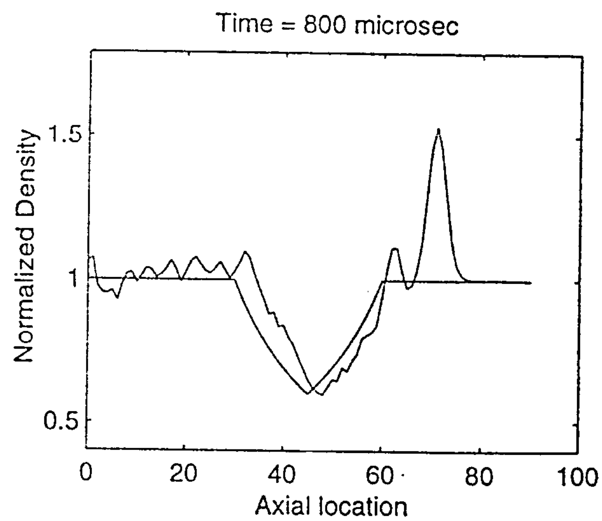

1/8/98

1) No radial tem. grad

2) Triangular axial temp gr

3) No plasma.

CASE III

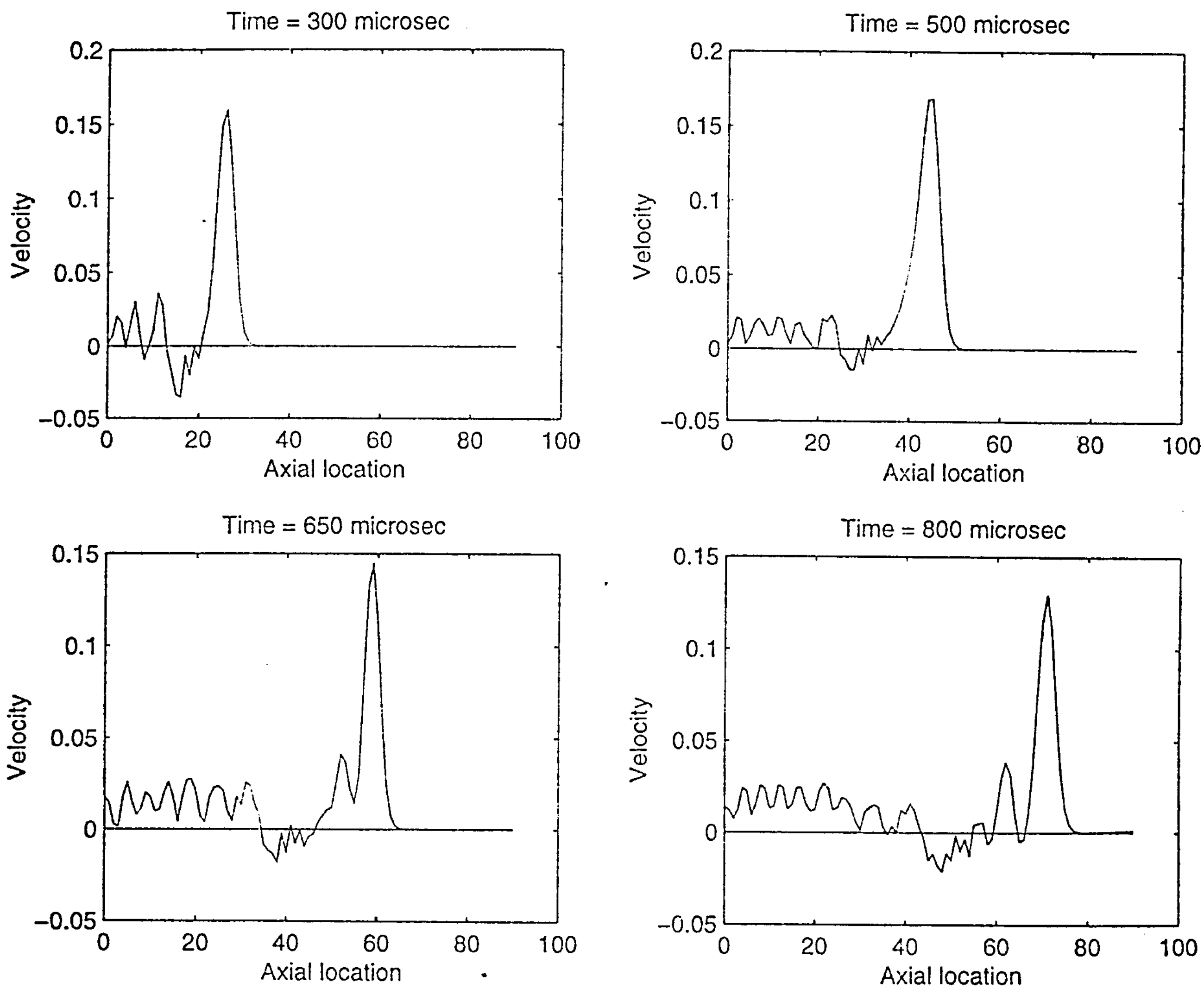

1/8/98

1) No radial temp g.
2) Triangular axial temp gra
3) No plasma

CASE III

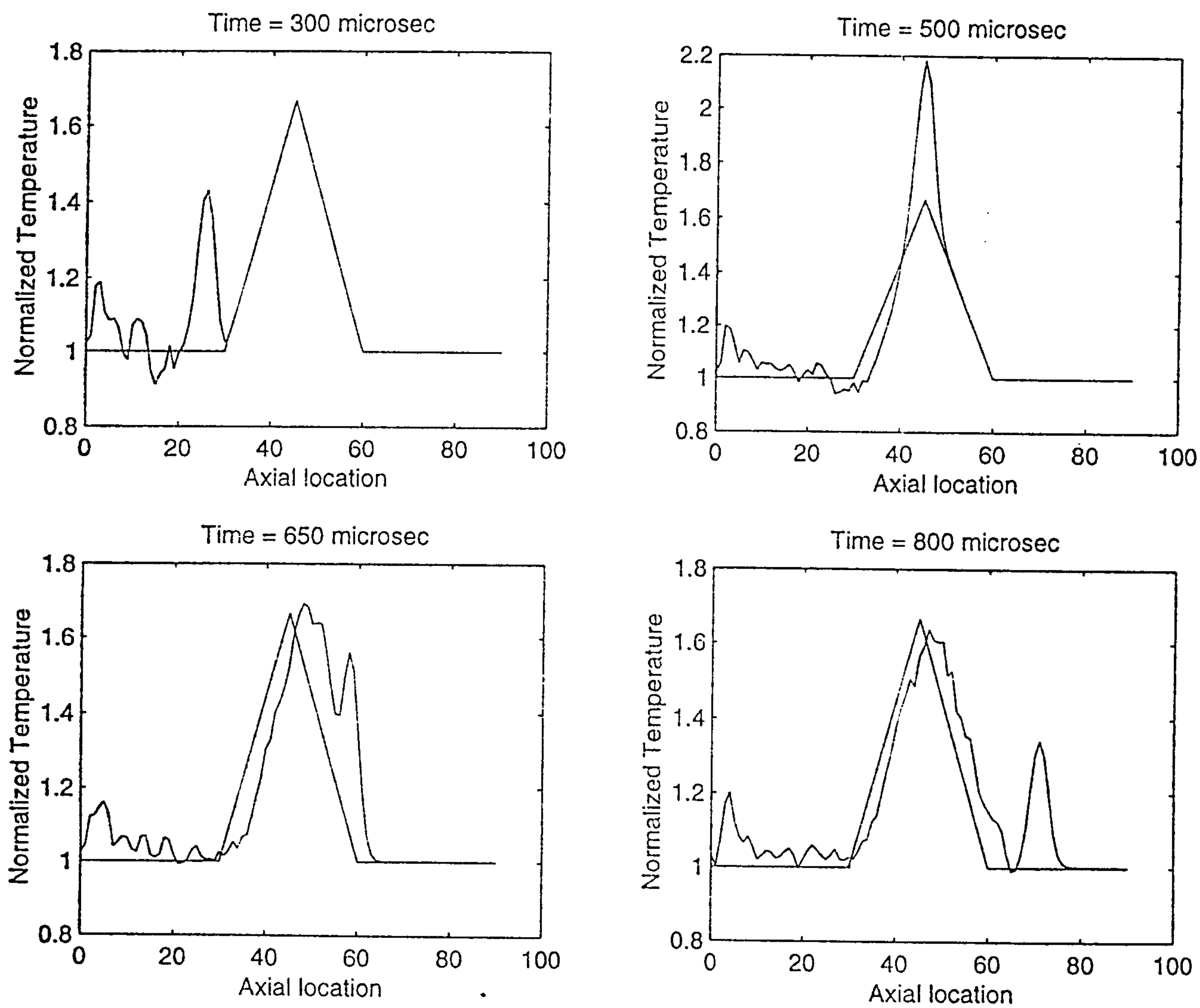

1/8/98

1) No radial temp gradient

2) Triangular axial temp grad

3) No plasma

CASE III

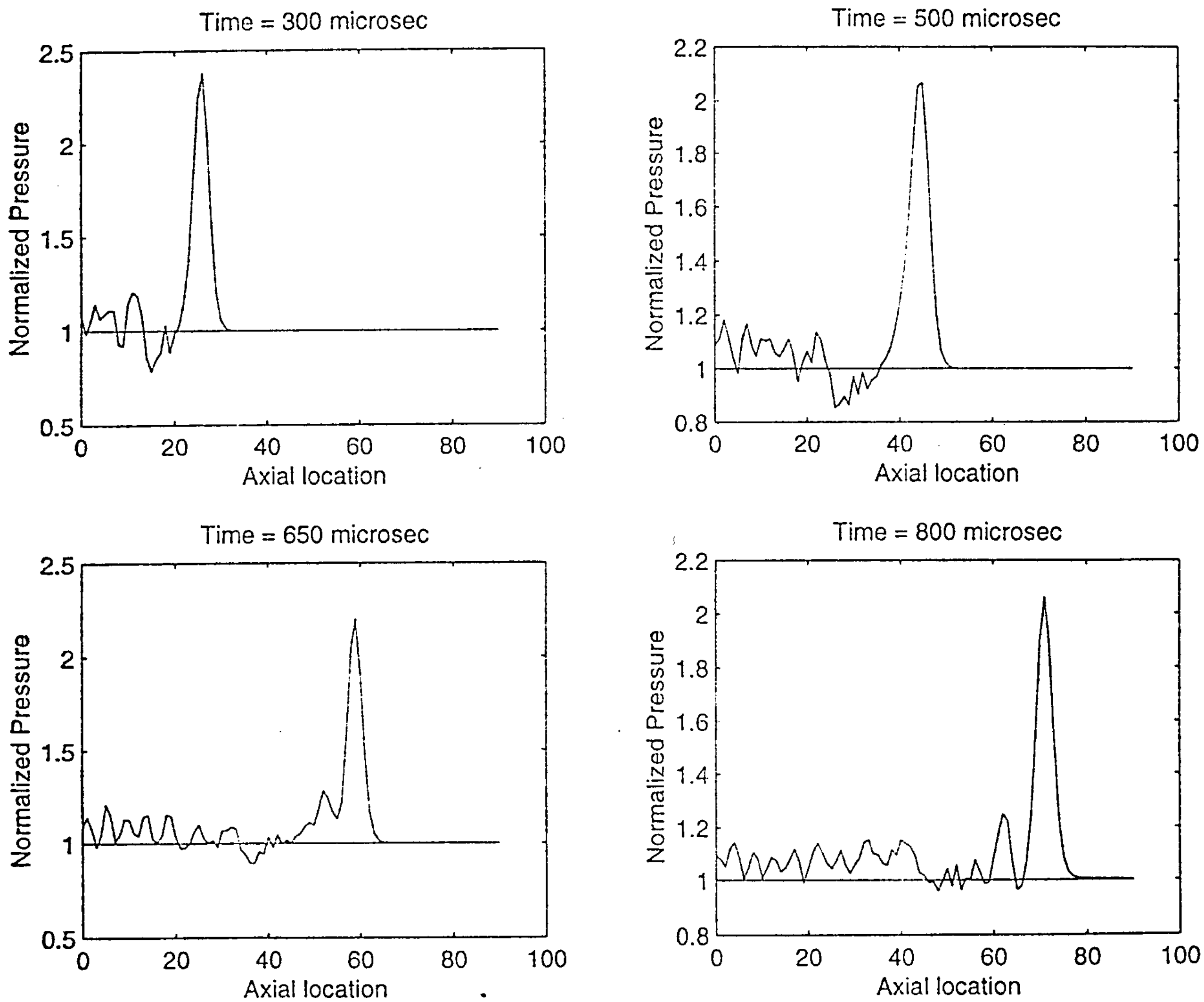

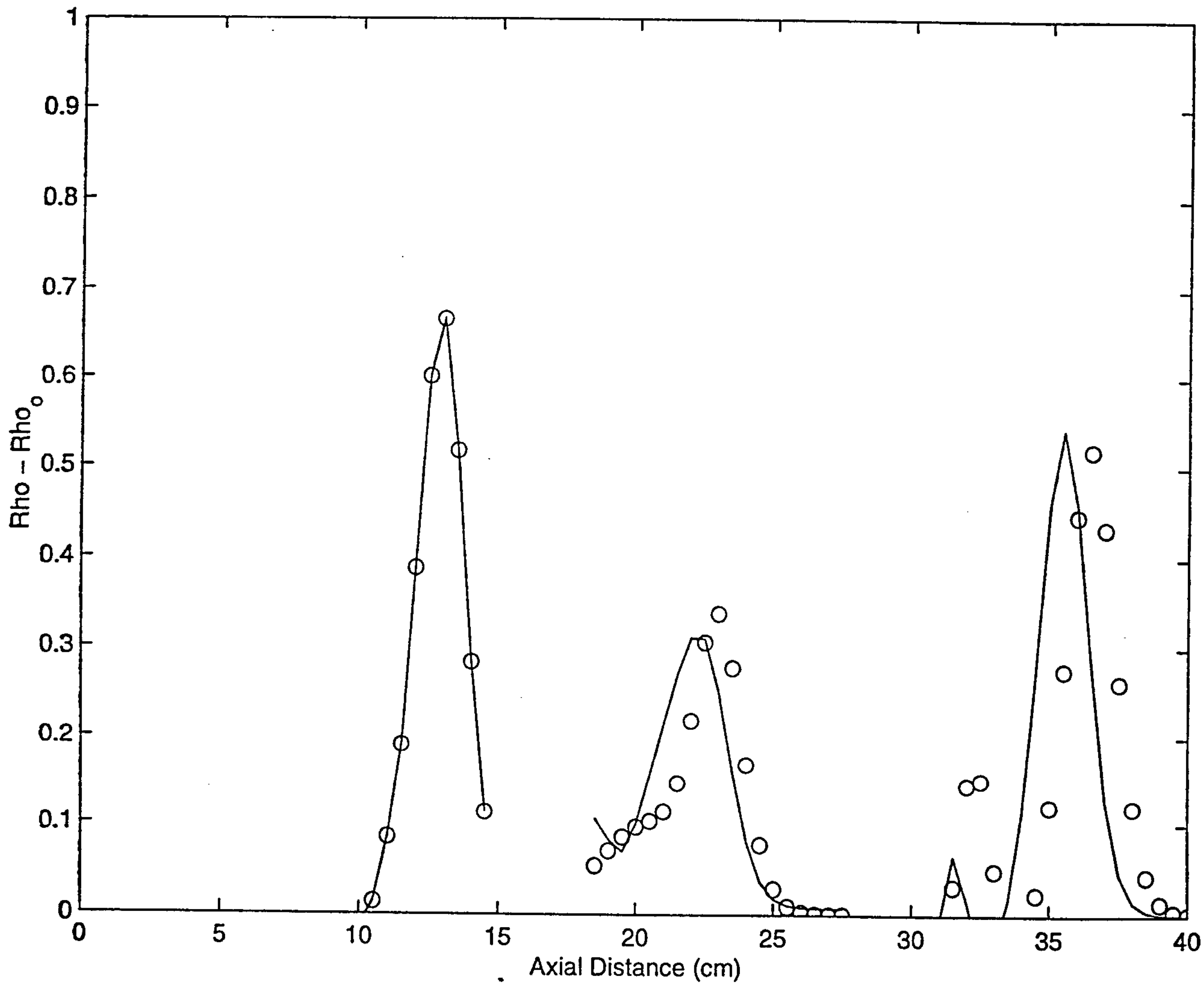

Rho - Rho$_o$
Axial Distance (cm)
0
0.1
0.2
0.3
0.4
0.5
0.6
0.7
0.8
0.9
1
0
5
10
15
20
25
30
35
40

DIAPHRAGM/PISTON - DRIVEN SHOCK

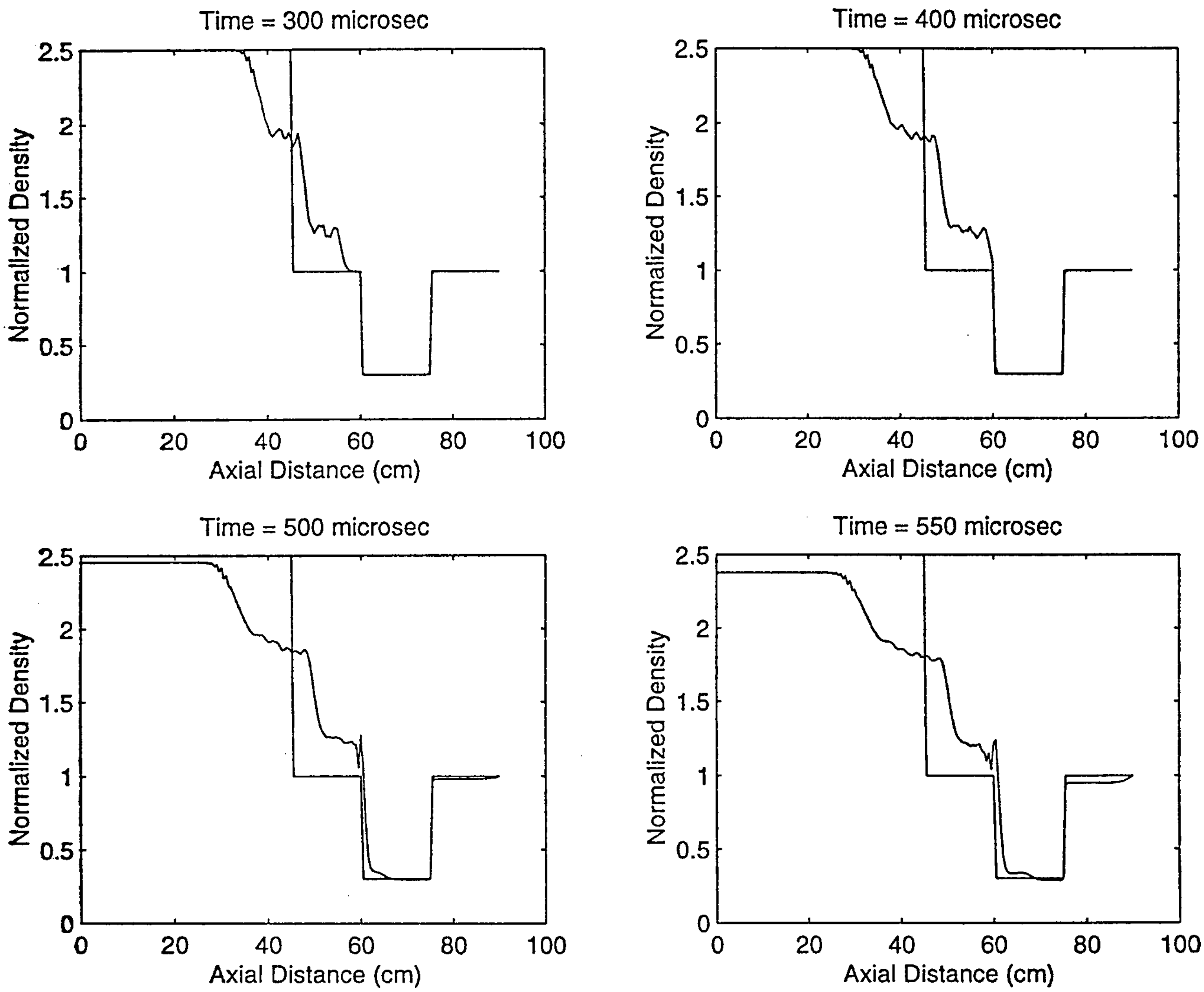

DIAPHRAGM/PISTON DRIVEN SHOCK

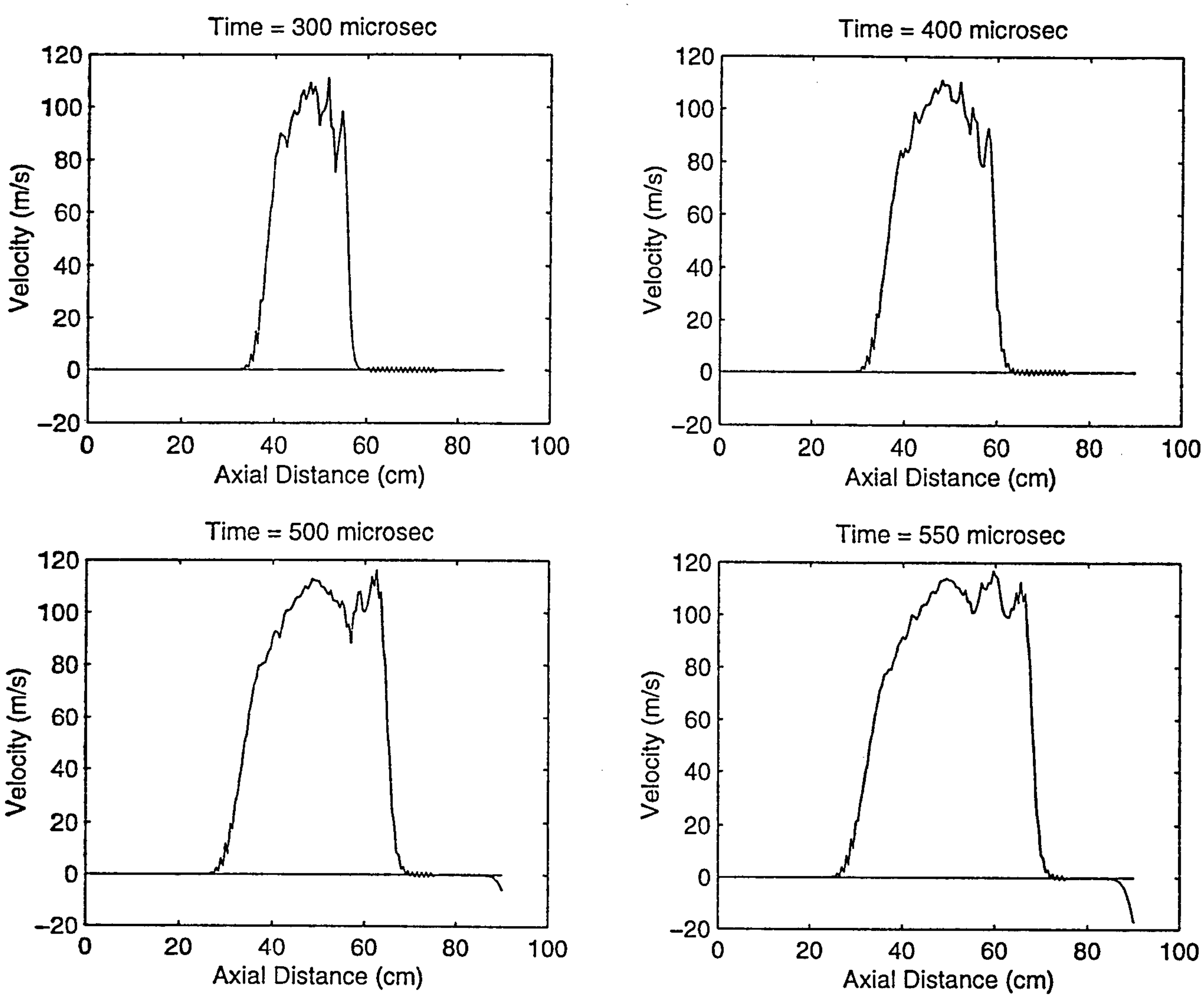

DIAPHRAGM/PISTON DRIVEN SHOC

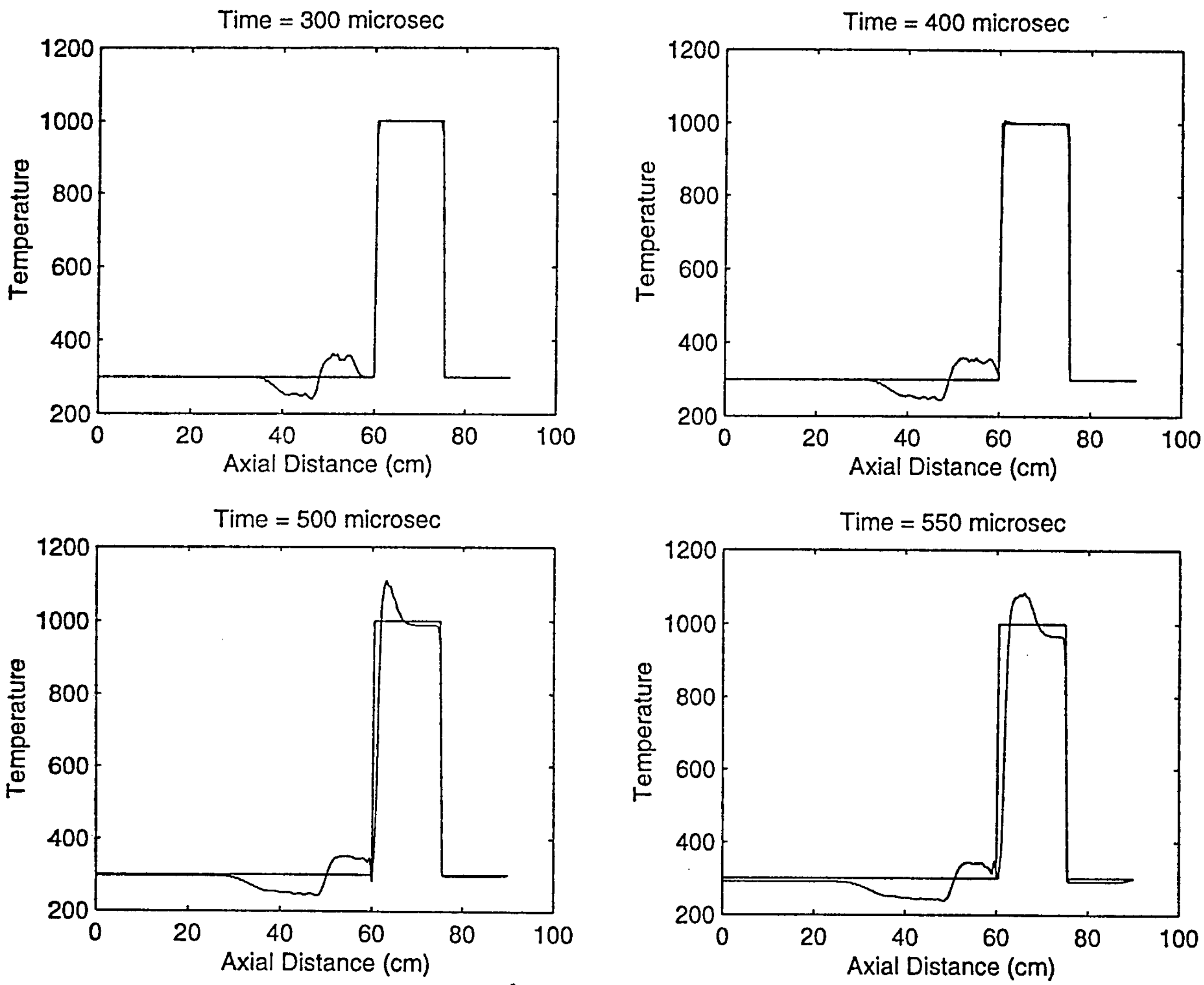

DIAPHRAGM/IN DRIVEN SHOCK

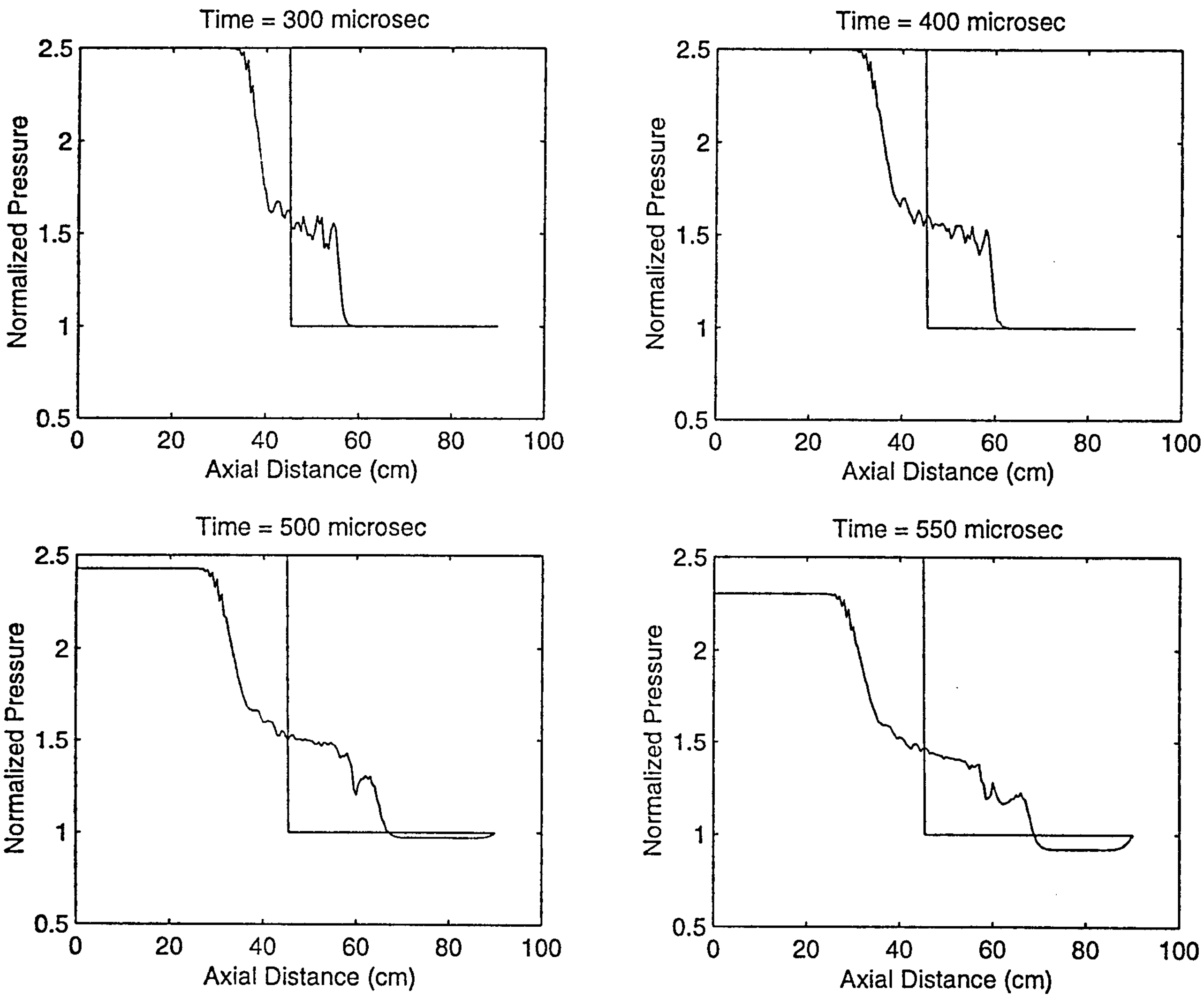

FINE GRID, ...-/1000/300

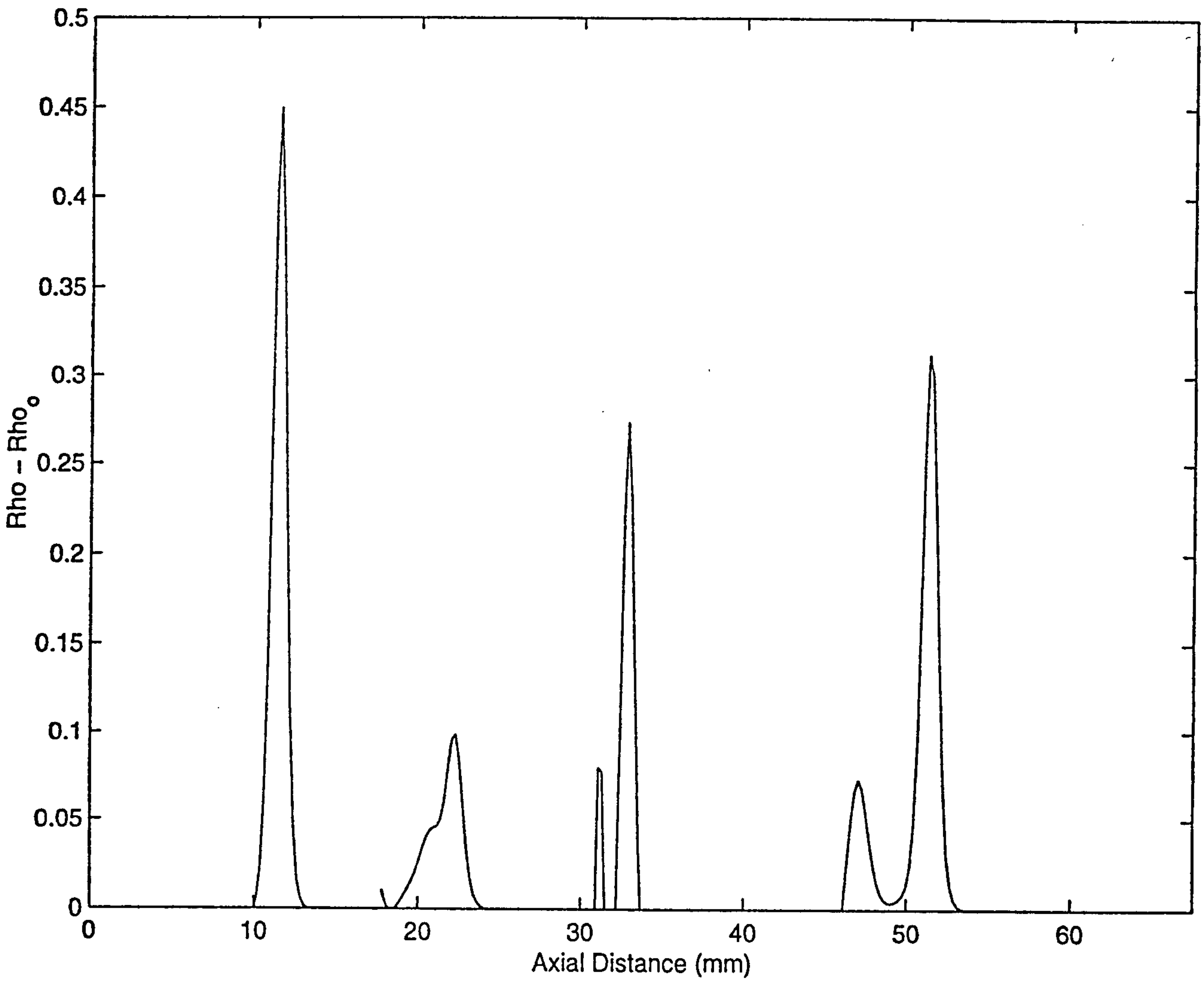

FINE GRID, 30/100/30

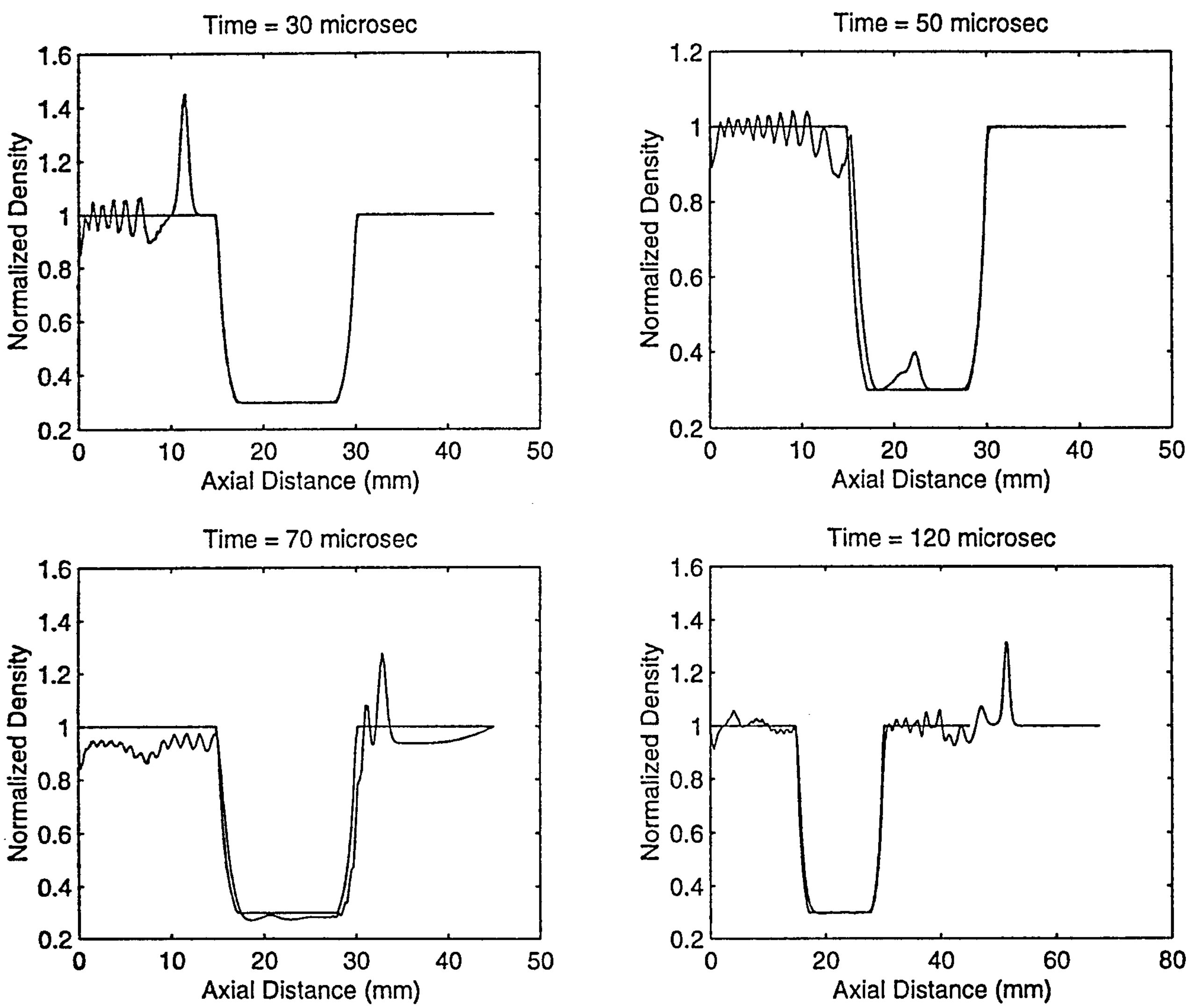

FINE GRID, 350/1000/350

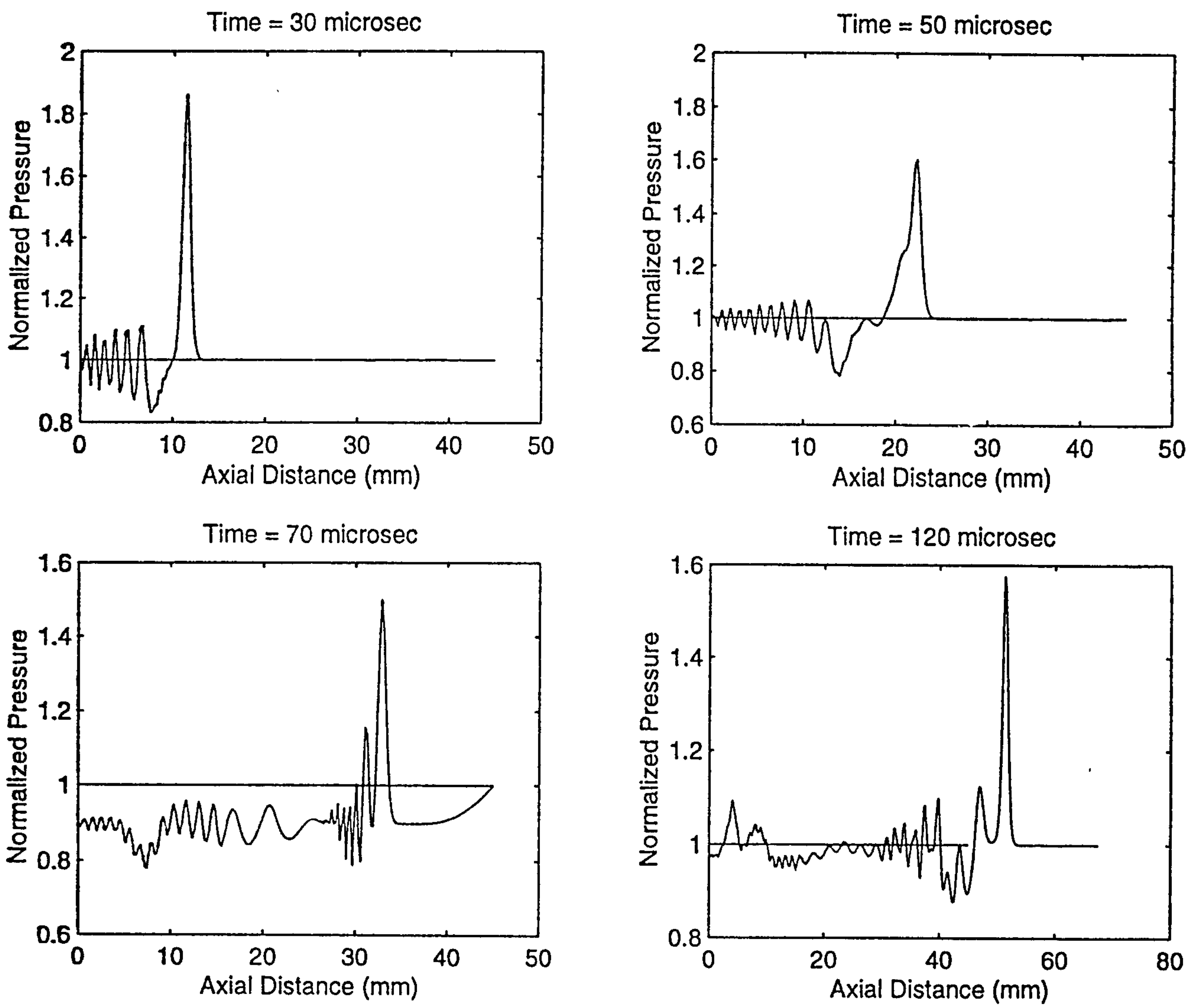

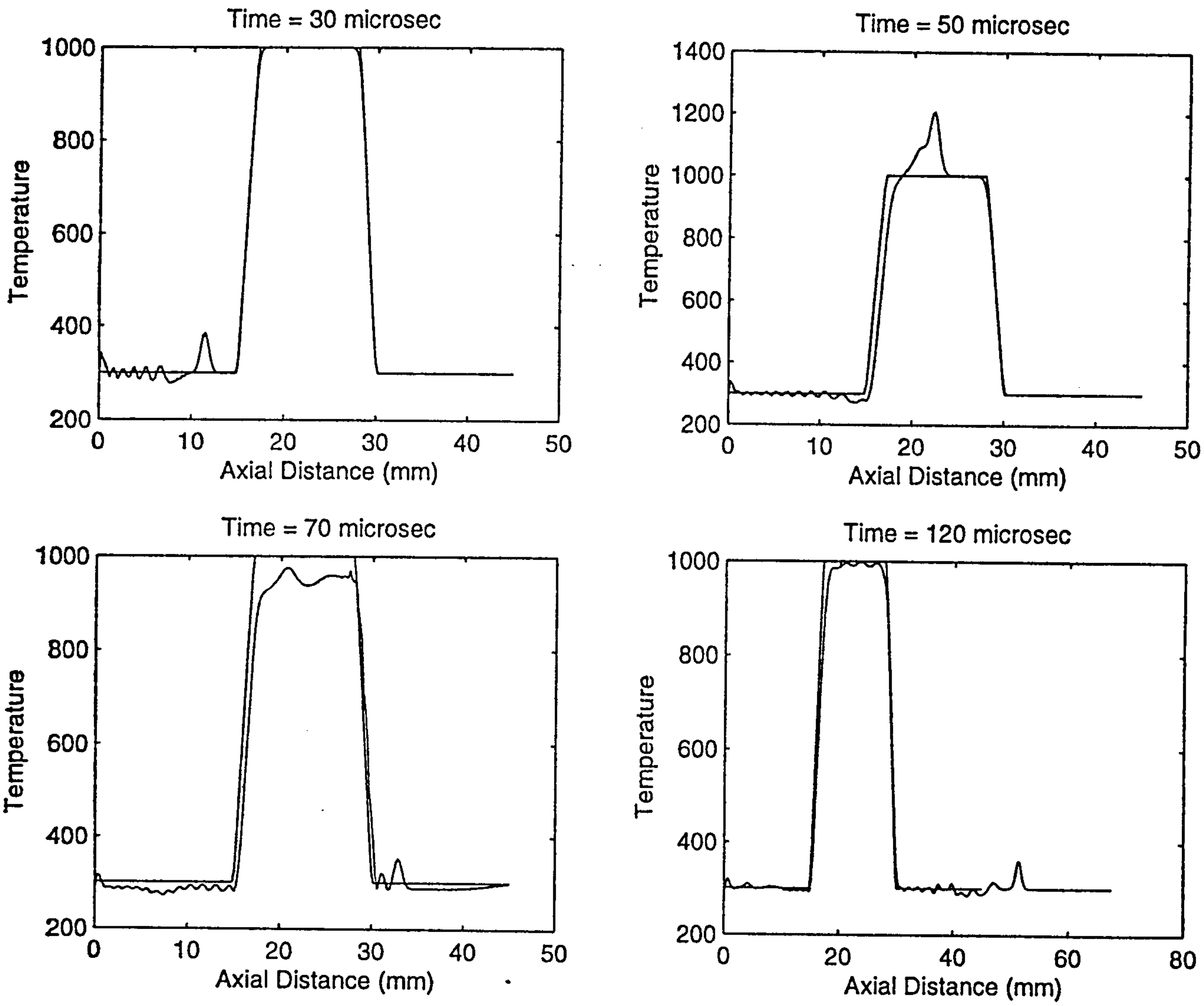

FINE GRID, 300/1000/300

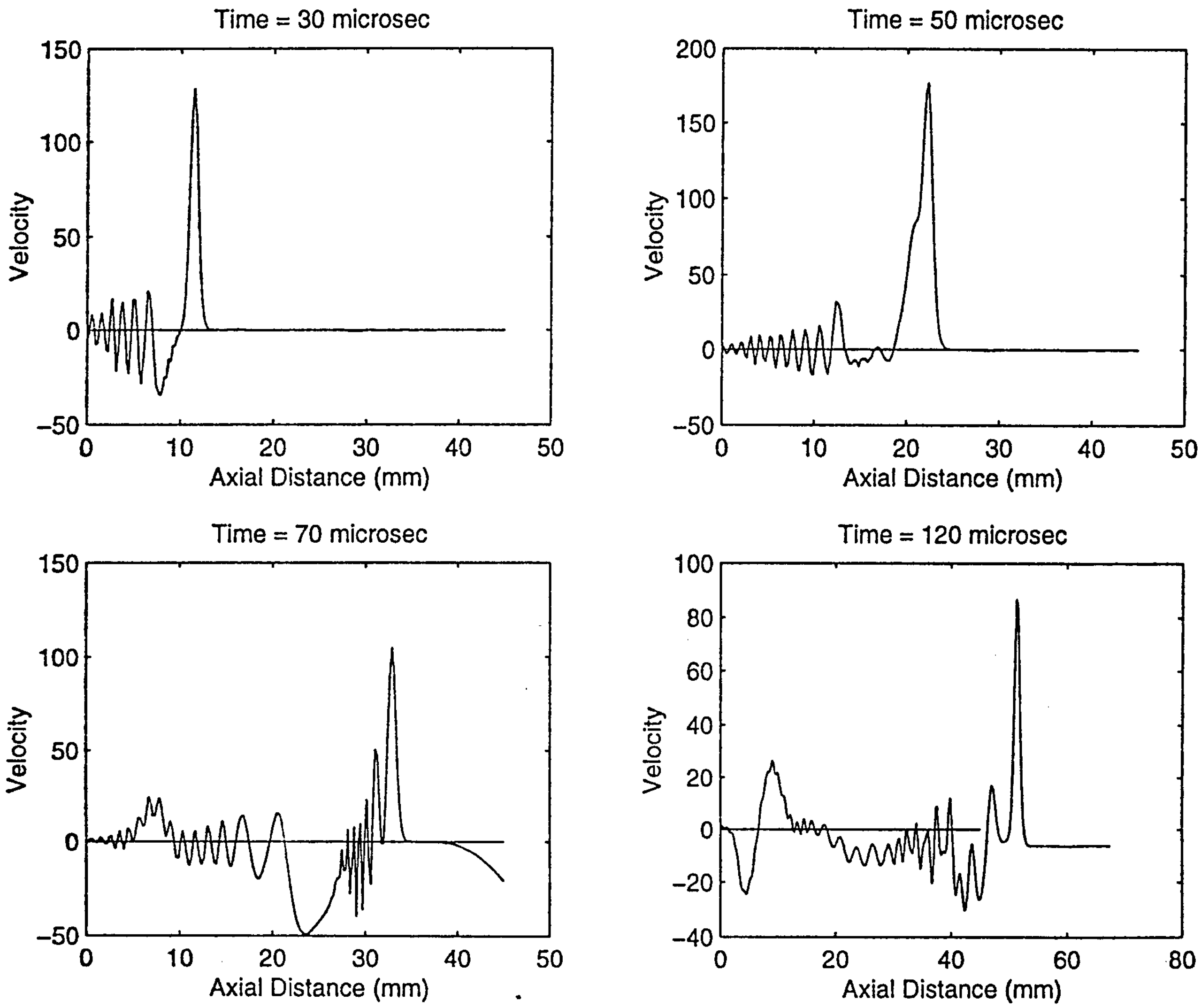

Fine Grid, 350/150/350

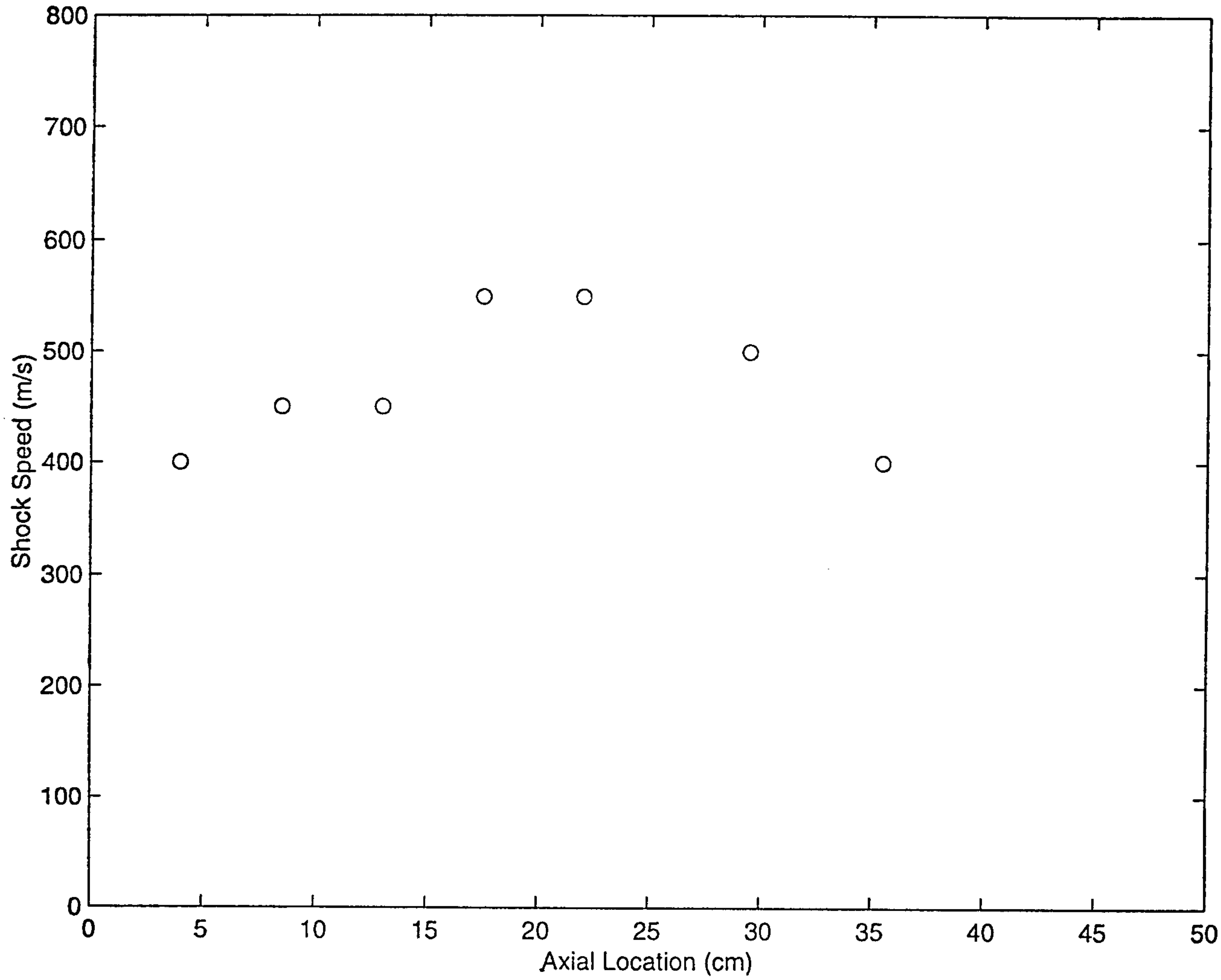

800
700
600
500
400
300
200
100
0
0
5
10
15
20
25
30
35
40
45
50
Shock Speed (m/s)
Axial Location (cm)

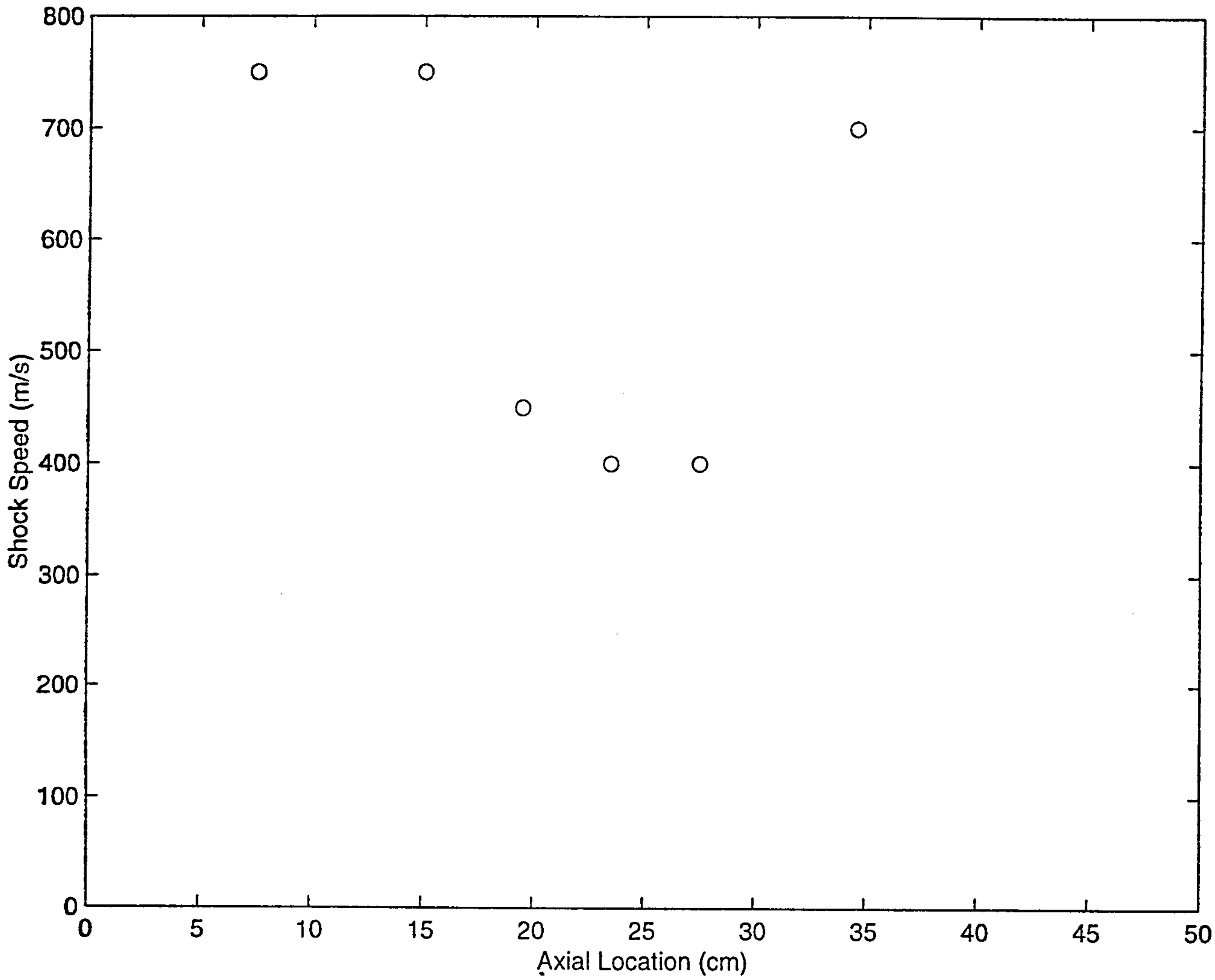

Shock Speed (m/s)
Axial Location (cm)
0
100
200
300
400
500
600
700
800
0
5
10
15
20
25
30
35
40
45
50

T · H · E OHIO STATE UNIVERSITY

Introduction

- Anomalous behavior of shock waves in weakly ionized plasmas:
  - shock wave accelerates
  - stand-off distance increases
  - shock splits into two or more structures
  - shock strength (as measured by density differences) diminishes
  - results occur in atomic and molecular gases
  - shock nearly recovers its original strength well downstream of the discharge.

- **Previous simulations (Bailey & Hilbun, Macheret & Martinelli) show radial thermal gradients can alter density profiles:**
  - **in piston-driven shock tubes**
  - **and when there is a curved boundary initially separating the hot and cold regions of a gas**

- **Thermal effects have been invoked to explain some experimental observations, but cannot explain others (such as shock recovery distance).**

- **Previous analysis (Adamovich et. al.) shows:**

(1) In order to change shock structure, an agent must have energy comparable to the incident kinetic energy density of the incident flow

(2) Two globally adiabatic shocks, able to exchange energy among themselves reproduces experimental observations:

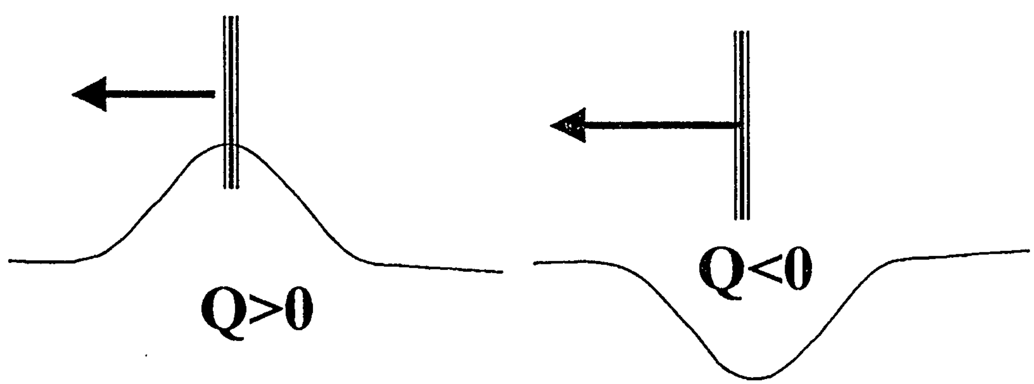

Effects of Radial Thermal Gradients (2-D axi-symmetric Navier-Stokes solution for Argon)

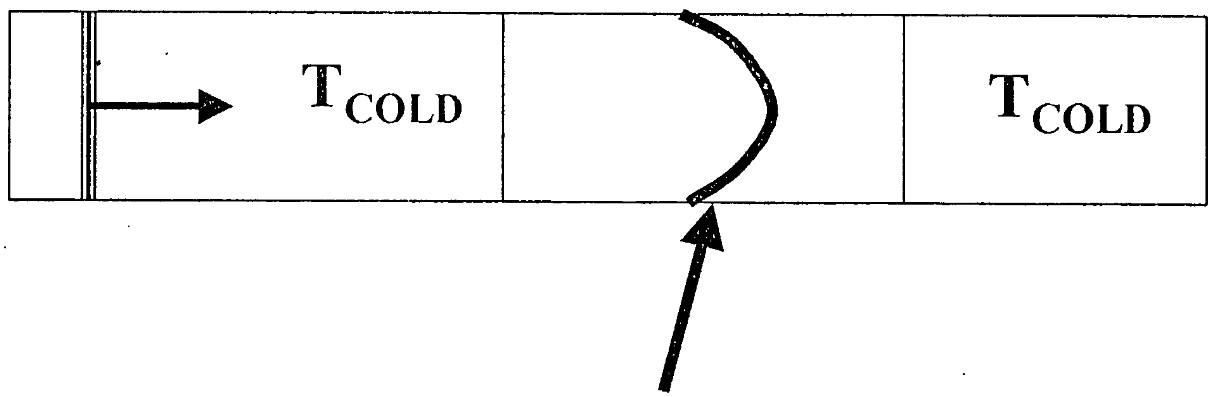

Initial parabolic temperature profile varying from T_{HOT} at the centerline to T_{COLD} at the wall.

Summary of Thermal Effects

- Axial temperature gradients cause splitting of an impulsive load into two distinct waves, a strong leader, and a weak follower.
- Radial gradients affect results quantitatively, but are not the cause of this splitting.
- Shock recovery is almost immediate, whereas they vary from 10 cm to 20 cm in the Ganguly-Bletzinger experiments.

$\therefore$ THERMAL EFFECTS CANNOT SOLELY EXPLAIN OBSERVED EXPERIMENTAL RESULTS.

Suppose that space charge layer induces a potential in the neutral gas, because neutrals are polarizable:

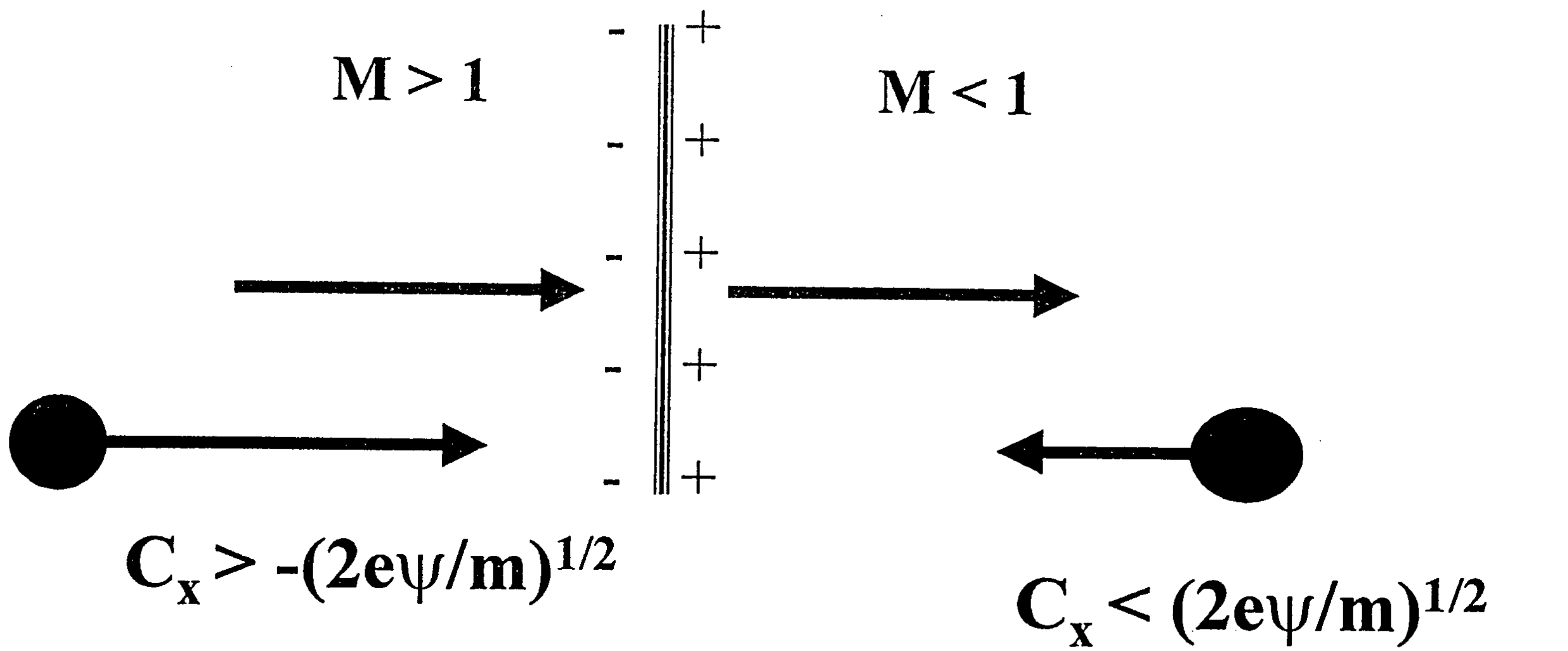

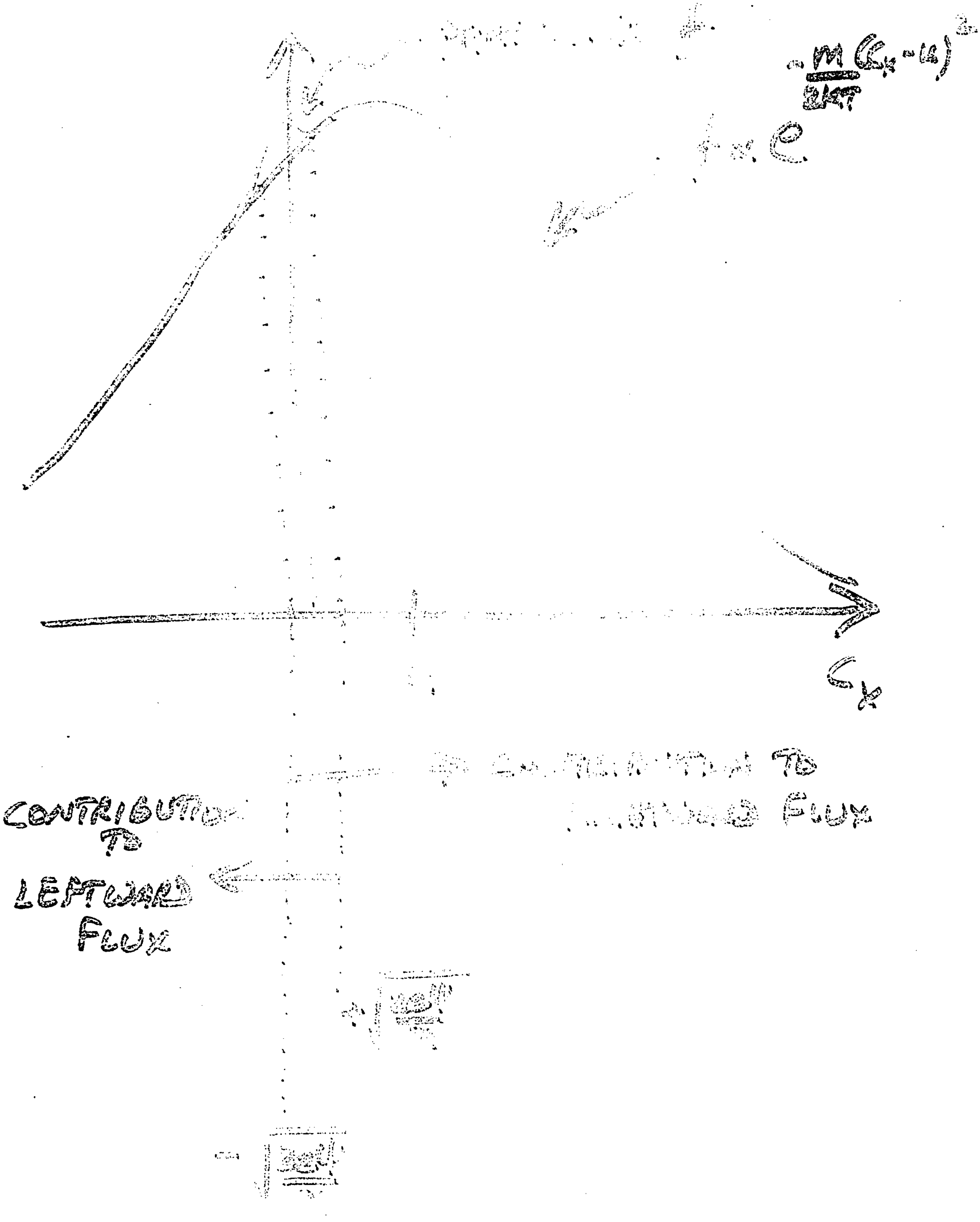

$-\frac{m}{2kT}(c_x - u)^2$
c_x
CONTRIBUTION TO LEFTWARD FLUX

Consequences

- **Let the force experienced by the neutral particles be:**

$$F_x = -e\left(\frac{\partial\psi}{\partial x}\right)\left[\Im\left(\sqrt{\frac{2e\psi}{m}} - C_x\right)\Im(x - x_o) + \Im\left(\sqrt{\frac{2e\psi}{m}} + C_x\right)\Im(x_o - x)\right]$$

where

$$\Im(z) = \begin{cases} 0 \ , \ z < 0 \\ 1 \ , \ z > 0 \end{cases}$$ *is the Heaviside step function,*

and C_x *is the x−component of the absolute particle velocity*

What would be the corresponding macroscopic equations to lowest order?

- Continuity

$$\frac{\partial n}{\partial t}+\frac{\partial}{\partial x}(nu)=N=\begin{cases} \dfrac{ne}{m}\left(\dfrac{\partial \psi}{\partial x}\right)\sqrt{\dfrac{m}{2\pi kT}}\; e^{-\left(\sqrt{\frac{e\psi}{kT}}-u\sqrt{\frac{m}{2kT}}\right)^2} & ;\; x>x_o \\ -\dfrac{ne}{m}\left(\dfrac{\partial \psi}{\partial x}\right)\sqrt{\dfrac{m}{2\pi kT}}\; e^{-\left(\sqrt{\frac{e\psi}{kT}}+u\sqrt{\frac{m}{2kT}}\right)^2} & ;\; x<x_o \end{cases}$$

- **x-momentum**

$$\frac{\partial(nu)}{\partial t}+\frac{\partial}{\partial x}\left(nu^2+\frac{nkT}{m}\right)=M=\begin{cases}\dfrac{en}{m}\left(\dfrac{\partial\psi}{\partial x}\right)\left(\sqrt{\dfrac{e\psi}{\pi kT}}\;e^{-\left(\sqrt{\frac{e\psi}{kT}}-u\sqrt{\frac{m}{2kT}}\right)^2}-\dfrac{1}{2}\left[1-erf\left(u\sqrt{\dfrac{m}{2kT}}-\sqrt{\dfrac{e\psi}{kT}}\right)\right]\right) & ;\ x>x_o\\[2ex] \dfrac{en}{m}\left(\dfrac{\partial\psi}{\partial x}\right)\left(\sqrt{\dfrac{e\psi}{\pi kT}}\,e^{-\left(\sqrt{\frac{e\psi}{kT}}+u\sqrt{\frac{m}{2kT}}\right)^2}-\dfrac{1}{2}\left[1-erf\left(-u\sqrt{\dfrac{m}{2kT}}-\sqrt{\dfrac{e\psi}{kT}}\right)\right]\right) & ;\ x<x_o\end{cases}$$

- **Energy**

$$\frac{\partial}{\partial t}\left(\frac{3}{2}nkT+\frac{1}{2}mnu^2\right)+\frac{\partial}{\partial x}\left(\frac{5}{2}nukT+\frac{1}{2}mnu^3\right)=S$$

$$where \quad S=\begin{cases} ne\left(\dfrac{\partial\psi}{\partial x}\right)\left[\left(\dfrac{2kT}{m\pi}\right)^{1/2}+\left(\dfrac{e\psi}{kT}\right)\left(\dfrac{kT}{2\pi m}\right)^{1/2}\right]e^{-\left(\sqrt{\frac{e\psi}{kT}}-u\sqrt{\frac{m}{2kT}}\right)^2} \\ \quad -\dfrac{neu}{2}\left(\dfrac{\partial\psi}{\partial x}\right)\left[1-erf\left(u\sqrt{\dfrac{m}{2kT}}-\sqrt{\dfrac{e\psi}{kT}}\right)\right] & ; \ x>x_o \\ -\ ne\left(\dfrac{\partial\psi}{\partial x}\right)\left[\left(\dfrac{2kT}{m\pi}\right)^{1/2}+\left(\dfrac{e\psi}{kT}\right)\left(\dfrac{kT}{2\pi m}\right)^{1/2}\right]e^{-\left(\sqrt{\frac{e\psi}{kT}}+u\sqrt{\frac{m}{2kT}}\right)^2} \\ \quad -\dfrac{neu}{2}\left(\dfrac{\partial\psi}{\partial x}\right)\left[1-erf\left(-u\sqrt{\dfrac{m}{2kT}}-\sqrt{\dfrac{e\psi}{kT}}\right)\right] & ; \ x<x_o \end{cases}$$

Source term in momentum equation

$$M_1 \approx -\frac{en_1}{m}\left(\frac{\partial \psi}{\partial x}\right)\bigg|_1 e^{-\frac{\gamma}{2}M_1^2}$$

$$M_2 \approx -\frac{en_2}{m}\left(\frac{\partial \psi}{\partial x}\right)\bigg|_2 e^{-\frac{\gamma}{2}M_2^2}$$

$$\Rightarrow \left|\frac{M_2}{M_1}\right| \approx \frac{n_2}{n_1}\frac{(\partial \psi / \partial x)|_2}{(\partial \psi / \partial x)|_1} e^{\frac{\gamma}{2}\left(M_1^2 - M_2^2\right)}$$

$\Rightarrow$ **Net Force is upstream**

Source terms in continuity equation

$$N_1 \approx \frac{en_1}{m}\left(\frac{\partial\psi}{\partial x}\right)\bigg|_1 \sqrt{\frac{m}{2\pi kT_1}}\, e^{-\frac{\gamma}{2}M_1^2}$$

$$N_2 \approx -\frac{en_2}{m}\left(\frac{\partial\psi}{\partial x}\right)\bigg|_2 \sqrt{\frac{m}{2\pi kT_2}}\, e^{-\frac{\gamma}{2}M_2^2}$$

$$\frac{N_2}{N_1} \approx -\frac{n_2}{n_1}\frac{(\partial\psi/\partial x)|_2}{(\partial\psi/\partial x)|_1}\sqrt{\frac{T_1}{T_2}}\, e^{\frac{\gamma}{2}\left(M_1^2 - M_2^2\right)}$$

$$\Rightarrow N_2 > N_1$$

Source term in energy equation

$$S_1 \approx e n_1 \left(\frac{\partial \psi}{\partial x}\right)\bigg|_1 \left(\frac{\gamma k T_1}{m\pi}\right)^{1/2} \left[\sqrt{\frac{2}{\gamma}} - M_1\right] e^{-\frac{\gamma}{2} M_1^2}$$

$$S_2 \approx -e n_2 \left(\frac{\partial \psi}{\partial x}\right)\bigg|_2 \left(\frac{\gamma k T_2}{m\pi}\right)^{1/2} \left[\sqrt{\frac{2}{\gamma}} + M_2\right] e^{-\frac{\gamma}{2} M_2^2}$$

$$\Rightarrow \quad \frac{S_2}{S_1} \approx \frac{n_2}{n_1} \frac{(\partial \psi / \partial x)|_2}{(\partial \psi / \partial x)|_1} \sqrt{\frac{T_2}{T_1}} \frac{\left[\sqrt{\frac{2}{\gamma}} + M_2\right]}{\left[M_1 - \sqrt{\frac{2}{\gamma}}\right]} e^{\frac{\gamma}{2}\left(M_1^2 - M_2^2\right)}$$

$\Rightarrow$ **Note change in sign when** $\mathbf{M}_1 = \sqrt{\frac{2}{\gamma}}$

THREE CASES

(A)

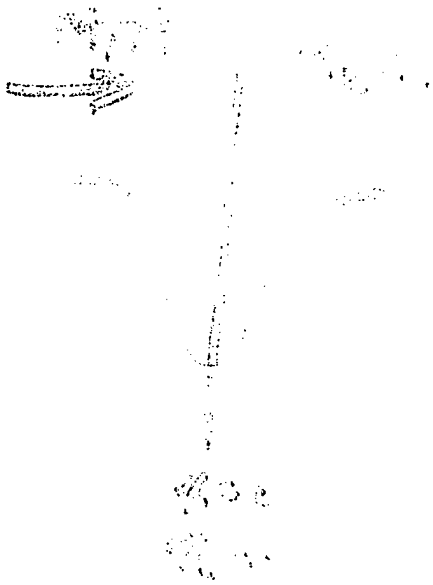

(B)

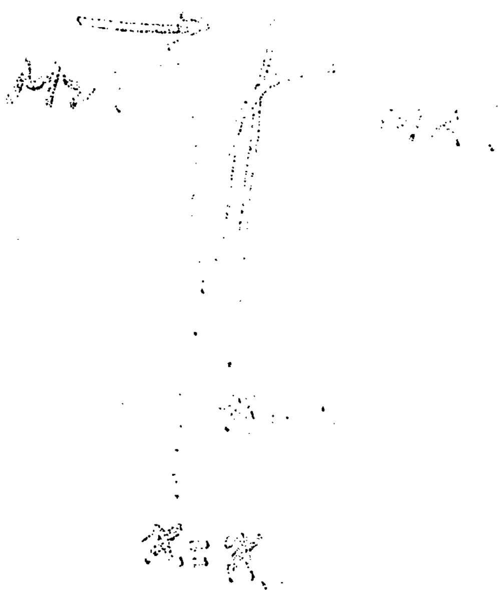

(C)

- **Distribution function will be non-M-B in the neighborhood of the shock**

  $\Rightarrow$ steep thermal, and density gradients will induce additional mass, momentum, and energy transfer from downstream region to upstream region.

- **Questionable as to whether a steady state can exist when sources are present in continuity, momentum, and energy equations.**

Case(B): Potential well ahead of shock

- Just upstream of the shock, for $x_o < x < 0$, $S > 0$, provided M_1 in the region is less than $(2/\gamma)^{1/2}$ while $S \rightarrow 0$ for $x > 0$ (downstream of the shock) since $\partial\psi/\partial x \rightarrow 0$ there

  $\Rightarrow$ SPLITTING ?
- For $M_1 > (2/\gamma)^{1/2}$, $S < 0$ in the same region

  $\Rightarrow$ STABLE
- Further, $\tilde{M} < 0$ for $x > x_o$ $\Rightarrow$ a body force driving shock upstream is present

  $\Rightarrow$ LARGER STAND-OFF DISTANCE

Summary

- **Classical gas dynamics predicts splitting of a pulse in the presence of a streamwise temperature gradient - But, split structure appears different from that observed in experiments.**

- **There may be special circumstances under which induced dipole effects cause the presence of local *adverse* thermal gradients at the shock front, by affecting the distribution function.**

Flow Control via MHD and EMHD

George Em Karniadakis

Division of Applied Mathematics
Center for Fluid Mechanics, Turbulence and Computation
Brown University
Providence, RI 02912

http://www.cfm.brown.edu/CRUNCH

AFOSR Workshop on

Understanding and Control of Ionized High-Speed Flows

February 26–27, 1998
Princeton, NJ

High-Speed Flow Features

- Strong shock wave effects/interactions
  - thin layers, small detachment distance, etropy layer
- Strong viscous effects/interactions
  - $\delta \sim \frac{M^2}{\sqrt{Re}}$
  - increased drag, heating at leading edge
- Transitional flow
  - $Re_c \sim 10^8$ vs. 10^5 (subsonic)
  - C_f and C_H are $3\times$ laminar
  - $Re_c^\theta \sim 100M_e$
- Nonequilibrium
  - thermal, chemical
  - introduction of length scale
  - multi-rate physics
- Ionization
  - 4000 K to 6000 K: $NO \rightarrow NO^+ + e^-$ (mild)
  - > 9000 K: $N \rightarrow N^+ + e^-$

    $O \rightarrow O^+ + e^-$
  - Above 20kM + 10 km/s
  - External B, E, frequencies
- Multiple boundary layers
  - hydrodynamics, thermal, species
  - electric conductivity, etropy layers

∴ - Multi-Rate Physics

- Multiple BLs

Non-Equilibrium Plasma Boundary Layer

- Effects on T_e, σ
- atmospheric-pressure potassium-seeded argon plasma

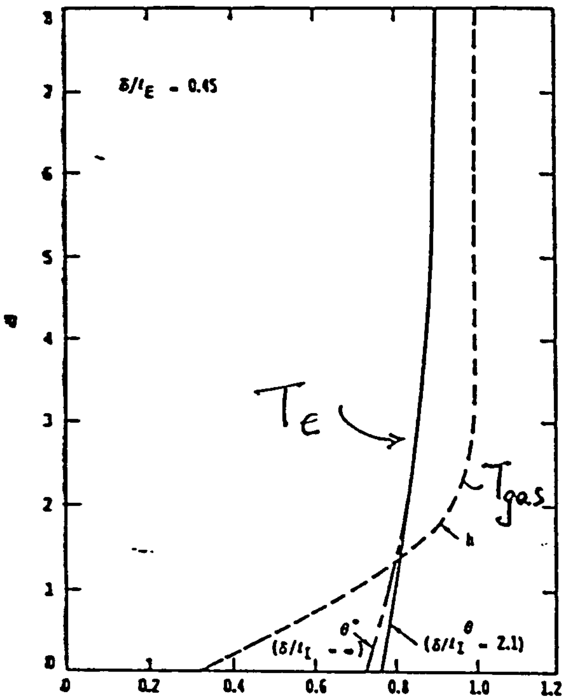

Normalized Temperature

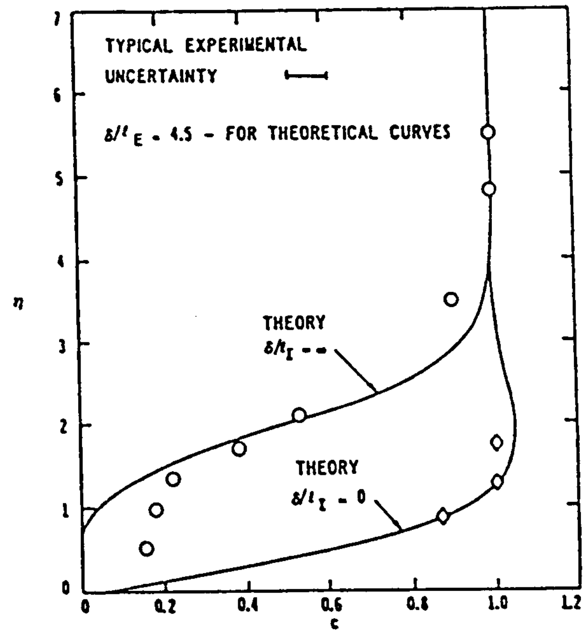

Normalized Conductivity

Ref: Brown & Mitchner (1971)

"... *Even in plasma which is strongly collision dominated, significant nonequilibrium may be present in the boundary layer adjacent to a cooled solid surface...*"

Note: Joule heating due to E could further increase conductivity.

Electrical Conductivity

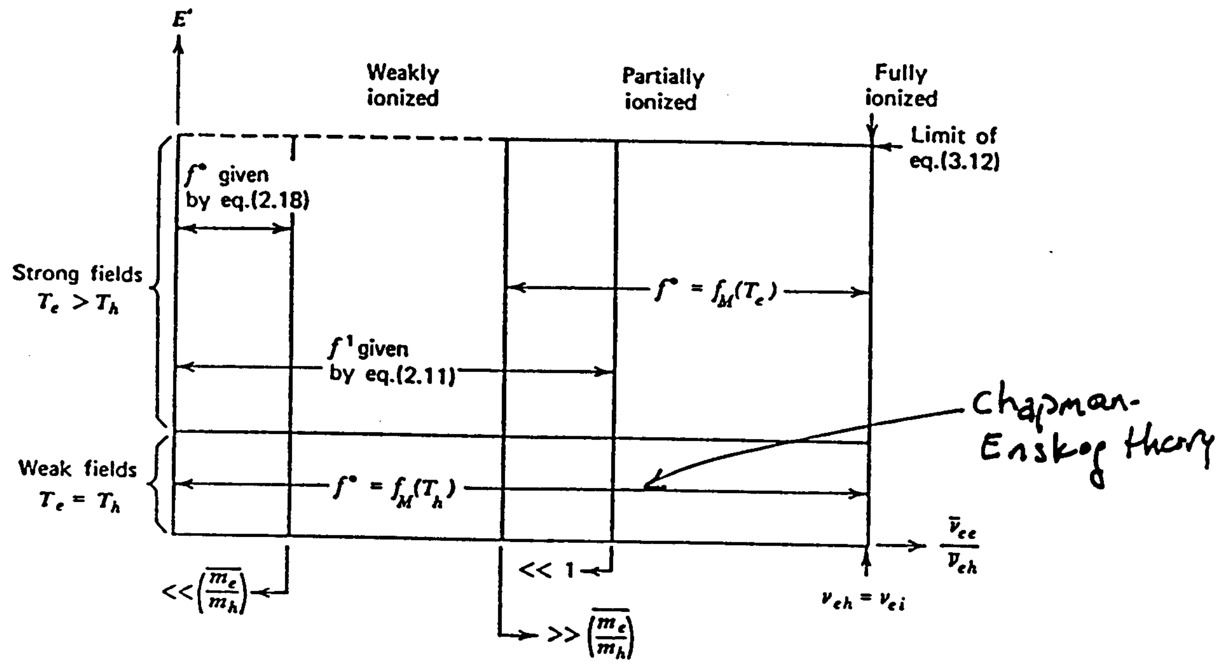

Electric Field vs. Ionization

- In constant E, B fields tensor conductivity

$$\text{Weakly-ionized}\begin{cases}\sigma_{\|} = \mathcal{F}(n_e, m_e, \nu_{eH}, f^0)\\ \sigma_{\perp} = \mathcal{F}(n_e, m_e, \nu_{eH}, f^0, \omega_e)\\ \sigma_H = \mathcal{F}(n_e, m_e, \nu_{eH}, f^0, \omega_e)\end{cases}$$

- If $B = 0 \Rightarrow \sigma_\perp = \sigma_\| = \sigma$
- If $E \sim e^{-i\omega t} \Rightarrow$ dependence of σ on ω , i.e. pulsing via tiles!

Note: $f^0 = \mathcal{F}(E^0_{11}, E_\perp, \nu_{eH}, T_H, m_e, m_H)$

Lorentz Force: Numerical Modeling

- Governing Equations for $\vec{B}$ and $\vec{E}$
- Boundary Conditions - The Motz problem

Example 1: Electromagnetic Tiles

Dirichlet: $\vec{F}_{\perp} \sim \frac{1}{3}\vec{F}_{\|}$; Neumann: $\vec{F}_{\perp} \sim \vec{F}_{\|}$

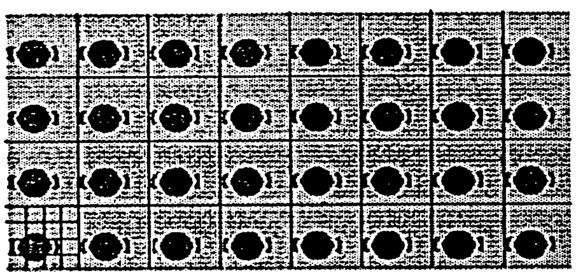

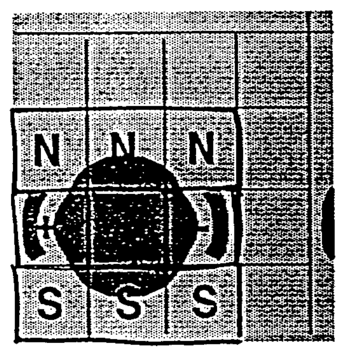

Example 2: Alternate stripes of electrodes/magnets $F_{\|} \sim e^{-\frac{\pi}{a}\lambda y}$? penetration

	Dirichlet	Neumann	D-N	Mixed
λ	4	2	8	8

Lorentz Force

- MHD Assumptions ($t_c > \omega_p^{-1}$)
  - Convection current neglected: $\frac{\rho_c U}{J} \ll 1$
  - Force due to net charge neglected: $\frac{\rho_c E}{|J \times B|} \ll 1$

Then:

$$\begin{aligned} \vec{F}_L &= \vec{J} \times \vec{B}; \;\; E_0 = \text{ external} \\ \vec{J} &= \sigma(\vec{E} + \vec{u} \times \vec{B}) + \sigma \vec{E}_0 \end{aligned}$$

simple Ohm's law

MHD-Control	**EMHD-Control**
• Apply $\vec{B}$	• Apply $\vec{B}$ and $\vec{E}$
• $E = -\nabla\Phi$	• $J \sim \sigma E_0$
• $\nabla^2\Phi = \nabla \cdot (\vec{u} \times \vec{B})$	• $I_{\text{applied}} = \frac{\sigma E_0 B L}{\rho U^2}$
• $I_{\text{induced}} = \frac{\sigma B^2 L}{\rho U}$	

where $R_{em} = \mu\sigma U L \ll 1$ in lab scale (neglect induced fields)

- But Ohm's law for partially ionized gas:

$$\vec{J} + \beta_e \vec{J} \times \vec{b} + s\vec{b} \times (\vec{J} \times \vec{b}) = \sigma(\vec{E} + \vec{u} \times \vec{B}) + \frac{\sigma}{e n_e} \nabla p_e$$

"Generalized Ohm's Law"

ion-slip

Discontinuous Galerkin Method - $\mathcal{N}\varepsilon\kappa\mathcal{T}\alpha r$

- dynamical Direct Numerical Simulation (dDNS)
- MHD, Compressible & Incompressible flows
- Full 3D Configurations - Arbitrary Geometric Complexity
- Unstructured/Hybrids Grids
- High-Order/Spectral Accuracy
- Conservative Formulation
- h-refinement for shocks/discontinuities
- ALE Algorithm for Moving Rotating Subdomains
- METIS/MPI-based Parallelization

$\therefore$ Convergence of (FV + FE + Spectral)
$\rightarrow$ DG

- MACH2/3 prototype - but high-order...

Hartmann-Hunt Flow : 3D

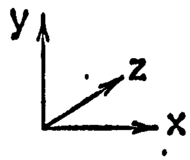

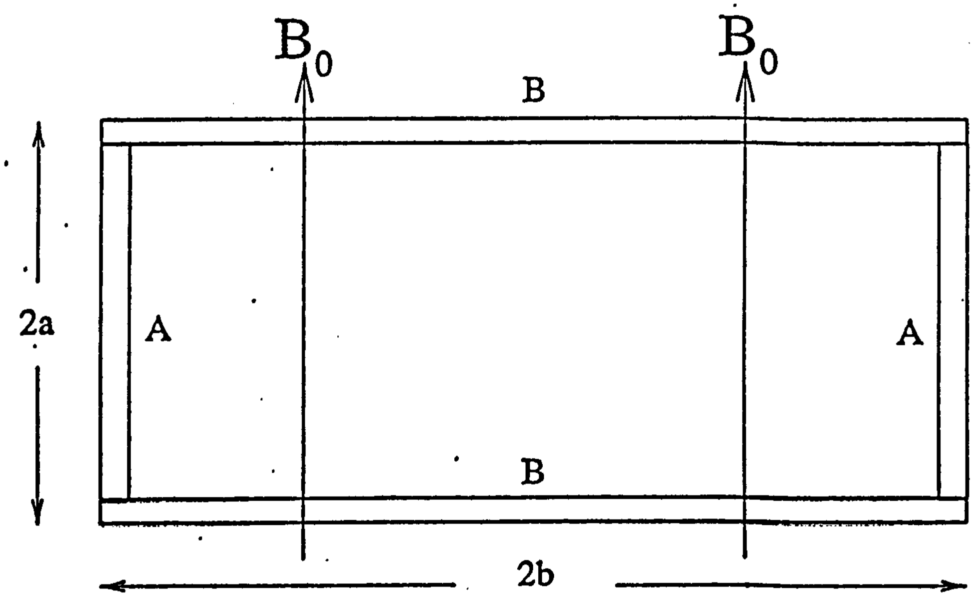

AA: Perfect Insulators

BB: Perfect Conductors

Flow is into the page

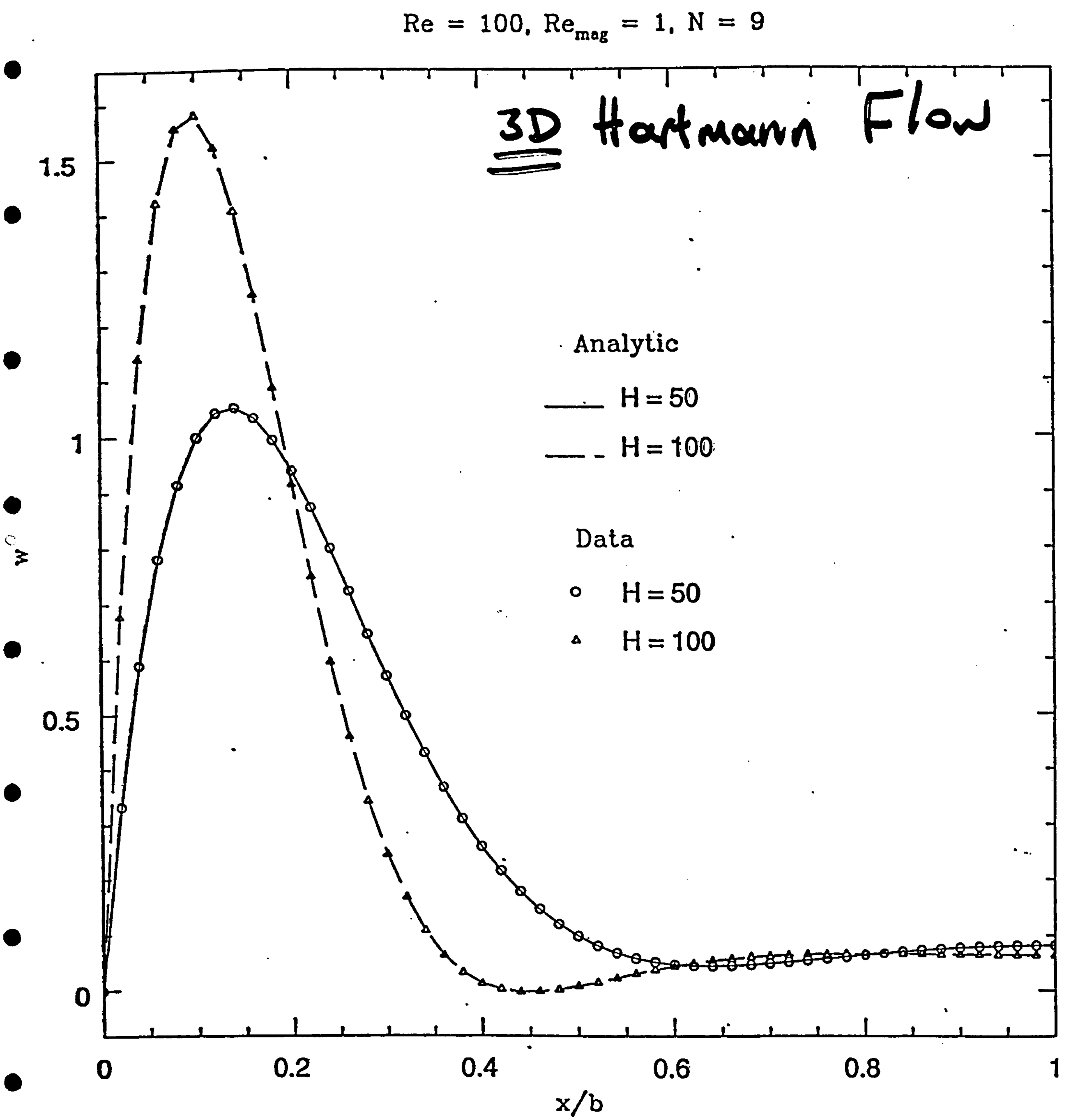

* Spectral/hp on Unstructured Grids.
(AFOSR)

Orszag-Tang MHD-Vortex

• Hybrid Grid

M=0.6

M=0

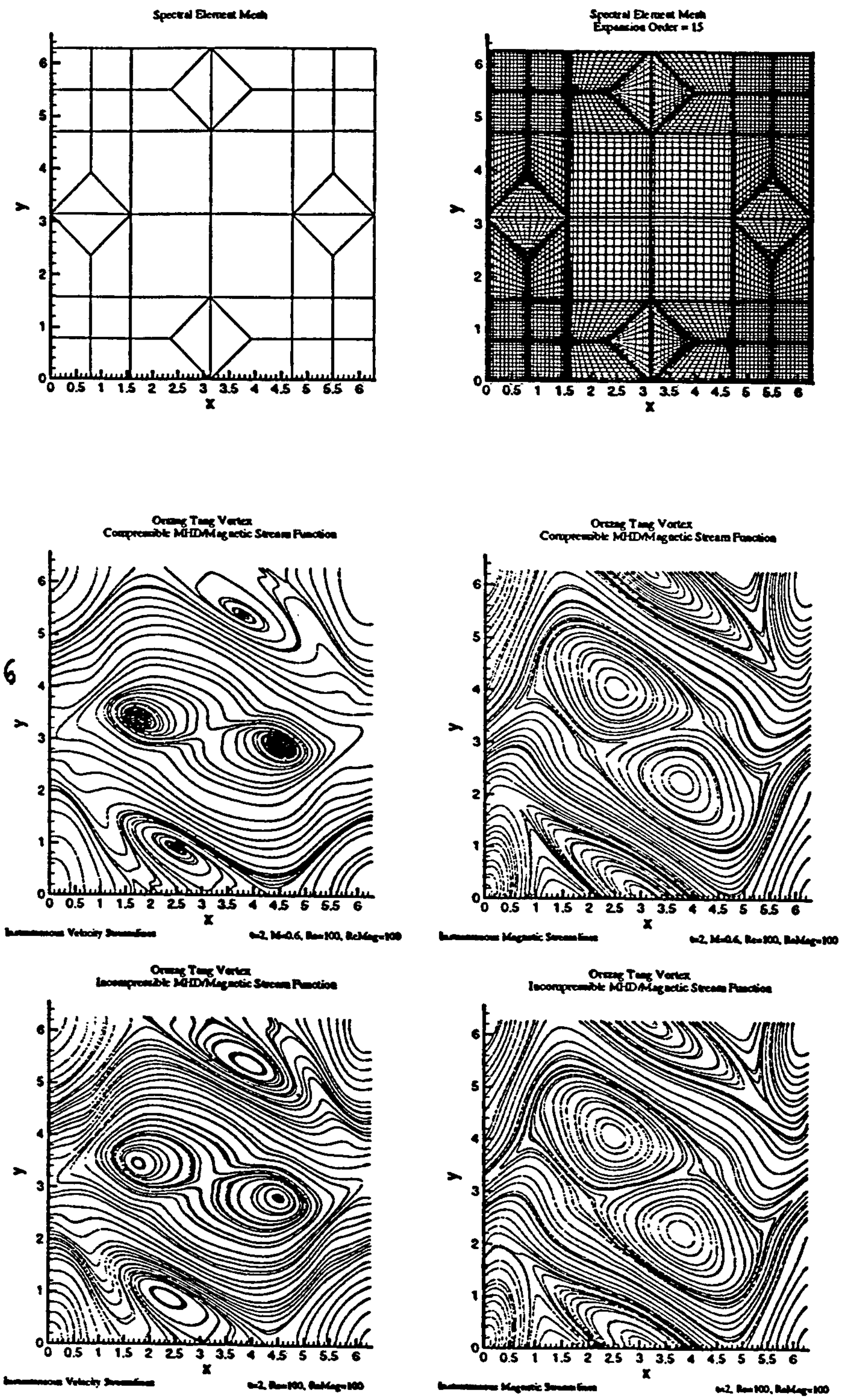

T.Warburton

H-P Adaptive Refinement: Viscous Supersonic Flows

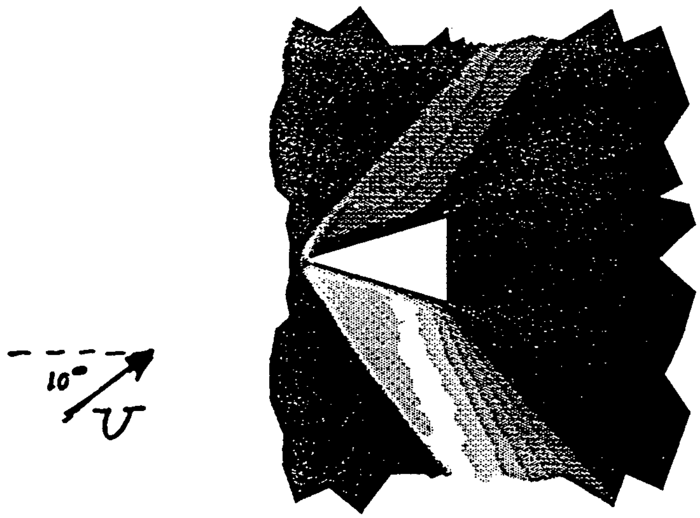

Figure 1: Discontinuous Galerkin Simulation: Density contours

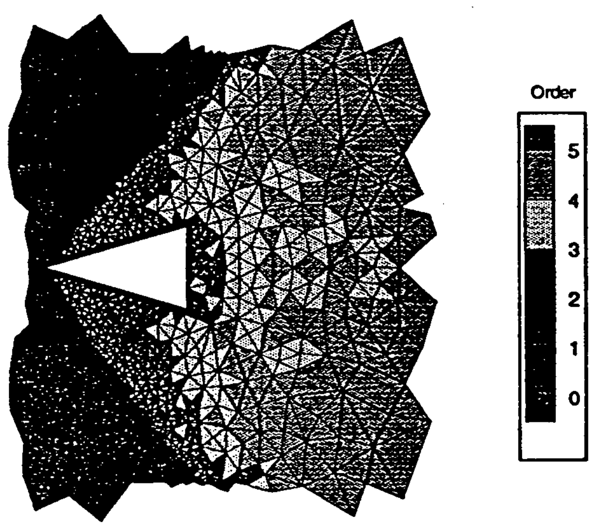

Figure 2: Unstructured grid and variable-order per element

* HYBRID APPROACH:

- DNS - near wall / structured
- LES in equilibrium regions

Hybrid-Element Boundary Layer Resolution

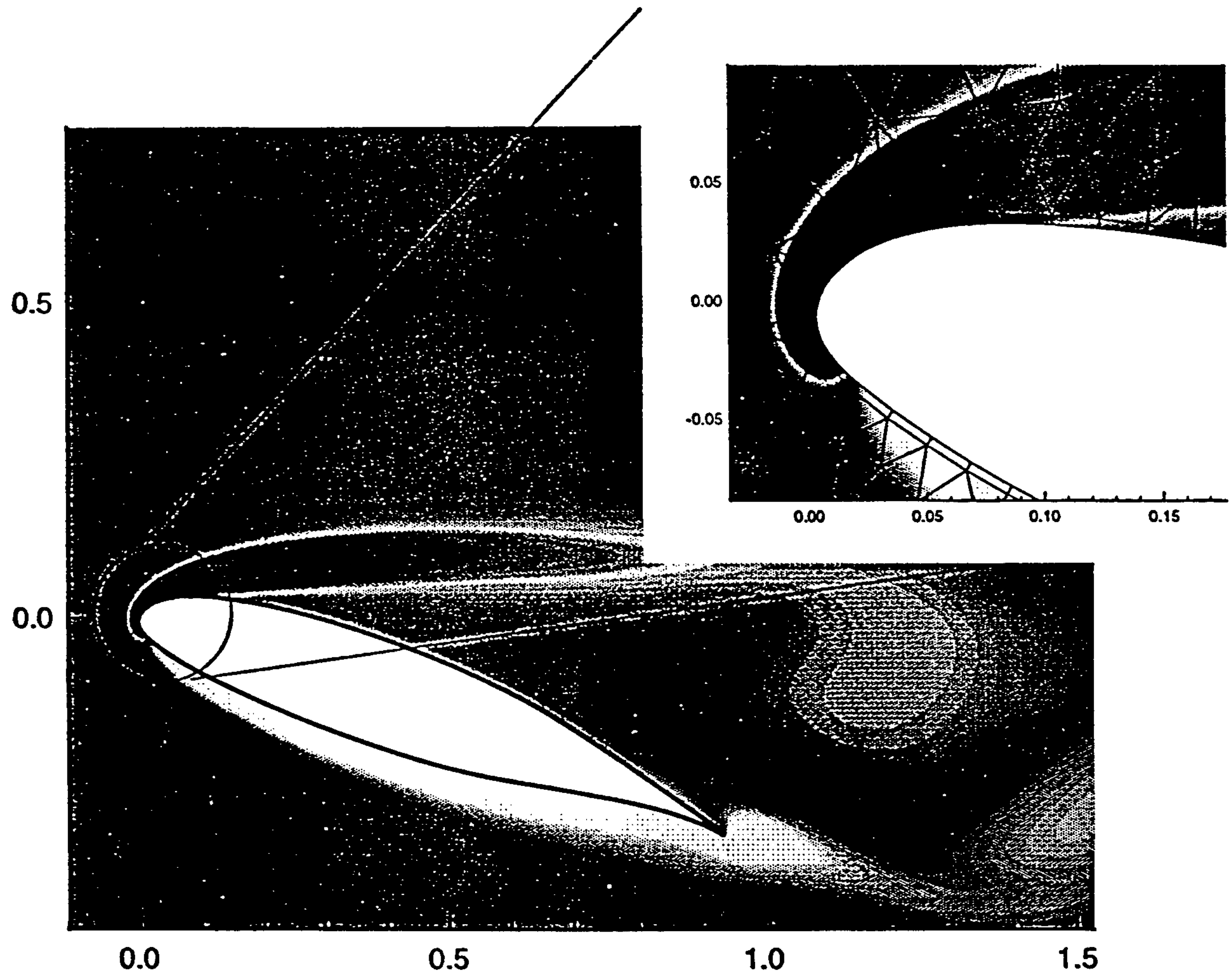

PhD Thesis: T.Warburton

Plan: { • DNS with h-p refinement.
• LES in equilibrium with h-p refinement }

→ high Re #, Complex Geometry

MHD/EMHD-Simulations

I. Laminar & Turbulent Wakes

- vortex street suppression
- phase/frequency control

II. Wall Turbulence

- High σ, spanwise forcing/MHD
- Low σ, steamwise forcing
- Low σ, "normal" forcing

Method: Parallel DNS - The $\mathcal{N}\varepsilon\kappa\mathcal{T}\alpha r$ Code

Experiments: Conflicting results

EMHD control of the flow around a circular cylinder

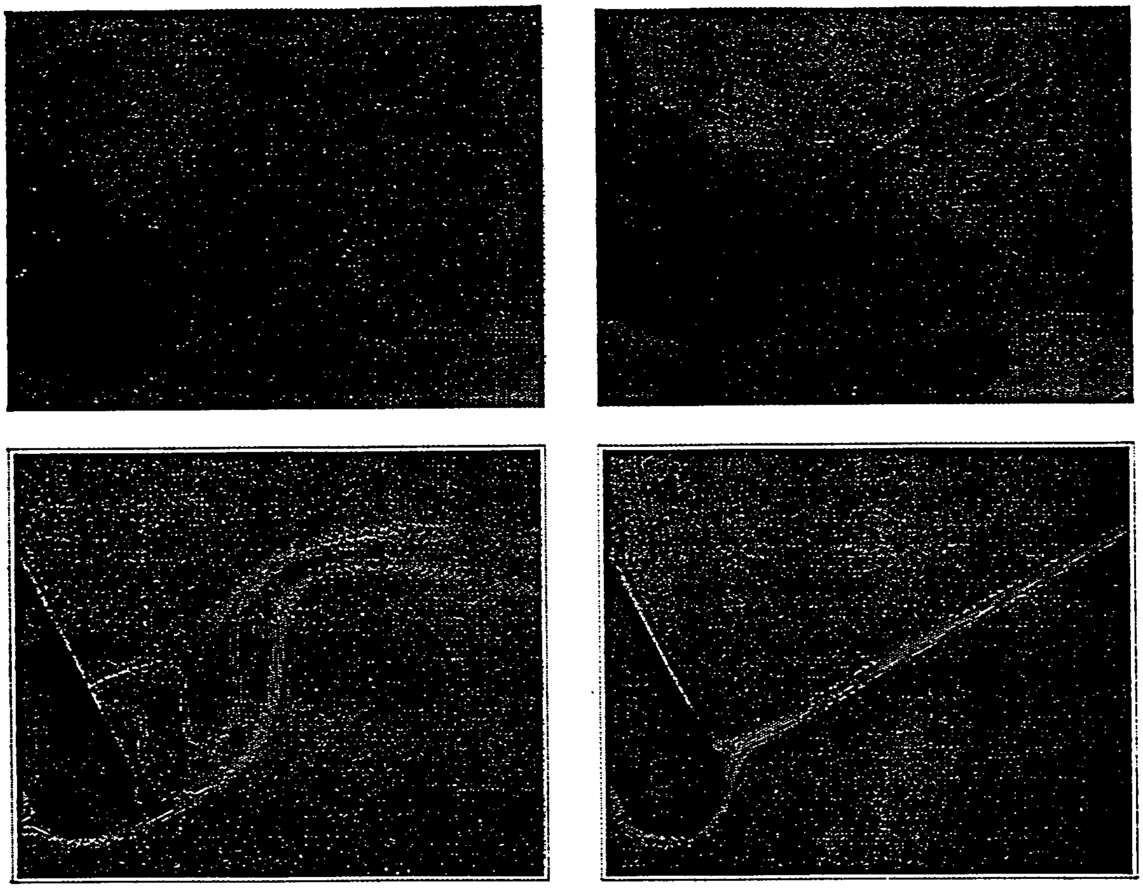

Dimensionless numbers:

$Re = \frac{v_\infty d}{\nu}$ - Reynolds number

$N = \frac{j_0 B_0 d}{\rho v_\infty^2}$ - Interaction Parameter

Suppression of the Kármán vortex street

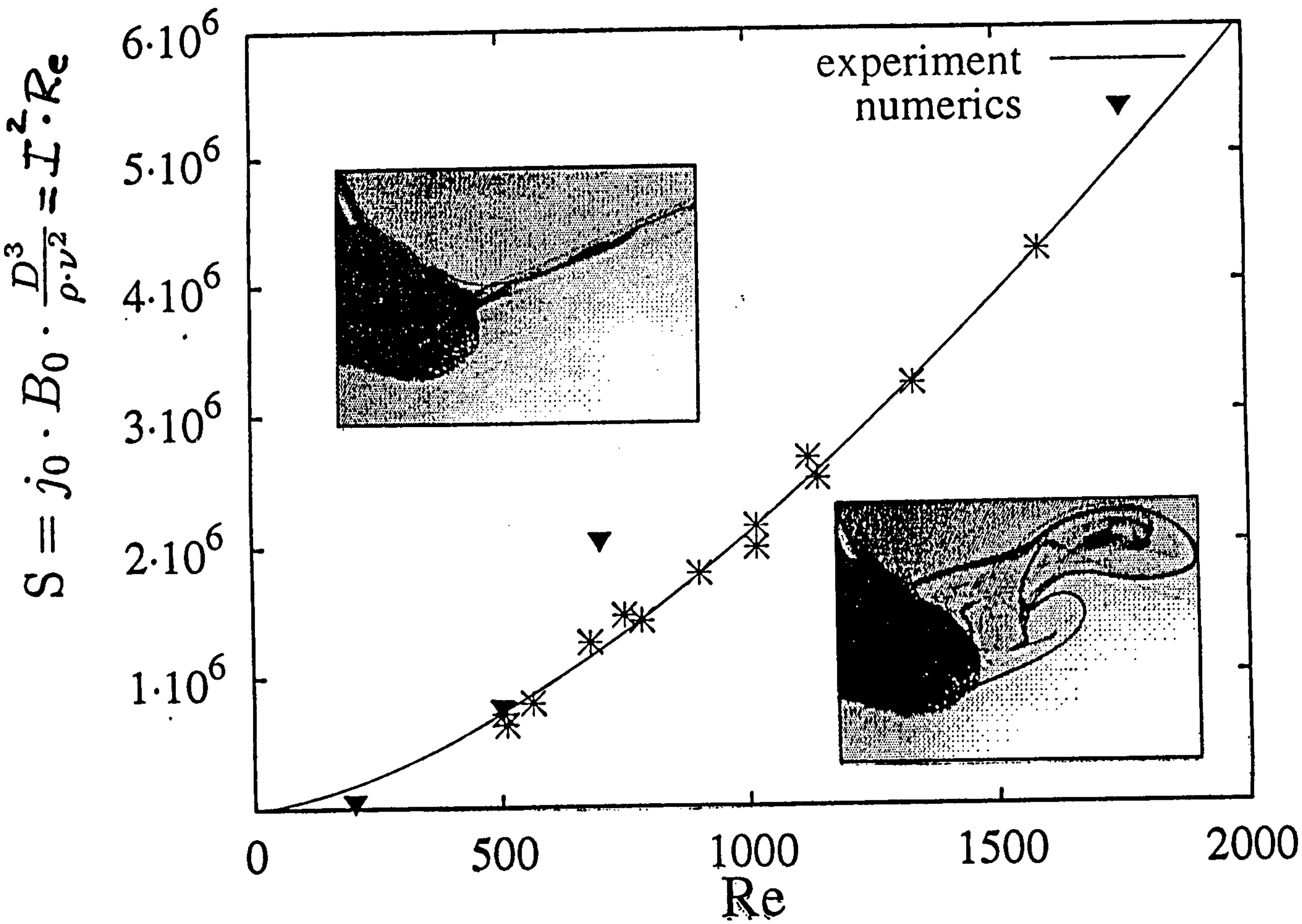

TURBULENT WAKES AIAA-95

Cylinder, Re = 500

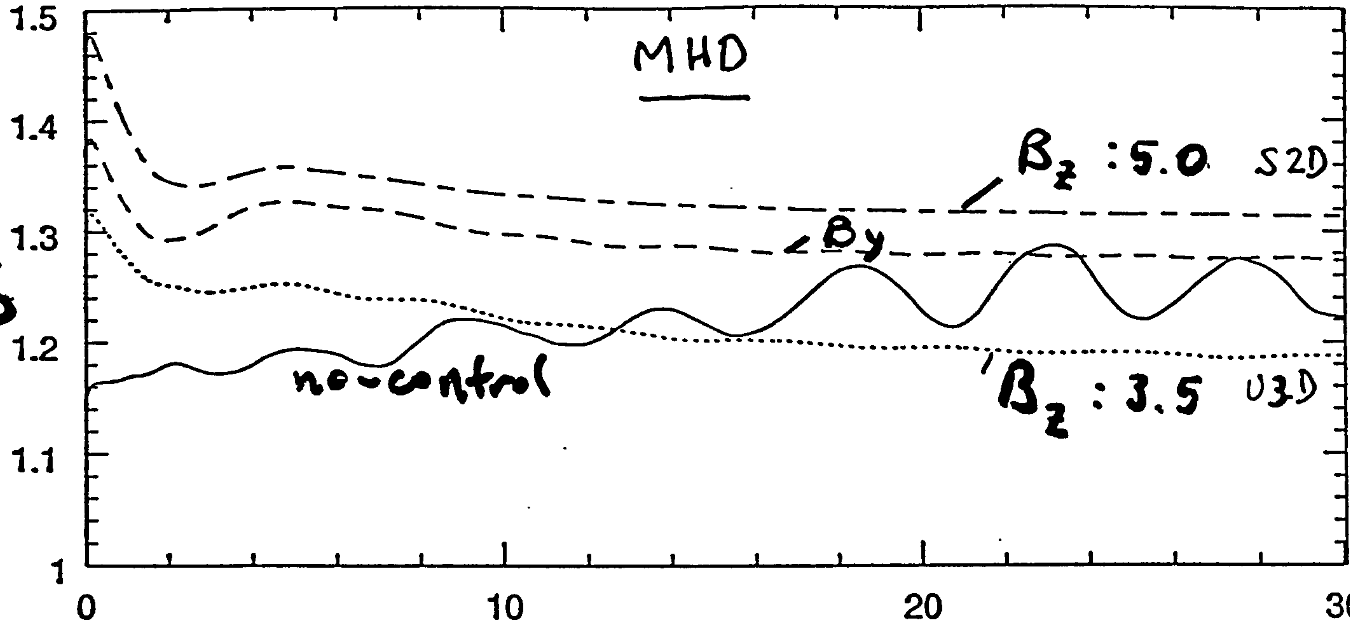

C_d vs. time (Mercury)

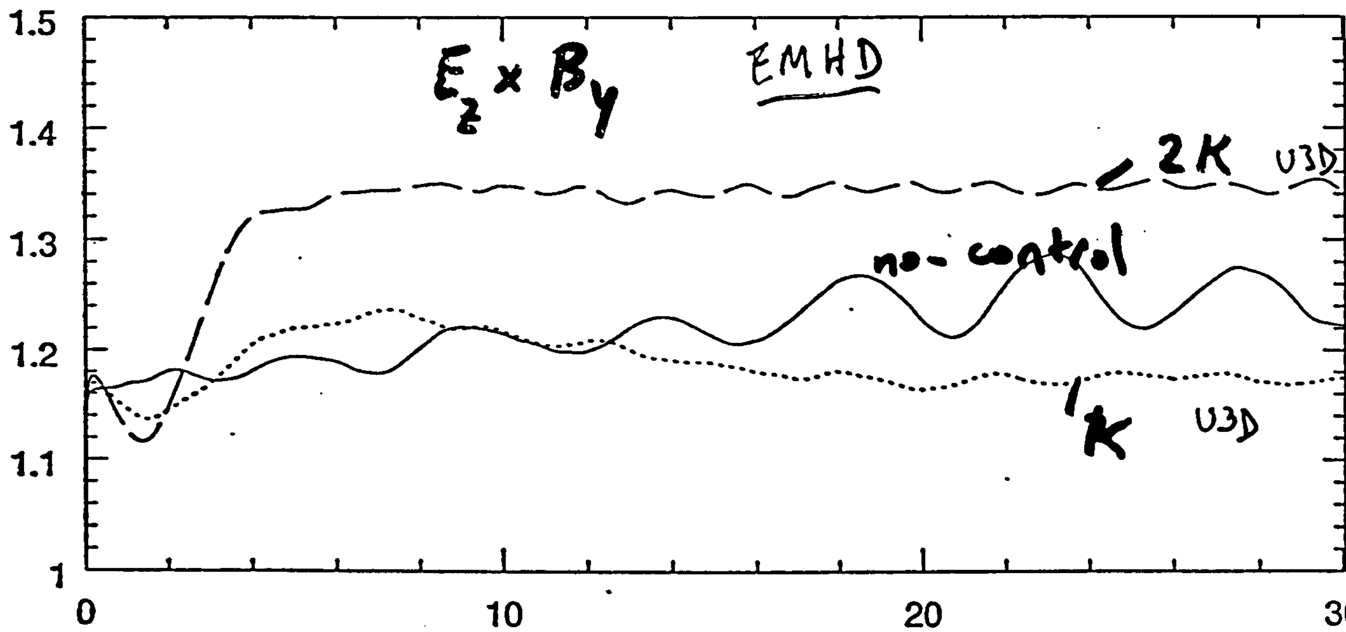

C_d vs. time (Sea Water)

∴ Changes are non-Monotonic!

Active Control: Lorentz Body Force

Phi.d.'s
Crawford
Y. du

Electric Field
Magnetic Field
Lorentz Force

DOE
AFOSR

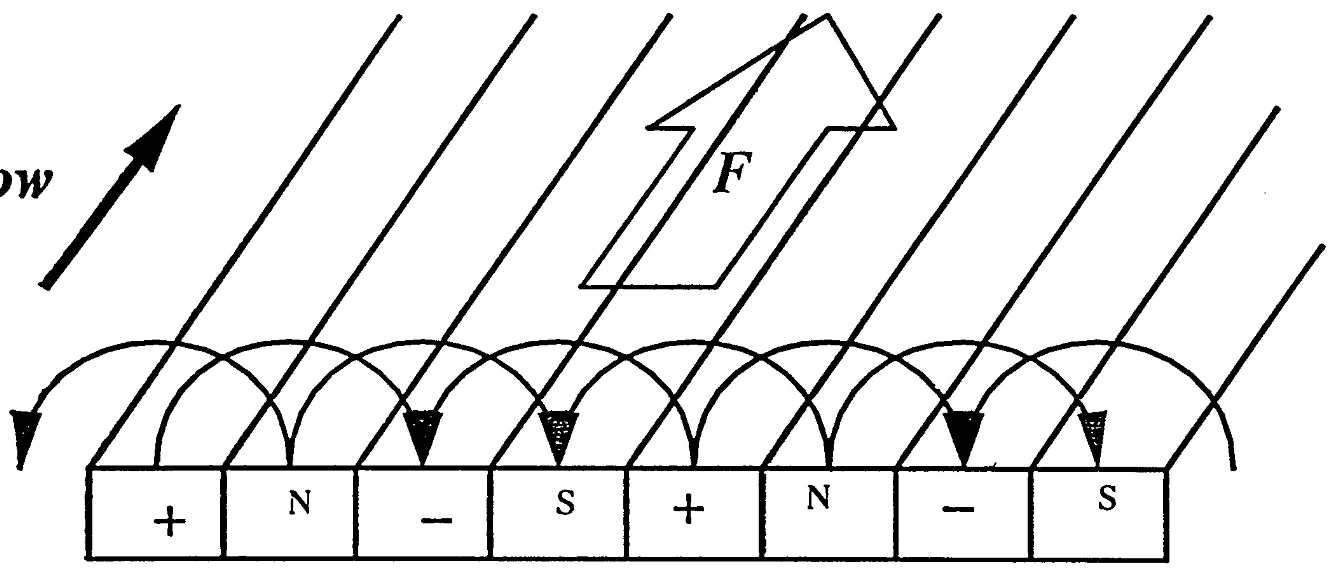

Henoch & Stace, 1995

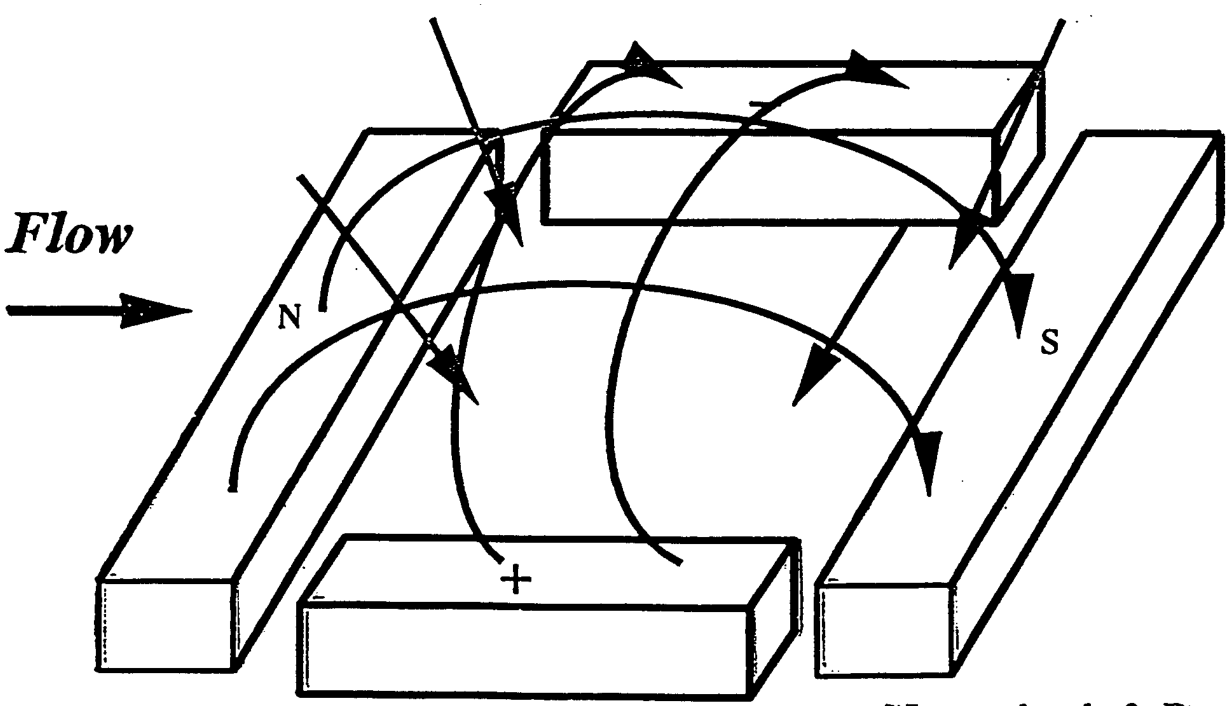

Nosenchuck & Brown, 1994

EMHD: Shear Stress History – Effects of BC

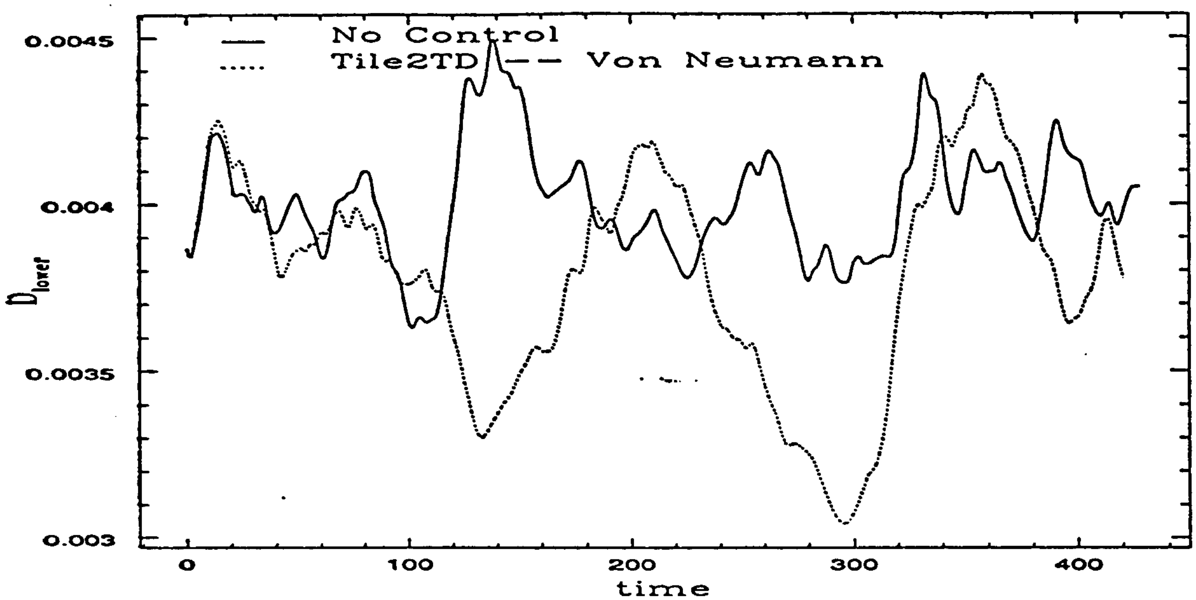

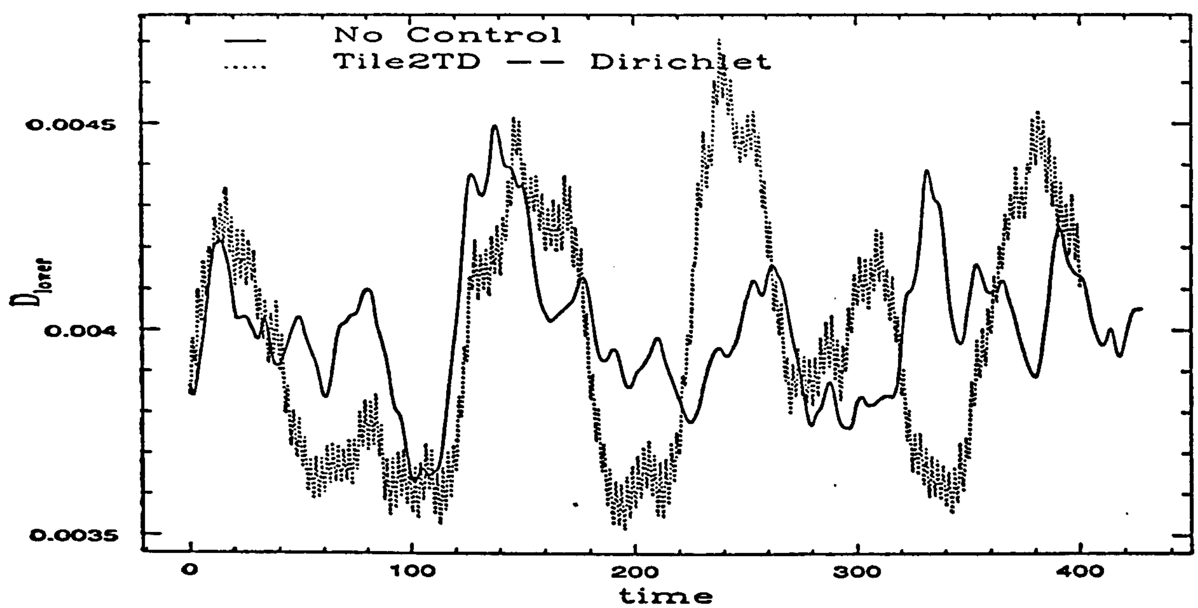

NEAR-WALL TURBULENCE and LAMB VECTOR

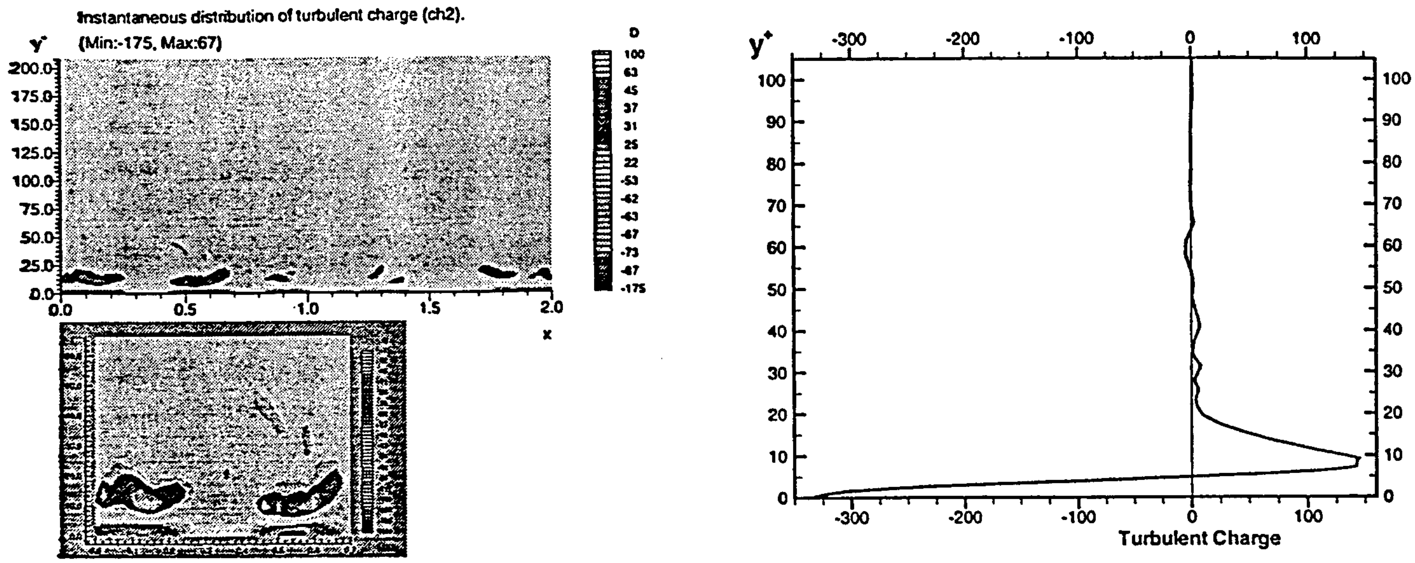

Figure 1: Dipole structure of the divergence of the Lamb vector: turbulent charge

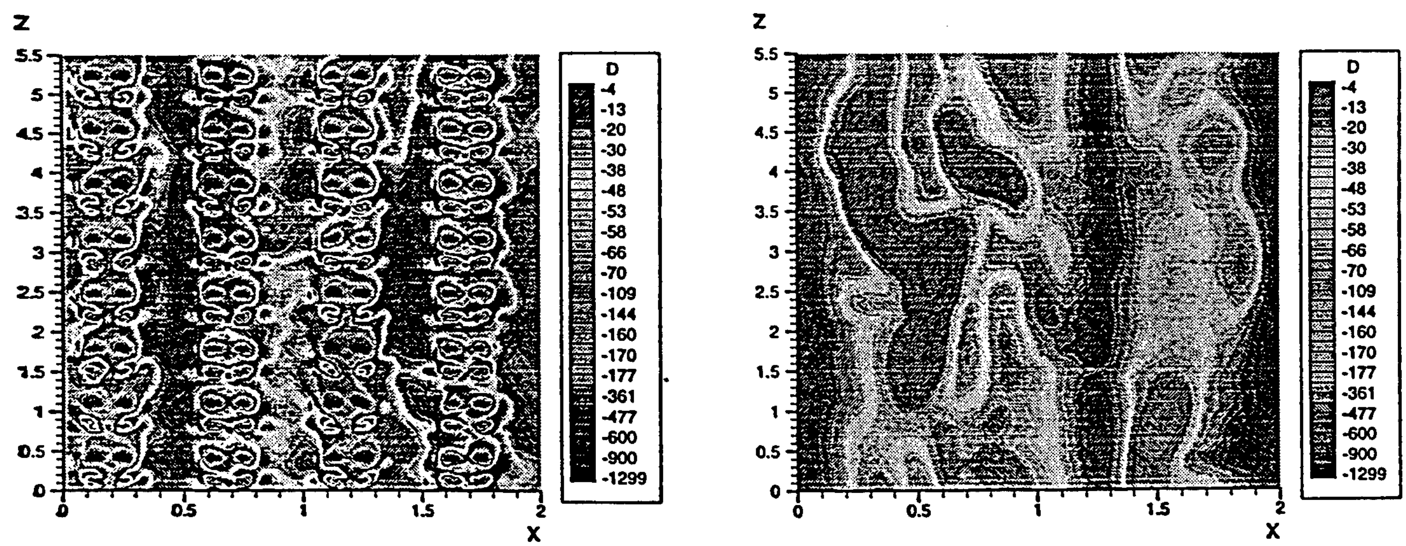

Figure 2: Footprint of the turbulent charge: LEFT – EMHD on; RIGHT: EMHD off

Summary

- Explore MHD, EMHD and EHD
- Strong electrical conductivity non-uniformity
- Selection of physical model is application-dependent
  - degree of ionization
- Transitional Flow - No *ad hoc* models
- Numerical Model ($\mathcal{N}\varepsilon\kappa\mathcal{T}\alpha r$):
  - High order
  - Hybrid grids
- Benchmark Experiments

2D vortex dynamics associated with shock splitting

Kremeyer, Nazarenko, Newell (Arizona).

Is observed shock splitting due largely to plasma electromagnetics or due solely to gas heating which accompony the introduction of non-equilibrium plasmas into a gas flow?

Shock wave attenuation in argon plasmas

Ganguly, Bletzinger & Garscadden ?1997

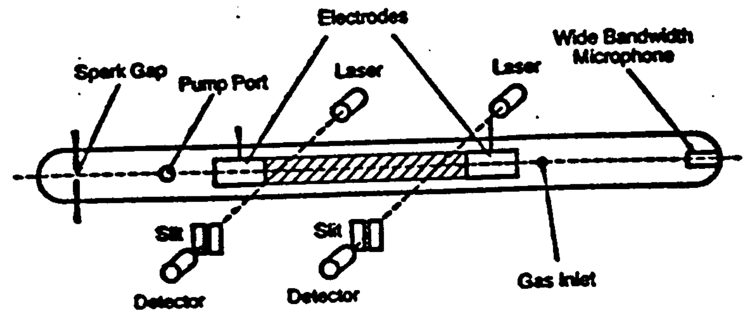

Fig. 1. Schematic of the experimental set-up.

- Shock attenuation & acceleration 1D effects ∇T.
- Shock splitting. ???

Ionisation unimportant, $\alpha \ll 1$?

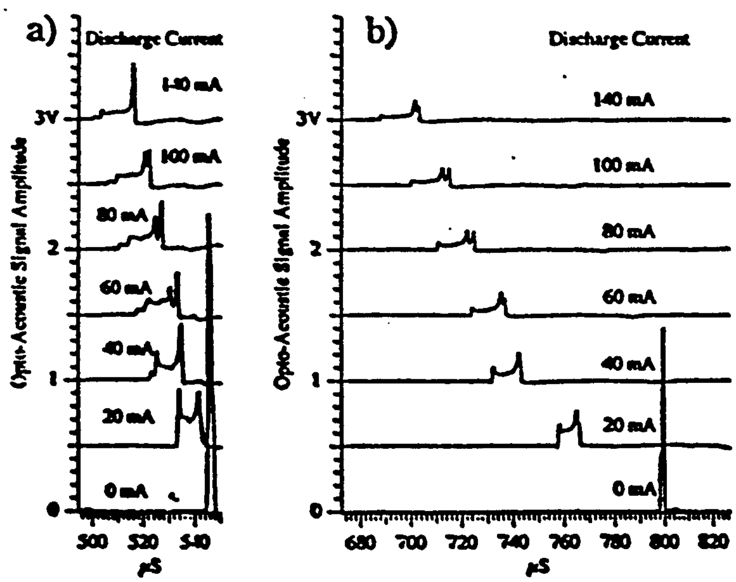

Fig. 2. Shock induced opto-acoustic signals in a 30 Torr argon discharge. (a) 30.2 cm from the spark source, (b) 42.2 cm from the sp source.

2D effects.

CFD of thermal effects,

Bailey & Hilbun '1997.

Spark Morphology

Velocity Contours

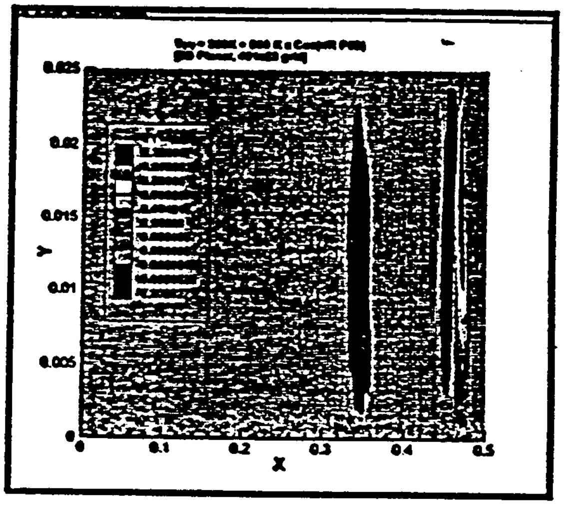

recirculation

Comparison with Experiment

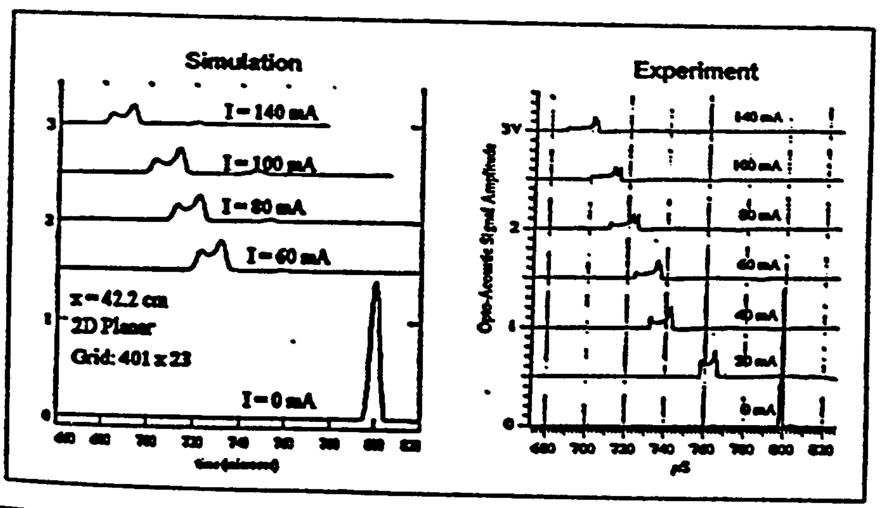

2D Shock Tube Simulation

Left Boundary: p = 1.0; d = 1.0; u = v = 0

Right Boundary: p = 0.1; d = "V"; u = v = 0

(top and bottom B.C's are "reflecting slip")

Initially, these two states meet at a discontinuity.

DENSITY: "V"

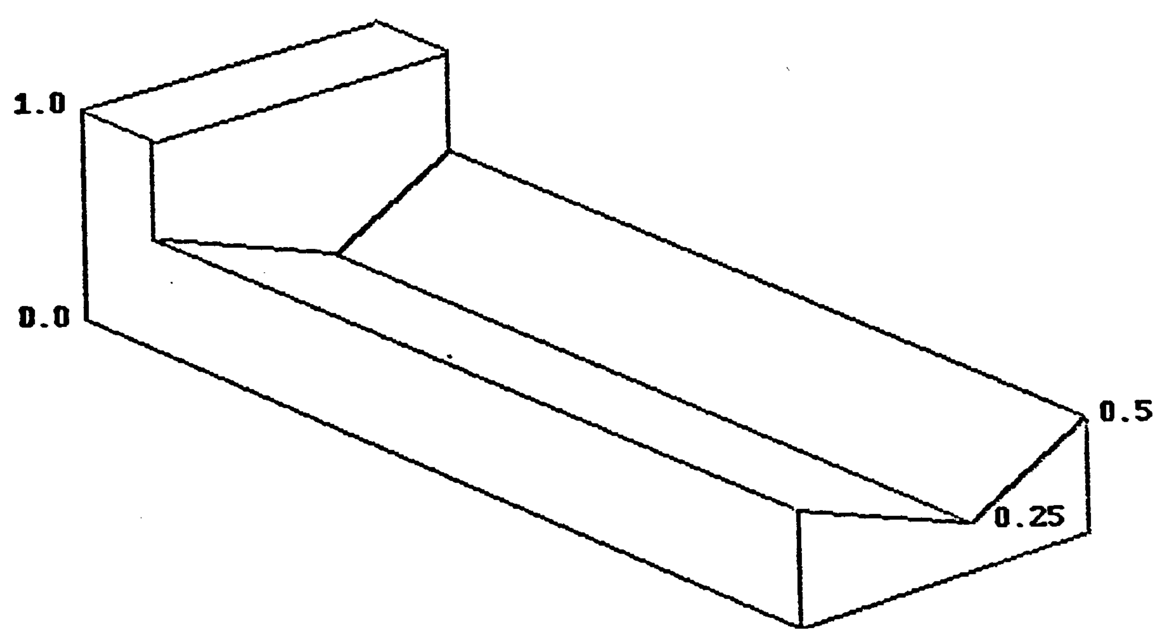

Baroclinic Vorticity Generation

$\underset{\sim}{\omega} = \nabla \times \underline{u}$ vorticity

$$\left[\partial_t + (\underline{u}\cdot\nabla)\right]\underset{\sim}{\omega} - (\underset{\sim}{\omega}\cdot\nabla)\underline{u} = -\underset{\sim}{\omega}\,\nabla\cdot\underline{u} - \underbrace{\nabla\frac{1}{\rho}\times\nabla p}_{\text{baroclinic term}}$$

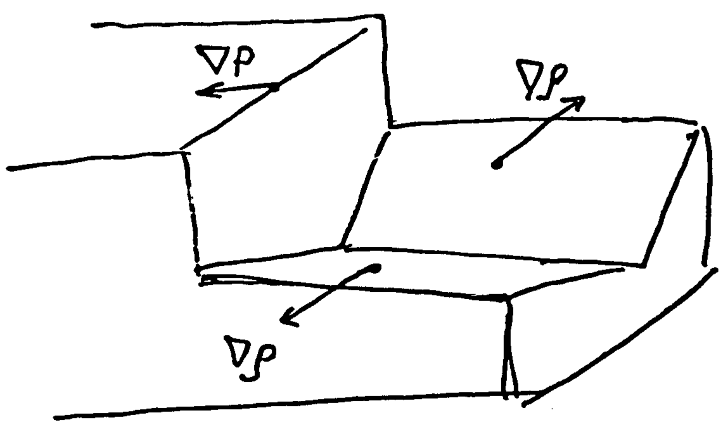

Potential Vorticity Conservation

2D Barotropic ($p = p(\rho)$) fluid

$$\left[\partial_t + (\underline{u}\cdot\nabla)\right]\frac{\omega}{\rho} = 0$$

Potential vorticity $\frac{\omega}{\rho}$ is conserved by each fluid element.

SIMULATION METHOD:

(of the 2D Euler equations)

PHYSICAL ASPECT RATIO (x:y) = 100:1

# of gridpoints in x direction = 400

# of gridpoints in y direction = 20

# of ghostpoints = 3 (on each side)

1: Given the fluid parameters at each gridpoint, find the eigenvectors to Roe's matrices.

2: Use a 5th order weighted ENO scheme to find the flux eigenvectors at half gridpoints.

3: Use a 3rd order Runge Kutta routine to propagate the half gridpoint fluxes and find the new fluid parameters at the real gridpoints.

4: Repeat.

(1) Vorticity Landscape

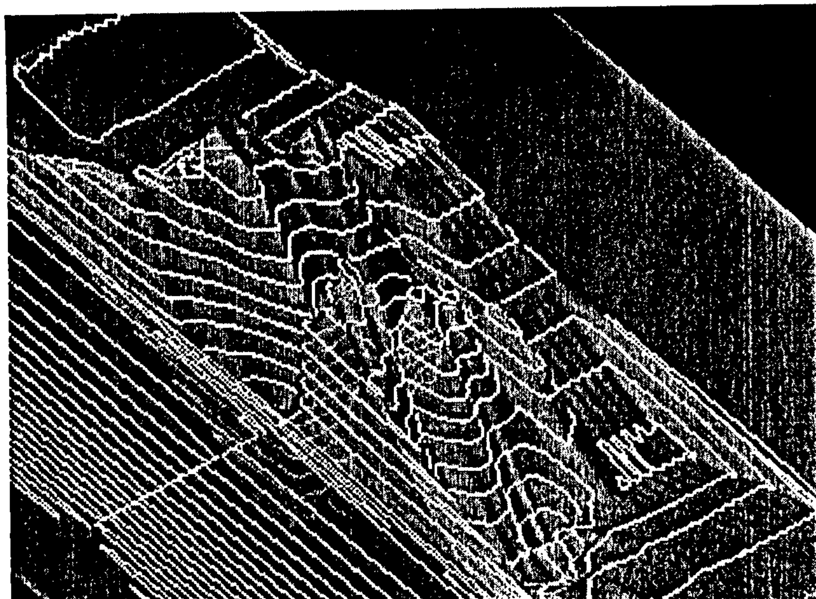

(2) Vorticity Contours

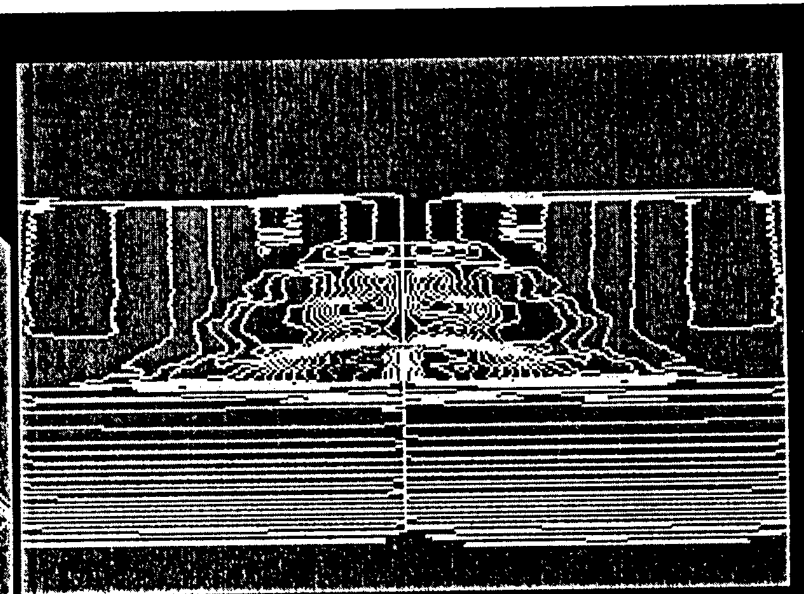

← front jump

← back jump

(3): half of (2)

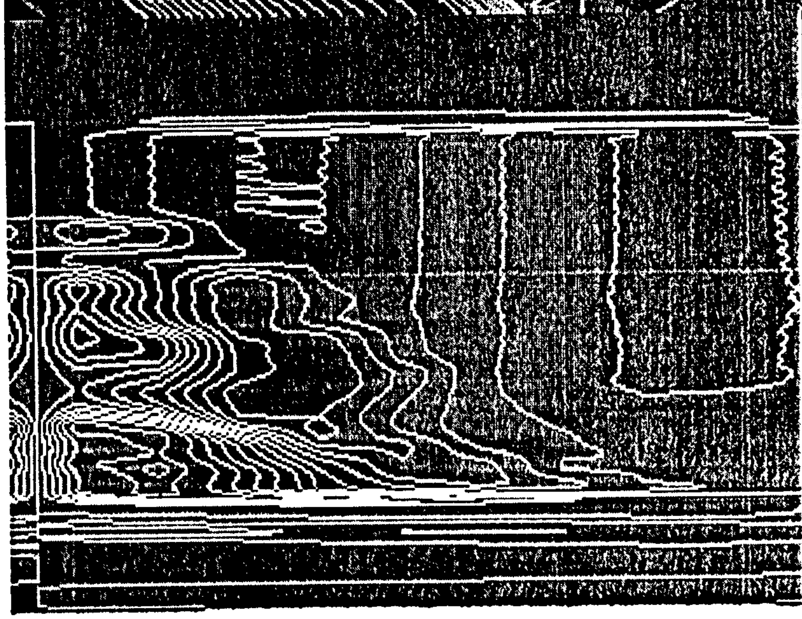

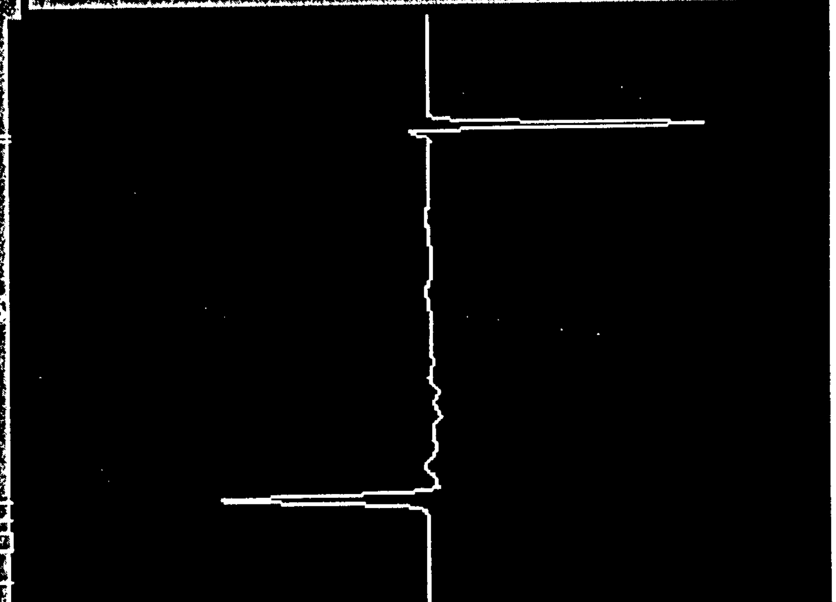

(4): $\frac{\partial}{\partial x}\int \xi \, dy$

Same scale as in (3).

Streamlines

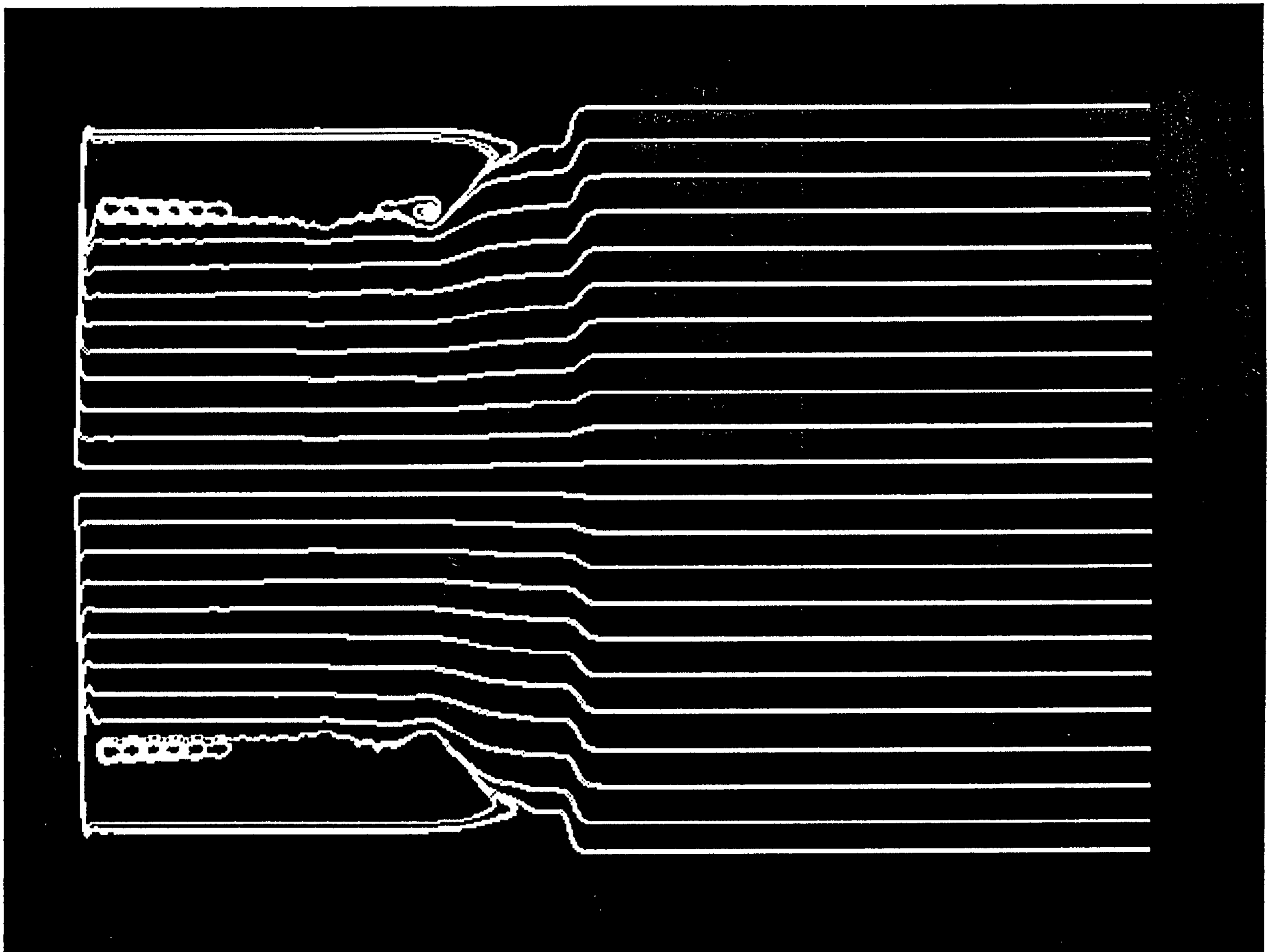

back

front

Flow Structure

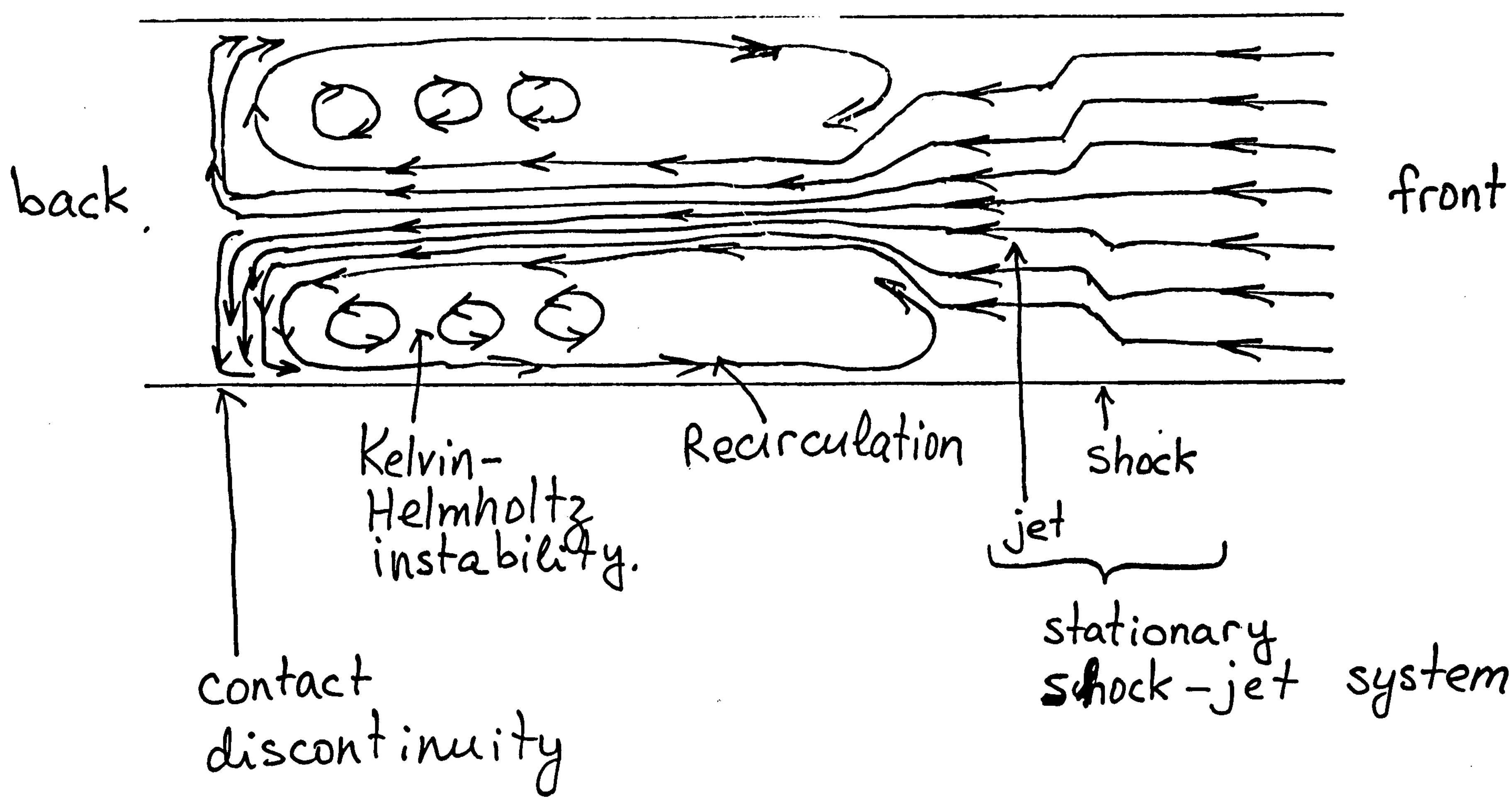

Profiles in front of the Shock

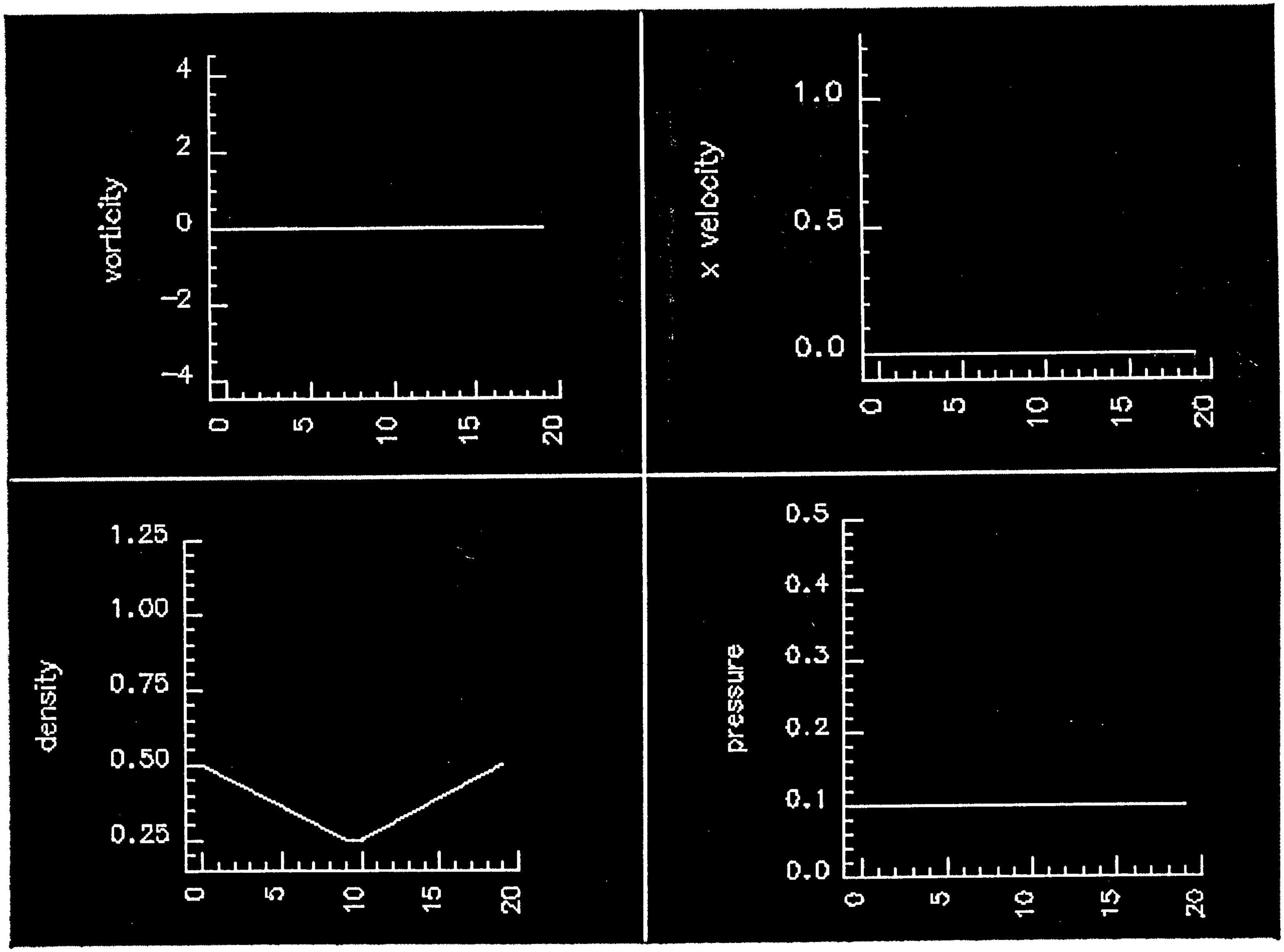

Profiles behind the contact discontinuity.

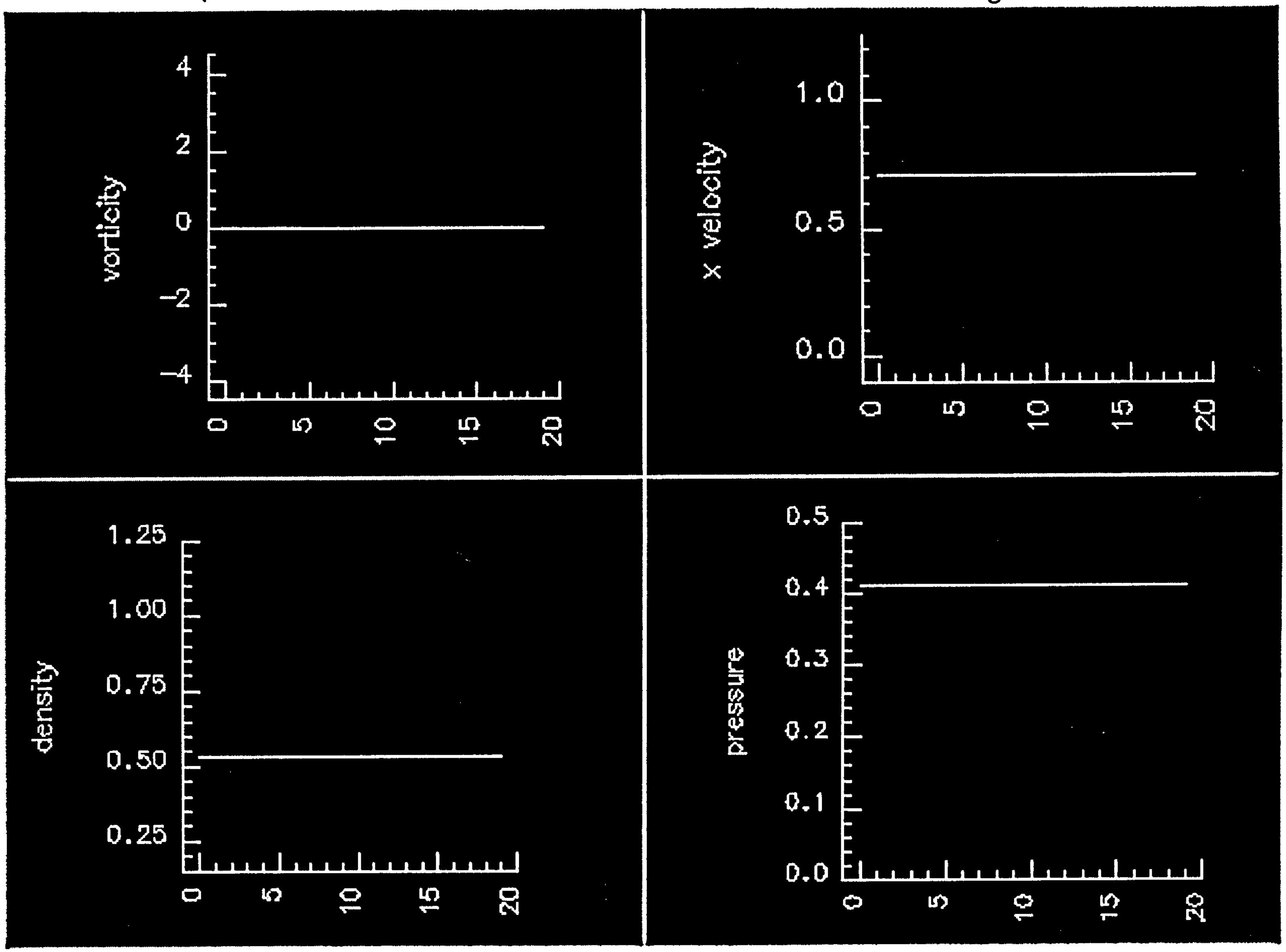

Shock-Jet System

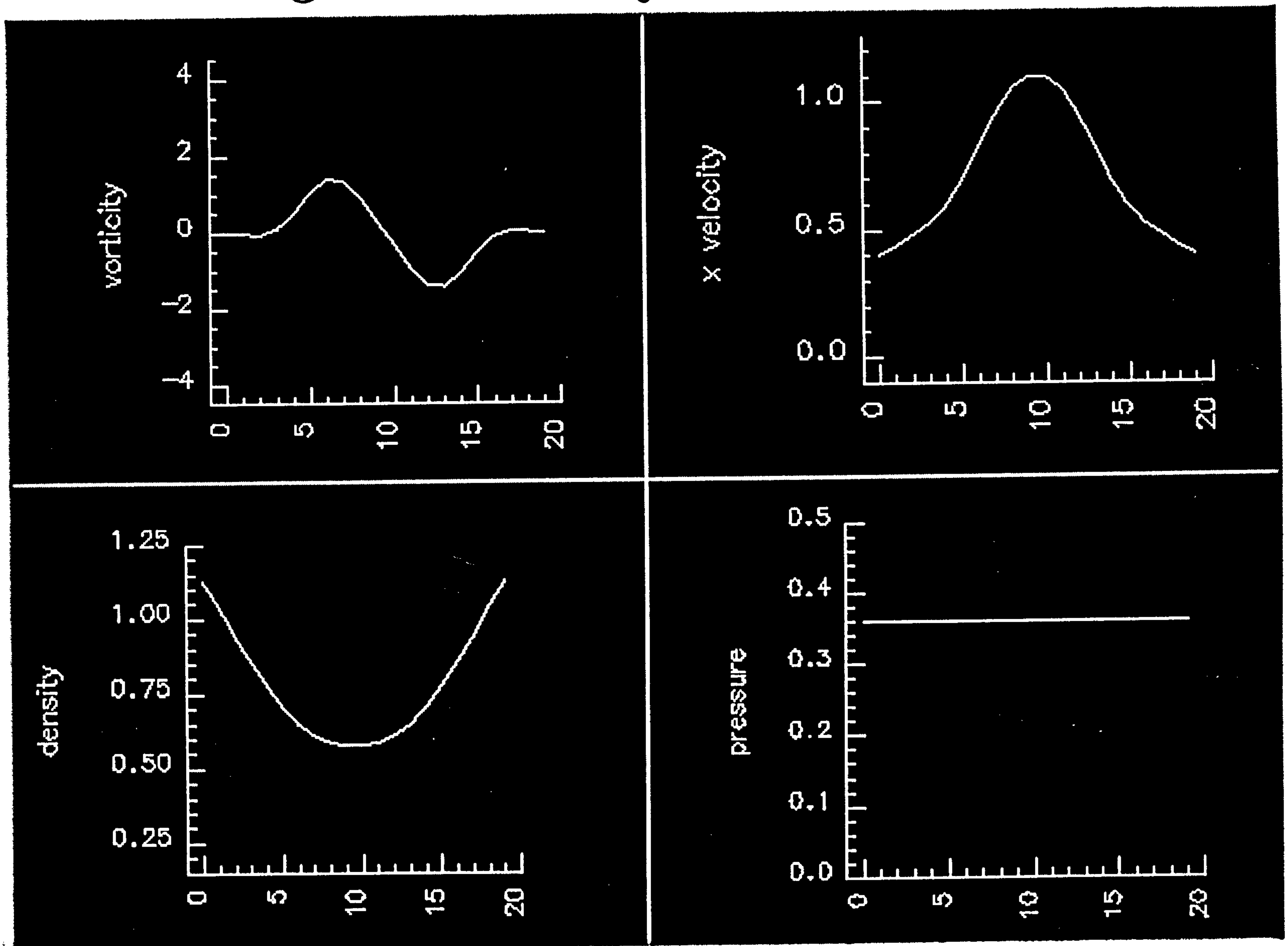

Averaged P, u_x, ρ

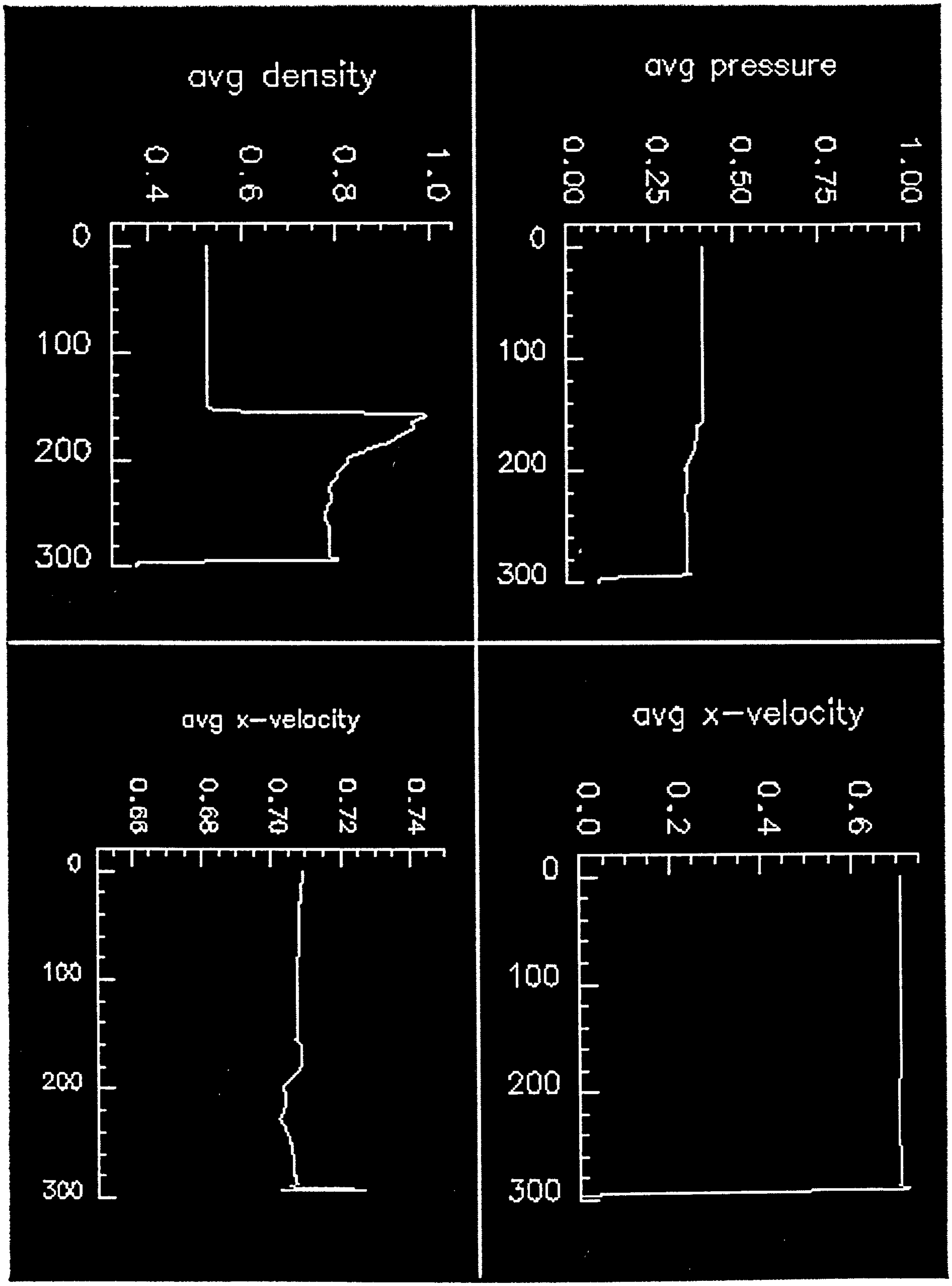

averaged vorticity   averaged potential vorticity

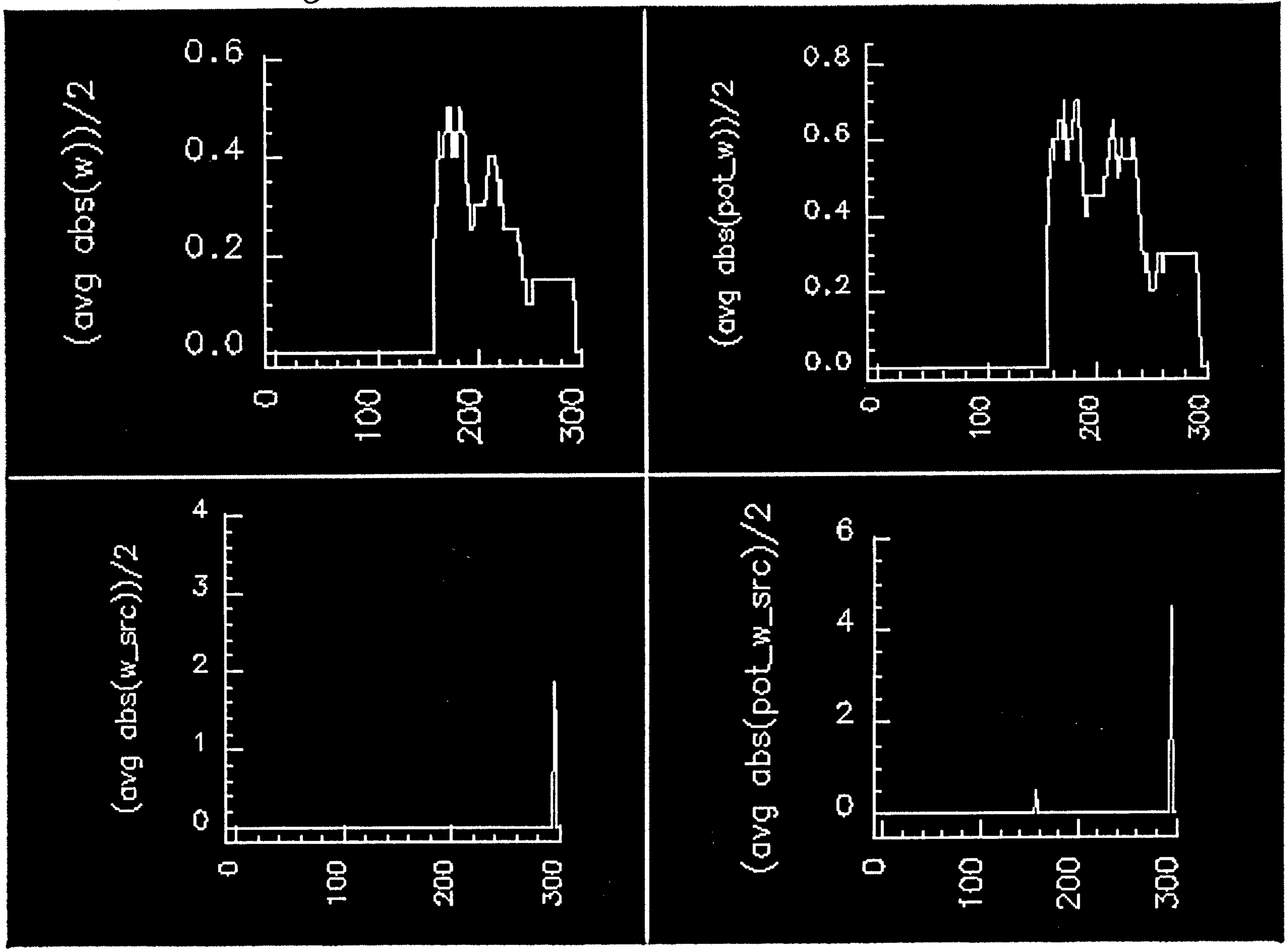

avg. rate of vorticity generation   avg. rate of pot. vorticity generation

RSI
Research
Support
Instruments

Further Investigation of Large Volume PIA (Persistent Ionizationin Air) Plasmas at Atmospheric Pressure

Mr. John F. Kline

Dr. John E. Brandenburg

Research Support Instruments

Lanham, Maryland

Presented at the Understanding and Control of

Ionized High-Speed Flows Workshop

Session IV: Plasma Generation and Maintenance

Princeton University

February 26, 1998

RSI

Research
Support
Instruments

Materials and Methods 2.45 GHz (1)

- Untuned cavity
- Field Enhancer
- Gas supply
- UV source
- Containment vessel

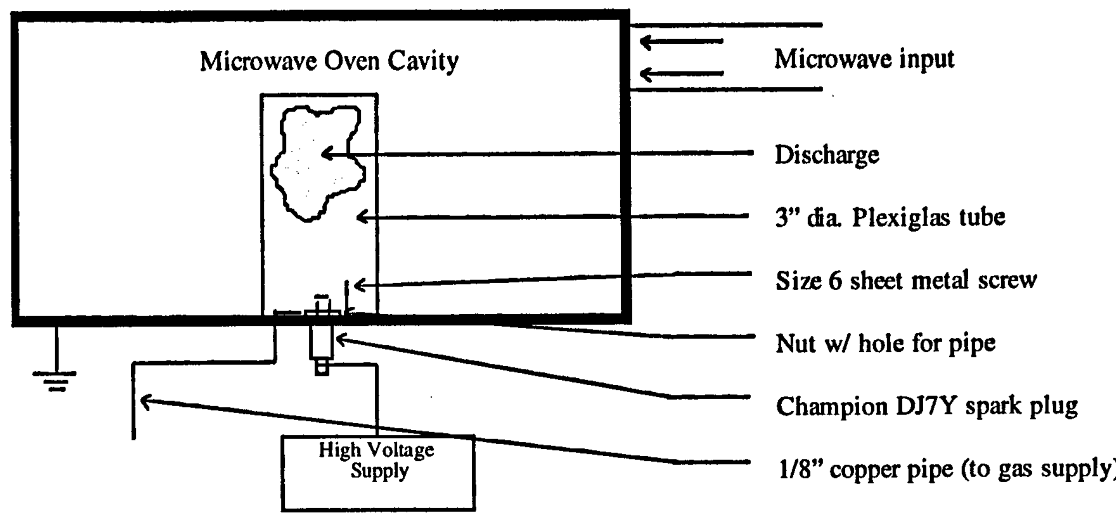

Materials and Methods 2.45 GHz (2)

- Top view of apparatus
- Gases - stagnant air, nitrogen, argon, and helium
- Langmuir single probe
- Videocamera - frame counting
- Microwave detector
- Photocell to measure light decay time

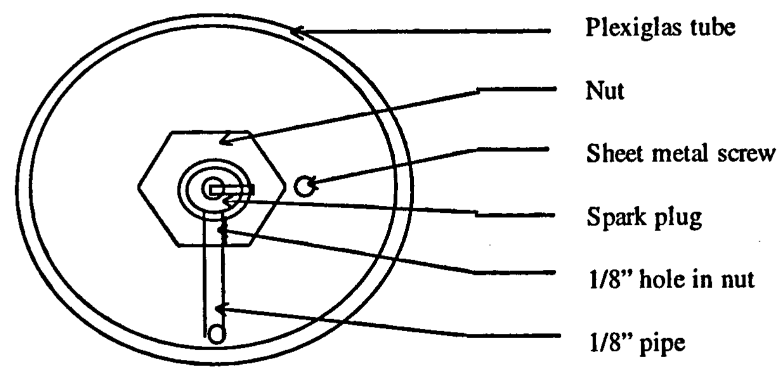

Materials and Methods 2.45 GHz (3)

- Replacement of spark plug by laser induced breakdown
  - » 1.06 μm, 0.3 - 1 J, 10 Hz Nd-Yag laser
  - » Field enchancement still necessary for microwave breakdown
  - » Elimination of field enchancer by using TM_{012} resonant cavity
- Vortex ring generator to provide local E/P enchancement
  - » Loudspeaker with plastic cone using voltage pulses
  - » Shapes plasma into flat disc that follows vortex ring
- Emissions spectra measurements
  - » 8-bit CCD viewing exit aperature of spectrometer
  - » Pixel values over a line give a time-resolved measurement over a broad range

RSI

Research
Support
Instruments

Materials and Methods 2.45 GHz (4)

- Time-resolved emissions spectra
- Broad range of wavelengths
- Pixel depth vs. position yields intensity vs. wavelength
- Calibration using Hg (Ar) source

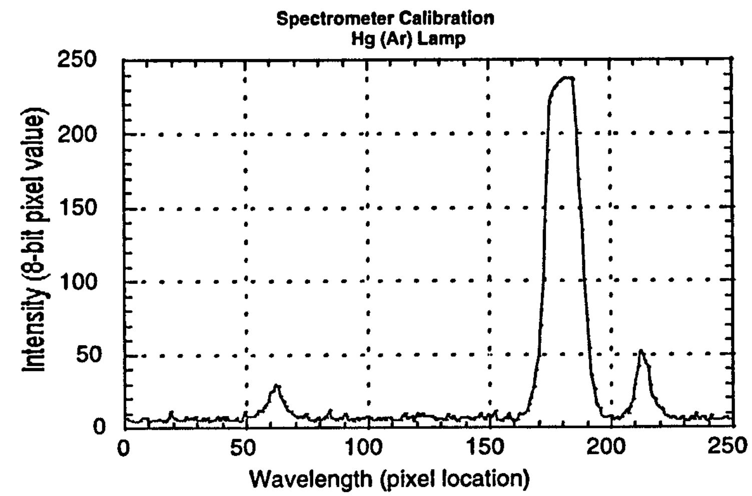

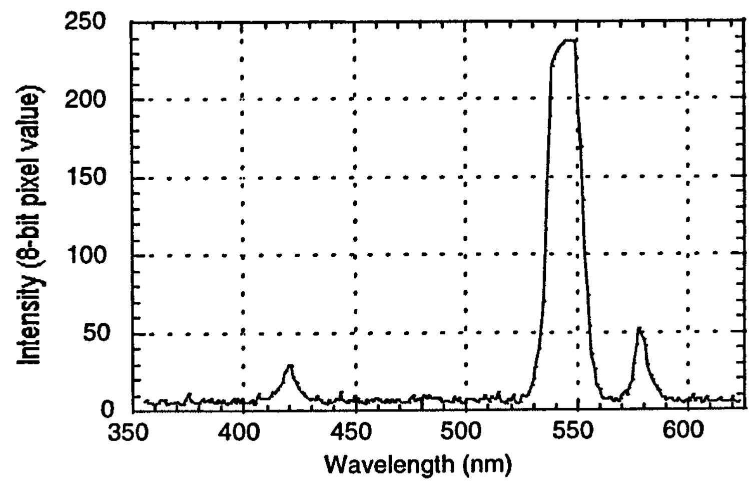

RSI

Research
Support
Instruments

Results (1)

- Temperature - 0.67 eV
- Density - 10^{10} cm^{-3}
- Low neutral gas temperature
- Turbulent, with toroidal core
- Optimal flow rate - 1.2 LPM
- Volume - 280 cm^3 average
- Microwave shielding - 1 order of magnitude increase with plasma (indicates 10^{11} cm^{-3})

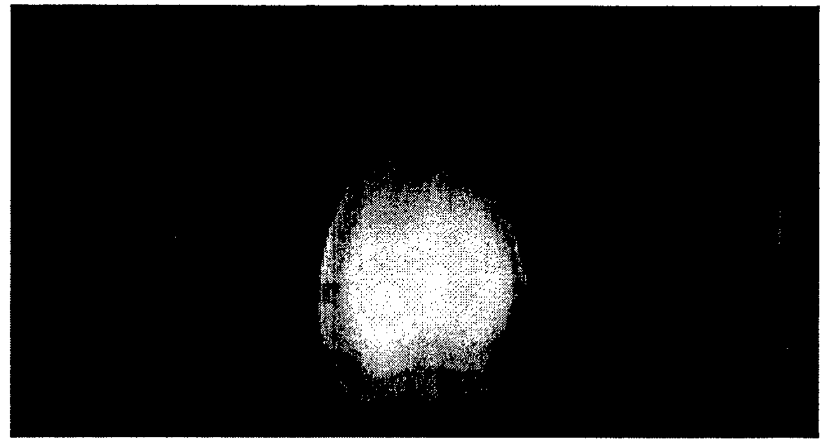

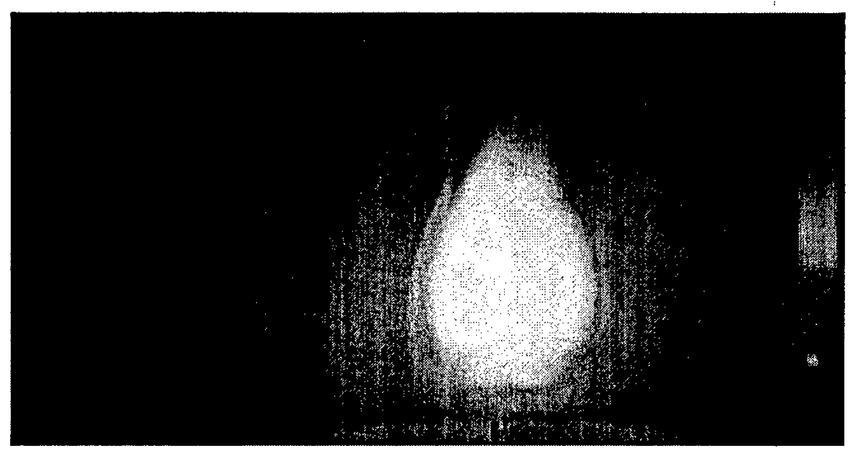

RSI

Research
Support
Instruments

Results (2)

- Unpowered lifetime - 200 ms average (3 e-folds at 60ms decay time)
- Upper channel shows photocell output
- Lower channel shows microwave detector output

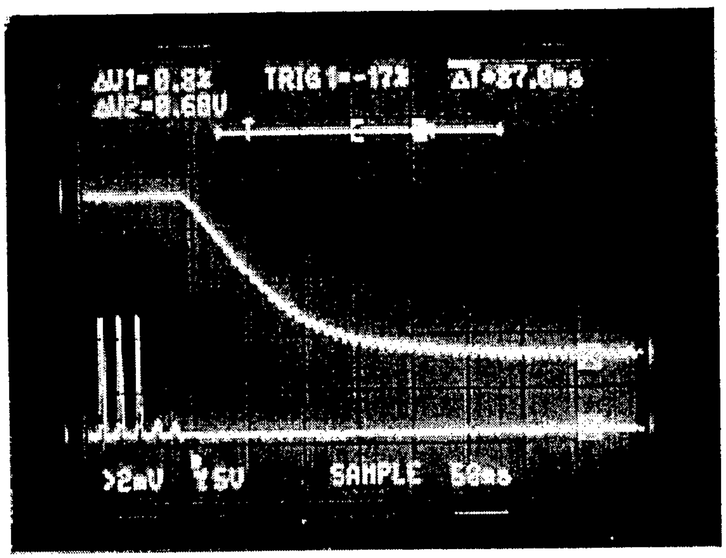

Argon

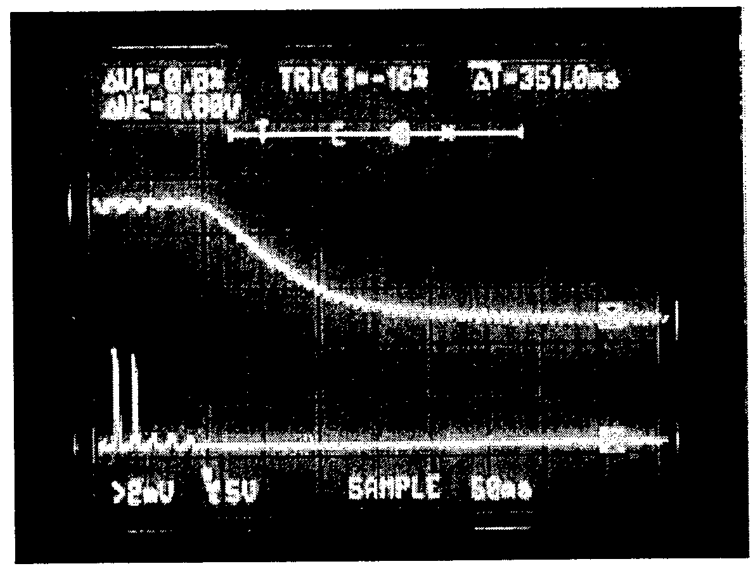

Air

RSI

Research
Support
Instruments

Results (3)

- Scaling of TM_{011} resonant cavity to 0.915 GHz
- 45 kW operation using vortex-stabilized compressed air

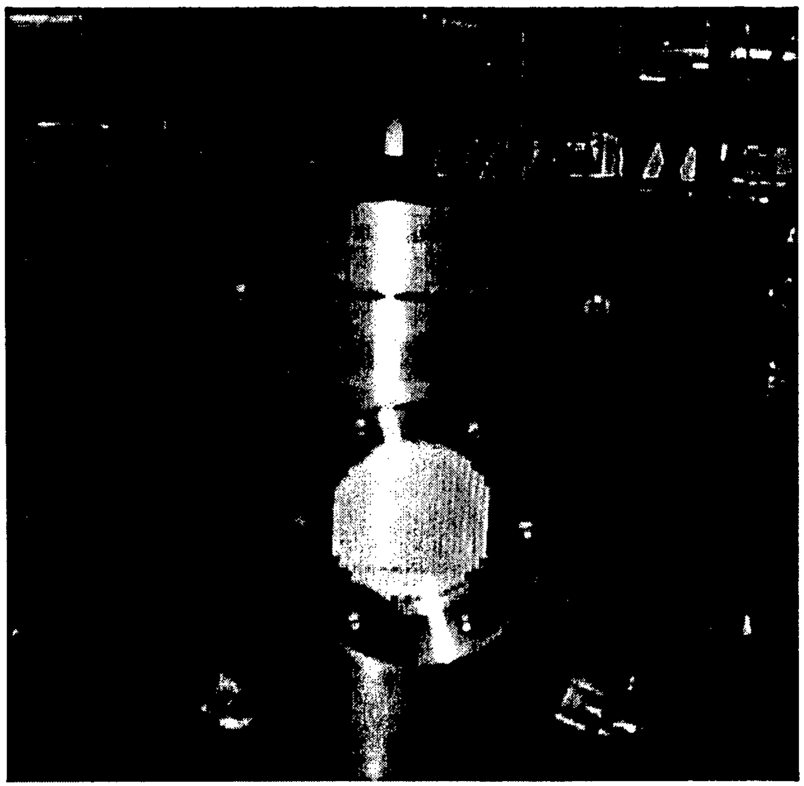

Results (4)

- Initial data on argon mixture
- Shows broad continuum (previously seen at Stanford)
- Can acquire time history data

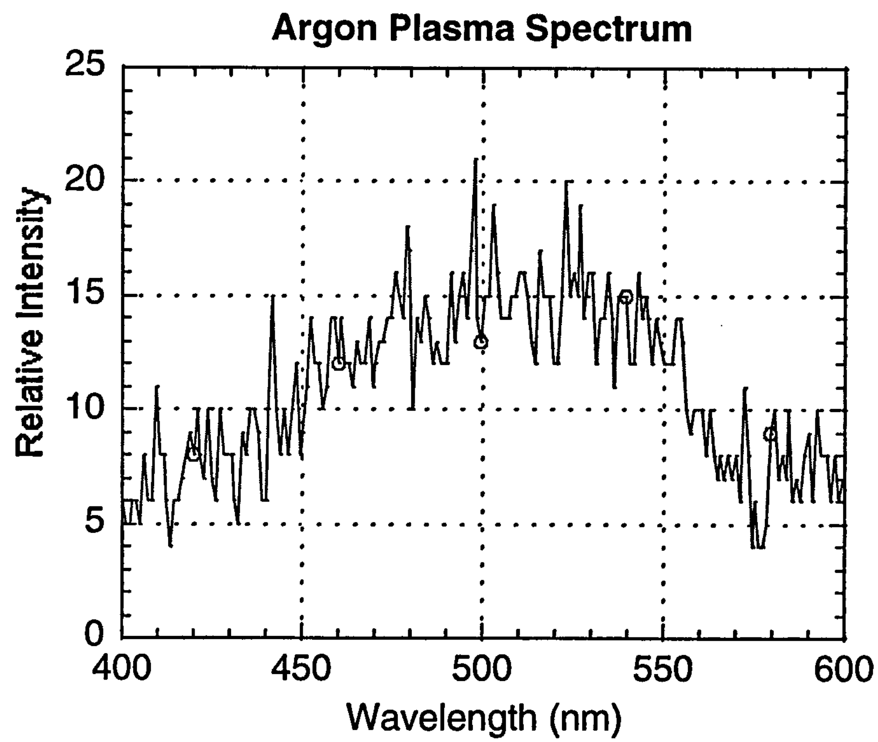

Discussion

- Shared Electron Orbital (SEO) Hypothesis
  - » Decoupling of electrons from collisions with neutrals
  - » Long collisional energy transfer times
  - » Long recombination times
  - » Electrons shared between orbitals
  - » Resemble conduction bands in liquid metals
  - » Vorticity suggests trapped magnetic fluxes and dynamo action (as in liquid metals)

Future Work

- Advanced diagnostics
  - » Continuing work on emissions spectra
  - » Triple probe with digital oscilloscope and function generator
- Investigate vorticity
  - » Pulsed power vortex ring generator
  - » Optically measure rotation

RSI

Research
Support
Instruments

Nitrogen Plasma - Low Flow

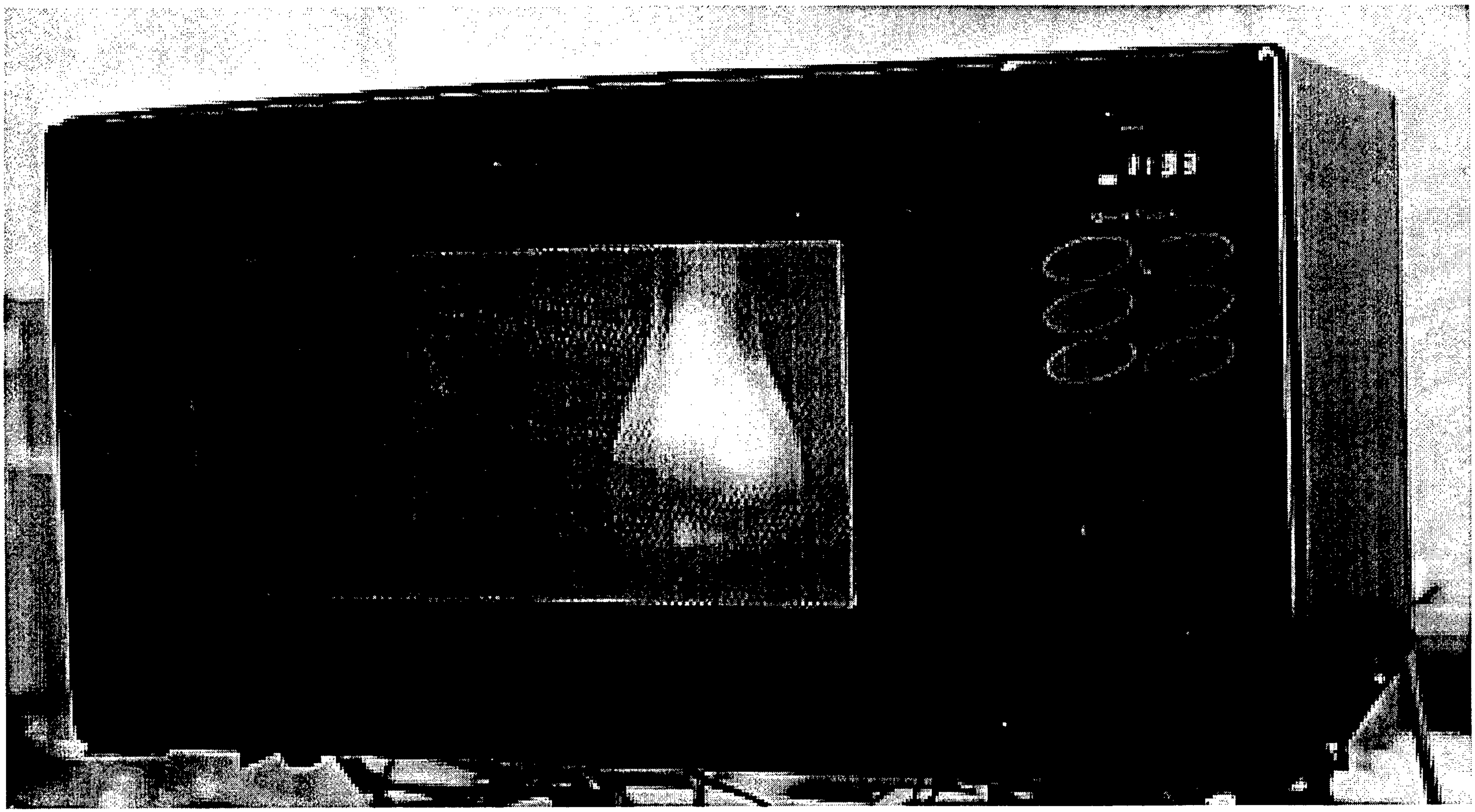

RSI

Research
Support
Instruments

Nitrogen Plasma - Stable

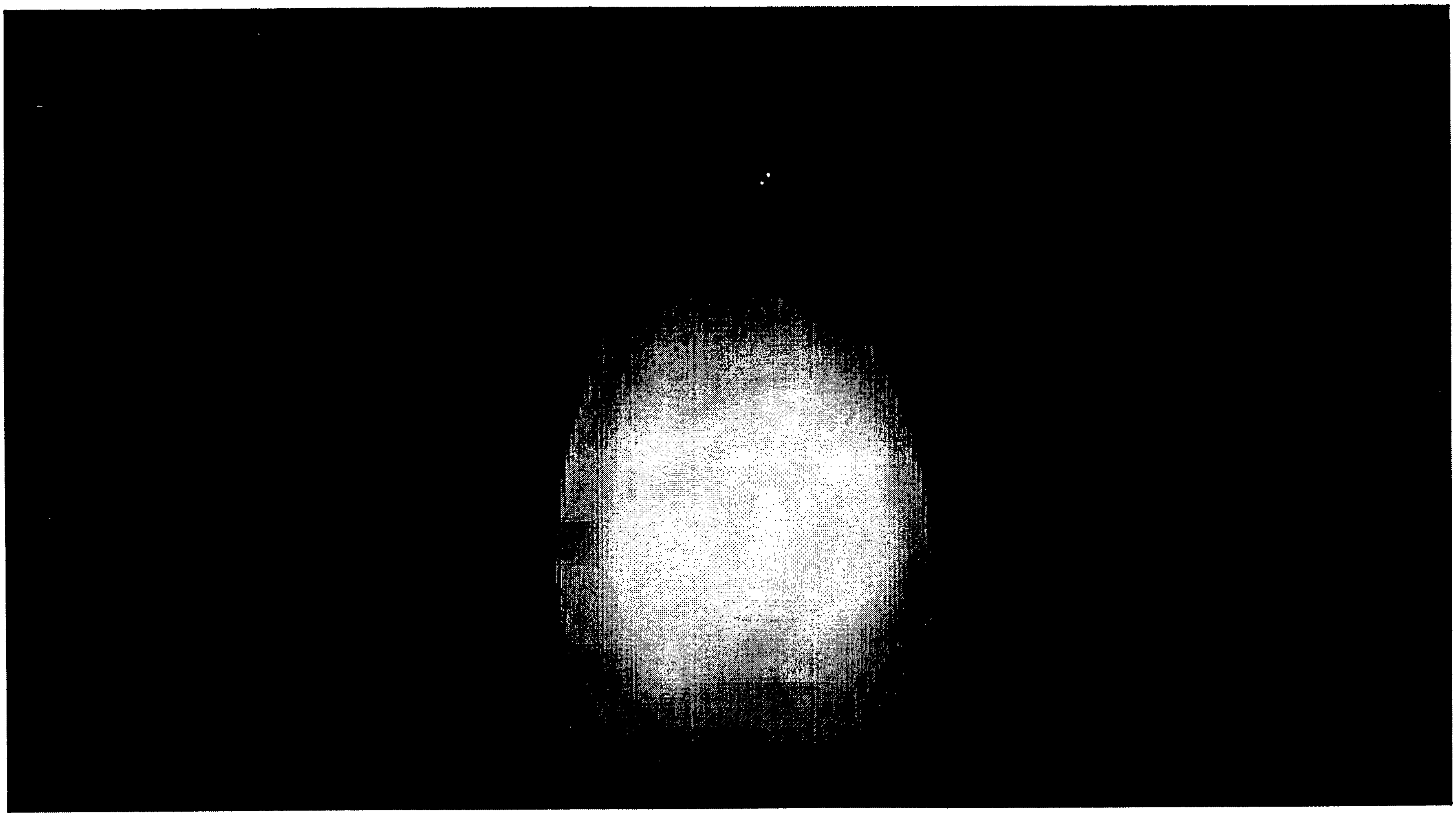

RSI
Research
Support
Instruments

Argon Plasma - Stable

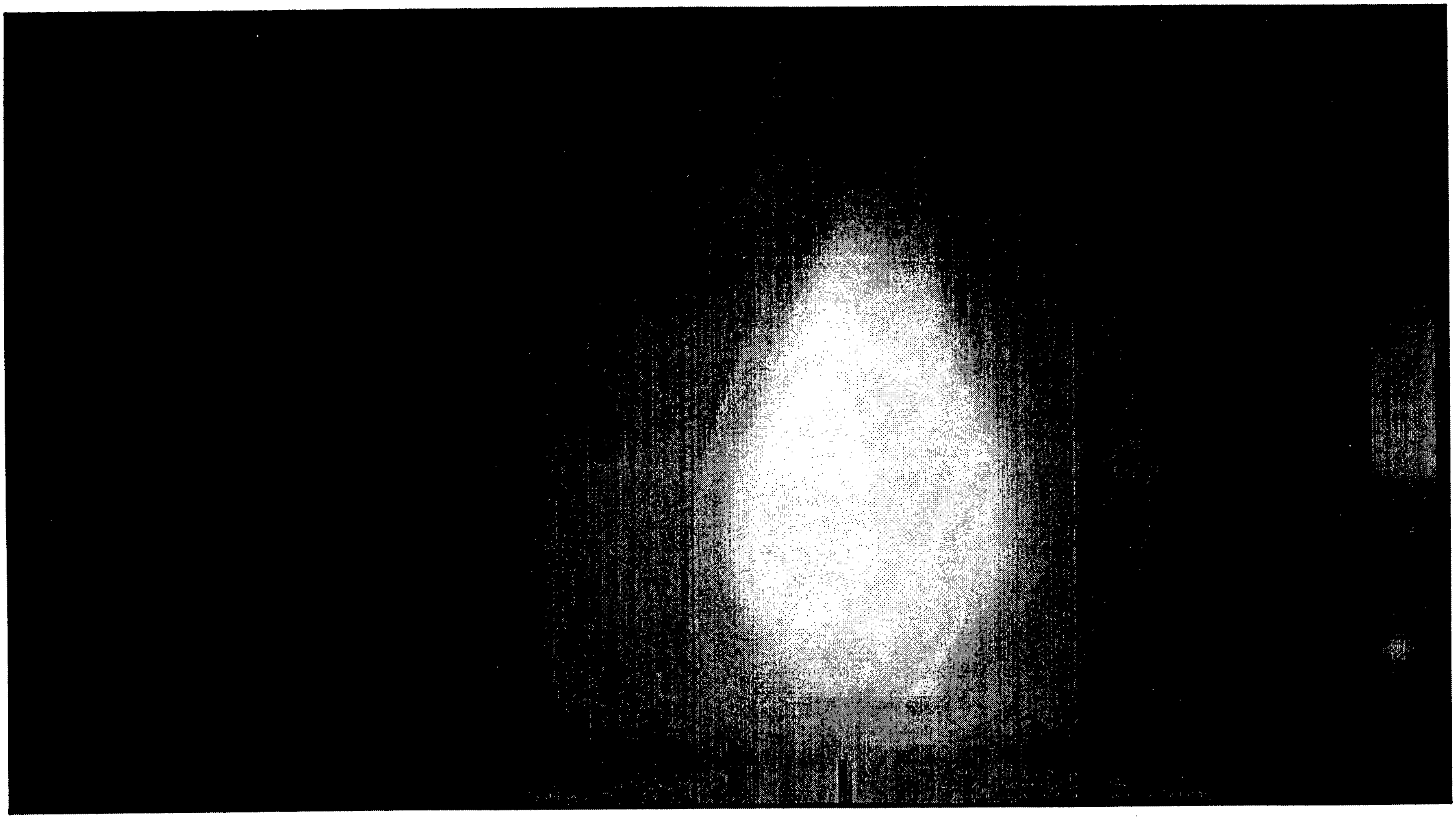

Plasma Torches and Their Demonstration

Spencer P. Kuo and Edward Koretzky

Department of Electrical Engineering

Polytechnic University

*Work supported by the AFOSR

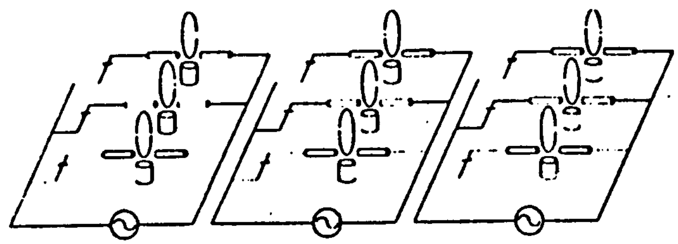

Figure 1.1: A schematic of the current arrangement for an array (3 × 3) of plasma torches. Tungsten electrodes are used. Each electrode pair is facilitated with an air jet nozzle.

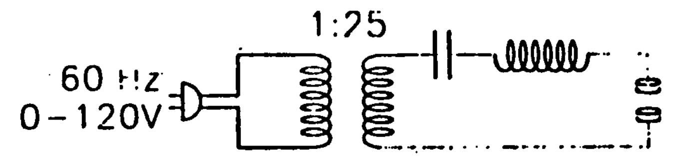

Figure 1.2: Circuit diagram of the plasma torch.

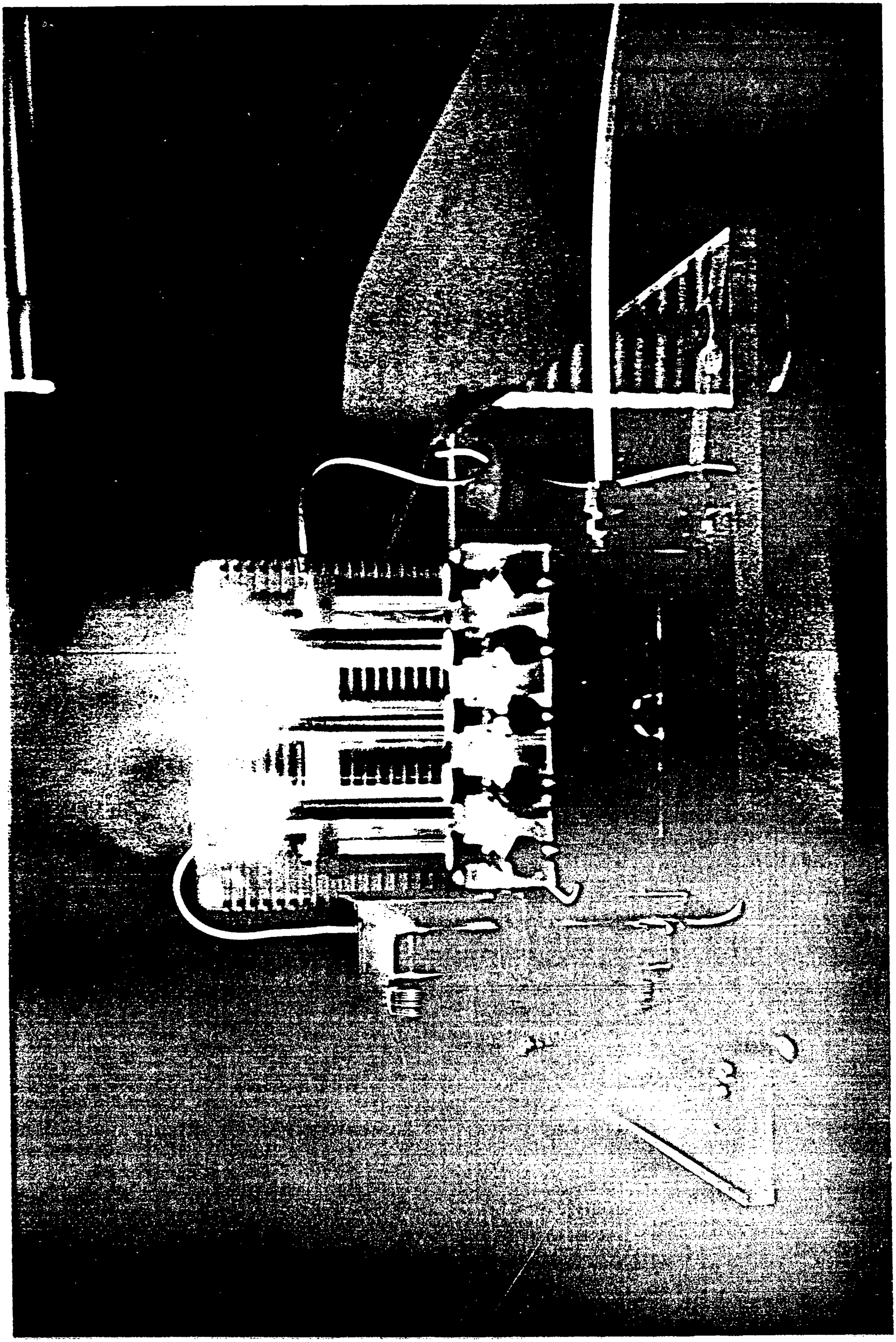

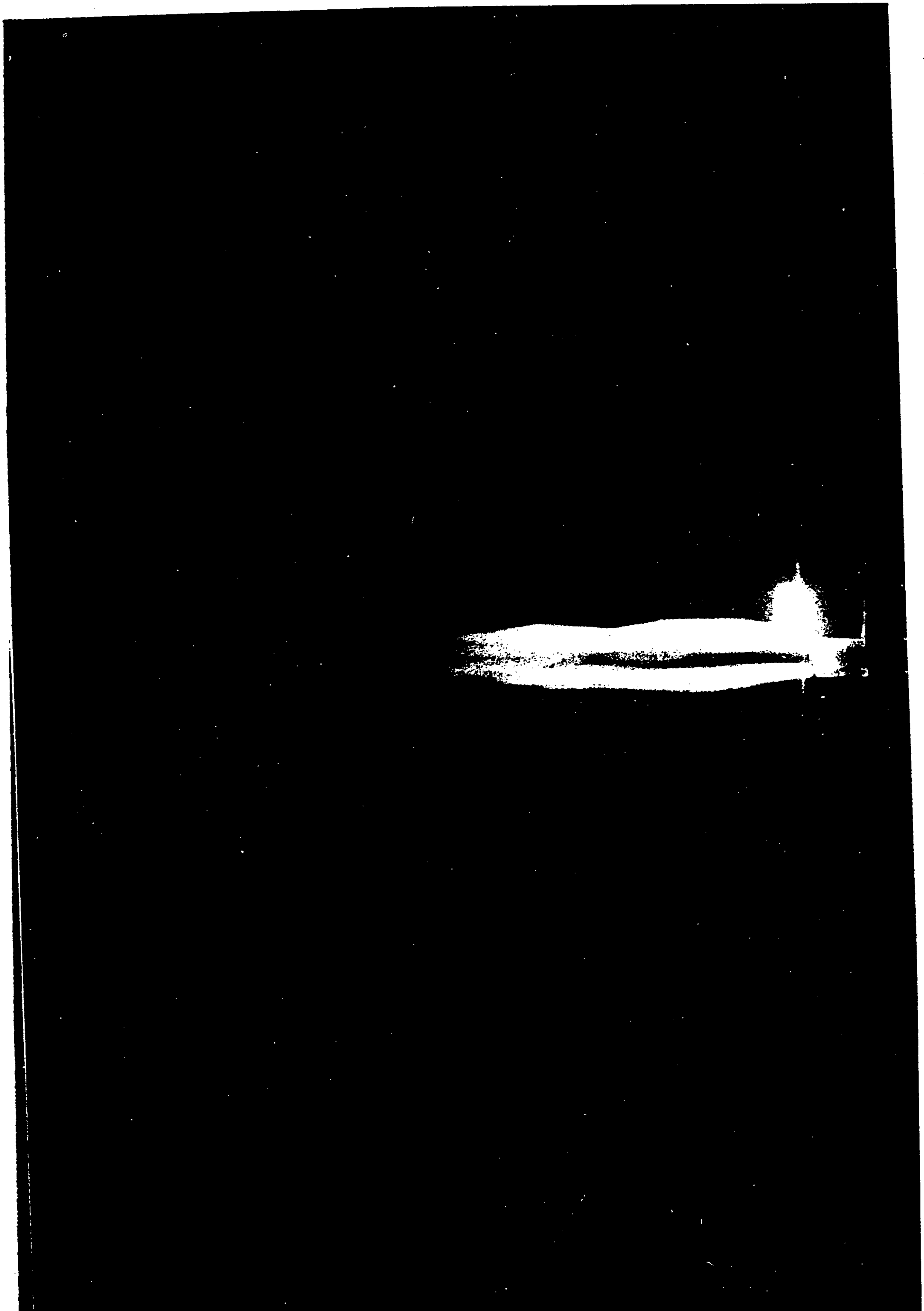

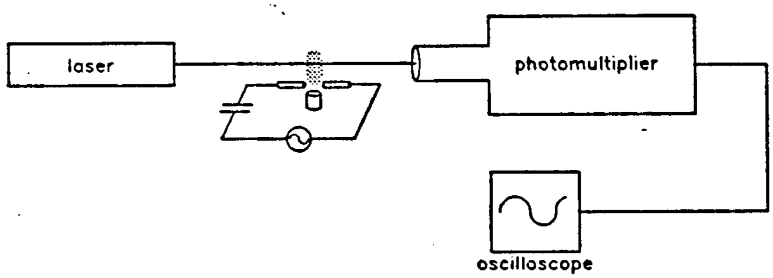

laser
photomultiplier
oscilloscope

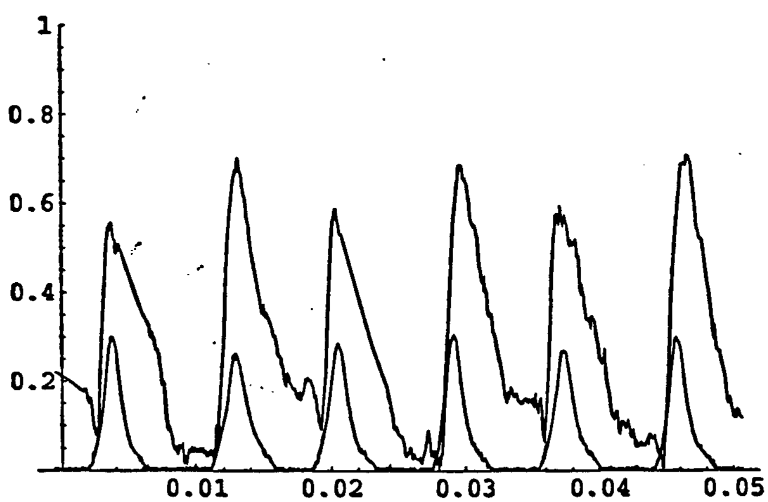

1
0.8
0.6
0.4
0.2
0.01
0.02
0.03
0.04
0.05

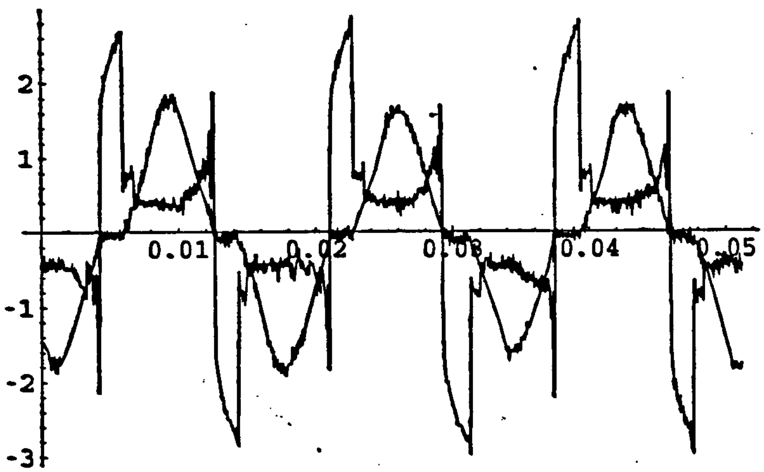
2
1
-1
-2
-3
0.01
0.02
0.03
0.04
0.05

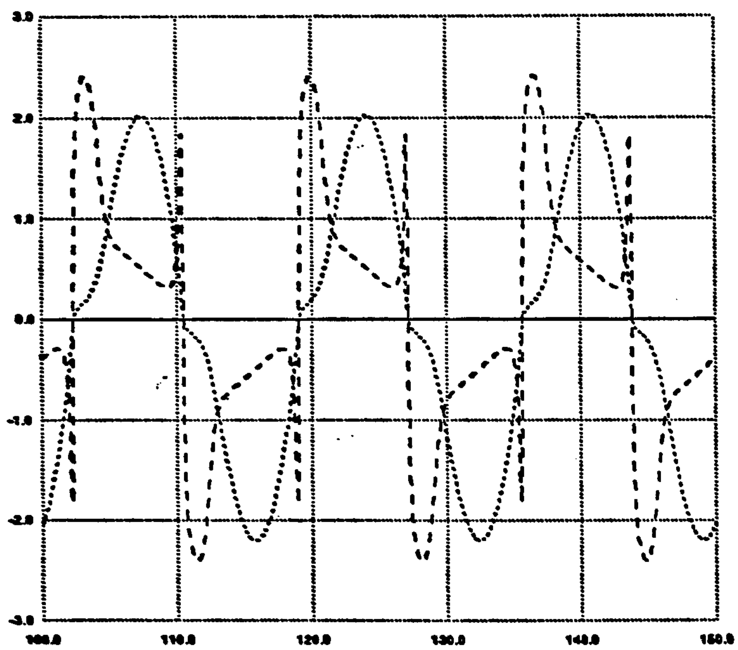
v(21)/1000
3.0
2.0
1.0
0.0
-1.0
-2.0
-3.0
100.0
110.0
120.0
130.0
140.0
150.0
mS

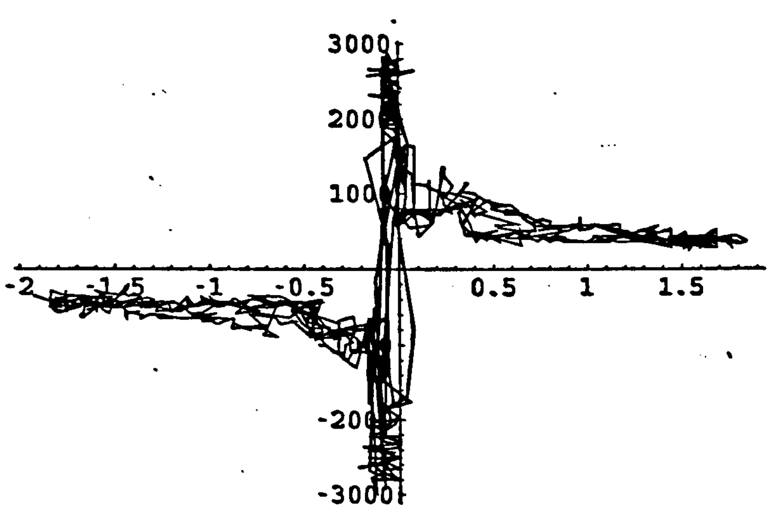
3000
2000
1000
-2000
-3000
-2
-1.5
-1
-0.5
0.5
1
1.5

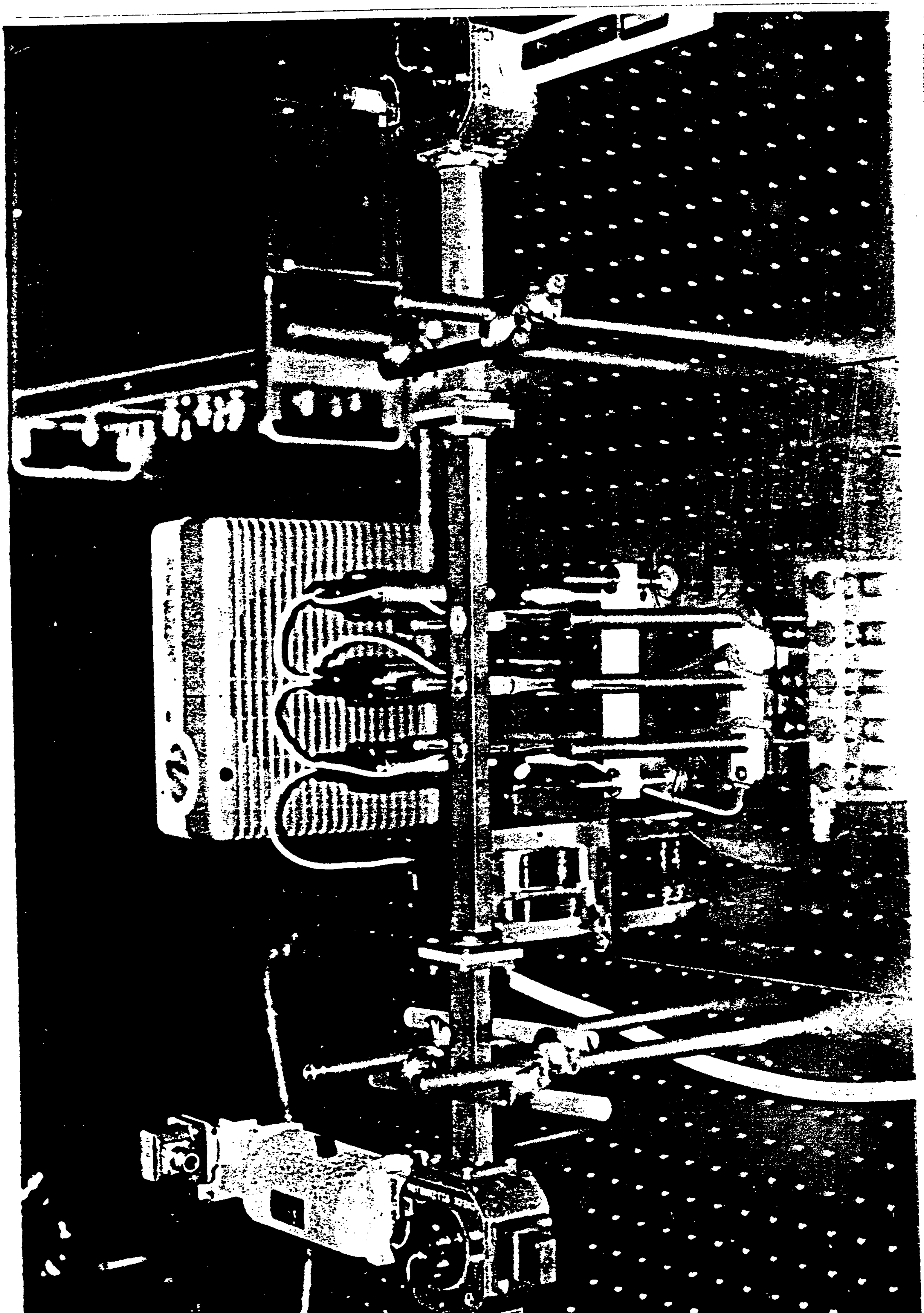

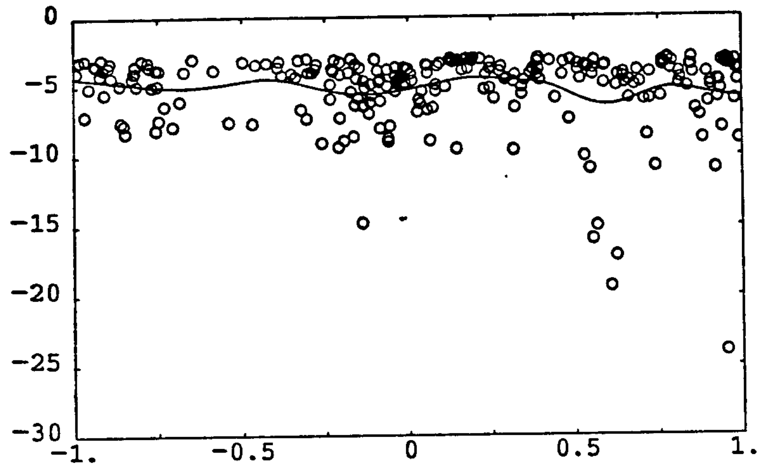
0
-5
-10
-15
-20
-25
-30
-1.
-0.5
0
0.5
1.

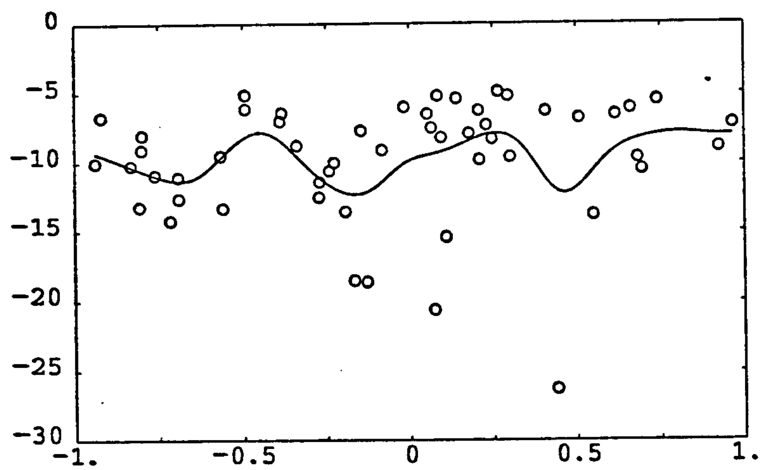
0
-5
-10
-15
-20
-25
-30
-1.
-0.5
0
0.5
1.

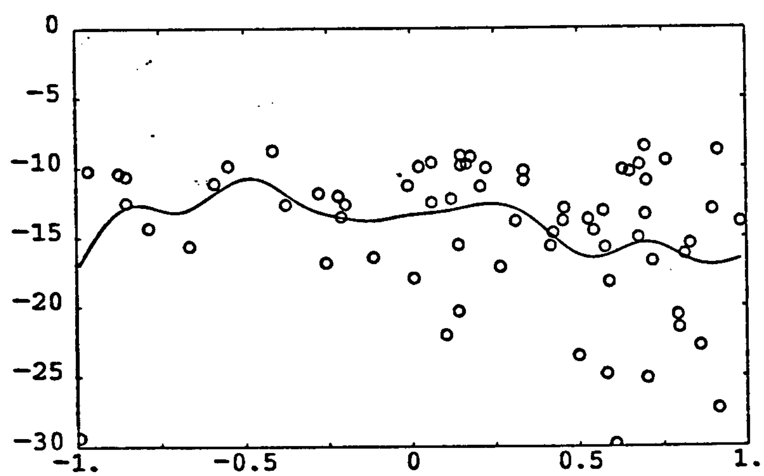
0
-5
-10
-15
-20
-25
-30
-1.
-0.5
0
0.5
1.

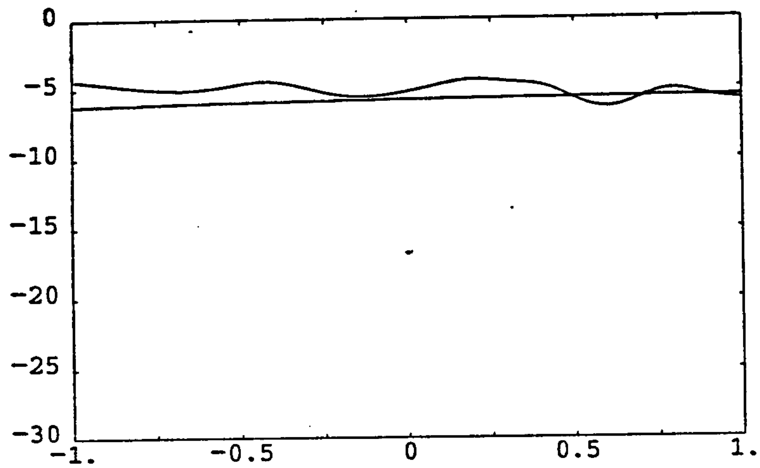
0
-5
-10
-15
-20
-25
-30
-1.
-0.5
0
0.5
1.

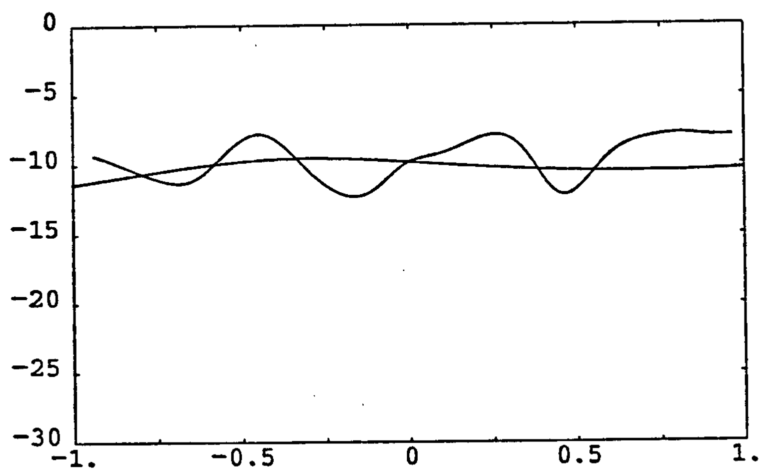
0
-5
-10
-15
-20
-25
-30
-1.
-0.5
0
0.5
1.

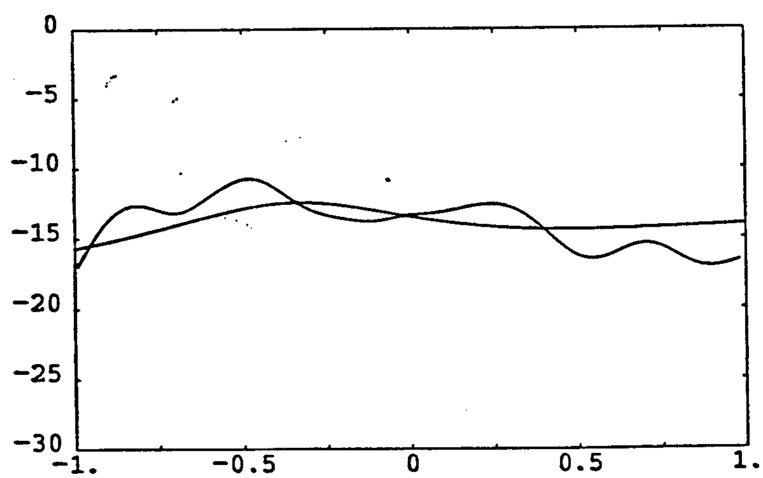
0
-5
-10
-15
-20
-25
-30
-1.
-0.5
0
0.5
1.

Plasma Torch

Pressure:	1 ATM
Density:	1.5×10^{13} (deduced from measurements based on two independent methods)
Temperature:	$1200° K$
Dimensions:	cylindrical shape having 1 cm radius and 7 cm length
Volume:	20 cm^3/torch
Power Consumption:	600 W/torch
Peak Voltage and Current:	2.8 kV and 2 A

Microwave Plasma Layers

Pressure:	20 torr
Density:	10^{11} cm^{-3}
Microwave Power:	1 MW peak, 1 μs pulse, 40 rps

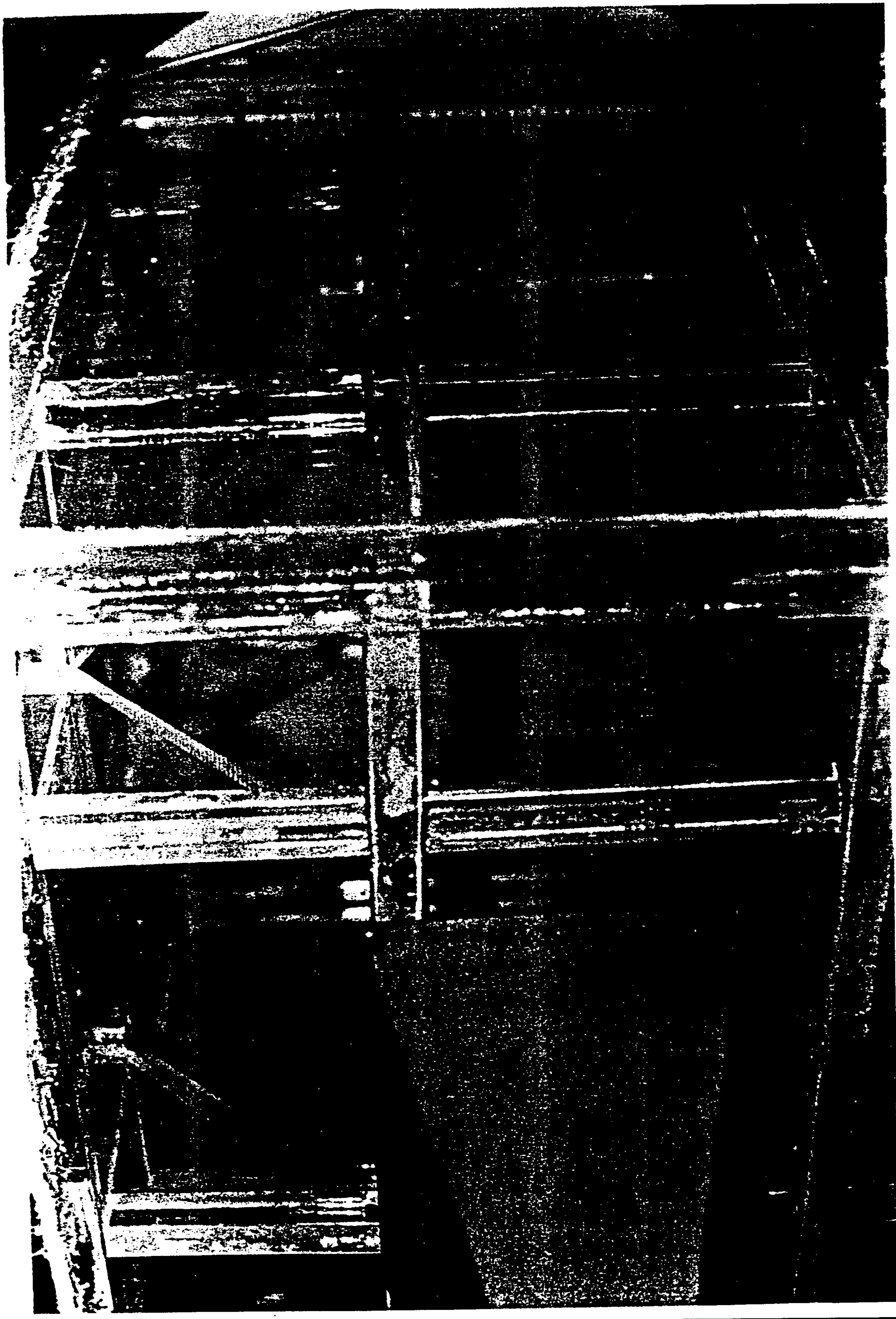

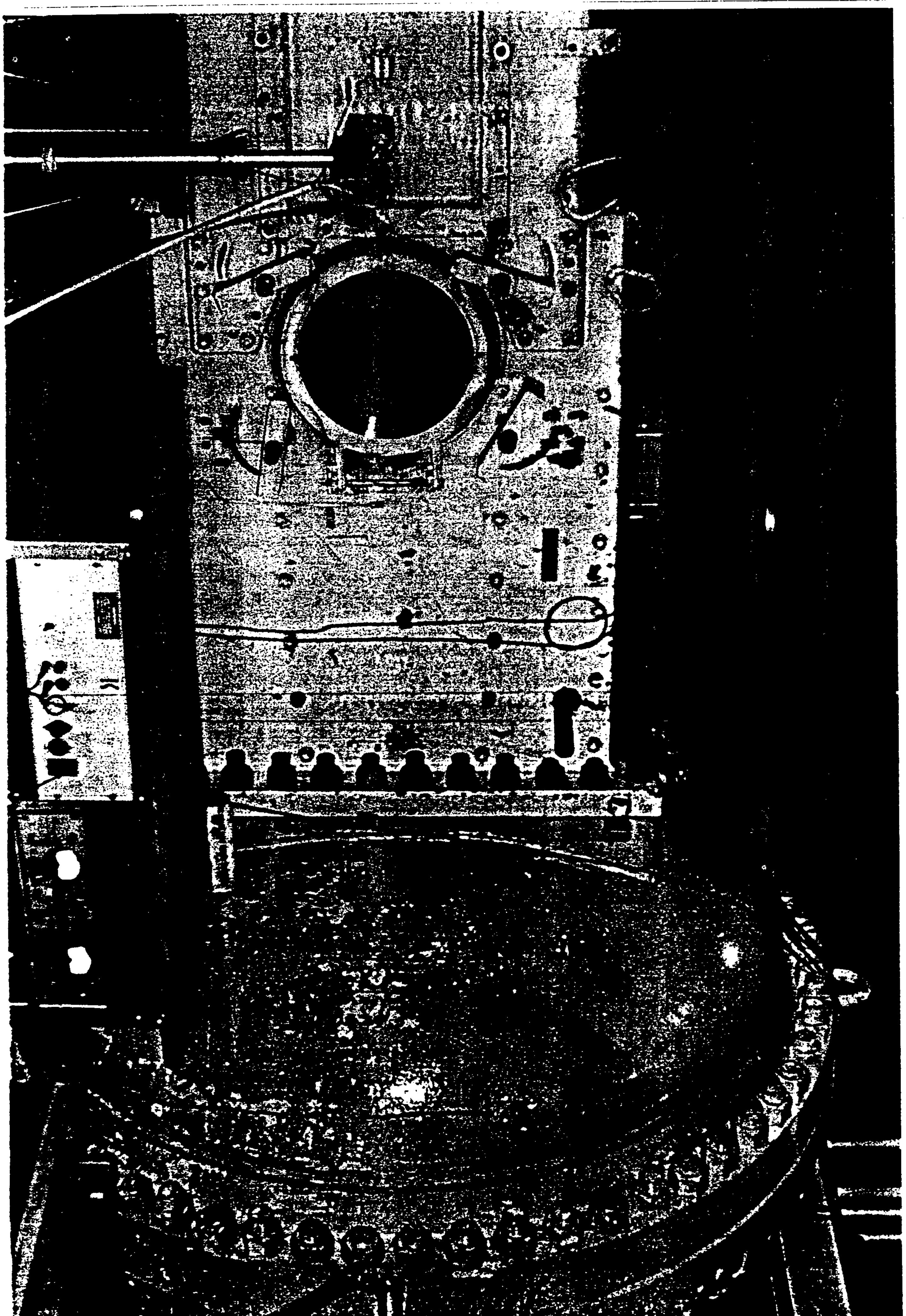

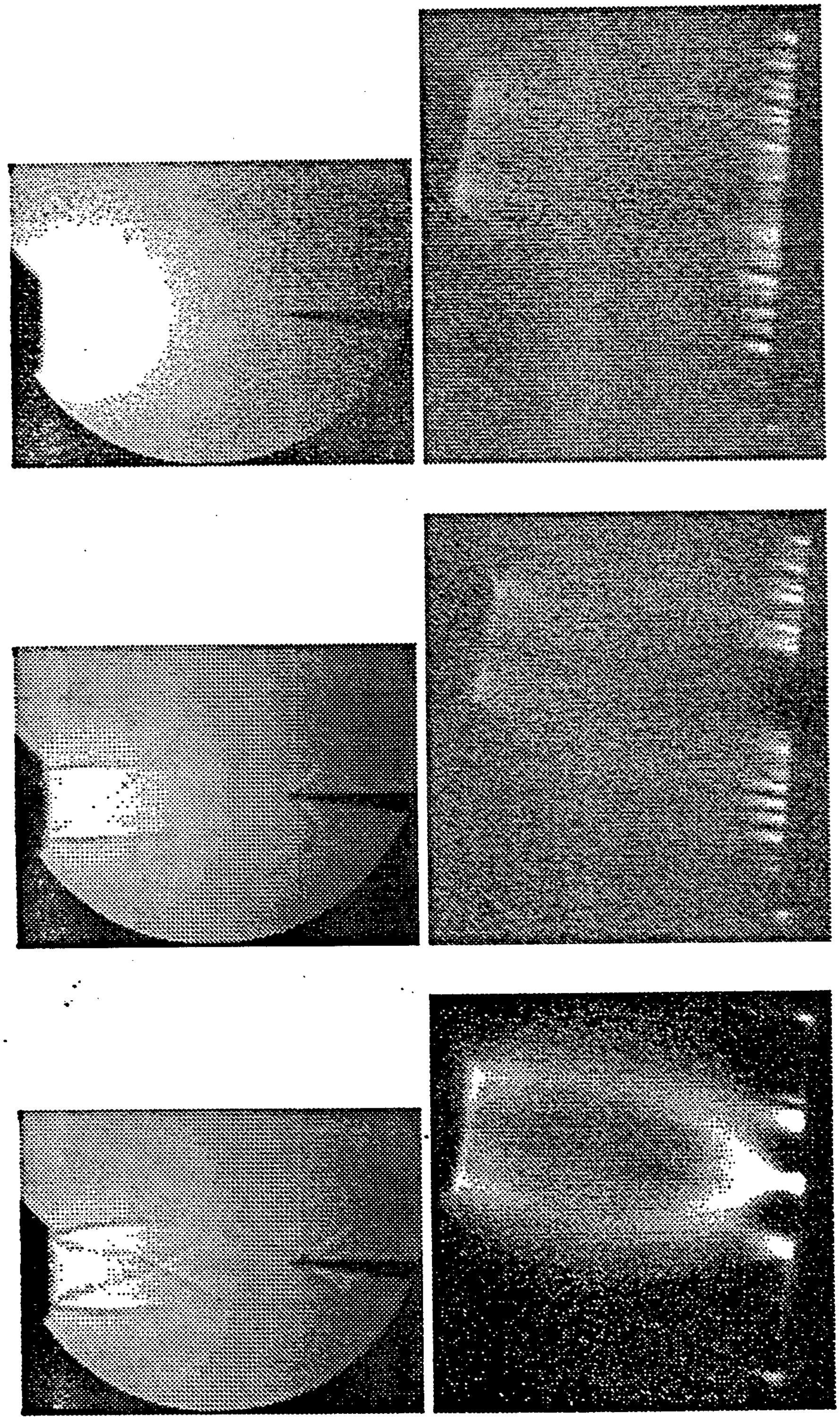

Plasma Ramparts Using Metastable Molecules

MURI Program

The Ohio State University
Princeton University

"Optically Pumped Nonequilibrium Plasmas"

I. Adamovich, V. Subramaniam, W. Rich

Presented at

AFOSR Workshop
"Understanding and Control of
Ionized High-Speed Flows"

Princeton University
Feb. 26-27, 1998

Work funded by the Director of Defense Research & Engineering (DDR&E) within the Air Plasma Ramparts MURI Program managed by AFOSR

Program Objectives:

- Create large volume ($O[m^3]$) free air plasma
- One atmosphere
- Free electron densities 10^{13} cm^3 or greater
- Gas temperature less than 2,000 K
- Energy efficient method

Approaches:

A. Thermal Plasmas (High Temperature Arcs, Reentry Plasmas)

Problems:

I) High Temperature

B. NonThermal Plasmas (Glow Discharges, Optically Pumped Plasmas)

Problems:

I) Requires thermodynamic work (electrical work, laser work)

II) Stability

OSU/Princeton Approach: Laser Pumped Metastable State Plasmas.

92 W cw broad-band lasing conditions

Date: 10-26-1992		
Gas	Partial Pressure (Torr)	mass flow rate (10^3 g/min)
He internal purge	4.15	18.9
He	9.00	75.5
N_2	2.75	138
CO	1.60	6.61
Air	.01	.89
Total	17.5	239
$He:CO:N_2$ molar ratio 751:92:157		
Discharge Conditions		
Current mADC	45	
Voltage kVDC	18	
Laser Power Broad Band W	92	
Physical Efficiency	30.3%	

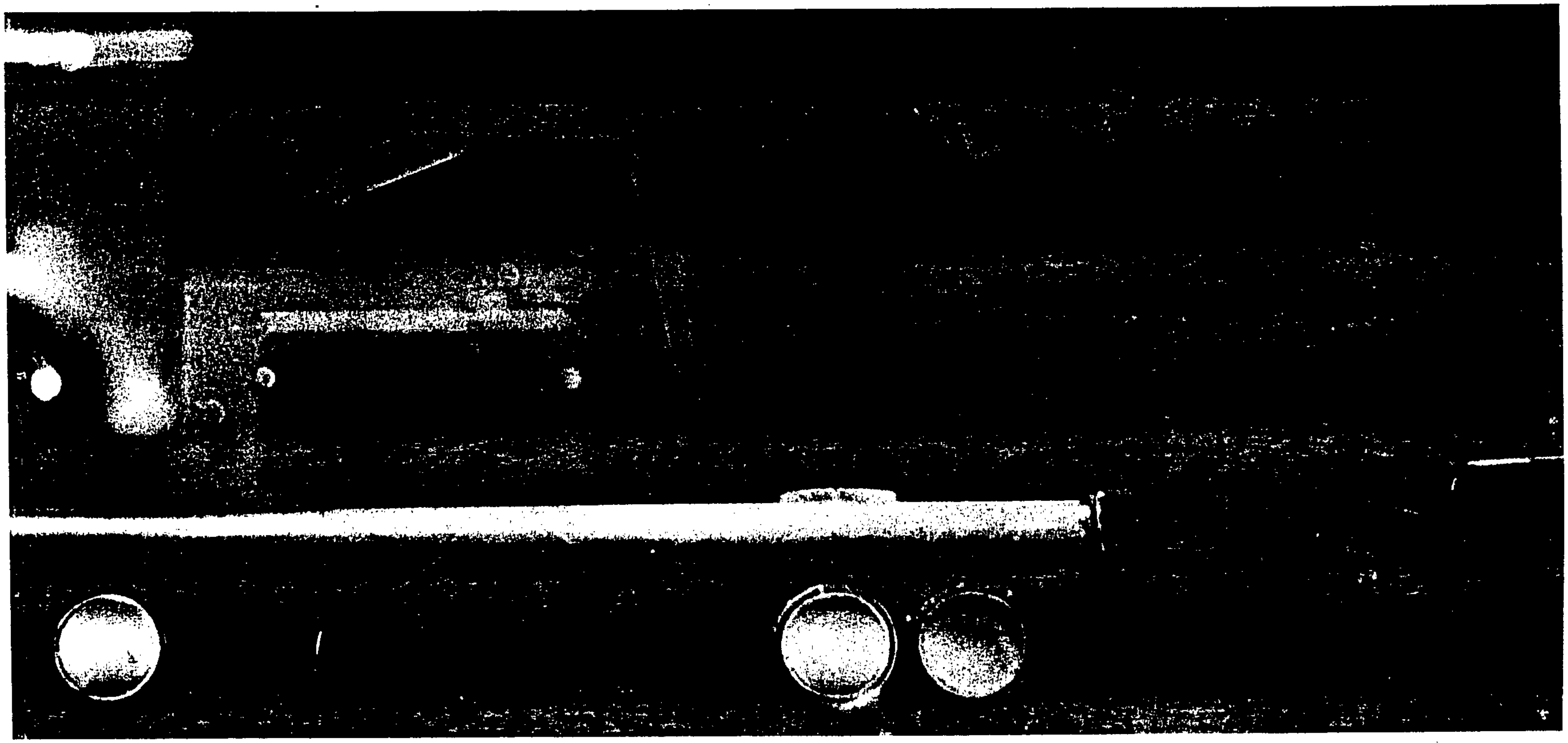

Advantages:

- Stable, large volume
- High pressure
- Low gas temperatures

Problems:

- Electron density
- Efficiency
- Non-air species

Three Level Laser

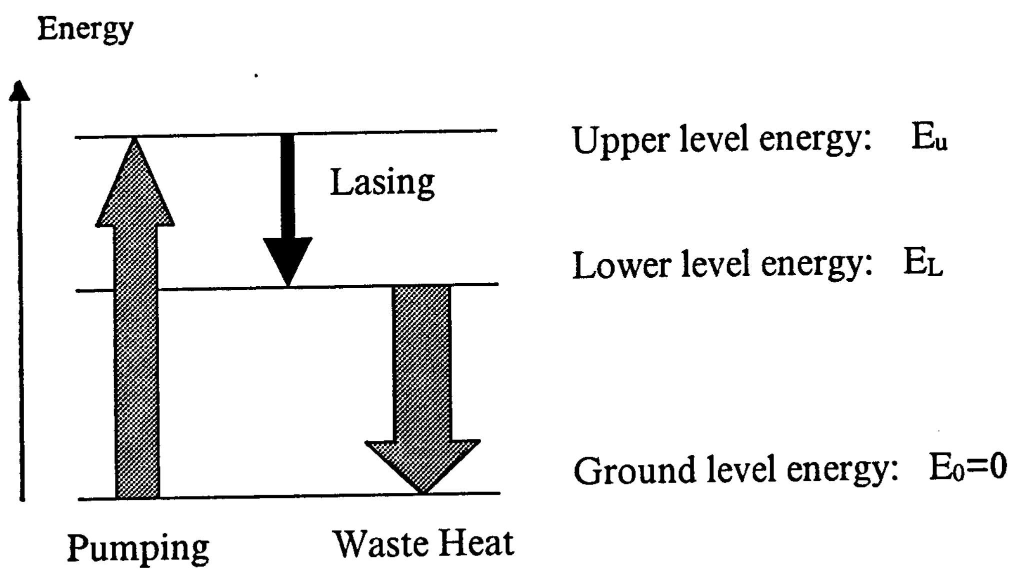

Quantum Efficiency

$$\eta_{quantum} = \frac{E_U - E_L}{E_L}$$

$\sim$ 40% for CO_2/N_2

$\sim$ 95% for CO/N_2

Scoville, 1954 showed equivalence with reversible engine efficiency

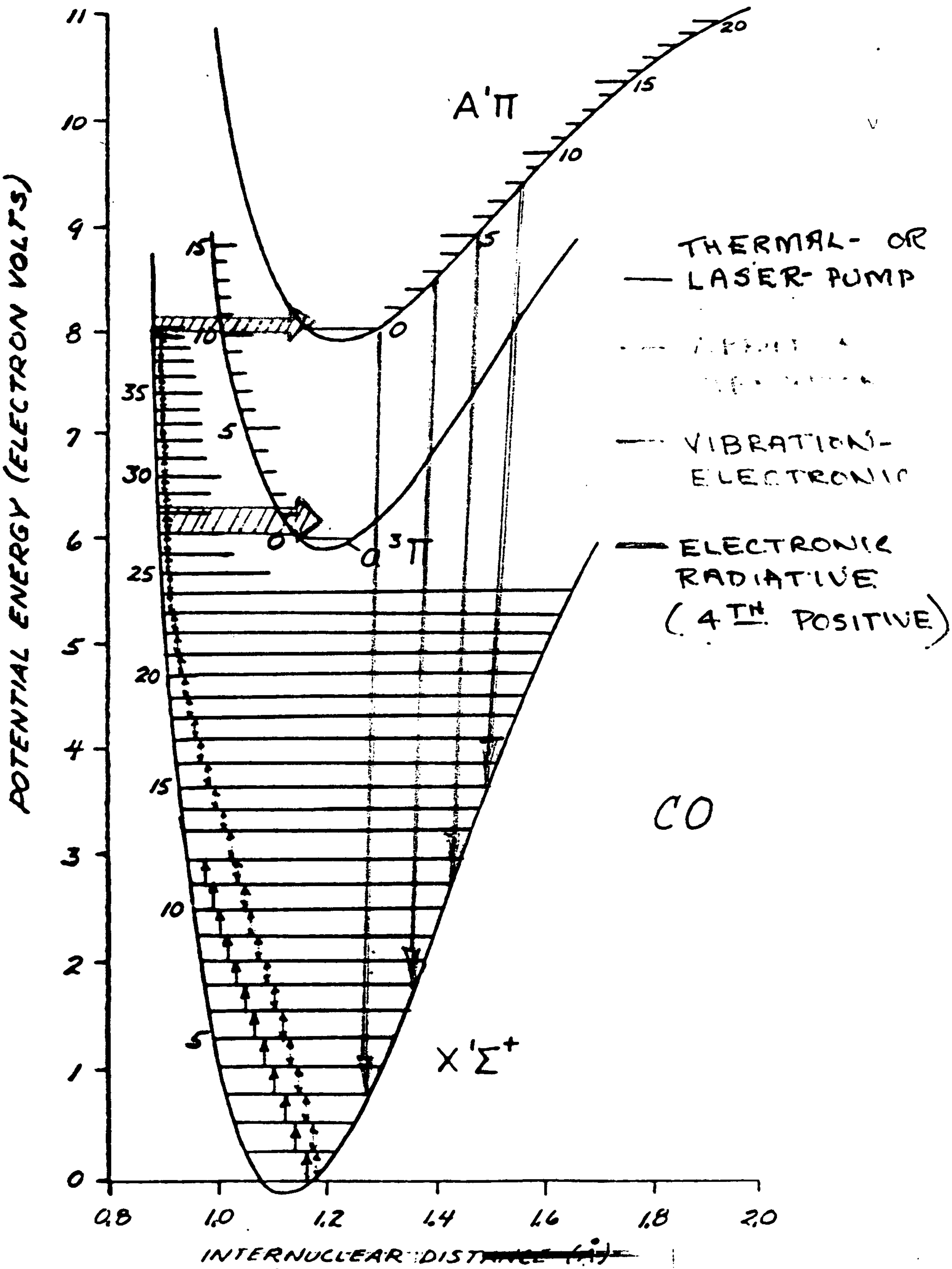

POTENTIAL ENERGY (ELECTRON VOLTS)
INTERNUCLEAR DISTANCE (Å)
A'Π
a³Π
X'Σ+
CO
THERMAL- OR LASER-PUMP
VIBRATION-ELECTRONIC
ELECTRONIC RADIATIVE (4TH POSITIVE)

IR/UV Radiation Conversion in Optically Pumped CO-Ar Plasma

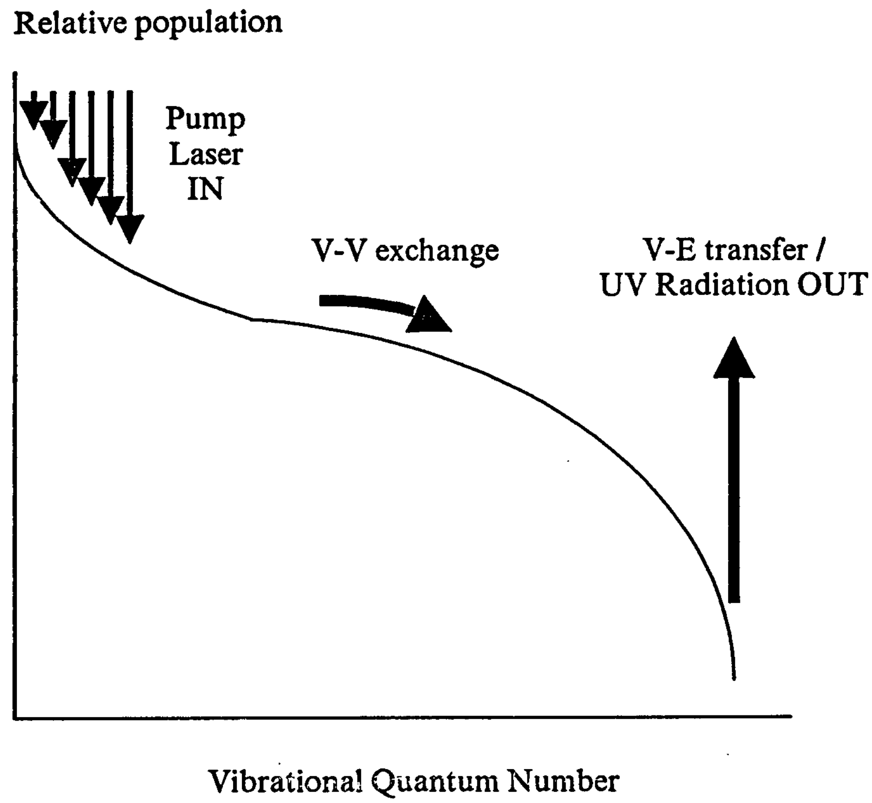

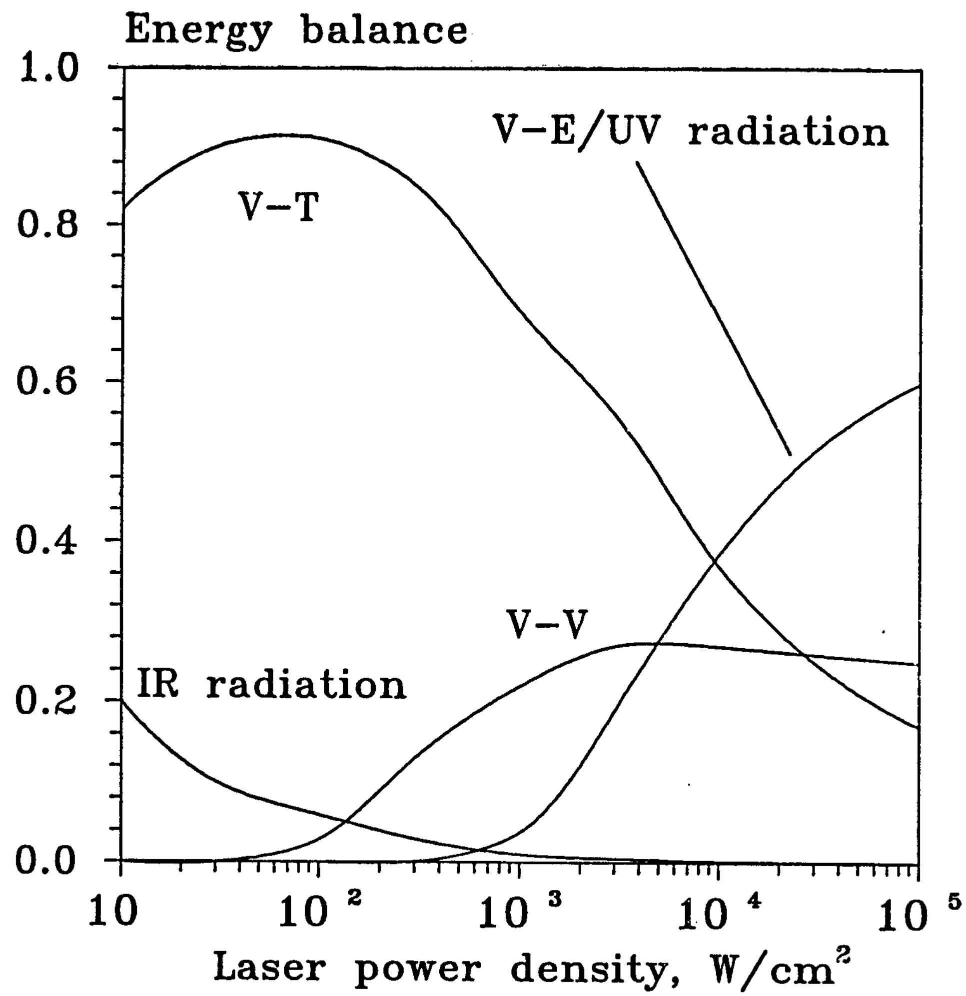

P=1 atm, T=1500 K

CO:Ar=5:95

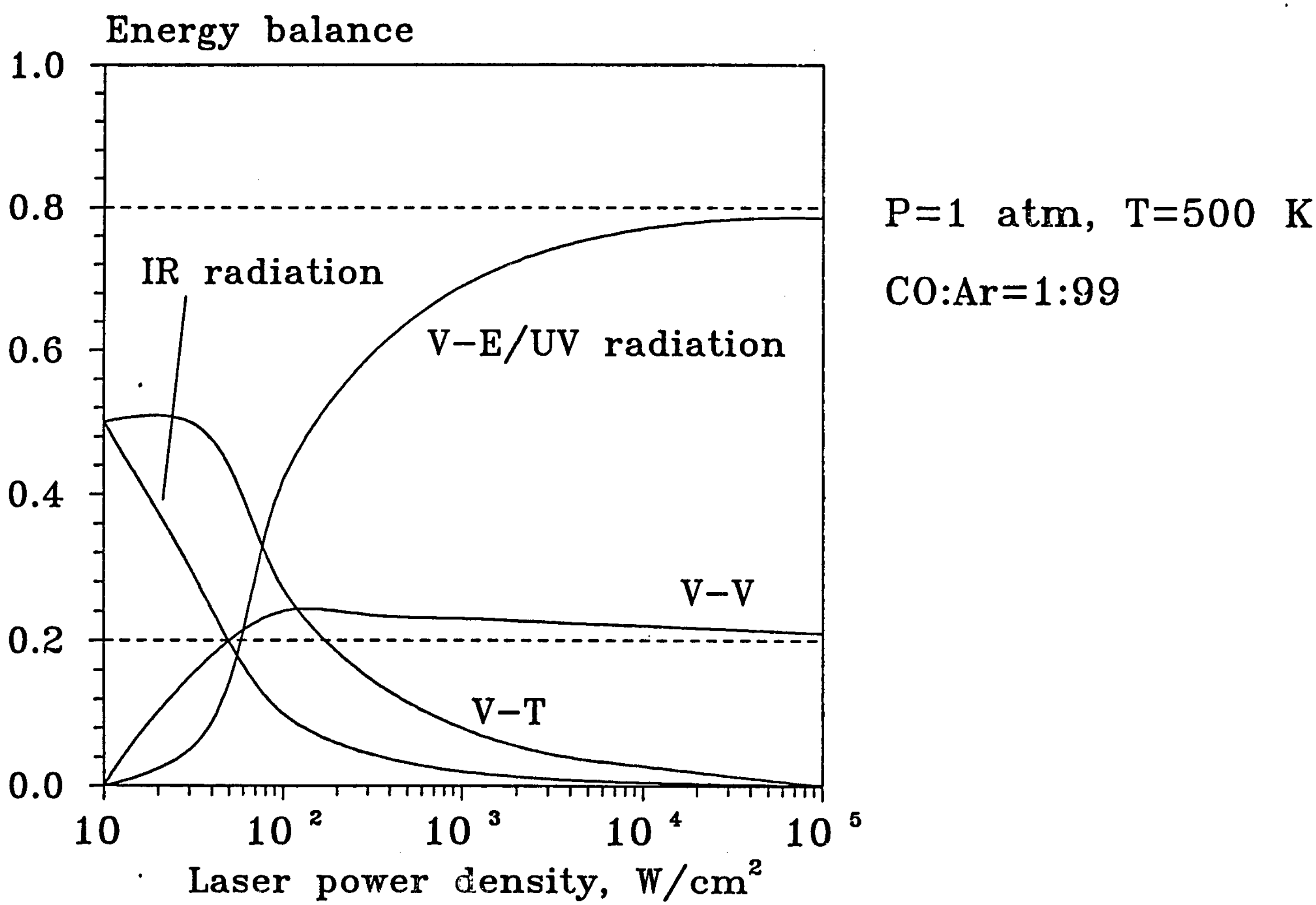
Energy balance
1.0
0.8
0.6
0.4
0.2
0.0
IR radiation
V–E/UV radiation
V–V
V–T
10
10 2
10 3
10 4
10 5
Laser power density, W/cm2
P=1 atm, T=500 K
CO:Ar=1:99

The Ohio State University

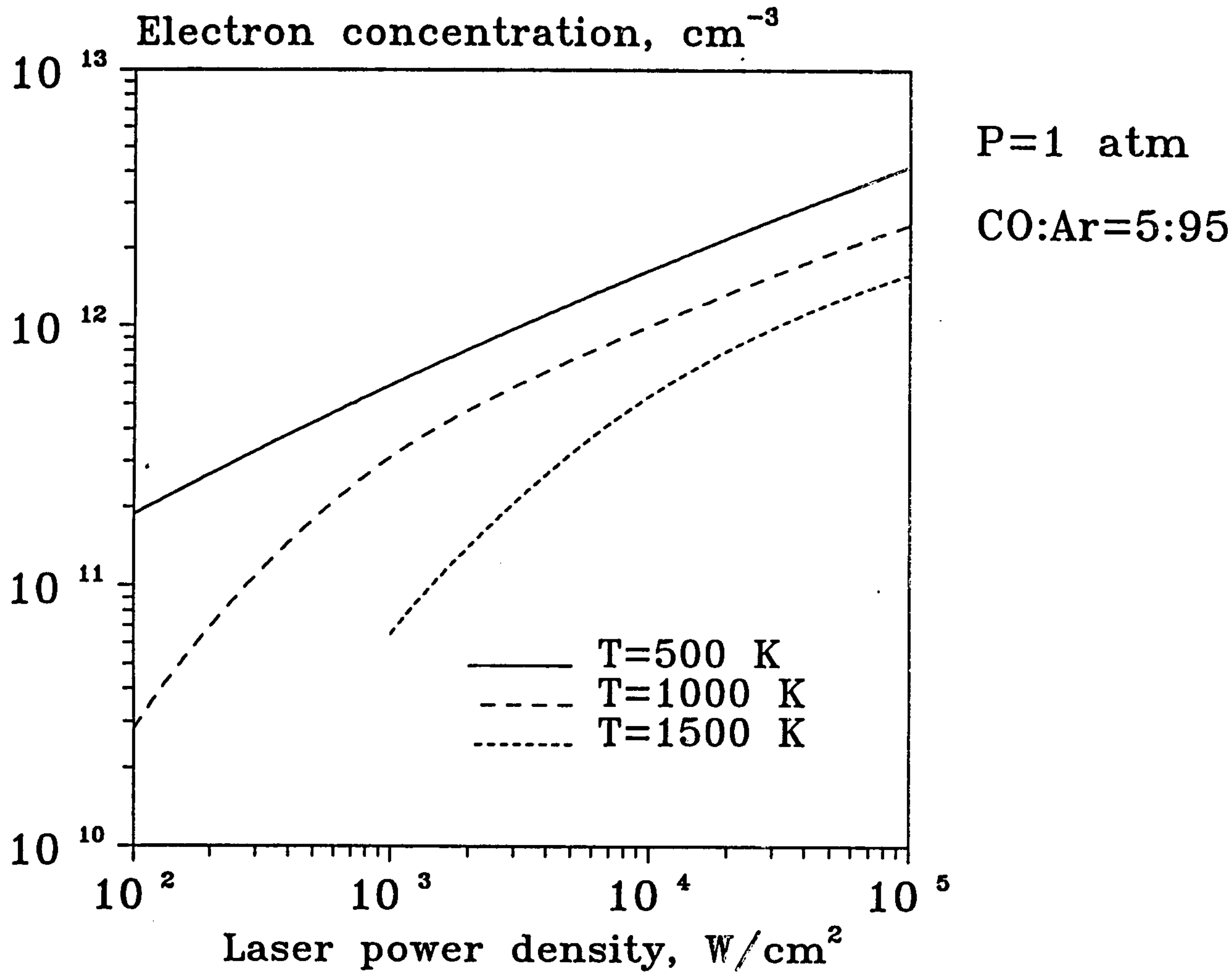

Nonequilibrium Thermodynamics Laboratories

IR/Visible Radiation Conversion in Optically Pumped CO-N_2-Na Plasma

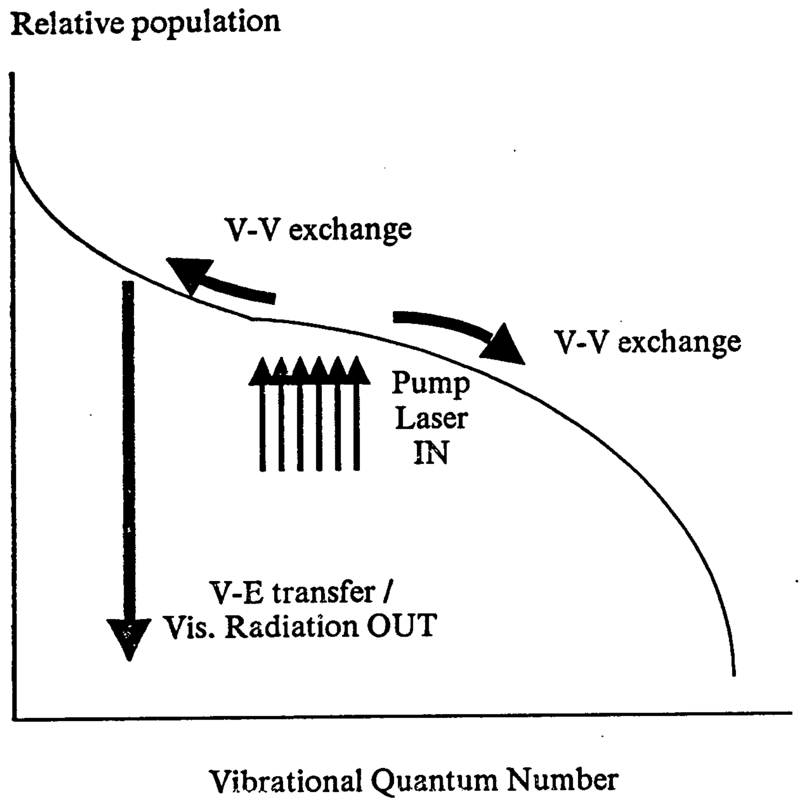

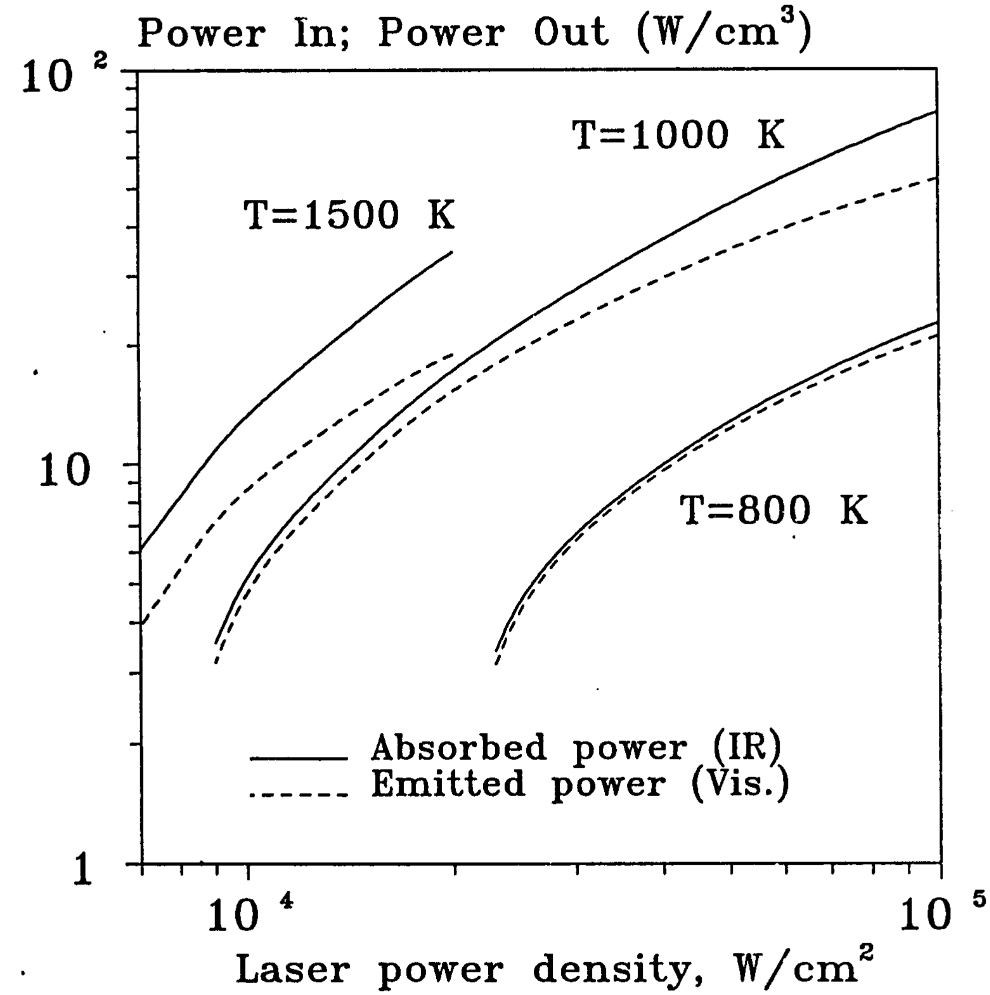
Power In; Power Out (W/cm3)
10 2
10
1
T=1500 K
T=1000 K
T=800 K
Absorbed power (IR)
Emitted power (Vis.)
10 4
10 5
Laser power density, W/cm2

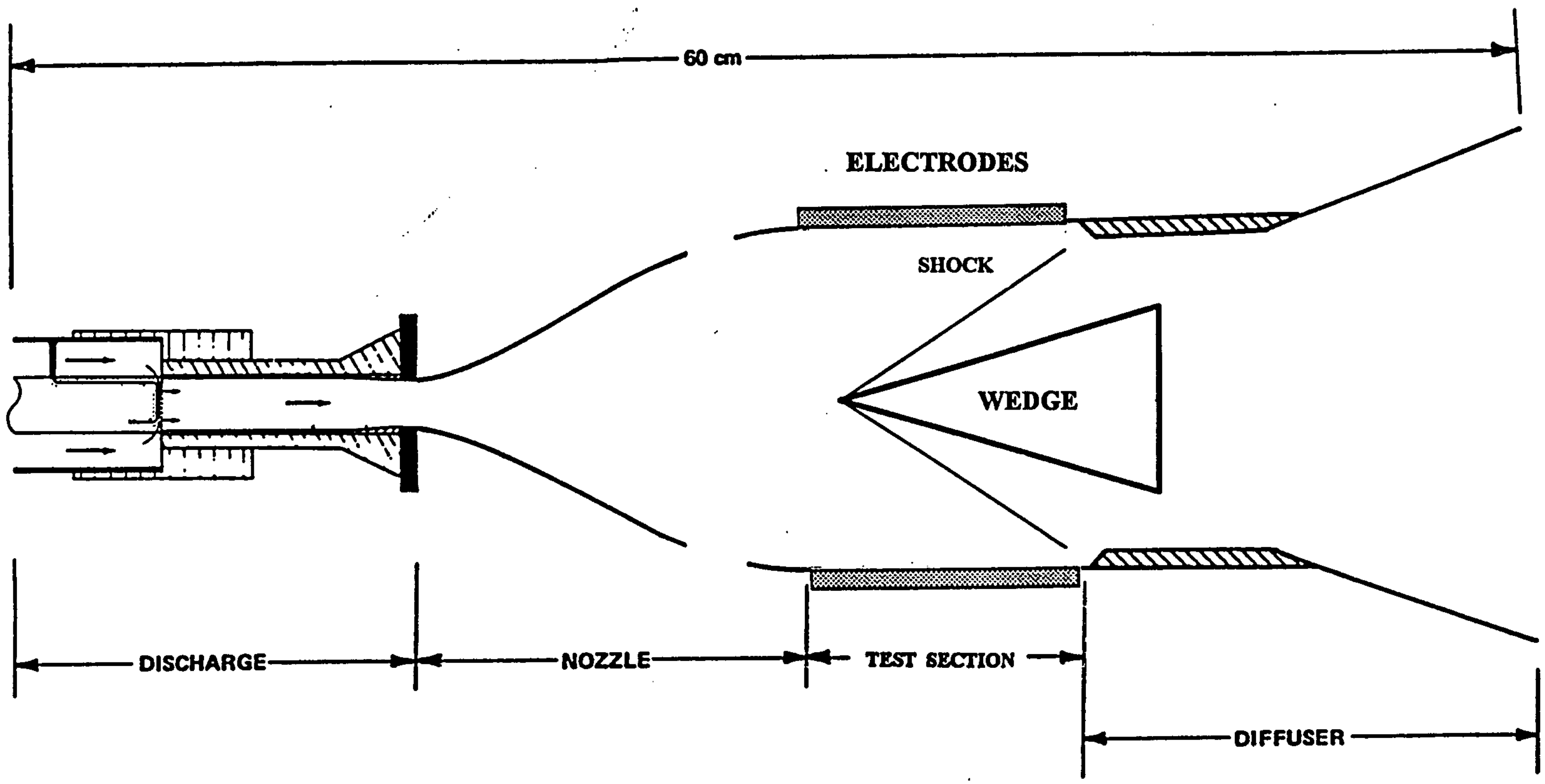

Figure 1. The schematic of the flowing afterglow experiment.

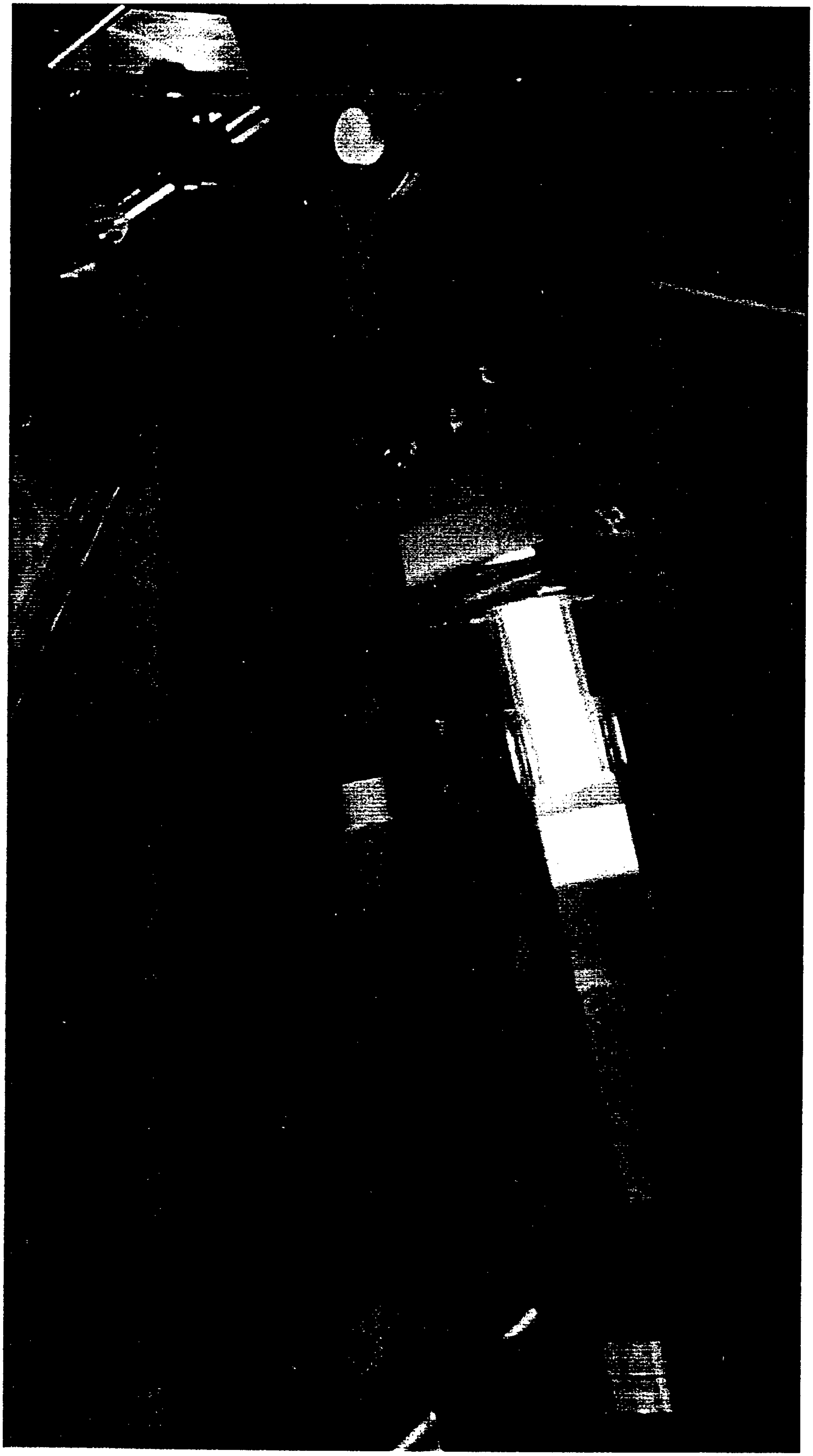

GRADIENT DISTORTION EXPERIMENT

- Transverse temperature gradient is created by absorption of CO laser radiation (1-2% CO is added to the flow to enable absorption and as a thermometric element).

  At P=100 Torr, dT/dr ~ 100 K/cm

Routinely used in CO and NO optical pumping kinetic experiments.

- Plane shock wave created by a capacitor bank discharge.

Measurements of:

- flow density distribution
- Gas temperature and transverse temperature gradient before the shock arrival

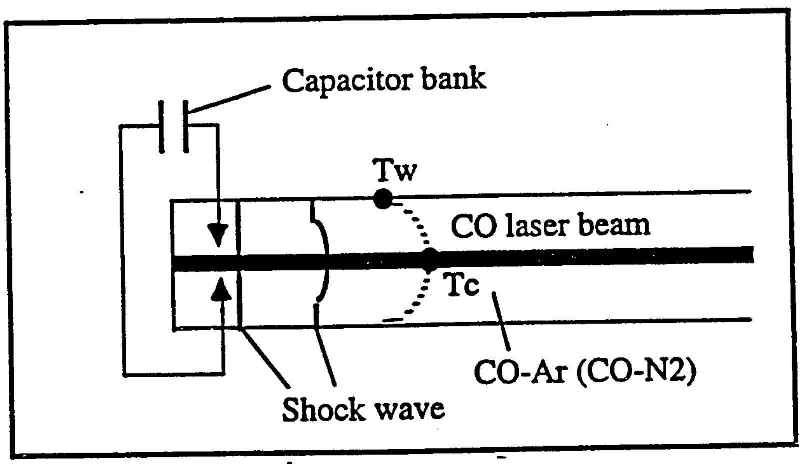

- Radial temperature profile is parabolic:
  $T(r) = T_c - (T_w - T_c)(r/R)^2$

Experimental verification

- Repeat Ganguly-Bletzinger experiment with thermal effects alone - pure, non-intrusive gas heating induced in CO-seeded Argon, using optical pumping.

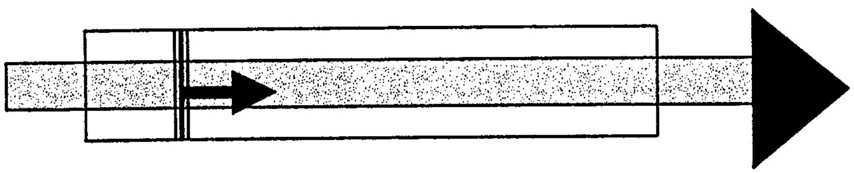

Axially directed CO laser beam

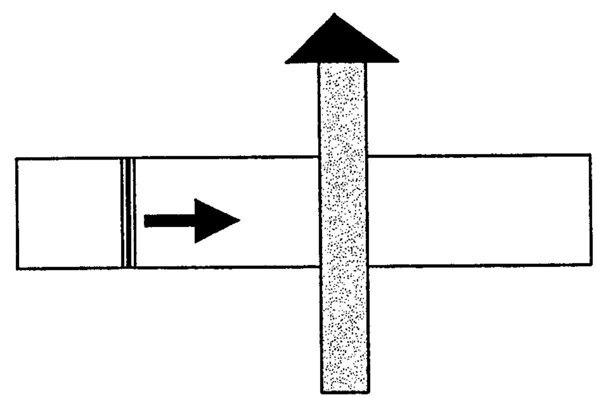

Transverse directed CO laser beam

Experimental Validation

- **Body in wind-tunnel; Thompson discharge by photo-ionization**

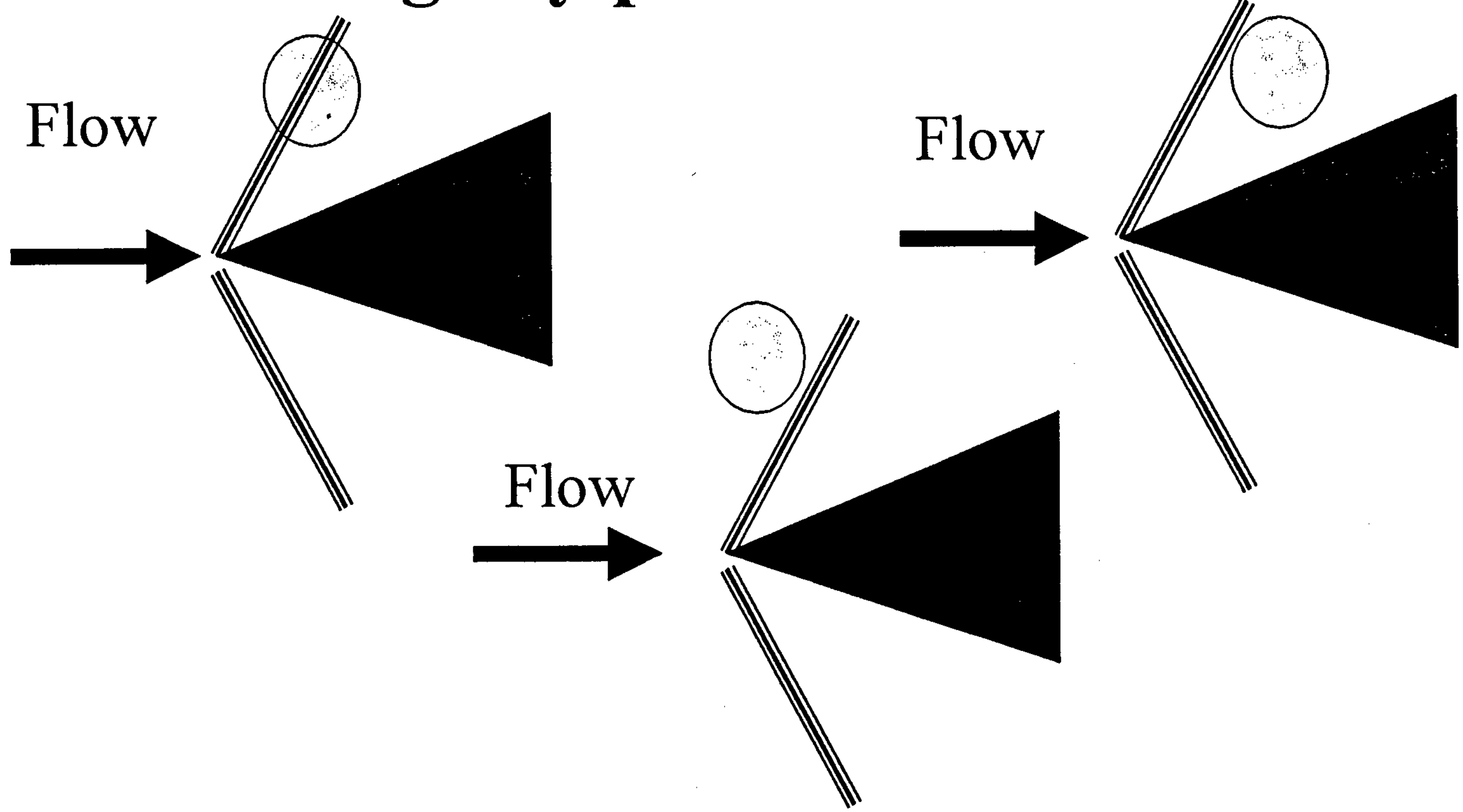

COMPRESSION OF A FIELD-FREE, NON-HOMOGENEOUS PLASMA

P. J. TURCHI *

AFRL/DE

KIRTLAND AFB, NM

* PROFESSOR OF AEROSPACE ENGINEERING, THE OHIO STATE UNIVERSITY.

BASIC FORMULATION

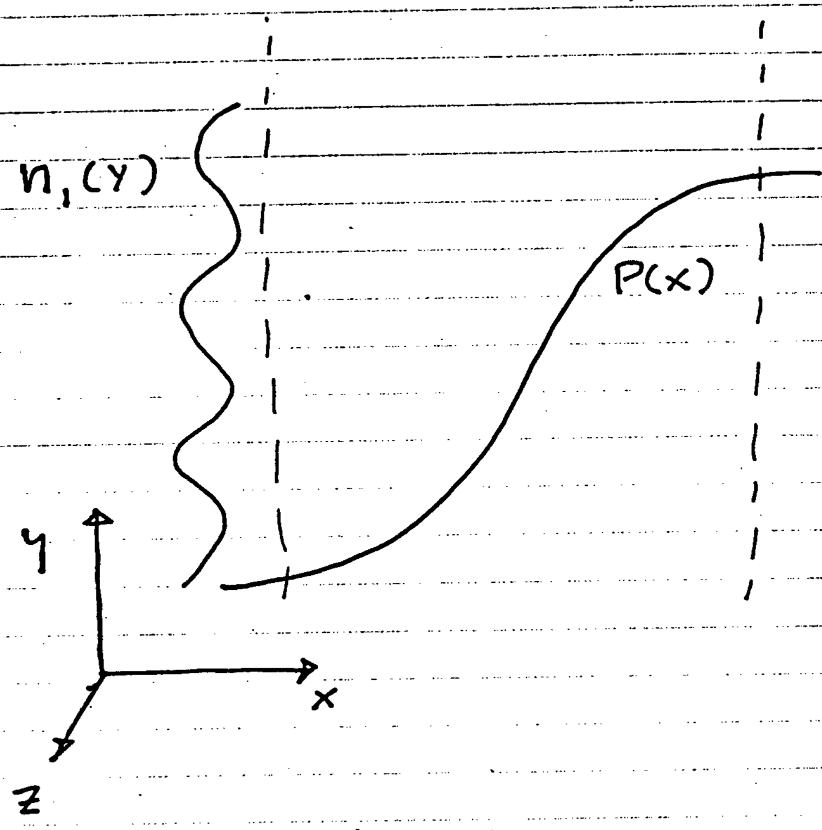

OHM'S LAW IN LIMIT OF HIGH DENSITY AND LOW CONDUCTIVITY

$$\Omega_e \to 0 \,, \; R_m \to 0$$

$$\vec{E} = \eta \vec{J} - \frac{1}{n_e e} \nabla P_e$$

(EXPECTATION THAT PLASMA IS TOO RESISTIVE INITIALLY TO PERMIT FLUX CONVECTION)

$$\frac{\partial \vec{B}}{\partial t} = -\nabla \times (\eta \vec{J}) - \left(\frac{k}{e}\right) \frac{\nabla n_e \times \nabla T_e}{n_e}$$

QUALITATIVE BEHAVIOR

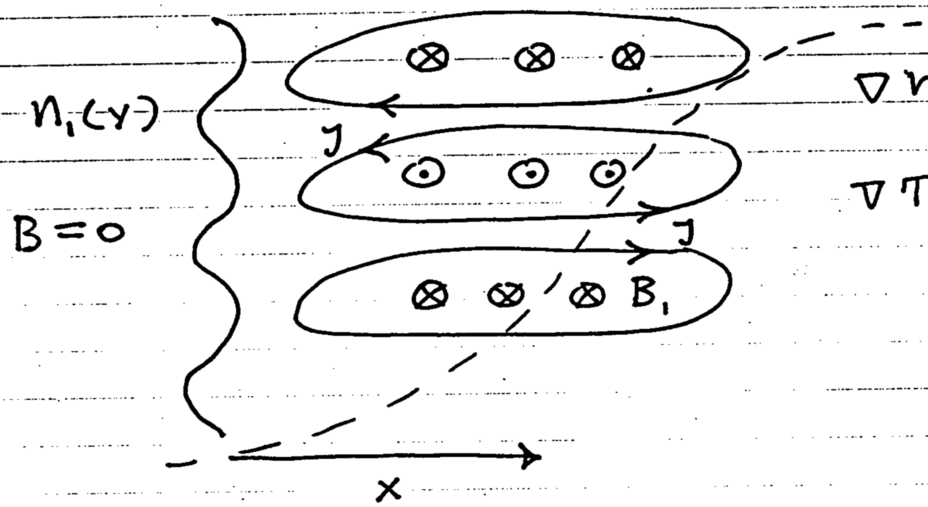

$$\nabla n_0 = \frac{\partial n_0}{\partial x}$$

$$\nabla T_0 = \frac{\partial T_0}{\partial x}$$

$\nabla n \times \nabla T$ TERM CAUSES GROWTH

OF MAGNETIC FIELD INTO AND OUT OF PLANE

AND ASSOCIATED IN-PLANE CURRENTS

TENDENCY TO TRANSFER AND CONCENTRATE

ENERGY FROM REGIONS OF GENERATION

TO REGIONS OF DISSIPATION

$$P_d = -\vec{E} \cdot \vec{J}$$

(CURRENT DENSITY DIRECTION ALTERNATES
MAIN PRESSURE-GRADIENT INDUCED
ELECTRIC FIELD MAINTAINS DIRECTION)

POSSIBLE NONLINEAR EFFECTS

RESISTIVE HEATING MAY CHANGE PLASMA

$$\eta J^2 \rightarrow \frac{dT_e}{dy}$$

CHANGING PLASMA MAY CHANGE TRANSPORT

$$\eta = \eta(n_e, T_e)$$

$$\mathcal{H} = \mathcal{H}(n_e, T_e)$$

THESE CHANGES GREATLY COMPLICATE THE ARITHMETIC, BUT MAY BE CRITICAL FOR DESCRIBING EXPERIMENTAL BEHAVIOR

- FURTHER CONCENTRATION OF CURRENTS AND IONIZATION

- OPPORTUNITY FOR HEAT TRANSPORT AT SHOCK VIA HOT COLUMNS

LINEARIZED ANALYSIS

LOOK FOR ELEMENTS OF BEHAVIOR WITH SIMPLIFIED ARITHMETIC

LET MAIN FLOW CARRY PRESSURE GRADIENT IN X-DIRECTION $\frac{\partial P_0}{\partial x}$

TRANSVERSE VARIATION OF DENSITY AND TEMPERATURE AT FIXED PRESSURE

$$\frac{\partial n_1}{\partial y}, \frac{\partial T_1}{\partial y} \quad \text{WITH} \quad \frac{\partial P_1}{\partial y} = 0$$

SOLVE FOR VARIATION OF (WEAK) MAGNETIC FIELD AS FUNCTION OF BOTH X AND Y

$$\vec{B} = B\hat{k} = B_0 + \epsilon B_1(x, y)$$

$$\text{WITH } B_0 = 0 \qquad \epsilon \ll 1$$

LINEARIZED ANALYSIS (CONTINUED)

SPECIFY
$$n(x,y) = n_0(x)(1 + \epsilon \sin Ky)$$

AT $\partial P/\partial y = 0$, THEN
$$T(x,y) \cong T_0(x)(1 - \epsilon \sin Ky)$$

WHERE $P_0(x) = n_0 k T_0$ ('0' REFERS TO ZEROTH ORDER, NOT STAGNATION)

ALSO, RESISTIVITY
$$\eta = \eta_0 + \epsilon \eta_1$$

SUBSTITUTION INTO FARADAY'S LAW YIELDS AT $O(\epsilon)$:

$$\frac{\partial B_1}{\partial t} = \frac{1}{\mu}\left\{\eta_0\left(\frac{\partial^2 B_1}{\partial x^2} + \frac{\partial^2 B_1}{\partial y^2}\right) + \frac{\partial B_1}{\partial x}\left[\left(\frac{\partial \eta_0}{\partial n_e}\right)\frac{\partial n_0}{\partial x} + \left(\frac{\partial \eta_0}{\partial T_e}\right)\frac{\partial T_0}{\partial x}\right]\right.$$

$$\left. + \frac{K \cos Ky}{e n_0}\frac{\partial P_0}{\partial x}\right\}$$

STEADY STATE, $\partial B_1/\partial t = 0$,

$$\left(\frac{\eta_0}{\mu}\right)\left[\frac{\partial^2 B_1}{\partial x^2} + \frac{\partial^2 B_1}{\partial y^2}\right] + \frac{1}{\mu}\frac{\partial B_1}{\partial x}\left[\left(\frac{\partial \eta_0}{\partial n_e}\right)\frac{\partial n_0}{\partial x} + \left(\frac{\partial \eta_0}{\partial T_e}\right)\frac{\partial T_0}{\partial x}\right]$$

$$= -\frac{K \cos Ky}{e n_0}\frac{\partial P_0}{\partial x}$$

LINEARIZED ANALYSIS (CONTINUED)

TRY SOLUTION OF FORM:

$$B_1(x,y) = b(x)\cos Ky$$

WHICH PROVIDES EQUATION:

$$\left(\frac{\eta_0}{\mu}\right)\left[\frac{d^2b}{dx^2} - K^2 b\right] + \frac{1}{\mu}\frac{db}{dx}\left[\left(\frac{\partial \eta_0}{\partial n_e}\right)\frac{\partial n_0}{\partial x} + \left(\frac{\partial \eta_0}{\partial T_e}\right)\frac{\partial T_0}{\partial x}\right]$$

$$= -\frac{K}{e n_0}\frac{dP_0}{dx}$$

EXPLORE SIMPLER CASE: LET η_0 = CONSTANT

$$\left(\frac{\eta_0}{\mu}\right)\left[\frac{d^2b}{dx^2} - K^2 b\right] = -\frac{K}{e n_0}\frac{dP_0}{dx}$$

OR

$$\frac{d^2b}{dx^2} - K^2 b = -\frac{\mu K}{\eta_0 e n_0}\frac{dP_0}{dx}$$

NORMALIZED EQUATIONS

LET $P_o(x) = \frac{b_c^2}{2\mu} \beta(\alpha)$ WHERE $\alpha = x/\lambda$

AND $K = 2\pi/\lambda$

$b(x) = b_c \, f(\alpha)$

$n_o(x) = \frac{P_o(x)}{k T_o(x)} = \frac{b_c^2}{2\mu k T_c} \frac{\beta(\alpha)}{\theta(\alpha)}$

SUBSTITUTION THEN PROVIDES:

$$\frac{d^2 f}{d\alpha^2} - 4\pi^2 f = -\left(\frac{2\pi\mu k T_c}{\eta_o e b_c}\right) \frac{\theta(\alpha)}{\beta(\alpha)} \frac{d\beta}{d\alpha}$$

WHICH FURTHER SIMPLIFIES TO:

$$\frac{d^2 f}{d\alpha^2} - 4\pi^2 f = -\frac{\theta(\alpha)}{\beta(\alpha)} \frac{d\beta}{d\alpha}$$

BY DEFINING $b_c = \frac{2\pi\mu k T_c}{\eta_o e}$

SOLUTION OF NORMALIZED EQUATION

HOMOGENEOUS PART:

$$\frac{d^2 f_H}{d\alpha^2} = 4\pi^2 f_H$$

$$f_H = c_1 e^{2\pi\alpha} + c_2 e^{-2\pi\alpha}$$

PARTICULAR SOLUTION, WITH FURTHER SIMPLIFICATION $\theta = 1$,

$$\frac{d^2 f_p}{d\alpha^2} - 4\pi^2 f_p = -\frac{1}{\beta}\frac{d\beta}{d\alpha}$$

TRY FORM OF $f_p(\alpha)$ THAT PROVIDES USEFUL FORM FOR $\beta(\alpha)$:

$$f_p(\alpha) = a \sin(m\pi\alpha)$$

THIS GIVES (BY SUBSTITUTION AND INTEGRATION):

$$\beta(\alpha) = \beta_1 e^{\frac{a\pi(m^2-4)}{m}\left[1-\cos(m\pi\alpha)\right]}$$

$$\alpha = 0, \quad \beta = \beta_1$$

$$\alpha = 1/m, \quad \beta = \text{MAXIMUM}$$

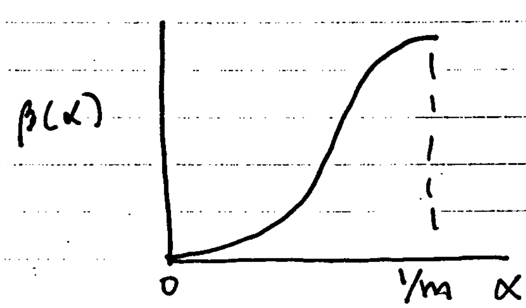

THICKNESS OF PRESSURE RISE:

$$\tau = \lambda/m$$

(WHICH GIVES m)

SOLUTION OF NORMALIZED EQUATION
(CONTINUED)

WITH $b_1 = 0$ AT $x = 0$ $\quad \Big(f(0) = 0$

AND $\dfrac{db_1}{dx} = 0$ ALSO $\quad \dfrac{df}{d\alpha} = 0 \Big)$

THE FULL SOLUTION IS:

$$B_1(x,y) = \frac{\mu k T_0}{\eta_0 e} \cos\left(\frac{2\pi y}{\lambda}\right) \frac{(\lambda/\tau)\ln r}{\left[\left(\frac{\lambda}{\tau}\right)^2 - 4\right]} \left\{ \sin\left(\frac{\pi x}{\tau}\right) - \frac{\lambda}{2\tau} \sinh\left(\frac{2\pi x}{\lambda}\right) \right\}$$

WHERE λ IS THE WAVELENGTH OF TRANSVERSE PERTURBATIONS OF PLASMA

τ IS THE COMPRESSION THICKNESS

AND r IS THE PRESSURE RATIO

THE SOLUTION IS RESTRICTED TO

$$0 \leq x \leq \tau \qquad \lambda/\tau > 2$$

(AND LINEARIZED ANALYSIS)

IT CAN MATCH TO $x \geq \tau$ WITH UNIFORM PRESSURE, FOR WHICH B DECREASES EXPONENTIALLY WITH x/λ.

CONCLUDING REMARKS

- INTERACTION OF COMPRESSION WAVE WITH FIELD-FREE, NONHOMOGENEOUS PLASMA CAN GENERATE CURRENT CONCENTRATIONS DUE TO $\nabla n \times \nabla T$ PROCESS.

- MAGNITUDES OF CURRENT DENSITIES INCREASE EXPONENTIALLY AS x/λ (FOR LINEARIZED SOLUTION) THROUGH THE THICKNESS OF COMPRESSION

- NONLINEAR EFFECTS IN PLASMA MAY RESULT IN FURTHER CONCENTRATION AND INCREASED TRANSPORT

- THE RESULT OF SUCH CONCENTRATION OF ENERGY AND INCREASED TRANSPORT MAY BE CHANGE IN FLOW STRUCTURE AND RELATED AERODYNAMIC DRAG